UNCLASSIFIED

AD 294 902

*Reproduced*
*by the*

ARMED SERVICES TECHNICAL INFORMATION AGENCY
ARLINGTON HALL STATION
ARLINGTON 12, VIRGINIA

UNCLASSIFIED

NOTICE: When government or other drawings, specifications or other data are used for any purpose other than in connection with a definitely related government procurement operation, the U. S. Government thereby incurs no responsibility, nor any obligation whatsoever; and the fact that the Government may have formulated, furnished, or in any way supplied the said drawings, specifications, or other data is not to be regarded by implication or otherwise as in any manner licensing the holder or any other person or corporation, or conveying any rights or permission to manufacture, use or sell any patented invention that may in any way be related thereto.

62-2-3

294 902

294902

# U. S. ARMY
# TRANSPORTATION RESEARCH COMMAND
# FORT EUSTIS, VIRGINIA

CATALOGED BY ASTIA
AS AD No.

TCREC TECHNICAL REPORT 62-88

# EXPERIMENTAL STUDIES OF THE AERODYNAMICS OF GROUND EFFECT MACHINES

Task 9R99-01-005-02

Contract DA 44-177-TC-776

November 1962

**prepared by:**

• UNIVERSITY OF MARYLAND
College Park, Maryland

ASTIA
JAN 8 1963

## DISCLAIMER NOTICE

When Government drawings, specifications, or other data are used for any purpose other than in connection with a definitely related Government procurement operation, the United States Government thereby incurs no responsibility nor any obligation whatsoever; and the fact that the Government may have formulated, furnished, or in any way supplied the said drawings, specifications, or other data is not to be regarded by implication or otherwise as in any manner licensing the holder or any other person or corporation, or conveying any rights or permission, to manufacture, use, or sell any patented invention that may in any way be related thereto.

## ASTIA AVAILABILITY NOTICE

Qualified requesters may obtain copies of this report from

Armed Services Technical Information Agency
Arlington Hall Station
Arlington 12, Virginia

This report has been released to the Office of Technical Services, U. S. Department of Commerce, Washington 25, D. C., for sale to the general public.

The information contained herein will not be used for advertising purposes.

The findings and recommendations contained in this report are those of the contractor and do not necessarily reflect the views of the U. S. Army Mobility Command, the U. S. Army Materiel Command, or the Department of the Army.

Task 9R99-01-005-02
Contract DA 44-177-TC-776
November 1962

# EXPERIMENTAL STUDIES OF THE AERODYNAMICS OF GROUND EFFECT MACHINES

TCREC Technical Report 62-88

Prepared by
University of Maryland
Wind Tunnel Operations Department
College Park, Maryland

For

U. S. ARMY TRANSPORTATION RESEARCH COMMAND
FORT EUSTIS, VIRGINIA

HEADQUARTERS
U. S. ARMY TRANSPORTATION RESEARCH COMMAND
Fort Eustis, Virginia

To confirm the existence of a critical velocity for air cushion vehicles, as postulated by N.K. Walker, the present series of wind tunnel tests was undertaken by the University of Maryland Wind Tunnel Operations Department under contract DA 44-177-TC-776. The tests were conducted primarily on two-dimensional models with provisions for pressure surveys and flow visualization. Four models with varying nose and tail cross sections were extensively tested at several ratios of dynamic pressure to jet total pressure. One of the nose shapes was geometrically similar to a large-scale three-dimensional vehicle that was tested in a larger wind tunnel for correlation of the results.

The results indicate the existence of a critical velocity; however, this velocity could not be defined as a point but rather as a band. No systematic effect of the nose shape on the critical velocity could be determined. The tests of the large-scale air cushion vehicle were hampered by mechanical breakdowns and were therefore of limited value for purposes of correlation.

Mr. N.K. Walker, under an ONR contract, is attempting to correlate these results with previous data from both Army and Navy programs.

FOR THE COMMANDER:

KENNETH B. ABEL
Captain, TC
Adjutant

WILLIAM D. HINSHAW
USATRECOM Project Engineer

# FOREWORD

The experimental studies described in this report were supported, in part, by the U.S. Army Transportation Research Command, Fort Eustis, Virginia, under Contract DA-44-177-TC-776. The studies were conducted by the Wind Tunnel Operations Department of the University of Maryland. The work was begun in July, 1961 and completed in June, 1962.

The engineers responsible for various parts of this work were Donald S. Gross, Jerrold V. Powers, Jr., and Richard I. Windsor. This report was prepared by Messrs. Gross and Powers.

Grateful acknowledgement is due many individuals and organizations for assistance in various phases of the work. Mr. George M. Levin and Mr. Robert F. Ryerson conducted the experiments to determine the center of gravity and moments of inertia and the initial stability tests of the full scale vehicle. This work was undertaken as their elective research project required for the Bachelor of Science degree in Aeronautical Engineering.

The cooperation of the Aeronautical Engineering Department, headed by Prof. A. W. Sherwood, in making the 24-Inch Low-Speed Student Wind Tunnel available was essential to this work.

The electric motor used in the full scale vehicle was loaned by the U. S. Navy David Taylor Model Basin.

Mr. Norman K. Walker supplied much valuable information concerning the current "state of the art" and ideas on information that would be of most value.

CONTENTS


| | Page |
|---|---|
| FOREWORD | III |
| LIST OF ILLUSTRATIONS | VII |
| LIST OF TABLES | XIV |
| LIST OF SYMBOLS | XV |
| SUMMARY | 1 |
| RECOMMENDATIONS | 2 |
| INTRODUCTION | 3 |
| TWO-DIMENSIONAL MODEL TESTS | 7 |
| Description of Models | 7 |
| Experimental Procedure | 7 |
| Experimental Results | 10 |
| FULL SCALE TESTS OF THE TINAJERO GEM | 13 |
| Description of the Vehicle | 13 |
| Hovering Tests | 13 |
| Wind Tunnel Tests | 16 |
| Presentation of Results | 18 |
| DISCUSSION OF RESULTS | 21 |
| Two-Dimensional Tests | 21 |
| Full Scale Tests | 24 |
| BIBLIOGRAPHY | 29 |
| TABLES | 31 |
| ILLUSTRATIONS | 37 |

Page

APPENDIXES . . . . . 135
I. Investigation of the Pitch and Roll Stability of the University of Maryland Ground Effect Machine (Tinajero), as written by G. M. Levin and R. E. Ryerson . . . . . 135
II. Test Program, Two-Dimensional Pressure Distribution . . . 169
III. Test Program, Two-Dimensional Flow Visualization . . . 197

DISTRIBUTION . . . . . 211

## ILLUSTRATIONS


| Figure | | Page |
|---|---|---|
| 1 | Front view of Tinajero GEM . . | 37 |
| 2 | Side view of Tinajero GEM . . . | 37 |
| 3 | Rear view of Tinajero GEM . . | 38 |
| 4 | Tinajero GEM mounted in wind tunnel . | 38 |
| 5 | Side view of two-dimensional model with symmetrical nose . . . . . | 39 |
| 6 | Bottom view of two-dimensional model with symmetrical nose . . . . . | 39 |
| 7 | Nose pieces for two-dimensional model | 40 |
| 8 | The 24-Inch Low-Speed Student Wind Tunnel | 40 |
| 9 | Two-dimensional model mounted in wind tunnel . . . . . | 41 |
| 10 | Rear view of two-dimensional model mounted in wind tunnel . . . . . | 41 |
| 11 | Nose profiles and jet configuration of 1/10 scale, two-dimensional GEM models . | 42 |
| 12 | Outline of 1/10 scale, two-dimensional GEM model . . . . . | 43 |
| 13 | Cutaway view of 1/10 scale, two-dimensional model of the Tinajero GEM . . | 44 |
| 14 | Center of gravity locations and dimensions of Tinajero GEM . . . . | 45 |
| 15 | Observed flow patterns about two-dimensional model, Tinajero nose, $^{h}/D = .050$, $\alpha = 0°$ | 47 |

| Figure | | Page |
|---|---|---|
| 16 | Observed flow patterns about two-dimensional model, Tinajero nose, $^{h}/D$ = .100, $\alpha$ = 5.0° | 50 |
| 17 | Observed flow patterns about two-dimensional model, Tinajero nose, $^{h}/D$ = .035, $\alpha$ = - 2.03° | 52 |
| 18 | Observed flow patterns about two-dimensional model, upper curv. nose, $^{h}/D$ = .050, $\alpha$ = 0° | 54 |
| 19 | Observed flow patterns about two-dimensional model, upper curv. nose, $^{h}/D$ = .035, $\alpha$ = - 2.03° | 56 |
| 20 | Observed flow patterns about two-dimensional model, upper curv. nose, $^{h}/D$ = .100, $\alpha$ = 5.0° | 57 |
| 21 | Observed flow patterns about two-dimensional model, lower curv. nose, $^{h}/D$ = .035, $\alpha$ = 0° | 58 |
| 22 | Observed flow patterns about two-dimensional model, lower curv. nose, $^{h}/D$ = .035, $\alpha$ = - 2.03° | 60 |
| 23 | Observed flow patterns about two-dimensional model, lower curv. nose, $^{h}/D$ = .100, $\alpha$ = 5.0° | 61 |
| 24 | Observed flow patterns about two-dimensional model, symm. curv. nose, $^{h}/D$ = .100, $\alpha$ = 0° | 62 |
| 25 | Observed flow patterns about two-dimensional model, symm. curv. nose, $^{h}/D$ = .050, $\alpha$ = - 5.0° | 64 |
| 26 | Observed flow pattern about two-dimensional model, symm. curv. model, $^{h}/D$ = .100, $\alpha$ = 5.0° | 65 |
| 27 | Observed flow conditions relative to $^{q}/P_{t}$ and $^{h}/D$ ratios, Tinajero nose, $\alpha$ = 0° | 66 |

| Figure | | Page |
|---|---|---|
| 28 | Observed flow conditions relative to $q/P_t$ and $h/D$ ratios, symmetrical curv. nose, $\alpha = 0°$ | 67 |
| 29 | Observed flow conditions relative to $q/P_t$ and $h/D$ ratios, lower curv. nose, $\alpha = 0°$ . . | 68 |
| 30 | Observed flow conditions relative to $q/P_t$ and $h/D$ ratios, upper curv. nose, $\alpha = 0°$ . . | 69 |
| 31 | Pressure distribution, two-dimensional model, Tinajero nose, $h/D = .05$, $\alpha = 0°$ . . | 71 |
| 32 | Pressure distribution, two-dimensional model, Tinajero nose, $h/D = .05$, $\alpha = -5.0°$ . . | 79 |
| 33 | Pressure distribution, two-dimensional model, Tinajero nose, $h/D = .05$, $\alpha = 5.0°$ . . | 81 |
| 34 | Change of lift coefficient with increasing forward speed. Comparison of nose shapes, $h/D = .035$, $\alpha = 0°$ . . . . . | 83 |
| 35 | Change of drag coefficient with increasing forward speed. Comparison of nose shapes, $h/D = .035$, $\alpha = 0°$ . . . . . | 84 |
| 36 | Change of pitching moment coefficient with increasing forward speed. Comparison of nose shapes, $h/D = .035$, $\alpha = 0°$ . . . | 85 |
| 37 | Change of center of pressure with increasing forward speed. Comparison of nose shapes, $h/D = .035$, $\alpha = 0°$ . . . . . | 86 |
| 38 | Change of lift coefficient with increasing forward speed. Comparison of nose shapes, $h/D = .035$, $\alpha = -2.03°$ . . . . | 87 |
| 39 | Change of drag coefficient with increasing forward speed. Comparison of nose shapes, $h/D = .035$, $\alpha = -2.03°$ . . . . | 88 |

| Figure | | Page |
|---|---|---|
| 40 | Change of pitching moment coefficient with increasing forward speed. Comparison of nose shapes, $^{h}/D = .035$, $\alpha = -2.03°$ | 89 |
| 41 | Change of center of pressure with increasing forward speed. Comparison of nose shapes, $^{h}/D = .035$, $\alpha = -2.03°$ | 90 |
| 42 | Change of lift coefficient with increasing forward speed. Comparison of nose shapes, $^{h}/D = .050$, $\alpha = 0°$ | 91 |
| 43 | Change of drag coefficient with increasing forward speed. Comparison of nose shapes, $^{h}/D = .050$, $\alpha = 0°$ | 92 |
| 44 | Change of pitching moment coefficient with increasing forward speed. Comparison of nose shapes, $^{h}/D = .050$, $\alpha = 0°$ | 93 |
| 45 | Change of center of pressure with increasing forward speed. Comparison of nose shapes, $^{h}/D = .050$, $\alpha = 0°$ | 94 |
| 46 | Change of lift coefficient with increasing forward speed. Comparison of nose shapes, $^{h}/D = .050$, $\alpha = -5.0°$ | 95 |
| 47 | Change of drag coefficient with increasing forward speed. Comparison of nose shapes, $^{h}/D = .050$, $\alpha = -5.0°$ | 96 |
| 48 | Change of pitching moment coefficient with increasing forward speed. Comparison of nose shapes, $^{h}/D = .050$, $\alpha = -5.0°$ | 97 |
| 49 | Effect of positive angle of attack for isolated cases where a critical point was detected, $C_L$ vs. $^{q}/P_t$ | 98 |

| Figure | | Page |
|---|---|---|
| 50 | Propeller r. p. m. vs. height . . . | 102 |
| 51 | Horsepower vs. height . . . . . | 103 |
| 52 | Comparison of height of Tinajero GEM at front and rear with no ballast aboard . . . | 104 |
| 53 | Comparison of height of Tinajero GEM inside wind tunnel and in free air. h vs. r. p. m. . | 105 |
| 54 | Comparison of height of Tinajero GEM inside wind tunnel and in free air. h vs. HP. . | 106 |
| 55 | Hovering pressure distribution under the Tinajero GEM . . . . . | 107 |
| 56 | Hovering pressure distribution under the Tinajero GEM, vehicle weighted to maintain level hover | 114 |
| 57 | Static pitching moment coefficient vs. angle of attack. Full scale vehicle hovering, propeller speed = 1917 r. p. m. Effect of changing vertical center of gravity position. . . . | 121 |
| 58 | Static rolling moment coefficient vs. angle of roll. Full scale vehicle hovering, propeller speed = 1917 r. p. m. Effect of changing vertical center of gravity position. . . . . | 122 |
| 59 | Lift coefficient vs. velocity, full scale vehicle, power off, $\alpha$ = 0°. Comparison of $^{h}/D$ ratios | 123 |
| 60 | Drag coefficient vs. velocity, full scale vehicle, power off, $\alpha$ = 0°. Comparison of $^{h}/D$ ratios | 124 |
| 61 | Pitching moment coefficient vs. velocity, full scale vehicle, power off, $\alpha$ = 0°. Comparison of $^{h}/D$ ratios . . . . . | 125 |
| 62 | Lift coefficient vs. $^{h}/D$ ratio, full scale vehicle, power off, $\alpha$ = 0°. Comparison of constant velocities . . . . . | 126 |

| Figure | | Page |
|---|---|---|
| 63 | Drag coefficient vs. $^{h}/D$ ratio, full scale vehicle, power off, $\alpha = 0°$. Comparison of constant velocities . . . . . | 127 |
| 64 | Pitching moment coefficient vs. $^{h}/D$ ratio, full scale vehicle, power off, $\alpha = 0°$. Comparison of constant velocities . . . . . | 128 |
| 65 | Pressure distribution across the jet of the Tinajero vehicle hovering, propeller speed = 1917 r.p.m., $^{h}/D = .020$, $\alpha = 0°$ . . . | 129 |
| 66 | Pressure distribution across the jet of the Tinajero vehicle, tethered, propeller speed = 1917 r.p.m., $^{h}/D = .020$, $\alpha = 3.23°$ . . | 130 |
| 67 | Pressure distribution across the jet of the Tinajero vehicle, tethered, propeller speed = 1917 r.p.m., $^{h}/D = .020$, $\alpha = 1.62°$ . . | 131 |
| 68 | Pressure distribution across the jet of the Tinajero vehicle, tethered, propeller speed = 1917 r.p.m., $^{h}/D = .020$, $\alpha = -2.52°$ . | 132 |
| 69 | Pressure distribution across the jet of the Tinajero vehicle, tethered, propeller speed = 1917 r.p.m., $^{h}/D = .020$, $\alpha = -1.26°$ . | 133 |
| 70 | Rear view of GEM . . . . . | 153 |
| 71 | Front view of GEM . . . . . | 154 |
| 72 | Side view of GEM . . . . . | 155 |
| 73 | Apparatus for weighing GEM . . . | 156 |
| 74 | Apparatus for determining longitudinal C.G. location . . . . . | 157 |
| 75 | Circuit for determining period of oscillation | 158 |
| 76 | Pitching moment versus angle of attack . | 159 |

| Figure | | Page |
|---|---|---|
| 77 | Rolling moment versus angle of roll . . | 160 |
| 78 | Angle of pitch versus time . . . | 161 |
| 79 | Residual pitching moment versus pitching velocity . . . . . | 162 |
| 80 | Residual pitching moment versus angle of pitch | 163 |
| 81 | Angle of roll versus time . . . . | 164 |
| 82 | Residual rolling moment versus rolling velocity | 165 |
| 83 | Residual rolling moment versus angle of roll | 166 |
| 84 | Peripheral jets and stability slots - Scale 1/20 | 167 |

# TABLES


| Table | | Page |
|---|---|---|
| 1. | Run Program, GEM in Tunnel . . . | 31 |
| 2. | Wind Tunnel Test Data . . . . | 33 |
| 3. | Damping Coefficients and Moments of Inertia in Pitch and Roll for Different Center of Gravity Positions . . . . . | 35 |
| 4. | Summary of Measured Physical Characteristics | 151 |

## SYMBOLS

| | | | |
|---|---|---|---|
| $L$ | Lift | | |
| $D$ | Drag, when used with $C_D$ | | |
| $M$ | Pitching moment | | |
| $\mathfrak{L}$ | Rolling moment | | |
| $q$ | Dynamic pressure, $1/2\ \rho V^2$ | | |
| $\rho$ | Density | | |
| $C_L$ | Lift coefficient | $= \frac{L}{qA}$ | (three-dimensional) |
| | | $= \frac{L}{ql}$ | (two-dimensional) |
| $C_D$ | Drag coefficient | $= \frac{D}{qA}$ | (three-dimensional) |
| | | $= \frac{D}{ql}$ | (two-dimensional) |
| $C_m$ | Pitching moment coefficient | $= \frac{M}{qAl}$ | (three-dimensional) |
| | | $= \frac{M}{ql^2}$ | (two-dimensional) |
| $C_l$ | Rolling moment coefficient | $= \frac{\mathfrak{L}}{qAb}$ | (three-dimensional) |
| $A$ | Base area of GEM | | |
| $l$ | Distance between jets, longitudinal | | |
| $b$ | Distance between jets, lateral | | |
| $D$ | Base diameter or representative diameter, equal to $l$ as used here; used with $h/D$ ratio | | |
| $h$ | Height of geometric center of base above ground | | |
| $\Delta p$ | Pressure difference, relative to ambient pressure | | |
| $P_t$ | Pressure in forward end of plenum relative to ambient pressure | | |

| | |
|---|---|
| $\alpha$ | Angle of attack (+ with nose up) |
| $\phi$ | Angle of roll (+ with left side facing forward up) |
| $\theta$ | Jet angle relative to base |
| G | Jet thickness |

## SUMMARY

This report describes and presents the results of a series of experiments conducted to investigate the basic aerodynamics of ground effect machines. Two-dimensional model tests and full scale tests of the Tinajero ground effect machine were made.

The objectives of the two-dimensional model tests were to investigate the flow patterns and pressure distributions around a vehicle at various flight conditions, and to determine the effects of nose shape on these patterns. It was found that nose shape had no significant effect on the cushion under the vehicle, but does have an effect on the basic external aerodynamic coefficients. Sketches of typical flow patterns, typical pressure distribution, and aerodynamic coefficients around "critical" points are presented.

The objectives of the full scale tests of the Tinajero ground effect machine were to investigate the aerodynamics of the machine, the static and dynamic stability characteristics, control effectiveness, and effects of changing center of gravity positions. Pressure distributions under the vehicle, static stability curves, dynamic damping coefficients, and some aerodynamic coefficients are presented. The machine was found to be basically unstable in yaw and the controls were ineffective. The directional stability problem prohibited a complete investigation at forward speeds.

## RECOMMENDATIONS

The work described in this report covers many phases of the ground effect machine problem. Probably too many subjects have been covered in a single report. It seems reasonable to suggest that future projects be broken into several tasks, with each task reported separately.

Based on the experience gained in this work, it also seems reasonable to recommend additional research directed toward a better understanding of the aerodynamics of ground effect machines, particularly at forward speeds. More background will certainly be necessary to insure adequately designed control systems for large, high speed ground effect machines. This research can be conducted most economically using models rather than expensive full scale vehicles. Any experimental model work should, however, be fully instrumented, including means of rapid data reduction. This last recommendation is also based on this work which has been seriously hampered by excessive times required for data reduction.

It would be impossible to make a specific recommendation regarding a preferred nose shape as a result of these tests, particularly without knowing the particular application. A GEM designed primarily for use over water would require considerable curvature of the lower surface to reduce wave impact and to keep the nose from being buried. However, these tests show that this imposes a considerable drag penalty if the GEM were to be used over land. Although it cannot be confirmed by facts, it is suspected that some overhang in front of the jet may be necessary to prevent sudden loss of the forward cushion if the nose should dip at high forward speeds.

# INTRODUCTION

At the time the work described in this report was initiated, the available knowledge of the pressure and flow patterns surrounding a ground effect machine (GEM) under all flight conditions was quite limited. The primary purpose of this work was to investigate the pressure and flow patterns around a specific vehicle throughout the flight envelope, and to attempt to determine the effects of these patterns on the performance and stability of the vehicle. In addition, the effects of changing the leading edge or nose shape was of considerable interest.

Additional items to be investigated were the lift height, power requirements, static and dynamic stability and control characteristics, and effect of changing the vertical center of gravity position of the specific vehicle.

Early in 1961 a GEM designed and constructed by Mr. A. Tinajero, as a personal project, was donated to the University of Maryland by Mr. Tinajero for use as a research tool and as an aid to student instruction. Mr. Tinajero had been hindered in his own experiments by engine difficulty and was unable to continue. The work described in this report is based on this vehicle.

The studies of the pressure and flow patterns were made on a two-dimensional model of the Tinajero GEM internal ducting, base, and leading and trailing edge shapes. The superstructure was not duplicated for these tests as its shape is rather odd. It was assumed that the data obtained would be of greater general value if a flat upper surface were used. The model was fitted with interchangeable noses, both front and rear, and was liberally fitted with pressure orifices.

The 24 inch Low Speed Student Wind Tunnel of the Aeronautical Engineering Department was converted for two-dimensional use with side plates for the small model tests. Although the speed range of this tunnel is limited, it was found satisfactory for this work. It had been hoped that the flow patterns could be observed and photographed using

a flourescent oil film technique. However, successful photographic recording of these data was not possible due to the many reflections off of the curved plastic outer walls of the tunnel. It was therefore necessary to make sketches of the flow patterns observed.

Test work on the full scale Tinajero GEM was conducted with a 100 horsepower induction motor installed. The use of this motor made it possible to accurately control the propeller speed and to measure the power output of the motor. Initial tests indicated that the propeller blades were operating in the aerodynamically stalled condition, resulting in excessive power requirements with too little flow output. The blade shanks were then modified to cut the blade angle at the three quarter radius by approximately one half. The modification made it possible to attain a propeller speed of 2000 r.p.m., just below the design speed, at a motor output of 51.5 horsepower, close to the maximum for the motor at that speed.

Tethered tests on the Tinajero GEM were made outdoors on a flat level platform, instrumented with pressure orifices on the surface.

Tests at forward speed were attempted in a section of the return circuit of the 7.75 x 11 foot low speed wind tunnel. This section measured 16 x 16 feet. A raised platform was built into this section to act as a ground board and to put the GEM in a previously surveyed area of good flow characteristics. Forces and moments on the vehicle were measured using a simplified type of wire balance with strain gage load cells in the cables. These attempts were not completely successful as the vehicle was violently unstable in yaw, making it very difficult to obtain any accurate data.

Following the electric powered tests of the GEM, a Model H-63 Nelson engine was installed with a "V" belt drive to the propeller. The intent was to be able to make free-flight tests to verify the results of the previous tests and to investigate the interaction of the human operator on guidance and control of the vehicle. Problems were encountered

with broken pulleys, failure of engine fan and pulley castings, and failure of the engine to attain more than one half of rated speed under load. It is probable that the engine drive parts were not originally designed for the high inertia loads of this particular propeller assembly. Last indications were that the engine did not produce full power because of ignition difficulties which are still unexplained.

Free flights, limited by the electric cables, were possible and were evaluated to obtain a qualitative impression of control effectiveness.

## TWO-DIMENSIONAL MODEL TESTS

### Description of Models

A single basic model was used for the two-dimensional tests. The model was one tenth scale of the Tinajero GEM platform. The general arrangement and dimensions of the model are shown in Figure 12 . The outer leading and trailing edge sections of the model were removable to provide for testing of different shapes. The various shapes used are shown in Figure 11 . The interior duct arrangement of the model is shown in Figure 13 . The screening shown was installed to insure a uniform flow distribution across the jets.

The nose shapes tested, in addition to the Tinajero GEM nose, were chosen as representative of the extremes of the shapes that would be likely to be used on other GEM vehicles. The interior nozzle configuration was held constant to insure that any effects would be due to exterior shape alone.

The construction of the model was basically simple. The base was mahogany and the upper surface a brass plate. Dowel type metal spacers were used at intervals to maintain the separation. In order to conform as closely as possible with exact scaling, the models of the Tinajero leading and trailing edge shapes were built up of one sixteenth inch brass tubing and externally filled with solder. The tubing base then also provided for the pressure orifices in the surface. This type of construction was necessary to preserve both the internal duct shape and the external shape as the full scale vehicle is built of sheet metal in this area. The other nose shapes were constructed around a mahogany base with epoxy resin used to mold in the internal shape. Brass tubing was set in the surface and flushed over with resin to provide for the pressure orifices. Pressure orifices were located in the model and ground board as shown in Figure 31 .

### Experimental Procedure

The two-dimensional models were mounted in the two foot diameter test section of the tunnel between side plates

spaced eight inches apart. As all pressure leads were brought out of one side of the model through the side plate, this side plate was fitted with a rotary section to avoid sealing problems as the angle of attack was changed. A wooden ground board of twice the model length was installed beneath the model. The ground board was adjustable in height. The angle of attack of the model could be changed around a fixed center. Tunnel dynamic pressure and all model orifices were connected to inclined multiple manometers for photographic recording of data.

Shop air supply was used for model power. A standard thin plate orifice meter, designed and built to American Society of Mechanical Engineers standards, was inserted in the line following a pressure regulator to permit recording of mass flows into the model. The use of this only available air-supply imposed several difficulties on the testing, primarily because the tunnel happened to be at the far end of the building from the compressor. The long piping run caused severe pressure drop at high flow rates and by the time the air reached the model jet, the model pressure became a limiting factor in the experiments and not the tunnel speed. This restriction was not serious however, as lower tunnel speeds provided the necessary model to tunnel dynamic pressure ratios. However, the long line lengths did make it necessary to blow out the line several times a day to eliminate condensed water in the piping.

A flourescent oil film technique was used to observe the flow patterns around and under the model. A splitter plate was fitted around the outside contour of the model at the center to carry the oil. The plate at the center of the model was used instead of one of the side walls to eliminate, as much as possible, the effects of boundary layer build up on the observed patterns.

To use this technique, the tunnel was arranged so that the model was mounted vertically. This put the splitter plate in a horizontal position and eliminated any gravity effects on the oil flow. A small amount of flourescent green dye was added to standard 40 weight automotive oil. The oil was

smeared evenly around the model on the splitter plate and the tunnel and model power brought up to the conditions desired. The oil film, moved by the air flow, was observed under ultraviolet light. When a pattern was established in the slow flowing oil, the pattern was sketched manually on prepared outlines of the model.

The original intention had been to photograph the flow patterns, a technique used successfully many times in the large wind tunnel. However, it was not possible to properly light the model, particularly at the critical areas under the leading and trailing edges, without getting reflections off the curved plastic outer surface of the tunnel back into the lens. The resulting quality was too poor for practical use.

Several other methods of flow visualization were attempted but were unsatisfactory. Lamp black mixed with kerosene was tried with the hope that, as the kerosene evaporated, the lamp black deposit would leave a trace of the pattern suitable for photographing. A mild hydrochloric acid solution was used with litmus paper for an indicator to try to determine a definite line marking the boundary of the model jet and the airflow ahead of the model. A similar method using an iodine solution was attempted. None of these methods proved to be satisfactory and were discontinued.

Normal procedure in running these tests was to obtain, first, a series of pressure data at different height to diameter ratios, angles of attack, and jet total pressure to tunnel dynamic pressure ratios. These tests were run prior to the oil studies as the oil quickly clogged the pressure orifices and it was necessary to thoroughly clean the model after each series of flow visualization runs. When the pressure data for a configuration had been recorded, the oil flow studies were conducted. A general exploratory study was made first at each height and angle of attack to determine the jet total pressure to tunnel dynamic pressure ratio at which the leading edge jet was blown under the model. When this point was determined, a series of sketches of the flow patterns leading up to the "blown under" conditions were made.

Schedules of all conditions tested, for both pressure data and flow visualization, are presented in Appendixes II and III.

## Experimental Results

The two-dimensional pressure data were plotted as shown in Figure 31. The data were plotted in this particular form in order to provide for both a pictorial representation of the pressure field around the model and a linear form for integration of the pressure fields. The pressures were then integrated using a polar planimeter to obtain the lift, drag, and pitching moment coefficients. The integration was made along the body axes and therefore the coefficients presented are relative to the body and not the wind axes.

Since it would have been impossible to plot all of the pressure data actually recorded in any reasonable length of time; points that were considered most significant were actually plotted and integrated. The significance of these points was determined by an evaluation of the flow visualization studies. Points were selected around and on either side of areas where there were changes in the flow patterns. Sufficient additional points were selected to insure that no major changes occured that were not indicated by changes in the flow.

In presenting the results of the pressure studies, only a few of the pressure plots are included, Figures 31 through 33. These are typical for a range of conditions.

The lift, drag, and pitching moment coefficients resulting from the integrated data were plotted to compare the four nose shapes. These data are presented in Figures 34 through 39.

It is difficult to estimate the precision of these data for several reasons. The slow speeds and pressures involved and the small model size all tend to degrade the precision. The reading of the data from film and the integration of the plotted data produce additional sources of possible error. However, considerable care was exercised throughout and double checks were made routinely and in all cases of suspected inconsistency. It is estimated, therefore, that results are accurate to within plus or minus five per cent. It should be noted that, although this is rather poor precision, it should not significantly affect the trends and comparisons which are the primary interests of the investigation.

The results of the flow visualization studies are inherently qualitative. A series of sketches of the flow patterns under various conditions are presented in Figures 15 through 26. The sketches were selected as representative of all of the patterns encountered for the four nose shapes.

Observations as to whether the front jet was or was not blown under the GEM have been plotted in Figures 27 through 30. The areas where it was difficult to determine whether the jet was fully blown under have also been indicated. A curve has been faired through the observed points to attempt to pinpoint the "critical" points.

## FULL SCALE TESTS OF THE TINAJERO GEM

### Description of the Vehicle

The Tinajero GEM is a peripheral jet type of ground effect machine with stabilizing slots. Air is supplied by a rear facing propeller having 16 blades. It is understood that these blades were originally used in some type of target drone and were adapted to this vehicle. Propulsion is provided by inclining vanes in the side jets. Yaw control is through inclining vanes in the front and rear jets. Pitch and roll control is obtained by slats closing over the entrance to the jet in the direction of the desired tilt. Pitch and roll controls are connected to an aircraft type control stick and the yaw control to pedals. The propulsion control is connected to a hand brake type of pull control.

The pertinent outlines and dimensions of the vehicle are presented in Figure 14.

A one hundred horsepower induction motor was installed to drive the propeller. A three to one reduction of motor speed to propeller speed was used. Drive was through a three inch timing type belt and appropriate pulleys. The motor was powered and controlled with the variable frequency system normally used to power model motors in the wind tunnel. This system made it possible to precisely control engine speed and to measure power requirements. Power calibration curves were provided with the motor by the David Taylor Model Basin.

### Hovering Tests

Prior to the beginning of the hovering tests, the center of gravity, both horizontal and vertical, and the moment of inertia about the pitch and the roll axes were determined as described in the Appendix I. This work was accomplished by Messrs. Levin and Ryerson.

A twelve by twenty foot ground plane was built of plywood for the hovering tests to provide a flat, level surface and to provide a means of installing pressure orifices under the vehicle. The Tinajero GEM was normally kept inside, out of the weather, but it was found to be quite easy to "fly" it onto the ground board. Two pieces of plywood were propped up on the edge of the board

which was about one foot off of the ground. The GEM, with power on, could then be pushed out of the building, up the ramp, and onto the board.

The cabling for the electric motor, water cooling lines, pressure tubing, etc., were bundled together and suspended to take their weight off of the vehicle. This was necessary as the electrical cables in particular had to be quite heavy in order to carry currents in excess of one hundred amperes. The loop in the cables from the vehicle to the support was kept quite long to keep the forces exerted by the cabling on the machine to a minimum.

In order to accurately measure both the height and angle of the GEM, a fluid reservoir was mounted on each corner of the vehicle. Each was connected through flexible tubing to a glass tube mounted against a calibrated scale. As the reservoir rose, so did the level in the tube. Knowing the location of the reservoirs, the angles were computed from the differences in heights.

Tests were made to determine the height of the GEM at progressively increasing propeller speeds. At each speed the power input to the motor was also measured. During the initial tests, the nose of the GEM rose first and continued to remain high up to the maximim propeller speed. A second test was then made with the nose weighted to maintain a horizontal attitude.

In the process of these first tests, it was found that the power required was saturating the electric motor before a propeller speed of 2000 r.p.m. could be obtained. The propeller was capable of 2100 r.p.m., according to the designer, and a speed of 2000 had been fixed as a safe operating speed.

It was fairly obvious that the propeller was operating at a stalled condition and the only reasonable solution was to reduce the blade angle. The blade angle was then reduced, from a nominal 37.5 degrees at the three quarter radius of the blade to 25.0 degrees, by milling off the flat of the blade shank where it is clamped in the hub. The new angle was chosen as a compromise between aerodynamic efficiency and strength of the shank.

The previous tests were then repeated with the modified propeller. The new blade angle made it possible to reach 2000 r.p.m. at 51.5 horsepower. This point is just within the maximum horsepower versus speed envelope of the motor. However, at this maximum speed it was found that the motor overheated rapidly.

All further tests were therefore made at a motor speed of 5750 r. p. m. (propeller speed of 1917 r. p. m. ) which permitted continuous operation.

To obtain the pressure distribution on the ground and on the base of the vehicle, the ground board and the bottom of the GEM were fitted with pressure orifices connected by flexible plastic tubing to inclined multimanometer boards. The pressure in the plenum of the GEM just before both the front and rear jets was also recorded on the manometer boards. The pressures were recorded photographically.

Pressures were recorded at each propeller speed at the time the power and height data were obtained.

In order to keep the GEM positioned properly over the ground board pressure orifices, it was necessary to place bumpers around the periphery of the vehicle with just enough clearance to allow free vertical movement.

Hovering pitch and roll static stability data were obtained with the GEM tethered over the ground board. To obtain pitching moment data, the GEM was tethered through rings on either side of the vehicle at the horizontal and vertical center of gravity position. Cables were fastened from the rings, fore, aft, and straight out to the sides, to points at least twenty feet away. This arrangement left the vehicle free to rotate in the angle of attack direction and to rise vertically, but not to roll or yaw. A small hydraulic crane was positioned over a premeasured point at the forward end of the vehicle and connected to the point through a spring scale. With the vehicle hovering at a constant propeller speed, the crane was raised to raise the nose of the vehicle. The angle of attack was measured and the load on the scale recorded. The process was repeated with increasing positive angles of attack up to the maximum where the rear of the vehicle was just clear of the ground. A similar process was repeated at the rear for negative angles of attack. Rolling moment was determines similarly, for positive roll angles only, as the vehicle was assumed symmetrical about the longitudinal axis.

To determine the effects of changing the vertical position of the center of gravity on the pitch and rolling moment static stability, a vertical mast was added over the venter of gravity. The mast was fitted with a platform to carry several weights and was adjustable vertically. With this arrangement, the pitch and rolling moment static stability was again determined, as described above, when the

center of gravity was raised first to 7.74 inches and then to 13.25 inches above the original location.

Dynamic stability tests of the Tinajero GEM were made with the same general arrangement as just described for the static stability data. Damping characteristics in pitch and roll were actually obtained by two distinct methods. The first, conducted by Levin and Ryerson, was accomplished by means of motion analysis from motion picture film and is described in the Appendix. This method produced the residual damping moment which is the damping due to the cushion under the GEM.

However, since the first results are not too readily usable for comparative purposes, and do not contain any effects of center of gravity height, additional tests were made to determine damping coefficients. A gyroscope with both pitch and roll potentiometers was installed in the GEM. The input signals from voltages across the potentiometers were recorded on an oscillograph. Curves of angle versus time were thus obtained directly. Recordings of the damping oscillations were made at three vertical center of gravity locations by manually displacing the vehicle in the desired direction.

There had been some discussion concerning the value of so called thick jets and thin jets, and the possibility that in some cases jets which were thought to be thick, because of their dimensions, might actually be thin due to the shape of the entrance to the jet or to separation problems. In order to check the jets of this particular GEM, total head and static pressure rakes were installed in the front and rear jets to check the pressure distribution. The rakes were connected to manometer boards for recording of data. The GEM was operated at normal maximum propeller r.p.m. of 1917 and data were recorded for level flight and several positive and negative angles of attack. Maximum angles were checked to determine whether the close proximity of the jet to the ground might induce flow separation.

## Wind Tunnel Tests

In order to obtain data at forward speeds, the GEM was mounted in a portion of the diffuser section of the larger subsonic wind tunnel. This section, about 16 by 16 feet in cross section had previously been surveyed to determine the flow characteristics. A ground board was built to put the vehicle in the best flow region and out of the boundary layer near the normal floor.

Hovering height and power versus propeller speed tests were repeated in the tunnel to determine whether the tunnel walls would have

any effect at zero wind speeds. Previous experiments with vertical take off types of aircraft models had indicated that recirculating flows caused by the tunnel walls washed away at low speeds. However, there was no previous experience available with models this large in the hovering condition. The differences noted as a result of these tests are discussed later in this report.

The vehicle was then suspended from a system of cables arranged to restrain the vehicle in lift, drag, and pitch. Strain gage type load cells were designed, fabricated, and calibrated. The load cells were installed in each cable to provide means of measuring the lift, drag, and pitching moment. A single drag cable and two lift cables were used. The pitching moment was derived from the difference in the lift cables. The cables were arranged so that the height of the vehicle from the ground board could be changed in one inch increments. Figure 4 shows the GEM installed in the tunnel.

To obtain an idea of the basic aerodynamic characteristics of the GEM without power, a series of tests was made at forward velocities up to 55 m.p.h., and heights from 2 to 12 inches. The lift, drag, and pitching moment were determined at each point. In the process of running these tests, it was found that the vehicle was very unstable in yaw. Bumpers had to be installed along the sides of the vehicle to restrain the yawing oscillations in order to record the data from the load cells. The angle of attack was maintained at zero throughout these runs.

As fifty pound weights were used on the front end of the GEM to maintain a level attitude with power on, a check was run to determine whether the weights had any effect on the aerodynamics of the GEM. No significant changes were evident.

It had been understood that a simulated cushion behind the front jet had produced appreciable increases in lift in some tests in Great Britain. To try to verify this, a wooden block, 1 7/8 inches thick, was installed under the base of the GEM immediately behind the front jet. A run was made at the 2 inch height, with velocities from 15 to 55 m.p.h., and data were recorded.

A series of tests was begun with power on. However, with air flowing from the jets, the vehicle became so unstable in yaw that no

data could be obtained. With the thought that perhaps the lift cables might be contributing to the instability, the cabling arrangement was changed. The lift cables were removed and the single drag cable was replaced with two cables, one leading forward at each side. It was hoped this might damp the yaw instability and also provide a measurement of the yawing moments. However, not only did the yawing oscillations remain, but without the pitching restraint of the lift cables, the nose of the vehicle dropped to the ground board. The latter was not totally unexpected as the power off tests had indicated a nose down pitching moment. A few drag data points were obtained; however, these are suspect because of the erratic behavior of the vehicle.

Presentation of Results

The positions of the center of gravity of the vehicle for the various loadings used for the full scale tests are shown in Figure 14.

The moments of inertia of the vehicle as rigged for the dynamic damping tests are presented in Table 3. The moments of inertia presented were derived from the basic moment of inertia as determined by Levin and Ryerson. The shift of the center of gravity and the moments of the added masses were accounted for using the following standard equations:

$$I' = I_{CG} + a^2 M$$

$$I = I'_1 + I'_2 + I'_3 + \ldots + I'_n$$

where $I'$ = moment of inertia transferred to new axis

$I_{CG}$ = original moment of inertia about original center of gravity

$a$ = distance between new and original centers of gravity, feet

$M$ = mass of item, slugs

$I$ = sum of all moments of inertia of vehicle and added masses

Curves of height and horsepower required for the original propeller and modified propeller are presented in Figures 50 and 51.

The pressure distributions on the ground and the base of the GEM in hovering flight are presented in Figures 55 through 56. It

should be noted that the distributions are presented for the cases where the GEM was not weighted to maintain a level attitude and for the cases where a level attitude was maintained, the pressures are presented as pressure ratios, $\Delta P/P_t$, where

$\Delta P$ = the pressure at the orifice relative to atmospheric pressure

$P_t$ = pressure in the forward end of the plenum relative to atmospheric

Curves of pitching and rolling moments versus angles of attack and roll respectively are presented in Figures 57 and 58 for the several center of gravity positions. The moments are presented as dimensionless coefficients based on the weight of the vehicle as tested and the characteristic length.

The dynamic damping coefficients obtained are presented as percentages of the critical damping. These data were obtained from the oscillograph recordings and were computed according to the analysis presented in Reference 1, chapter 1. The rate of decay of the amplitude of the oscillations is dependent upon the value of n in the following equation:

$$n = \frac{\ln x_o/x_r}{r\tau}$$

where:

$r$ = number of cycles between points $x_o$ and $x_r$

$x_o$ and $x_r$ = amplitudes of two points of tangency within the envelope of the curve

$\tau$ = period between $x_o$ and $x_r$ in seconds

The points $x_o$ and $x_r$ were chosen so that r equals 1. The amplitudes of $x_o$ and $x_r$ and the frequency were measured from the recording . and the equation solved for n. The frequency, $\omega$, in radians per second, was similarly determined. The damping coefficient is then equal to $n/\omega$. The ratio, $n/\omega$ equals 1, indicates that point at which no oscillatory motion occurs. When the ratio equals 0, there is no damping.

The difference in hovering height and power required versus propeller speed between the GEM outside and in the wind tunnel is presented in the curves of Figures 53 and 54.

The lift, drag, and pitching moment of the GEM at forward speed, with power off, are presented in Figures 59 through 61 at constant height and increasing speed and in Figures 62 through 64 at constant speed and increasing height. All of the data obtained in the tunnel are presented in Table 2. The coefficients are defined in the list of symbols.

The pressure distributions across the jets are presented in Figures 65 through 69. The pressures are presented in inches of water, as the object is to show only the shape of the distribution curve. Total and static pressures are presented separately.

## DISCUSSION OF RESULTS

### TWO-DIMENSIONAL TESTS

A study of the flow patterns, around the four leading and trailing edge shapes investigated, shows that the flow patterns beneath the vehicle are basically similar regardless of nose shape. They are similar primarily with respect to the sequence of changes that occur as the $^{q}/P_{t}$ ratio increases.

The flow patterns are best described by the series of sketches presented in Figures 15 through 26 . It may be noted that, at the zero forward speed or hovering condition, the air flows outward from the bottom of the cushion as predicted by all theories and demonstrated in many previous studies. As the forward speed increases, a bubble forms ahead of the vehicle and cushion. Of course, this is not truly a bubble, but resembles one in the pattern. There is circulation within this bubble as in a vortex. The external flow follows the outside boundary of the bubble, flowing up and over the vehicle as though the vehicle and cushion were a solid mound.

As the forward speed continues to increase, the front of the bubble begins to be pushed in toward the vehicle, forming effectively a more blunt mound. As the forward speed continues to increase, the bubble is compressed still further until external air begins to leak under the leading edge of the cushion. This process continues until the forward jet no longer blows forward but is bent backwards into the cushion. The point at which the front jet is bent to the rear has been called variously the "critical point" or "blow under point".

The process of reaching the "critical point" is a gradual one and is, therefore, difficult to determine precisely. This phenomenon probably should not be called a "critical point" because there really is no point, but only a gradual change in flow pattern.

The primary effect of the nose shape on the flow pattern is the shape of the bubble formed ahead of the cushion and the flow over the top of the vehicle. In this respect, the nose shape has an effect similar to angle of attack changes. The shape of the bubble formed appears to be determined by the pocket formed by the shape of the lower surface, the jet boundary, and the ground.

The height to diameter ratio, $^{h}/D$, has a considerable effect on the $^{q}/P_{t}$ ratio at which the front jet "blows under". The observed flow conditions have been plotted in Figures 27 through 30 . A curve has been faired between those points where the front jet was observed to be blown away and where it was not. These curves should represent fair approximations of where the jet blows under. They can only be approximations, however, as there is no definite "point" as discussed previously. The definite relationship of $^{h}/D$ ratio to $^{q}/P_{t}$ ratio is readily noted; the jet blowing under at lower $^{q}/P_{t}$ ratios as the height increases.

A comparison of the data plotted for each nose shape does not indicate any significant change in where the jet blows under caused by a change in the nose shape. This conclusion is, of course, based on qualitative data. However, since the variation in nose shapes investigated is quite radical, it is apparent that external shape cannot be of major significance.

Qualitative observations of the effect of angle of attack on where the jet blows under are inconclusive. It is apparently even more difficult to determine a "blow under point" at either positive or negative angle of attack. An attempt to plot results similar to those plotted for the level flight case produced only a confusing hash. A contributing factor to the uncertainty is the fact that, at the $^{h}/D$ ratios investigated, the range of angle of attack is quite small, particularly at the lowest $^{h}/D$ ratios. A qualified opinion at the moment would be that increasing positive angle of attack raises the speed at which the jet blows under, and the blow under speed is lowered as the angle of attack becomes more negative.

A study of the plotted pressure data, as in Figures 31 through 33 , does not indicate any significant changes in the pressure distribution on the vehicle as the jet blows under. An attempt to determine whether the jet was blown under from the pressure plots proved fruitless. There is an indication of where the jet strikes the ground pressure distribution at very low speeds; however, this peak flattens out under the front jet at relatively low speeds where the flow patterns definately indicate that the jet is still blowing forward.

The aerodynamic coefficients obtained are presented in Figures 34 through 39 . Nominal "critical points" have been indicated on each curve; however, as noted previously there is no true "point".

It is when trying to analyze data such as this that a moment of truth arrives and it is realized just how much additional data would be helpful. Although much more data were recorded, it was impossible to reduce more than was considered most necessary because of the great amount of time consumed in reducing this type of data.

The following trends are evident, however:

1. The lift coefficient decreases with increasing speed regardless of nose shape.
2. The nose with curvature on the lower side only consistently has the highest drag coefficient.
3. The nose shape with curvature on the upper side only has the lowest drag coefficient.
4. The Tinajero nose and the symmetrical nose had about equal drag, falling between the other limits.
5. The vehicle was unstable in pitch, regardless of nose shape.
6. The lift and drag coefficients are functions of angle of attack as would be expected. Particular note should be made here that the force coefficients are along the body axes. This explains why a negative drag does not result from a negative angle of attack as might be anticipated, knowing that dropping the nose of a GEM usually produces forward motion.

It may be noted in several of the tables that mention is made of a negative pressure in the forward portion of the plenum when the nose was close to the ground. This occured at $^{h}/D$ ratios above 0.100 at large negative angles of attack and at higher $q/P_t$ ratios. It did not happen with the nose shape with upper curvature only. The indication is that there is venturi effect between the ground and curved lower surface with possibly some augmentation from the jet itself. Possibly, it is the other way around and a jet formed by the surfaces is augmenting the model jet and drawing it out.

This phenomenon is not really understood. However, if this should be a general case, it might possibly help explain the question of why several operating GEM vehicles have had sudden severe contact of the nose with the surface at relatively high speeds. Coupling of a naturally unstable pitching moment with a loss of cushion pressure could cause sudden impact.

## Full Scale Tests

The curves of Figures 50 and 51 show the relation between propeller speed, horsepower input, and height obtained. It may readily be seen that the reduction to the smaller blade angle had no effect on the height relative to propeller speed but resulted in a saving in horsepower of about 34 per cent. The reduction in horsepower required made it possible to obtain a maximum height of 3.1 inches. This is a ratio of $^{h}/D$, based on distance between front and rear jets, of only 0.022. The $^{h}/D$ ratio for most of the following tests was only about 0.020. Although a higher ratio would be highly desirable, this seems to be in the same order of magnitude as GEM vehicles currently operating.

It is interesting to note that the above curves could easily be faired into a power off height of minus 0.5 inch. Due to a strip running just inside the jet under the GEM, 0.5 inch is just the height of the jet when sitting on the ground.

The pressure distributions on the ground and the base of the GEM, without ballast, are presented in Figure 55. In this condition, the rear of the GEM never got off the ground. In addition to the fact that the center of gravity was slightly to the rear of the center of the GEM, Figure 55a shows that the pressure was higher under the front end than the rear. The combination of these two factors made it necessary to use ballast to maintain a level attitude. Some effort was made early in the testing to equalize the pressure distributions with baffling but with no substantial success. This condition was created by the intake configuration which drew air in the rear and blew toward the front.

It is also interesting to note in Figure 55a that the ground pressure decreases toward the rear, but the base pressure on the vehicle is much more constant. As the propeller speed increased, the difference in pressures between ground and base disappeared. The pressures thereafter remained essentially the same, as would be expected.

As the nose of the GEM rose higher, the relative pressures toward the nose of the GEM dropped off. This is to be expected, as the air could more readily escape. However, with the GEM ballasted to maintain level flight, the pressure dropped off to the rear as the height increased as shown in Figures 56a through 56g. This was caused by the basically bad distribution noted previously and made it necessary to use considerable ballast. Negative pressure peaks may be noted under the jets as the height increases. These negative pressures are caused by the turning outward of the jets which flow parallel to the ground at these points.

The variation of static pitching and rolling stability with increasing center of gravity height is shown in Figures 57 and 58. Unfortunately, the normal center of gravity data were taken by students, while the raised center of gravity data were taken by more experienced personnel. The difference is obvious. All data, however, indicate high stability as would be expected at $h/D$ ratios of 0.020. The difference between the raised center of gravity curves shows a slight decrease with increasing height as would be expected. However, there is no serious decrease in stability, even though the higher center of gravity is quite high for this type of vehicle.

It may be seen that pitching stability is higher with the nose down than nose up. This is certainly caused by the fact that the forward jet has a higher pressure than the rear.

The comparison of dynamic damping and moments of inertia with center of gravity height is presented in Table 3. The moment of inertia increased, of course, when mass was added to raise the center of gravity. Damping in roll decreases from 23.2 per cent of critical to 12.9 per cent when the center of gravity is raised 13.25 inches. This seems reasonable. Damping in pitch, from displacement in the direction of positive angle of attack, decreases from 17.0 per cent of critical to 13.2 per cent when the center of gravity is raised 7.74 inches. However, the damping in pitch increases with increasing center of gravity height when displaced in the direction of positive angle of attack. This does not seem reasonable and is unexplained at this time.

The comparison of height versus propeller speed and horsepower in free air and in the wind tunnel is shown in Figures 53 and 54. There is a height loss of about 16 per cent in the tunnel for the same propeller speed or horsepower. This is quite probably caused by a recirculation of the jet flow due to the pressure of the tunnel side walls.

The lift, drag, and pitching moment coefficients of the GEM are plotted versus forward velocity in Figures 59 through 61 for $^{h}/D$ ratios from 0.014 to 0.084. The same data are replotted in Figures 62 through 64 for constant forward speed versus $^{h}/D$ ratios. It should be noted that these data must not be compared with the two-dimensional data. The two-dimensional model had none of the superstructure of the full scale vehicle.

A detailed analysis of the results is rather difficult. A considerable effect of increasing forward speed is readily apparent; quite possibly due to Reynolds Number effects. There is a general increase in negative lift and pitching moment and a positive drag increase with increasing $^{h}/D$ ratio. There are definite humps in the lift and drag curves at an $^{h}/D$ ratio of 0.070. These may or may not be significant. It is certainly apparent however, that this is a very bad shape for a GEM. The lift coefficient is negative which will require more lifting power. The drag coefficient, approximately 0.250 at the higher speeds and heights, is quite high which will require high propulsion power. The pitching moment coefficient is constantly negative. For this particular GEM, negative pitching moments might be advantageous as this would help counteract the high jet pressures at the front and would keep the nose down. However, as negative angles of attack add thrust, some sort of powerful controls would be necessary to stop the vehicle.

Although only a few drag data points were obtained with the GEM with power at forward speed, those that were obtained show a drag coefficient of about 0.262. These data are presented in Run 16 of Table 2. The low point noted at 35 m.p.h. may be discarded as a bad point as there is no other reason to suspect a low drag in this area. The $^{q}/P_{t}$ ratio at this point

is only about 0.16, which, at the $^{h}/D$ ratio of 0.020, is considerably below the region where the jet might be expected to "blow under" based on the observations of the two-dimensional tests.

It should be noted that the highest $^{q}/P_{t}$ ratio obtainable in the full scale tests was approximately 0.40. This is considerably below the so called "critical point" where the jet begins to blow under the cushion. Again, however, this is based on two-dimensional observations.

The pressure distributions, across the front and rear jets are presented in Figures 65 through 69. There is no evidence of any flow separation in the jet even when there is considerable back pressure with the jet close to the ground. These curves again show high pressure in the front jet relative to the rear.

It is unfortunate that completely free flight tests could not be made because of repeated engine failures. However, free flights, limited by electric cables, were possible. Although the cables did not permit any appreciable forward speed to be attained, if such is possible, the operator could get a qualitative impression of the control system.

The Tinajero GEM has a natural tendency to move to the rear in the control neutral, level attitude. This is due to the rear facing propeller. With the side, or propulsion vanes inclined to the rear about 15 degrees, the GEM would hover over a spot. With the side vanes fully deflected to the rear, the GEM would move slowly forward. Releasing the side vanes halted the forward motion and started motion rearward.

The nose down pitch control had no effect whatever. Full deflection of the nose up pitch control seemed to drop the aft end slightly.

Roll control seemed to tilt the GEM slightly. However, this may actually have been caused by the operators natural tendency to lean in the roll direction desired. A sideslipping

motion accompanied roll.

Yaw control was totally ineffective.

The GEM in free flight was at the mercy of any prevailing breeze or gusts. If flown over a surface that was not level, the GEM tended to slide downhill, just as water seeks the lowest level.

The best available control was kinesthetic control or control by shift of the operator's weight. Using kinesthetic control, roll was quite easy. Pitch changes could be obtained if the operator stood up and leaned far forward or back. Yaw control was not possible by any means. Motion could be obtained in any direction by tilting the GEM in the direction desired.

In summarizing the results of the free flight tests, it may be said that the installed controls were essentially ineffective. There was not enough propulsive power to attain any appreciable forward speed. Based on the behavior of the vehicle at forward speed in the wind tunnel, if any forward speed had been obtained, the GEM would have become directionally uncontrollable.

# BIBLIOGRAPHY


1 Abramson, H. Norman, The Dynamics of Airplanes, The Ronald Press Co., New York, 1958, Chap. 1.

2 Chaplin, Harvey R., Theory of Annular Nozzle in Proximity to the Ground, David Taylor Model Basin Aero Report 923, July 1957.

3 Chaplin, Harvey and Stephenson, Bertrand, Preliminary Study of the Hovering Performance of Annular Jet Vehicles in Proximity to the Ground, David Taylor Model Basin, Aero Report 347, August 1958.

4 Foltz, Claude A., Ground Effect Machine Investigations at the University of Wichita: Final Report Summarizing the Test Program and Data Obtained, Wichita, Kansas, 1961.

5 Loving, Donald L., and Katsoff, S., The Flourescent Oil Film Method and Other Techniques for Boundary-Layer Flow Visualization, NASA MEMO 3-17-59L, 1959.

6 Marks, Lionel S., Mechanical Engineer's Handbook, McGraw-Hill Book Co., Inc., New York, 1951.

TABLE 1

RUN PROGRAM, GEM IN TUNNEL

| Run | q (p.s.f.) | Prop. Speed (r.p.m.) | $h_F$ | $h_R$ | h (in.) | Remarks |
|---|---|---|---|---|---|---|
| 1 | 0 | 333 | 0 | 0 | - | - |
| 1 | 0 | 666 | 0 | 0 | - | 50 lb. added to front |
| 1 | 0 | 1,000 | 0 | 0 | - | 100 lb. added to front |
| 1 | 0 | 1,166 | 0.1 | 0.1 | - | 150 lb. added to front |
| 1 | 0 | 1,333 | 0.3 | 0.3 | - | 150 lb. added to front |
| 1 | 0 | 1,500 | 0.75 | 0.75 | - | 150 lb. added to front |
| 1 | 0 | 1,666 | 1.00 | 1.05 | - | 150 lb. added to front |
| 1 | 0 | 1,833 | 1.65 | 1.75 | - | 200 lb. added to front |
| 1 | 0 | 1,833 | 1.70 | 1.75 | - | 175 lb. added to front |
| 1 | 0 | 1,916 | 2.10 | 2.20 | - | 175 lb. added to front |
| 1 | 0 | 2,000 | 2.50 | 2.60 | - | 175 lb. added to front |
| 2 | 0.58 to 1.60 | 0 | - | - | 2 | - |
| 3 | 0.58 to 7.74 | 0 | - | - | 2 | - |

TABLE 1 (Continued)

| Run | q (p.s.f.) | Prop. Speed (r.p.m.) | $h_F$ | $h_R$ | h (in.) | Remarks |
|---|---|---|---|---|---|---|
| 4 | 0.58 to 7.74 | 0 | - | - | 4 | - |
| 5 | 0.58 to 7.74 | 0 | - | - | 6 | - |
| 6 | 0.58 to 7.74 | 0 | - | - | 8 | - |
| 7 | 0.58 to 7.74 | 0 | - | - | 10 | - |
| 8 | 0.58 to 7.74 | 0 | - | - | 12 | - |
| 9 | 3.13 to 7.74 | 0 | - | - | 12 | Weights added to GEM |
| 10 | 0.58 | 1,916 | - | - | 12 | GEM unstable @ q = 1.60 p.s.f. |
| 11 | 0.58 to 3.13 | 1,916 | - | - | 2 | GEM unstable @ q = 3.13 p.s.f. |
| 12 | 5.18 | 1,916 | - | - | - | Observation only |
| 13 | 5.18 | 1,916 | - | - | - | Lift cables off. Observation only |
| 14 | 0.58 to 5.18 | 0 | - | - | 2 | Simulated cushion |
| 15 | 0.58 | 1,916 | - | - | 2 | Simulated cushion |
| 16 | 0.58 to 5.18 | 1,916 | - | - | - | Lift cables off. Two drag cables. Drag data only |

TABLE 2

WIND TUNNEL TEST DATA

| Run No. | h (in.) | Prop. Speed (r.p.m.) | Velocity (m.p.h.) | $C_L$ | $C_D$ | $C_m$ |
|---|---|---|---|---|---|---|
| 3 | 2 | - | 15 | -.070 | .175 | -.025 |
| | | - | 25 | -.111 | .206 | -.040 |
| | | - | 35 | -.114 | .228 | -.041 |
| | | - | 45 | -.086 | .245 | -.042 |
| | | - | 55 | -.079 | .261 | -.041 |
| 4 | 4 | - | 15 | -.048 | .131 | -.084 |
| | | - | 25 | -.129 | .190 | -.079 |
| | | - | 35 | -.116 | .220 | -.066 |
| | | - | 45 | -.114 | .245 | -.064 |
| | | - | 55 | -.103 | .258 | -.063 |
| 5 | 6 | - | 15 | .080 | .174 | -.061 |
| | | - | 25 | -.036 | .269 | -.078 |
| | | - | 35 | -.086 | .261 | -.080 |
| | | - | 45 | -.105 | .260 | -.073 |
| | | - | 55 | -.122 | .268 | -.073 |
| 6 | 8 | - | 15 | -.174 | .217 | -.063 |
| | | - | 25 | -.253 | .316 | -.091 |
| | | - | 35 | -.229 | .301 | -.090 |
| | | - | 45 | -.192 | .283 | -.084 |
| | | - | 55 | -.184 | .280 | -.081 |
| 7 | 10 | - | 15 | -.048 | .305 | -.084 |
| | | - | 25 | -.129 | .269 | -.087 |
| | | - | 35 | -.149 | .277 | -.091 |
| | | - | 45 | -.168 | .264 | -.086 |
| | | - | 55 | -.177 | .280 | -.083 |
| 8 | 12 | - | 15 | -.158 | .201 | -.080 |
| | | - | 25 | -.191 | .253 | -.093 |
| | | - | 35 | -.189 | .285 | -.093 |
| | | - | 45 | -.187 | .274 | -.090 |
| | | - | 55 | -.193 | .280 | -.085 |

TABLE 2 (Continued)

| Run No. | h (in.) | Prop. Speed (r.p.m.) | Velocity (m.p.h.) | $C_L$ | $C_D$ | $C_m$ |
|---|---|---|---|---|---|---|
| 9 | 2 | 0 | 35 | -.189 | .285 | -.068 |
| | | 0 | 45 | -.202 | .284 | -.069 |
| | | 0 | 55 | -.193 | .280 | -.065 |
| 10 | 12 | 1,916 | 0 | - | - | - |
| | | 1,916 | 15 | 7.134 | .742 | .069 |
| 11 | 2 | 1,916 | 0 | - | - | - |
| | | 1,916 | 15 | 22.660 | .131 | -.047 |
| | | 1,916 | 25 | 7.935 | .411 | -.103 |
| 14 | 2 | - | 15 | .153 | .209 | -.039 |
| | | - | 25 | -.049 | .215 | .001 |
| | | - | 35 | -.062 | .266 | -.001 |
| | | - | 45 | -.074 | .260 | 0 |
| | | - | 55 | -.079 | .251 | 0 |
| 16 | - | 1,916 | 15 | - | .263 | - |
| | | 1,916 | 35 | - | .098 | - |
| | | 1,916 | 45 | - | .264 | - |
| | | 1,916 | 55 | - | .261 | - |

TABLE 3

DAMPING COEFFICIENTS AND MOMENTS OF INERTIA IN PITCH AND ROLL FOR DIFFERENT CENTER OF GRAVITY POSITIONS

| C. G. Position | Configuration | $n/\omega$ (Percent) | Moment of Inertia at Centroidal Axis (slug ft.$^2$) |
|---|---|---|---|
| Original | Roll | 23.2 | 165.5615 |
| | Positive Pitch | 17.0 | 497.6855 |
| | Negative Pitch | 18.5 | 497.6855 |
| Raised 7.74 in. | Roll | 17.9 | 188.5930 |
| | Positive Pitch | 20.1 | 551.4835 |
| | Negative Pitch | 13.2 | 551.4835 |
| Raised 13.25 in. | Roll | 12.9 | 213.6830 |
| | Positive Pitch | 22.5 | 565.3133 |
| | Negative Pitch | * | 565.3133 |

* Data not reliable due to small negative angle attainable.

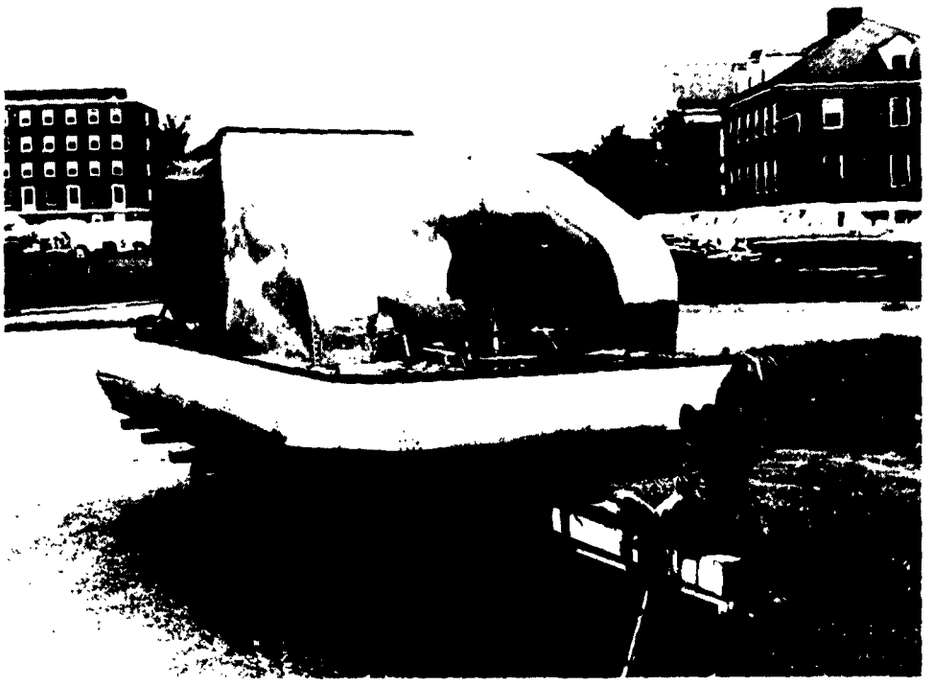

Figure 1. Front view of Tinajero GEM.

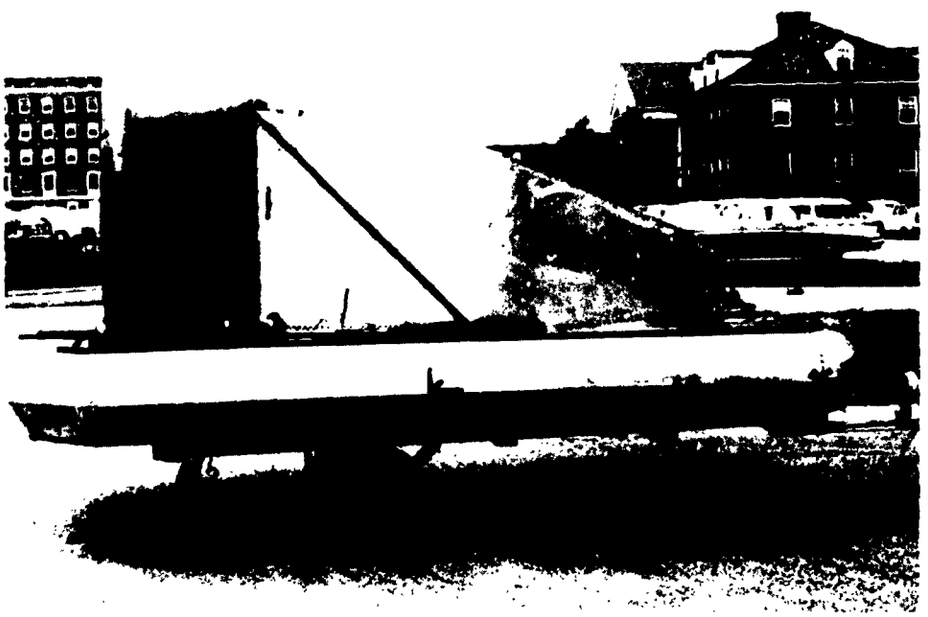

Figure 2. Side view of Tinajero GEM.

Figure 3. Rear view of Tinajero GEM.

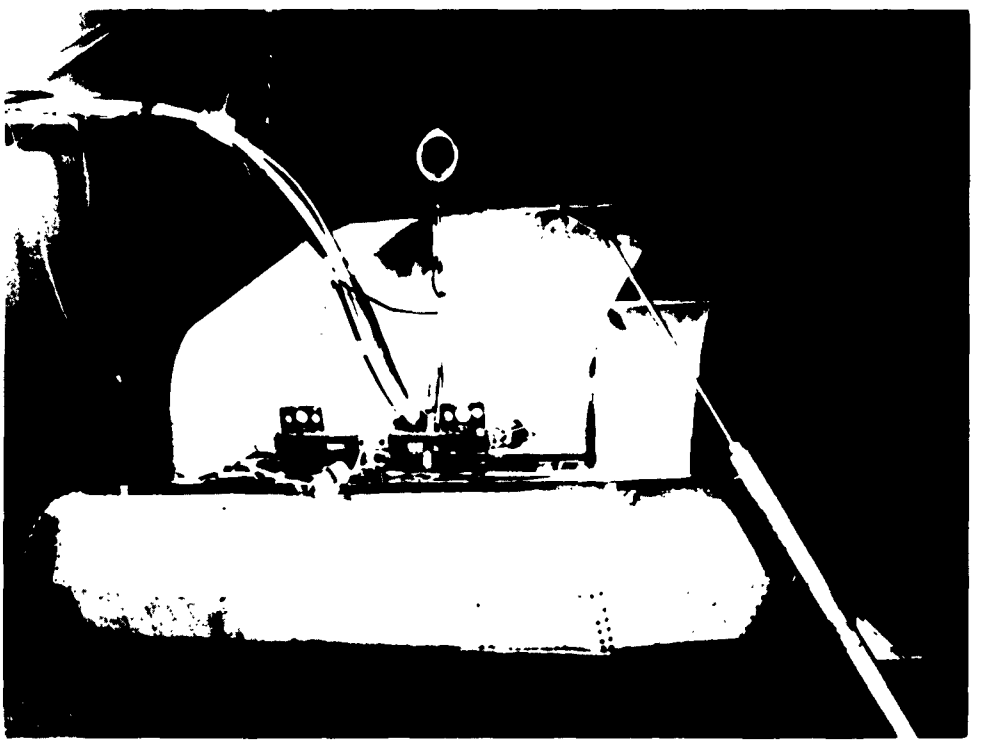

Figure 4. Tinajero GEM mounted in wind tunnel.

Figure 5. Side view of two-dimensional model with symmetrical nose.

Figure 6. Bottom view of two-dimensional model with symmetrical nose.

Figure 7. Nose pieces for two-dimensional model.

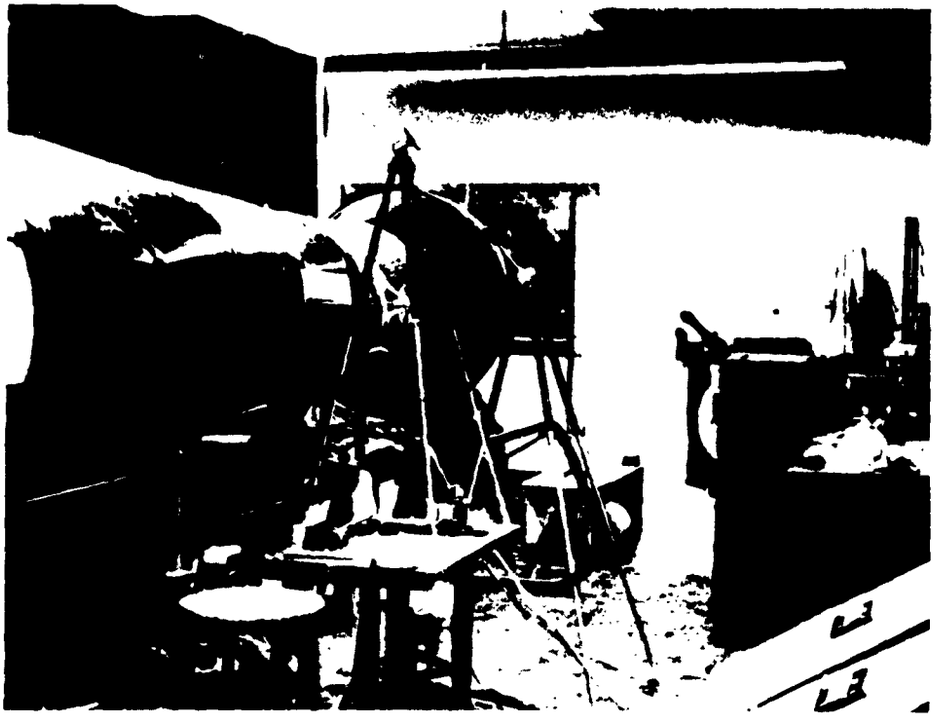

Figure 8. The 24 Inch Low Speed Student Wind Tunnel.

Figure 9. Two-dimensional model mounted in wind tunnel.

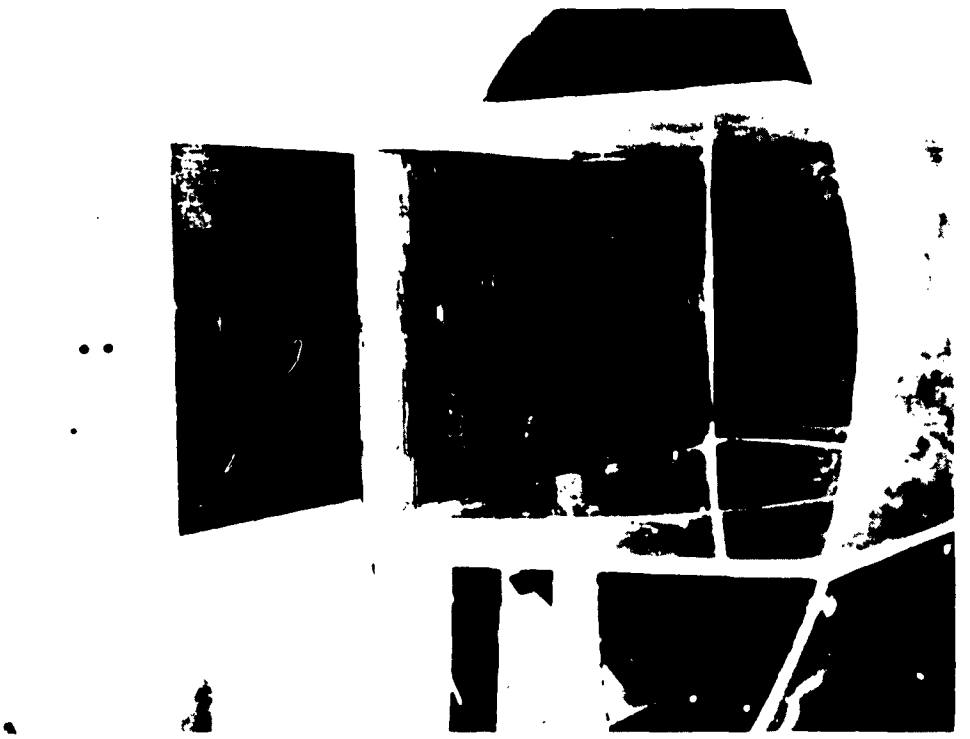

Figure 10. Rear view of two-dimensional model mounted in wind tunnel.

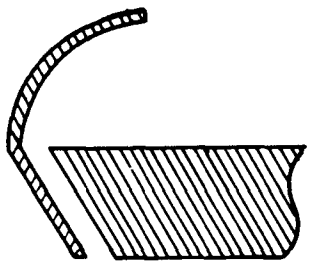

TINAJERO GEM

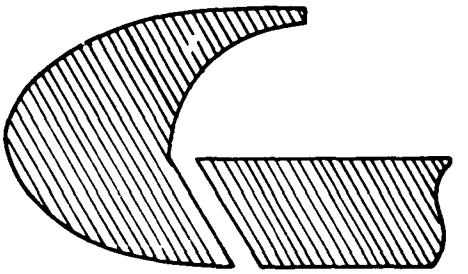

SYMMETRICAL CURVATURE

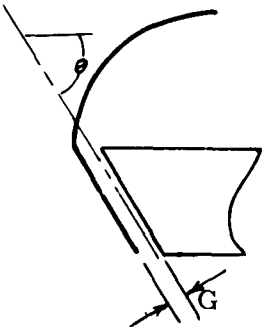


INTERIOR CONFIGURATION

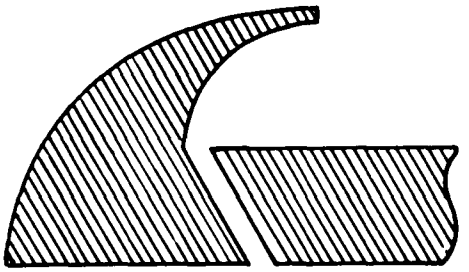

UPPER CURVATURE

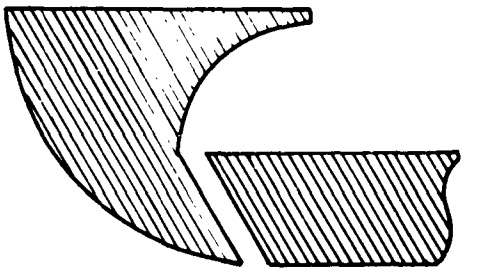

LOWER CURVATURE

Figure 11 . Nose Profiles and jet configuration of 1/10 Scale, two-dimensional, GEM models.

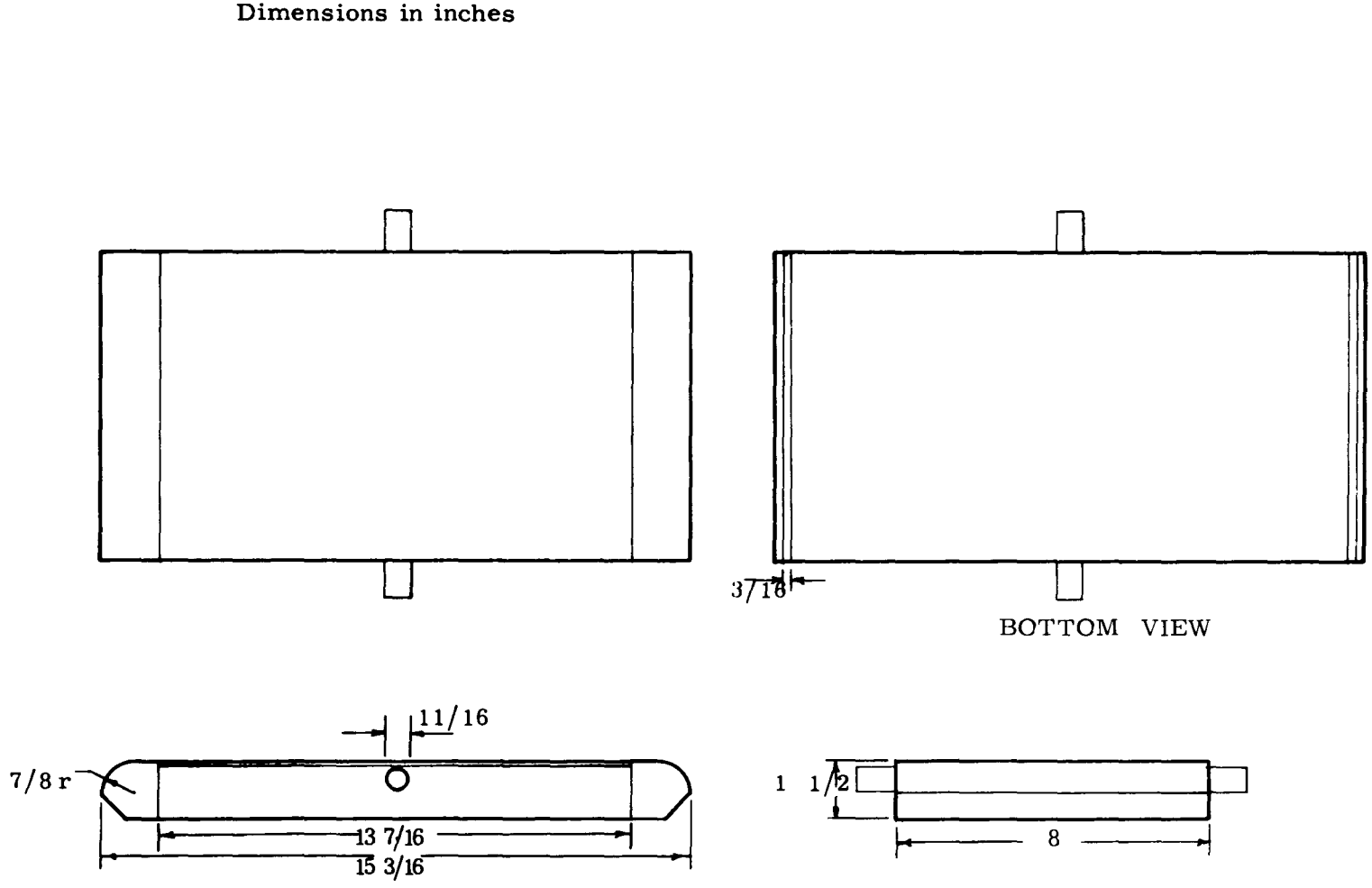


Figure 12 . Outline of 1/10 scale, two-dimensional GEM model

KEY

① FORWARD PLENUM TOTAL PRESSURE TUBE

② DIFFUSION SCREEN

③ PLENUM CHAMBER AIR DELIVERY TUBE

④ INTERIOR WALL OF JET

⑤ EXTERIOR SKIN OF MODEL

⑥ NOSE OF MODEL

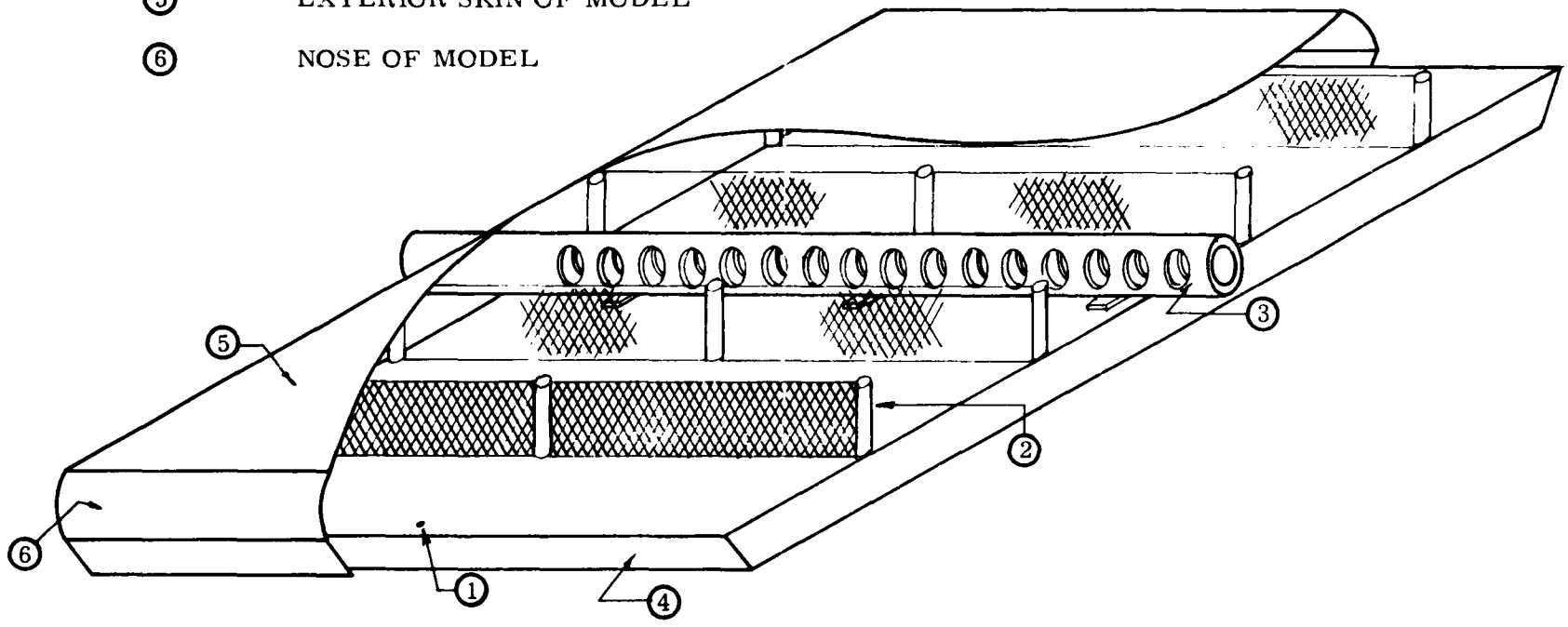


Figure 13 . Cut away view of 1/10 scale, two-dimensional model of the Tinajero GEM.

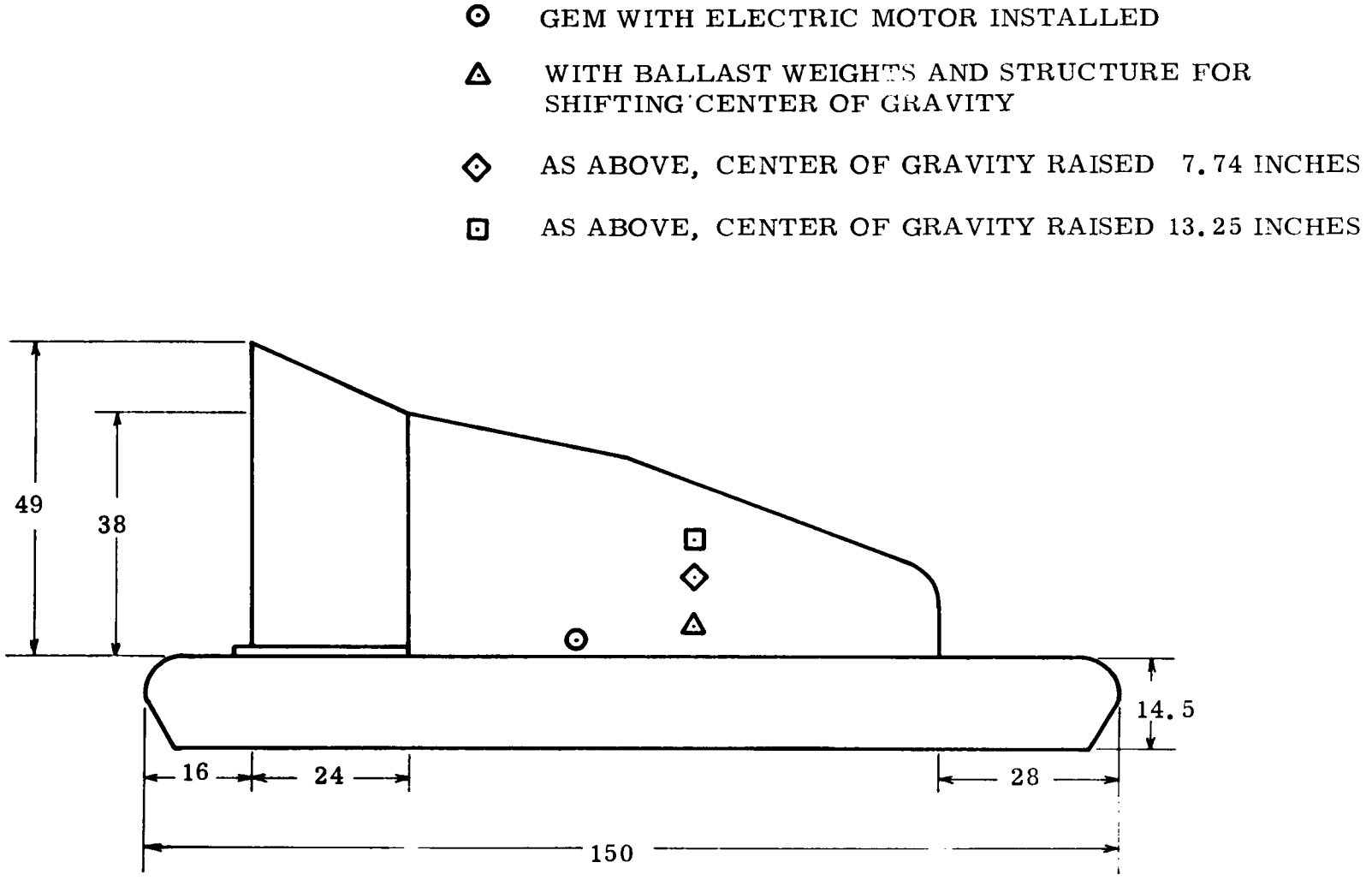


**Figure 14a.** Center of gravity locations and dimensions of Tinajero GEM. Dimensions in inches.

PERIPHERAL JET AND STABILITY SLOTS

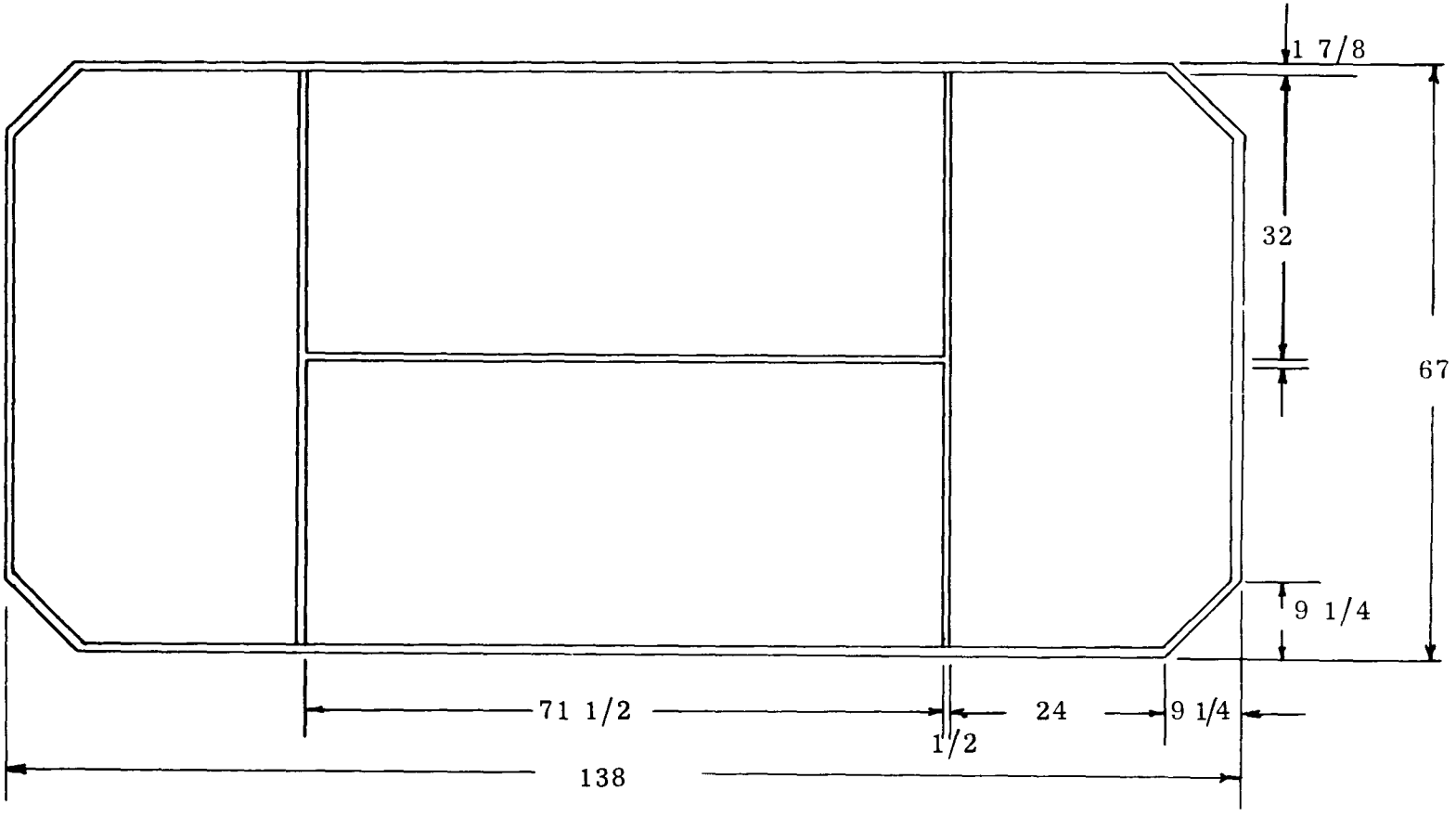


Figure 14b . Center of gravity locations and dimensions of Tinajero GEM . Dimensions in inches.

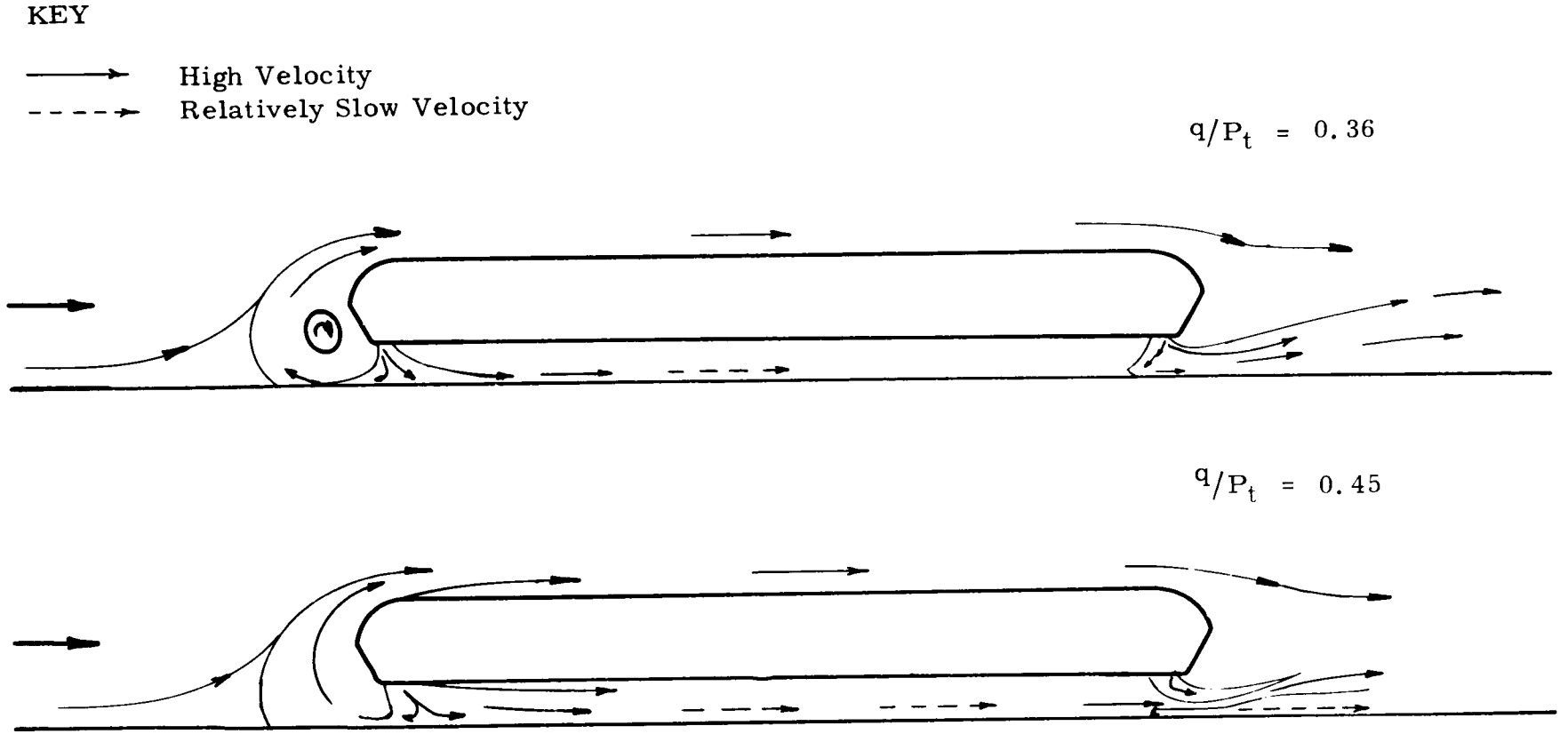


Figure 15a . Observed flow patterns about two-dimensional model, Tinajero nose, $h/D$ = .050, $\alpha$ = 0°.

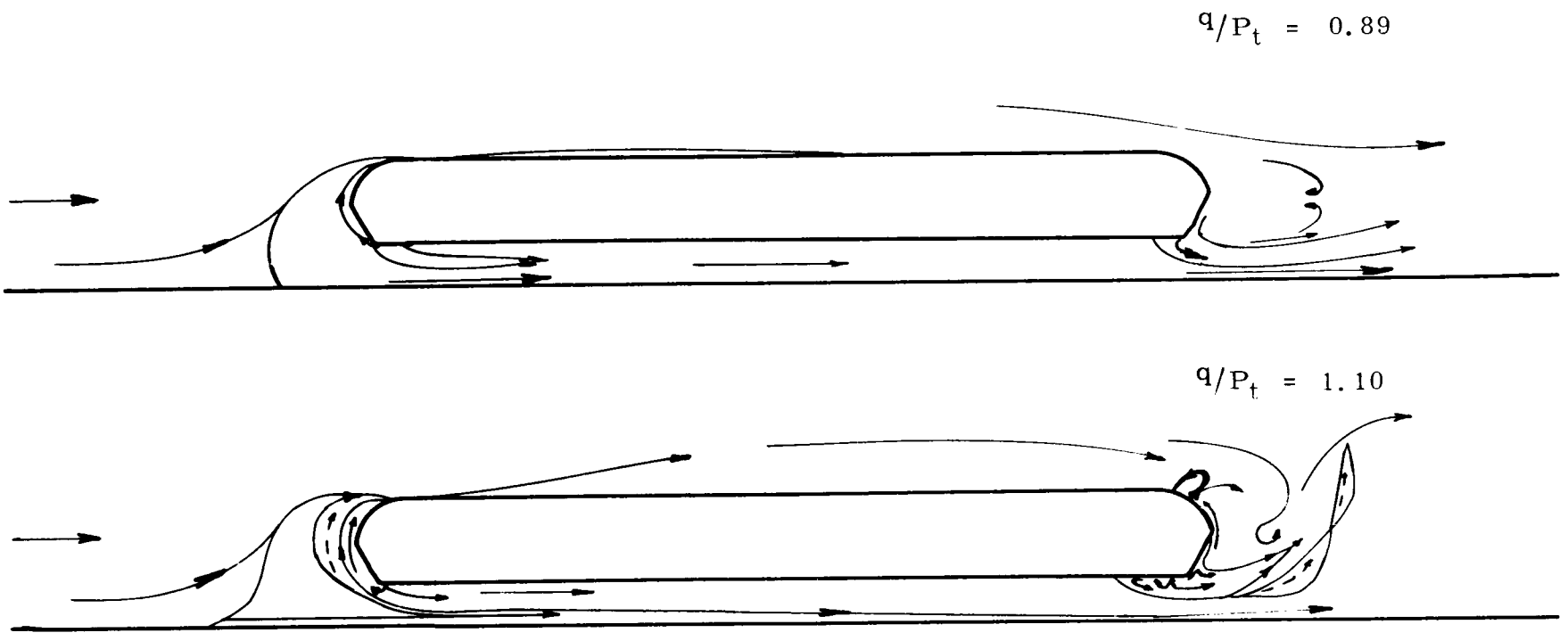


Figure 15b . Observed flow patterns about two-dimensional model, Tinajero nose, h/D = .050, $\alpha$ = 0°.

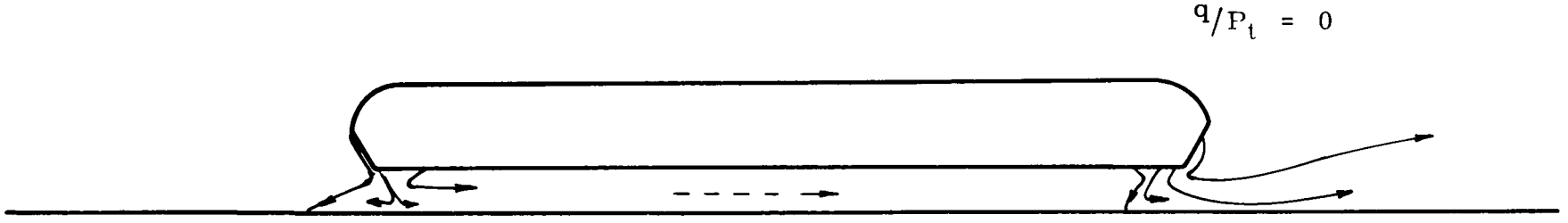


Figure 15c. Observed flow pattern about two-dimensional model, Tinajero nose, $h/D = .050$, $\alpha = 0°$.

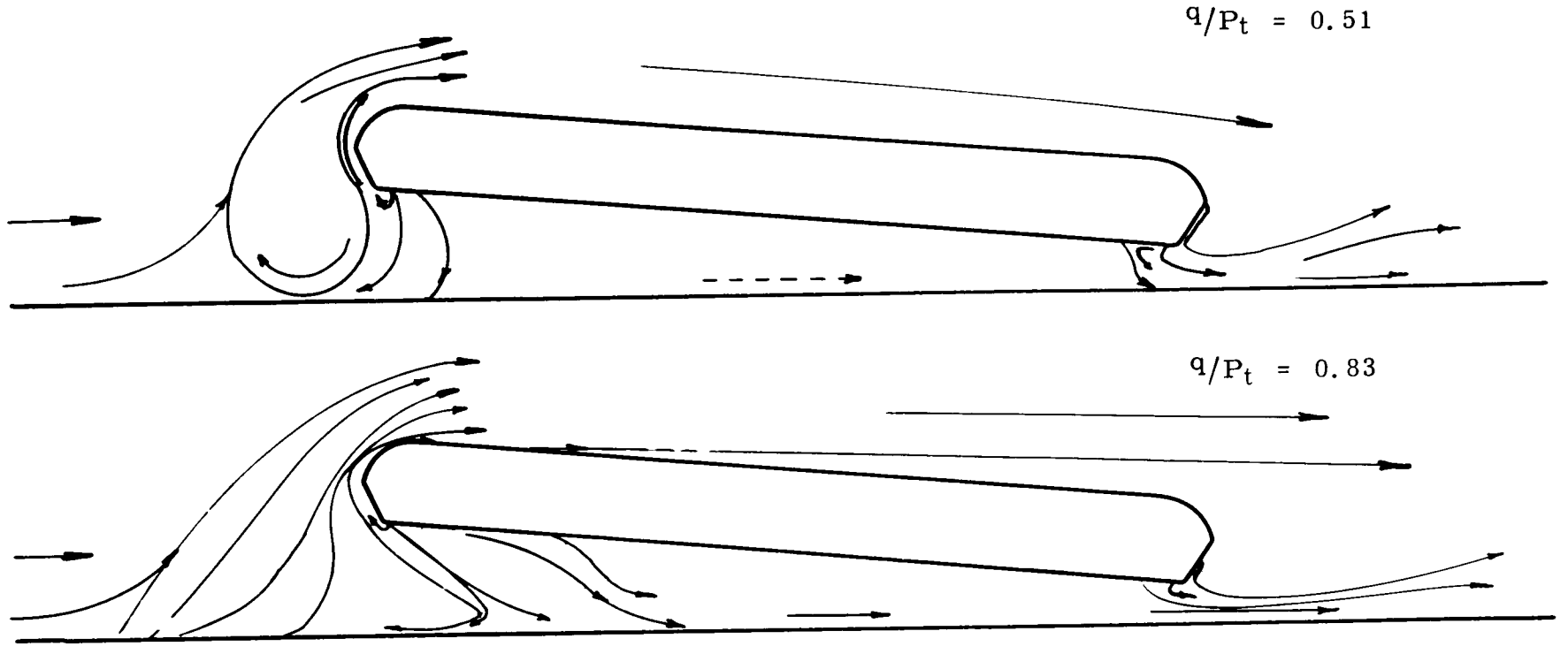


Figure 16a . Observed flow patterns about two-dimensional model, Tinajero nose, $h/D$ = .100, $\alpha$ = 5.0°.

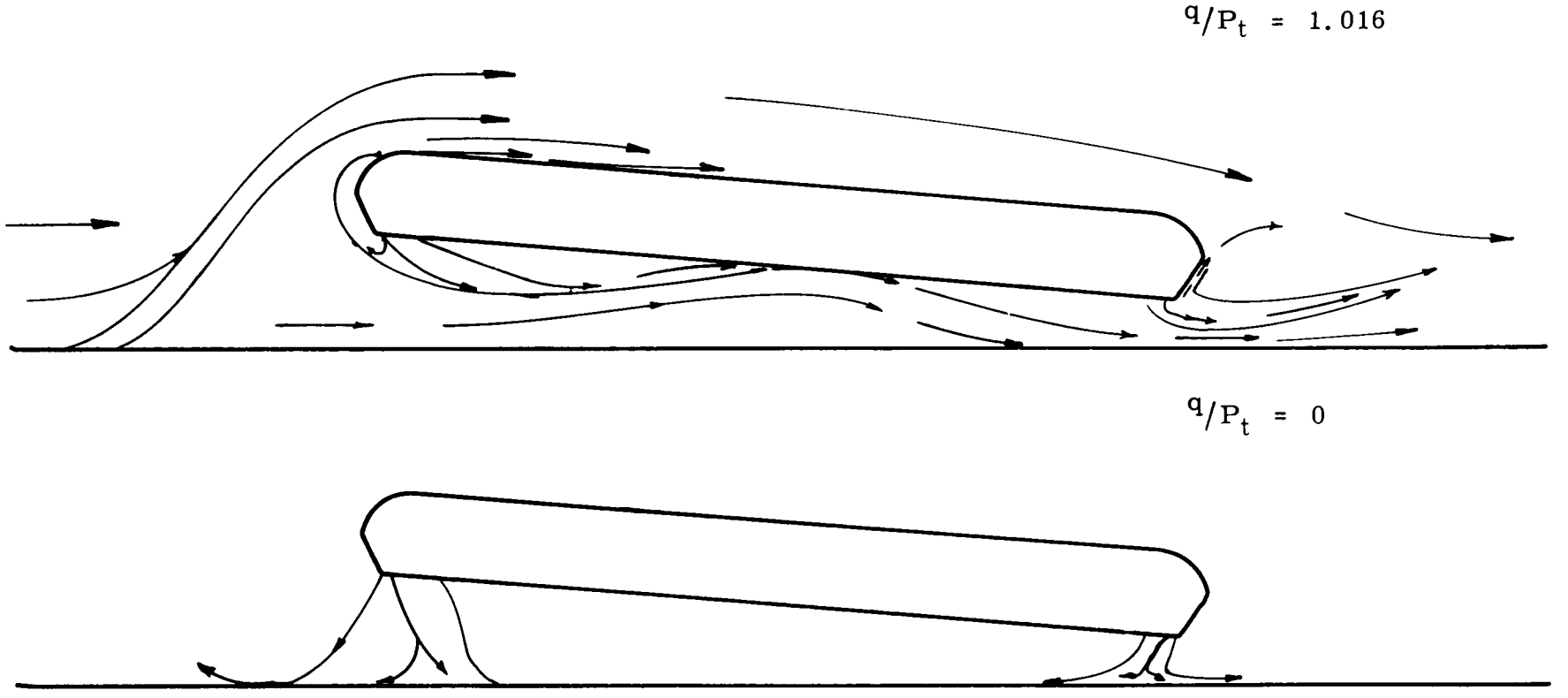


Figure 16b . Observed flow patterns about two-dimensional model, Tinajero nose, $h/D$ = .100, $\alpha$ = 5.0°.

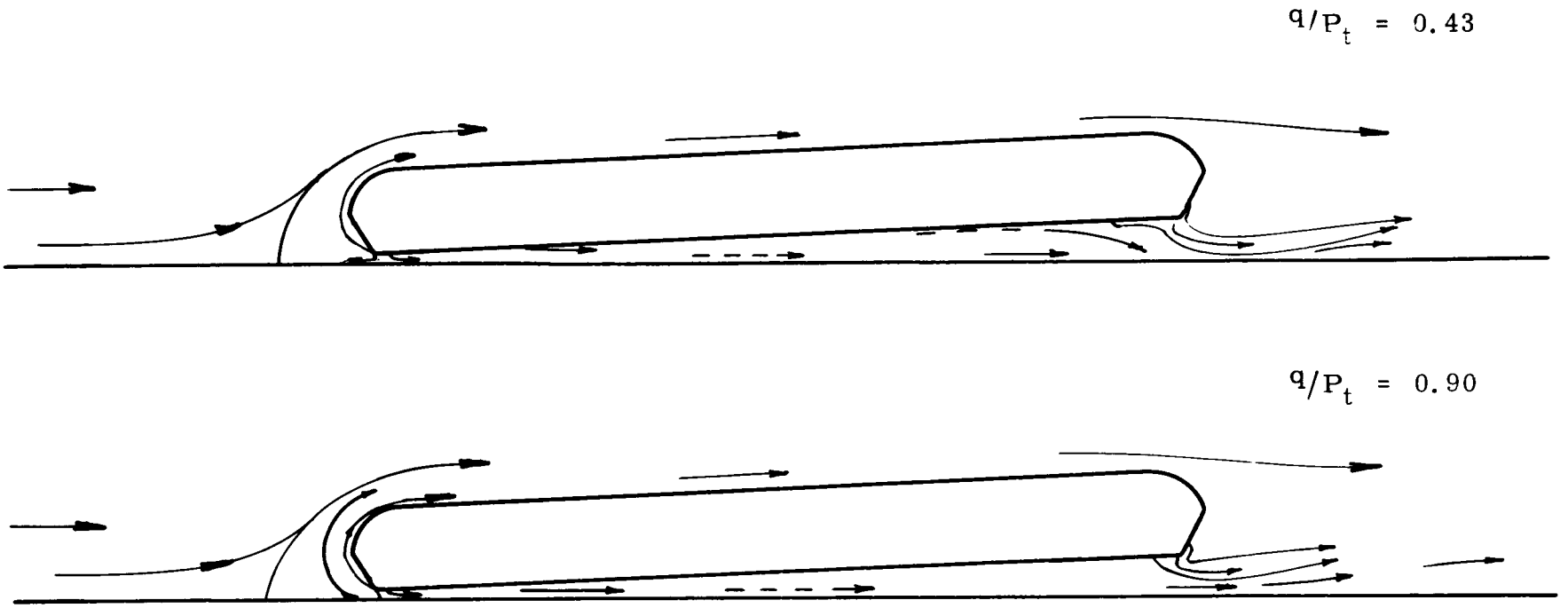


Figure 17a . Observed flow patterns about two-dimensional model, Tinajero nose, $h/D$ = .035, $\alpha$ = - 2.03°.

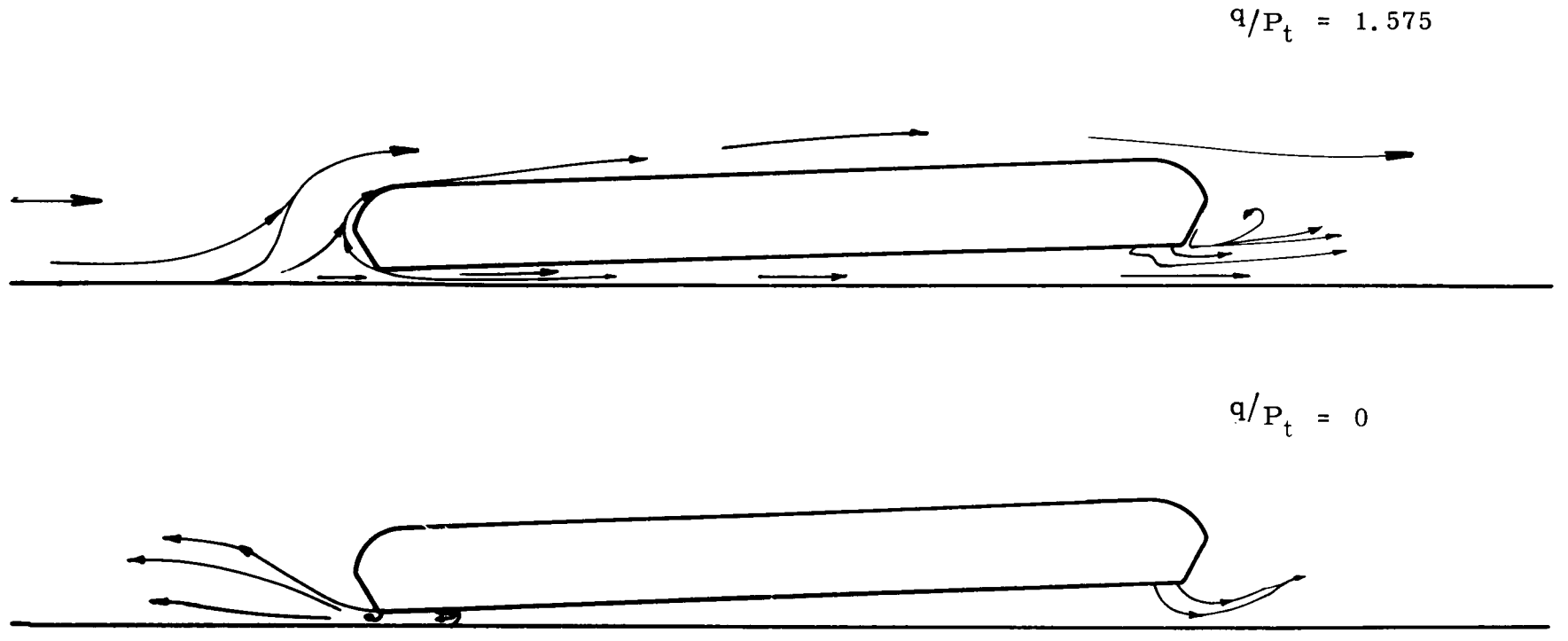


Figure 17b . Observed flow patterns about two-dimensional model, Tinajero nose, $h/D$ = .035, $\alpha$ = - 2.03°.

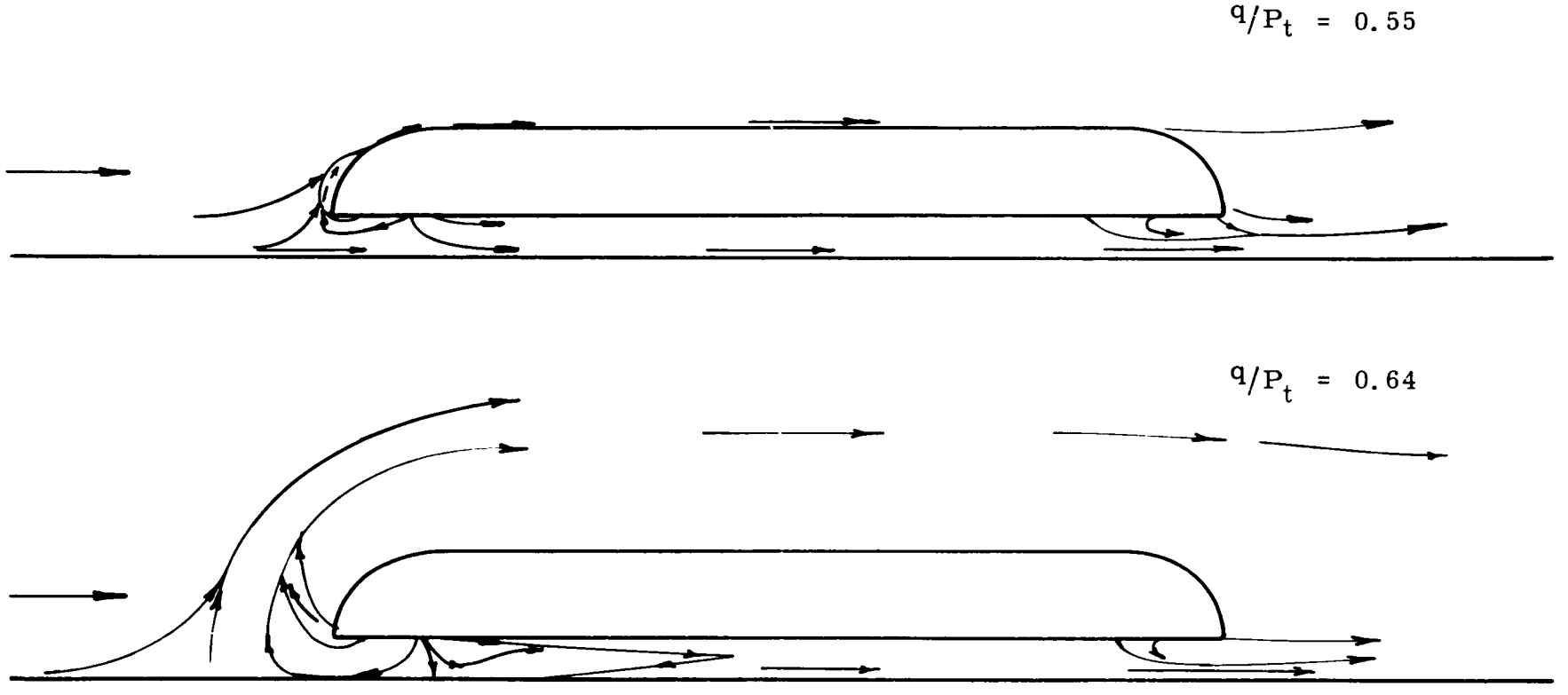


Figure 18a . Observed flow patterns about two-dimensional model, upper curv. nose, $h/D$ = .050, $\alpha$ = 0°.

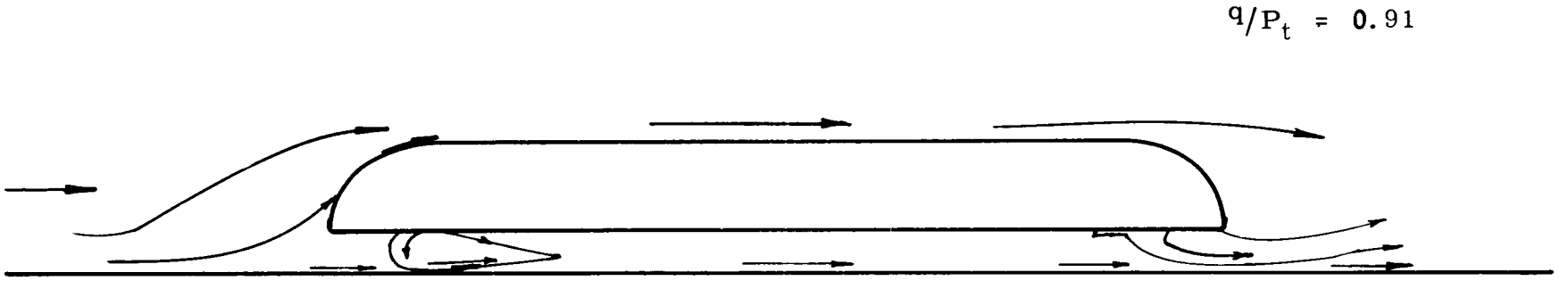


Figure 18b . Observed flow pattern about two-dimensional model, upper curv. nose, $h/D$ = .050, $\alpha$ = 0°.

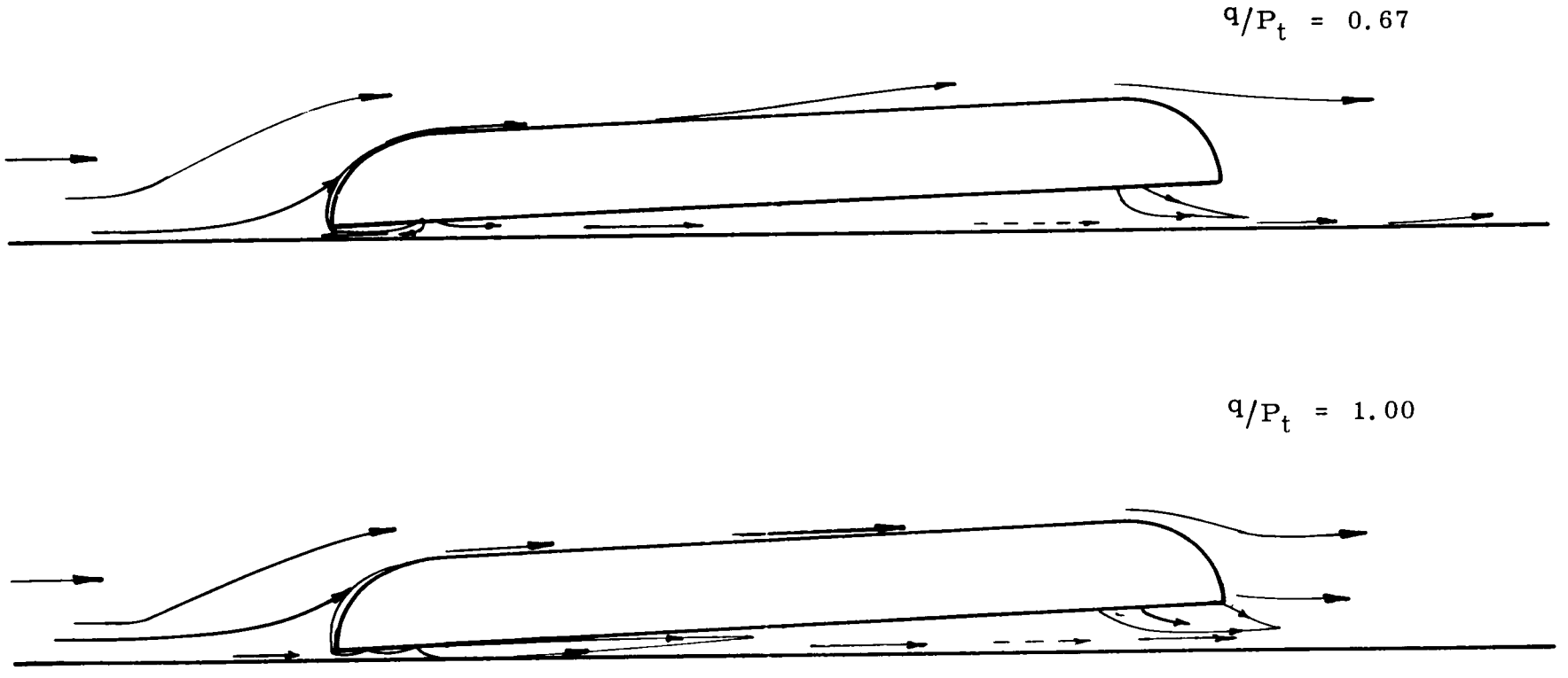


Figure 19 . Observed flow patterns about two-dimensional model, upper curv. nose, $h/D$ = .035, $\alpha$ = - 2.03°.

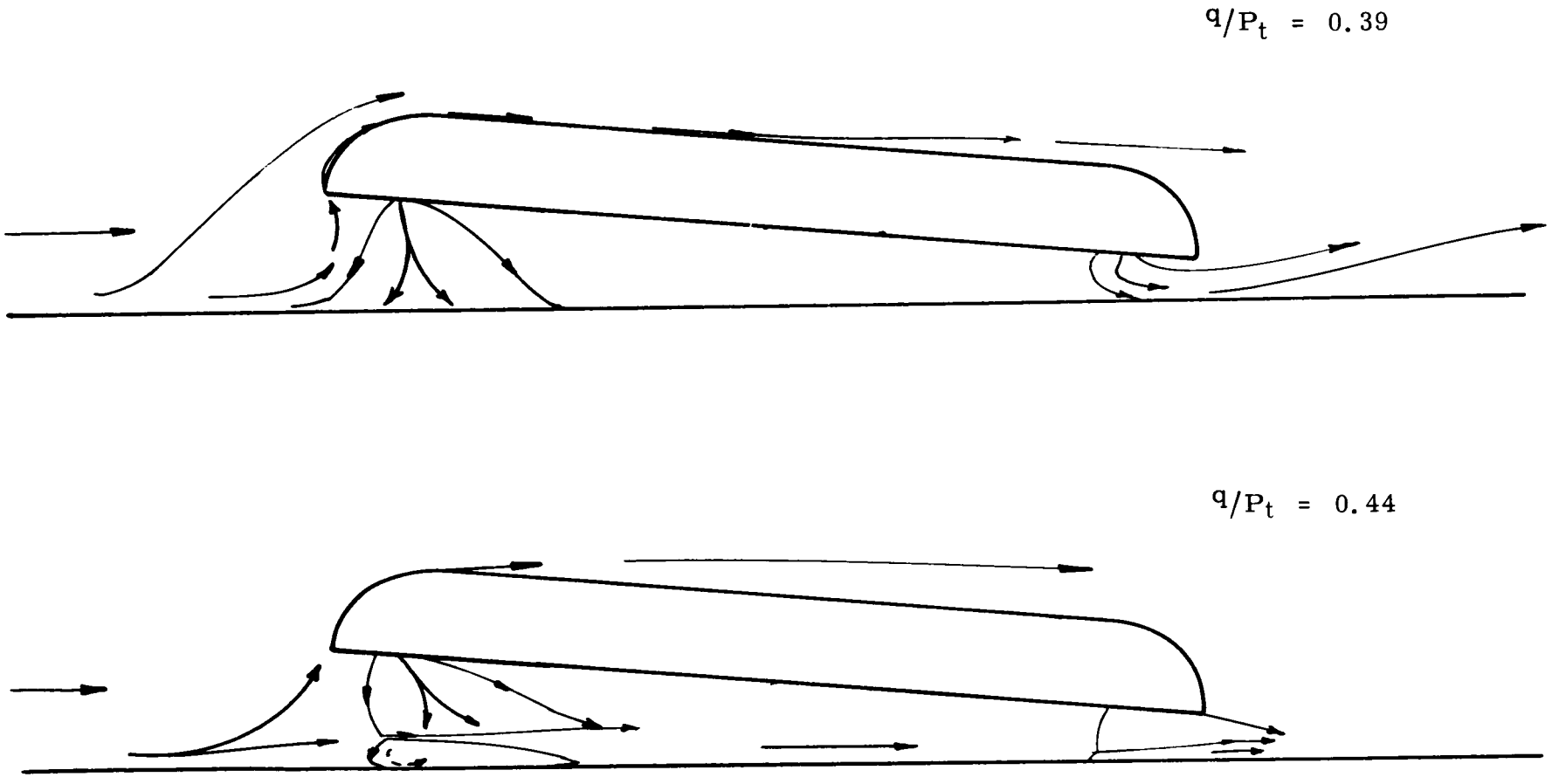


Figure 20 . Observed flow patterns about two-dimensional model, upper curv. nose, $h/D$ = .100, $\alpha$ = 5.0°.

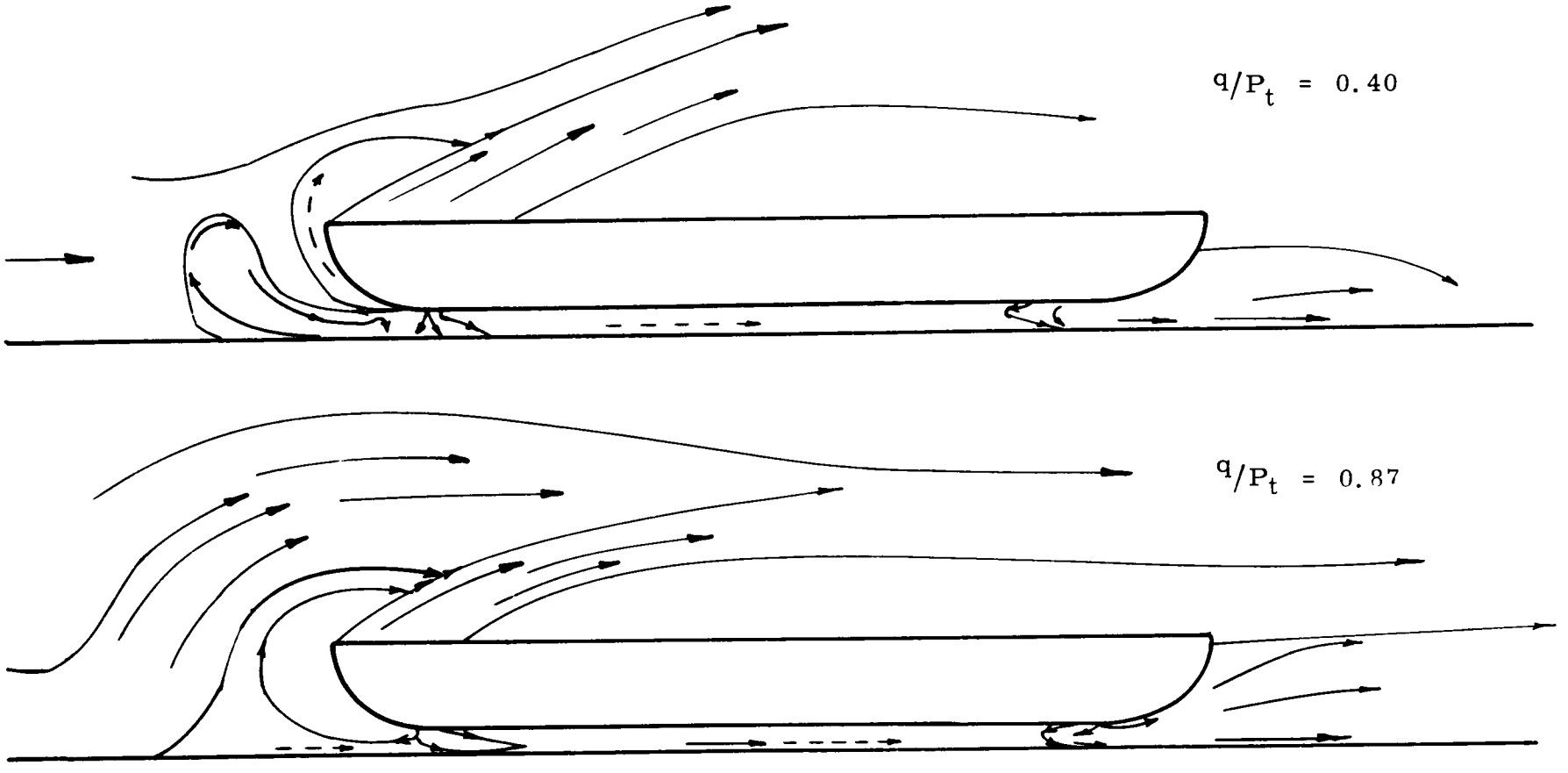


Figure 21a . Observed flow patterns about two-dimensional model, lower curv. nose, $h/D$ = .035, $\alpha$ = 0°.

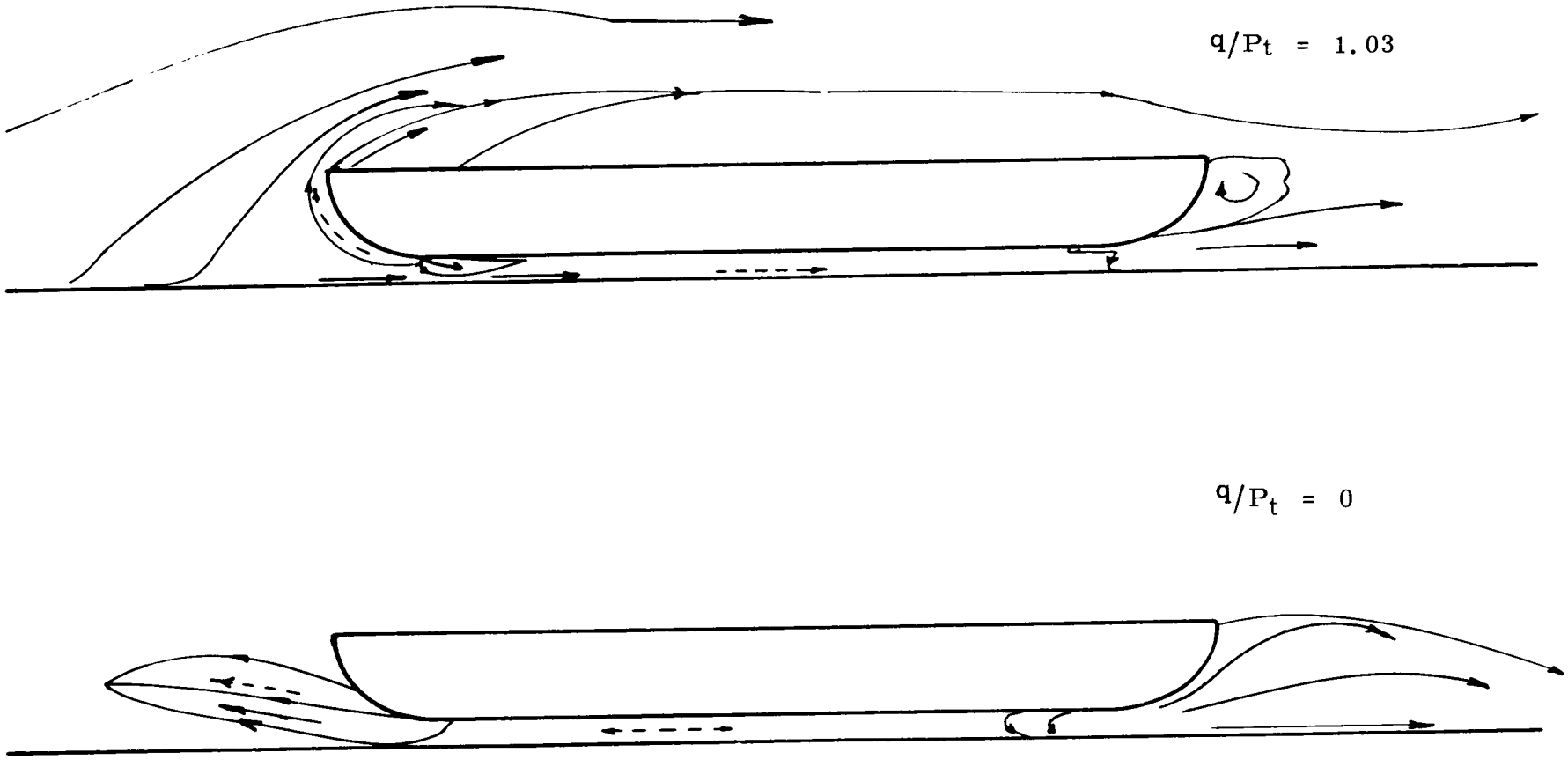


Figure 21b . Observed flow patterns about two-dimensional model, lower curv. nose, $h/D$ = .035, $\alpha$ = 0°.

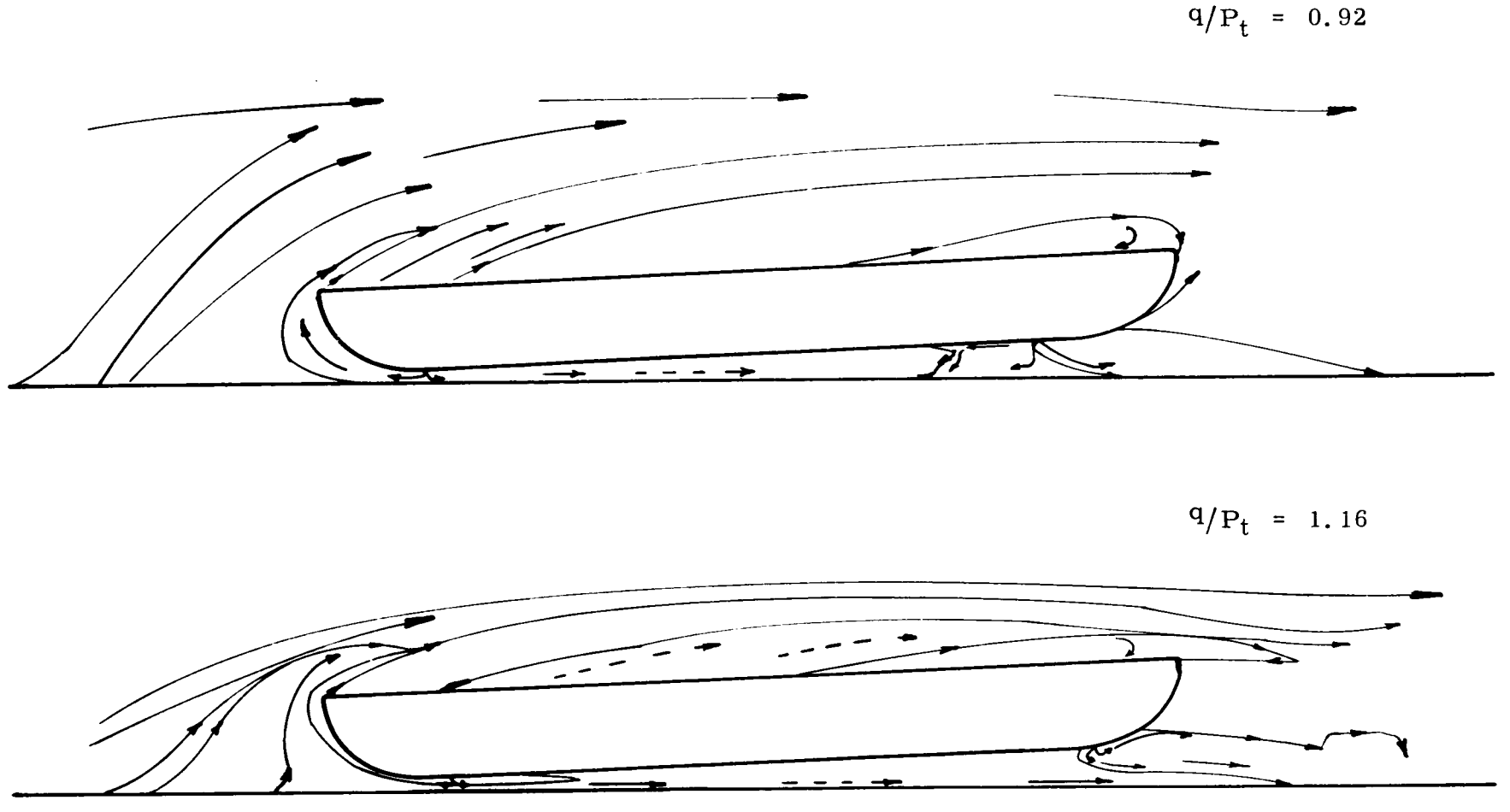


Figure 22 . Observed flow patterns about two-dimensional model, lower curv. nose, $h/D$ = .035, $\alpha$ = - 2.03°.

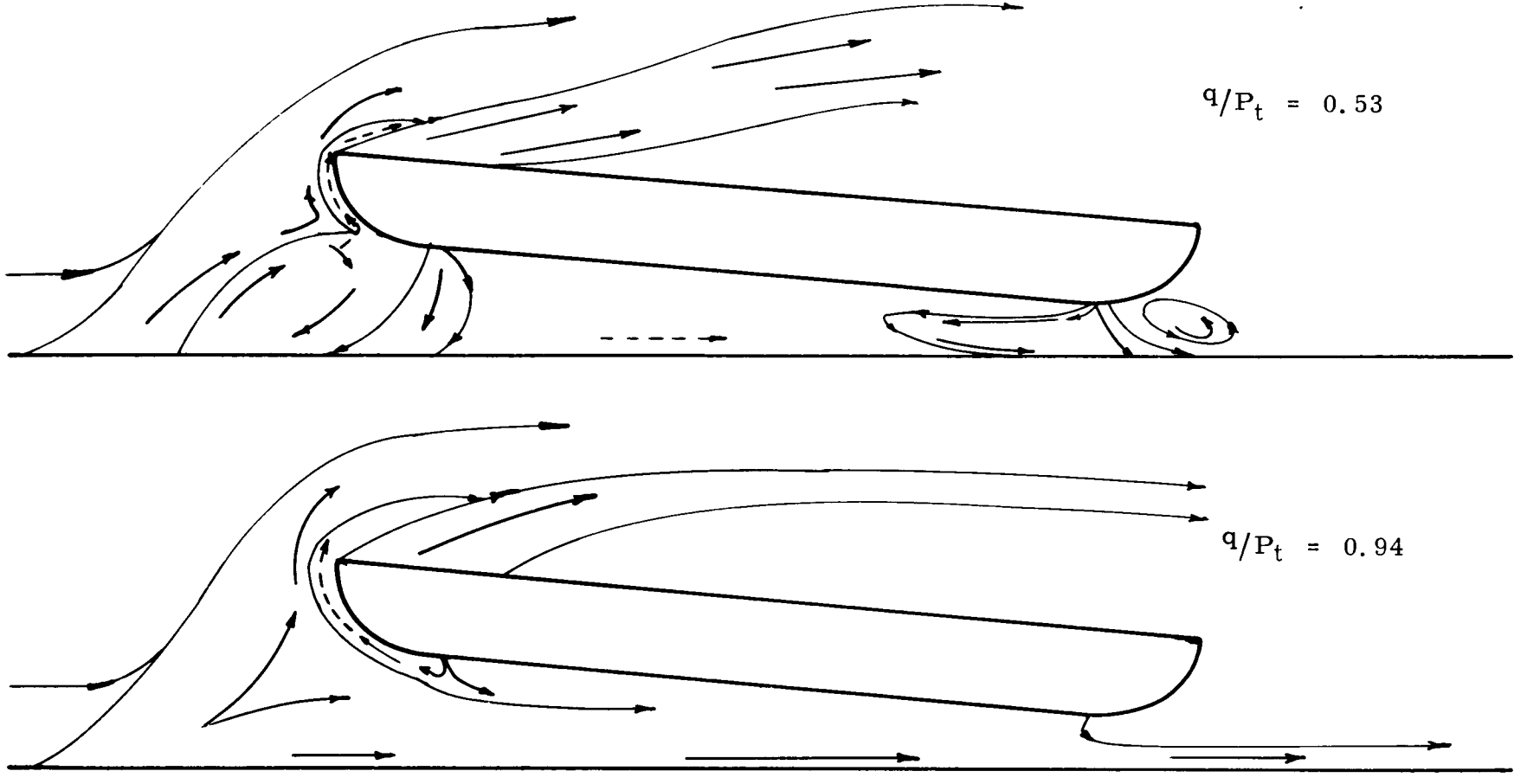


Figure 23 . Observed flow patterns about two-dimensional model, lower curv. nose, $h/D$ = .100, $\alpha$ = 5.0°.

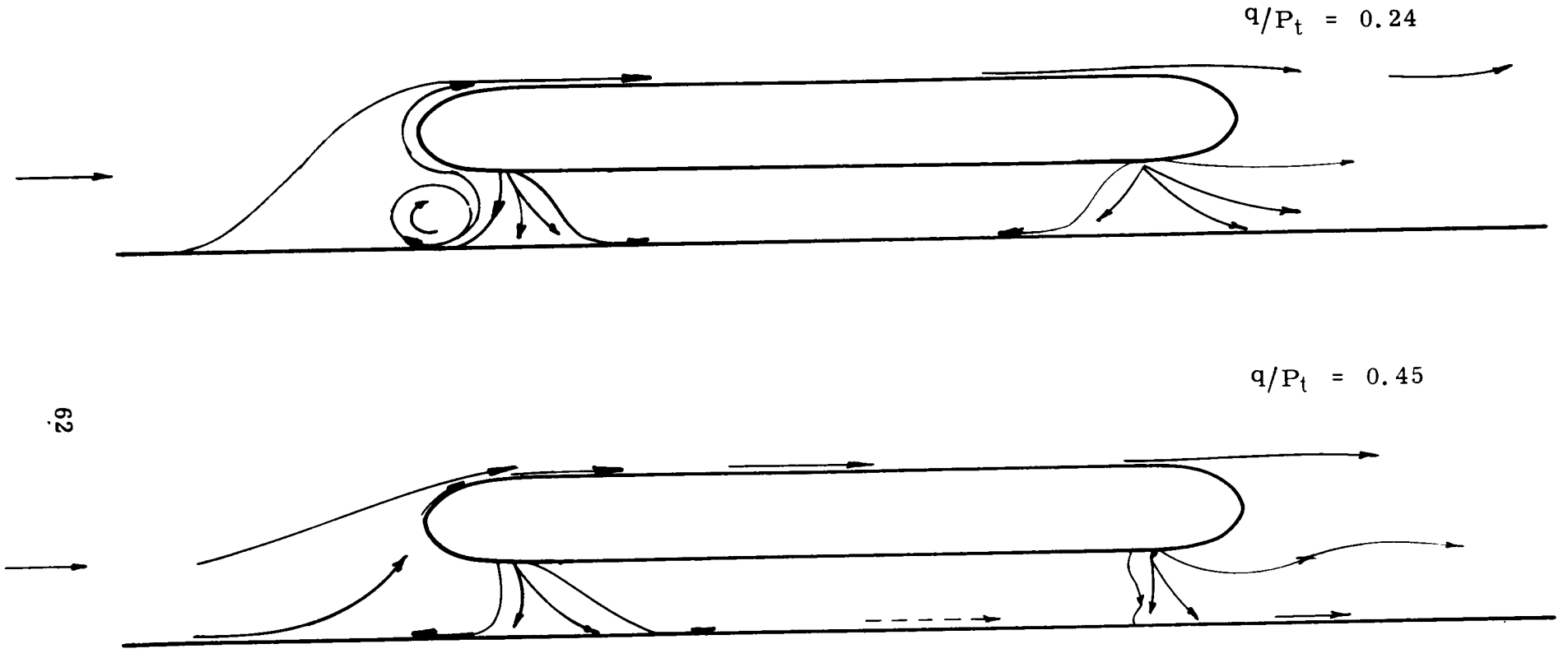




Figure 24a . Observed flow patterns about two-dimensional model, symm. curv. nose $h/D$ = .100, $\alpha$ = 0°.

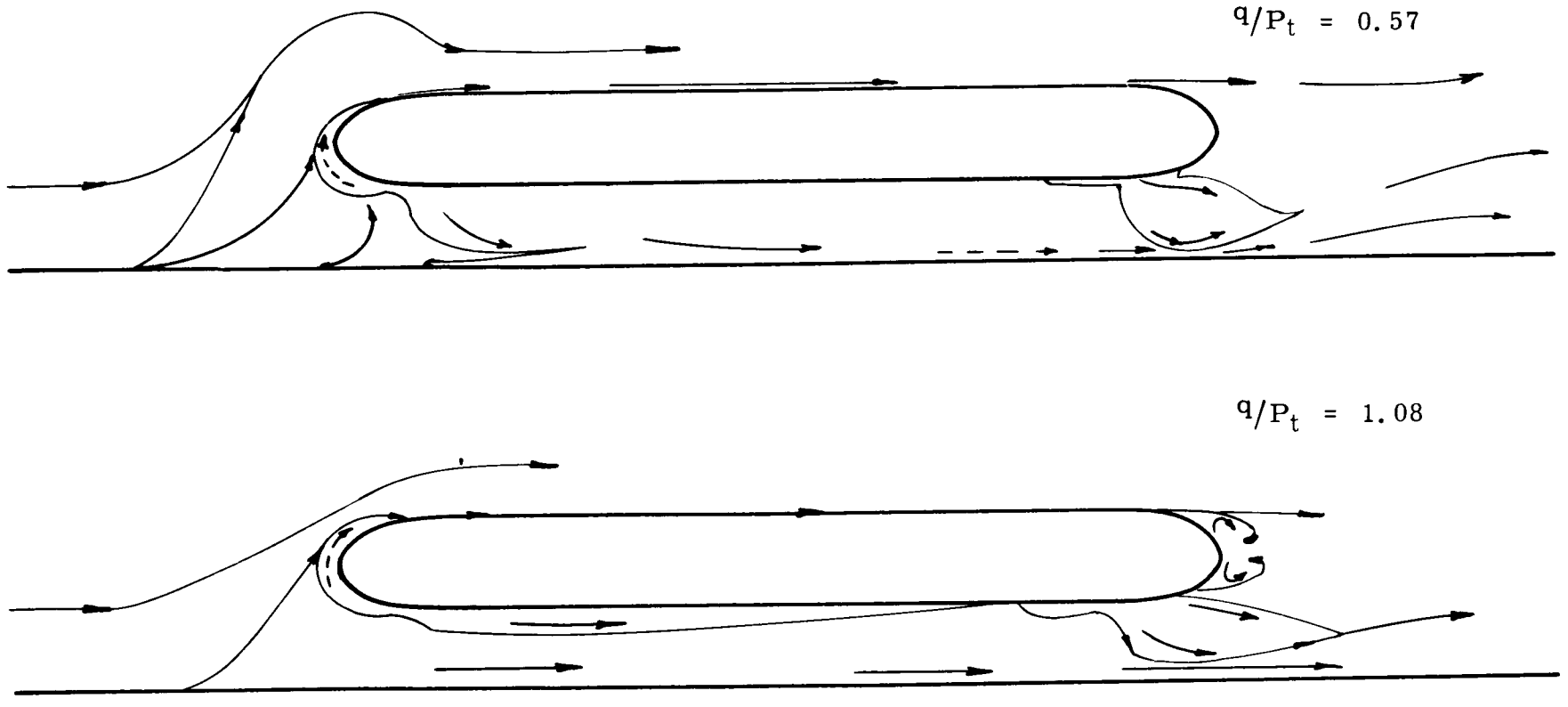


Figure 24b . Observed flow patterns about two-dimensional model, symm. model nose, $h/D$ = .100, $\alpha$ = 0°.

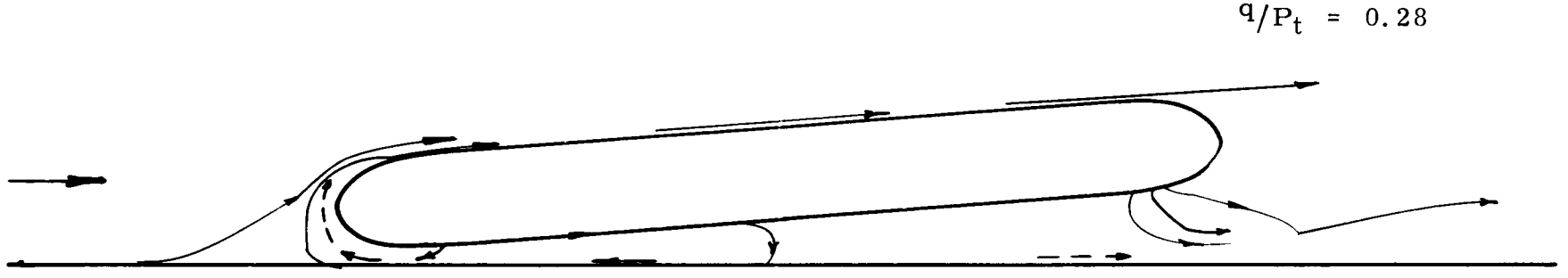


Figure 25 . Observed flow pattern about two-dimensional model, symm. model nose, $h/D$ = .050, $\alpha$ = - 5.0°.

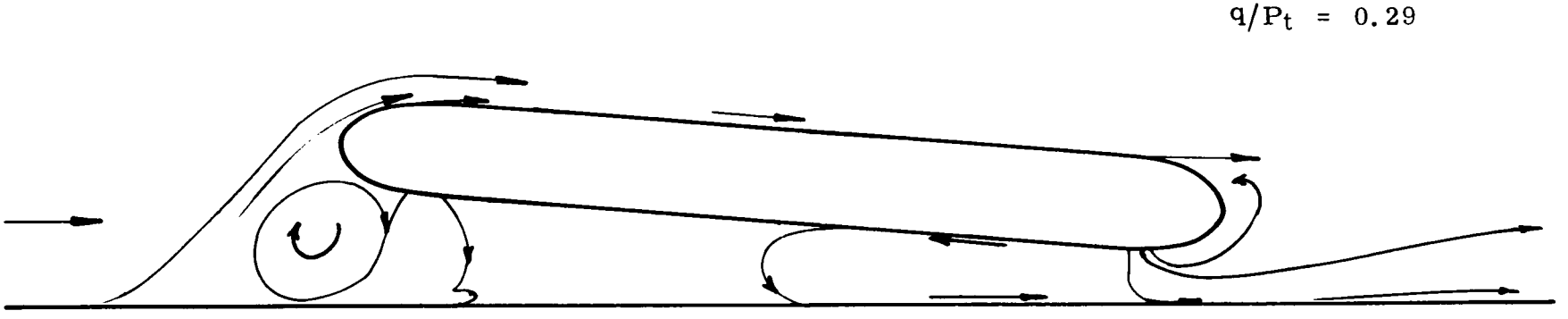


Figure 26 . Observed flow pattern about two-dimensional model, symm. curv. model, $h/D$ = .100, $\alpha$ = 5.0°.

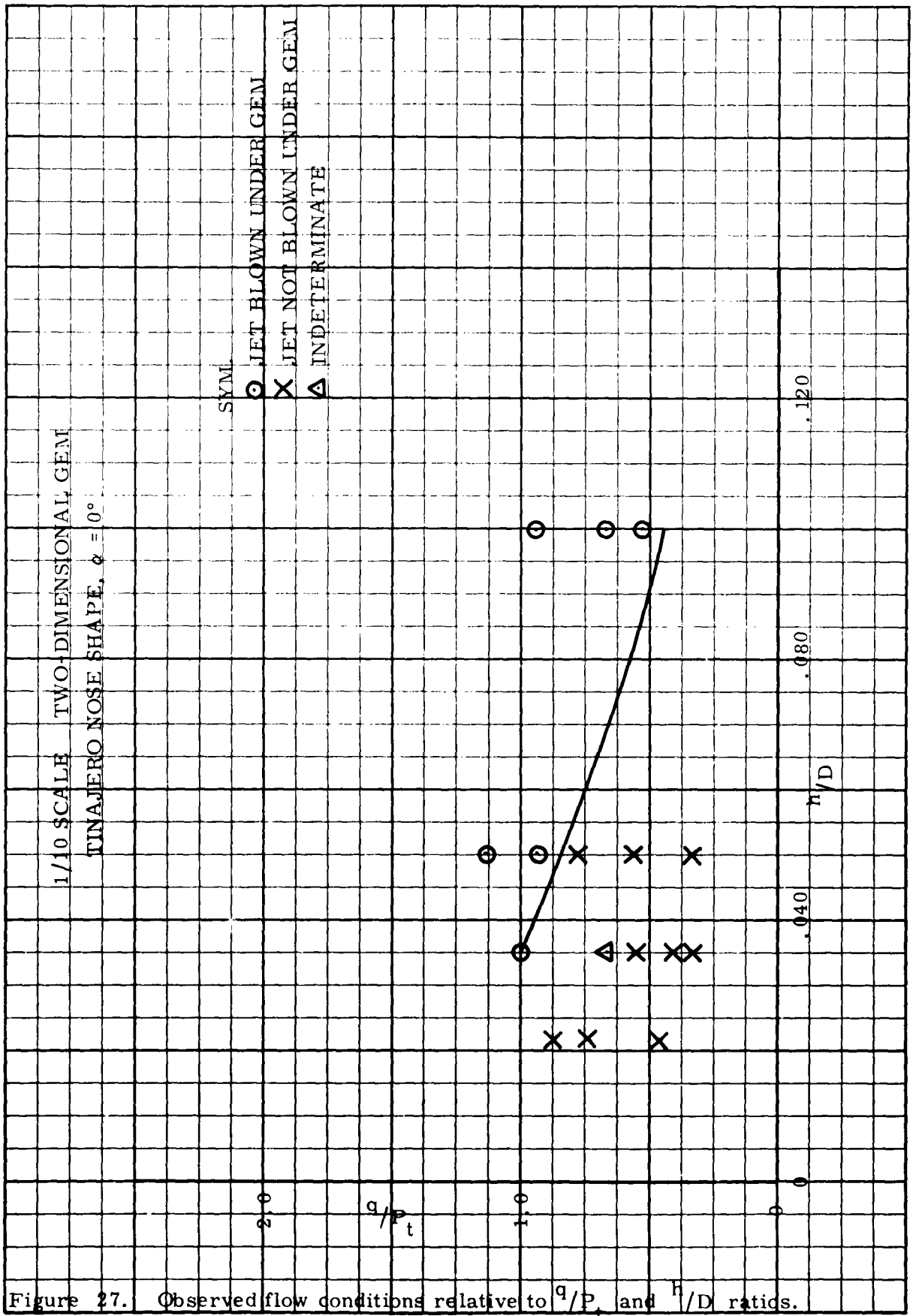


Figure 27. Observed flow conditions relative to $q/P_t$ and $h/D$ ratios.

Figure 28 . Observed flow conditions relative to $^{q}/P_{t}$ and $^{h}/D$ ratios.

Figure 29. Observed flow conditions relative to $q/P_t$ and $h/D$ ratios.

Figure 30. Observed flow conditions relative to $q/P_t$ and $h/D$ ratios.

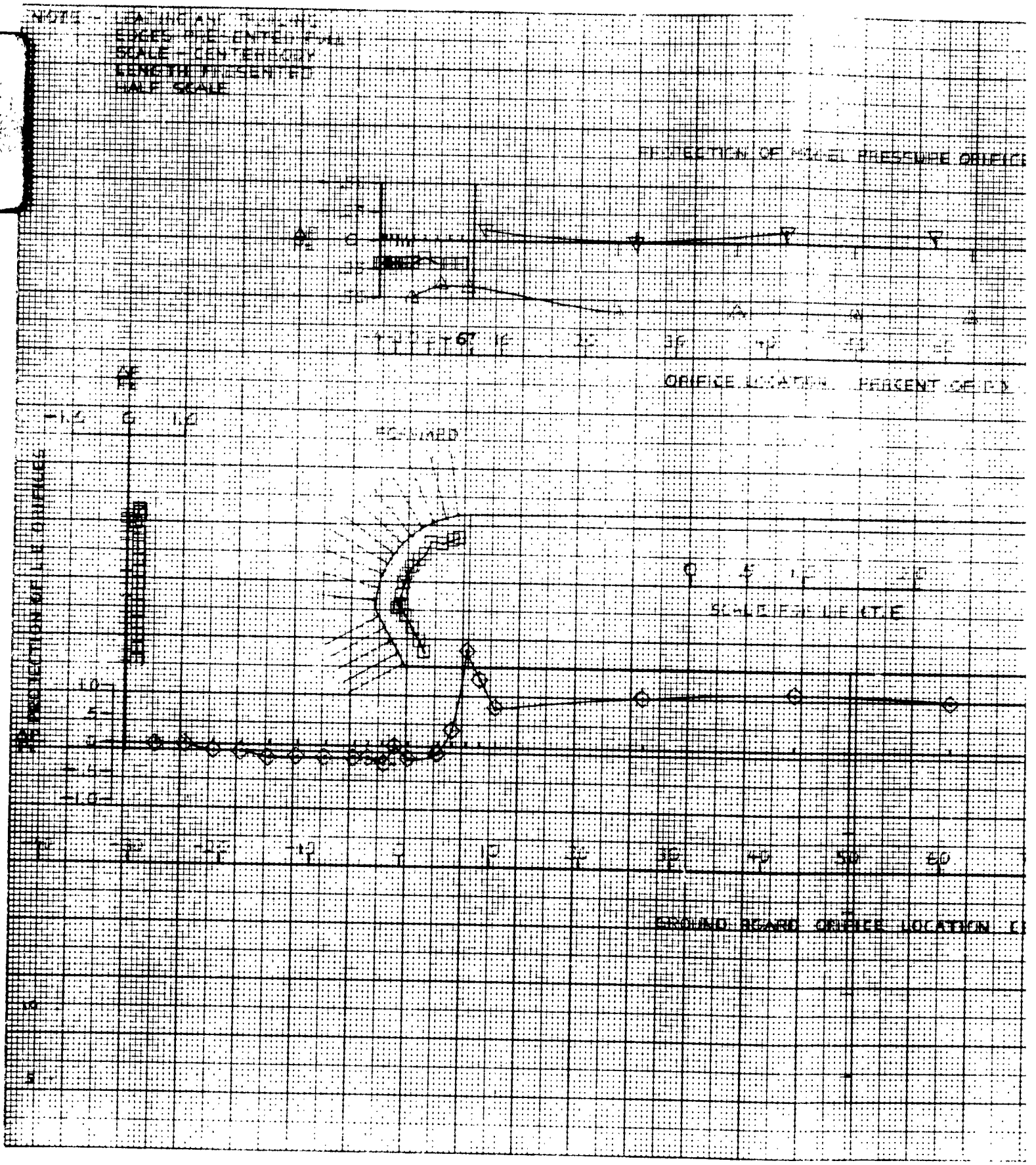

NOTE - LOADING AND TRIPLING
EDGES PRESENTED FULL
SCALE - CENTERBODY
LENGTH PRESENTED
HALF SCALE
PROTECTION OF NOSEL PRESSURE ORIFICE
ORIFICE LOCATION PERCENT OF D.D.
FORWARD
SCALE FOR L.E. (T.E.
PROTECTION OF L.E. ORIFICES
GROUND BOARD ORIFICE LOCATION

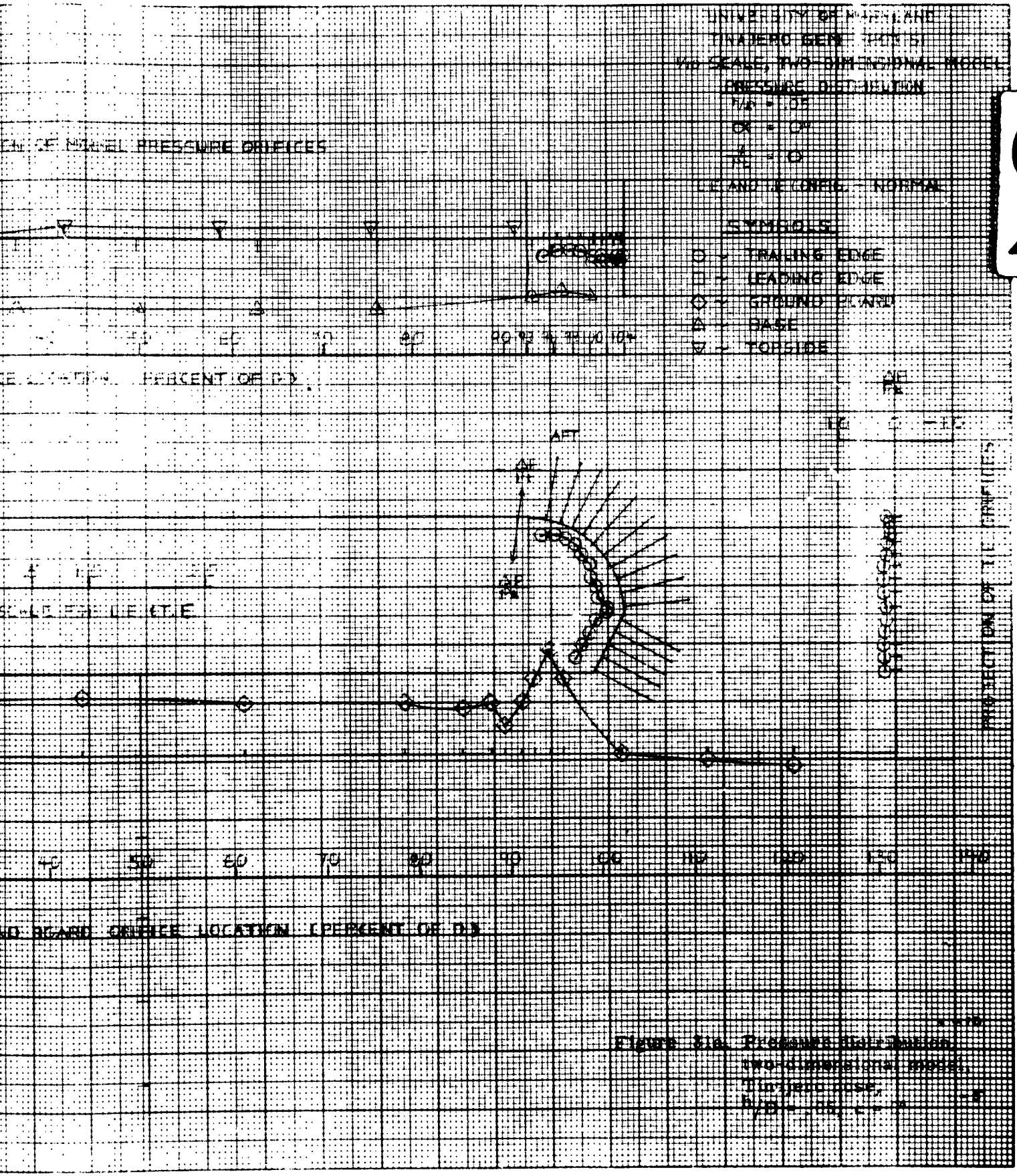


Figure 31a. Pressure distribution, two-dimensional model, Tinajero nose, h/D = .05, c = 0°

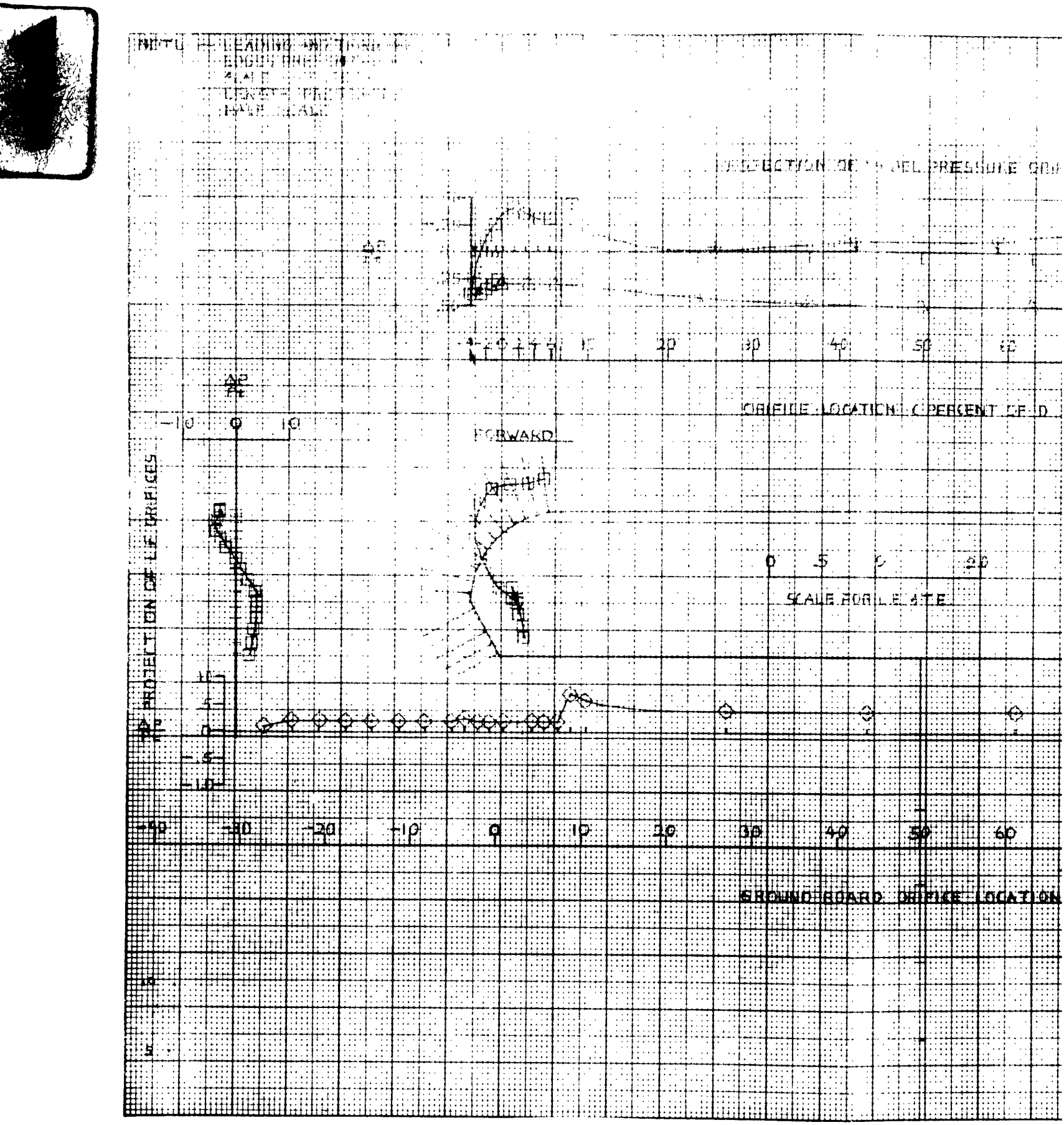
FORWARD
ORIFICE LOCATION (PERCENT OF D
SCALE FOR L.E. & T.E.
GROUND BOARD ORIFICE LOCATION

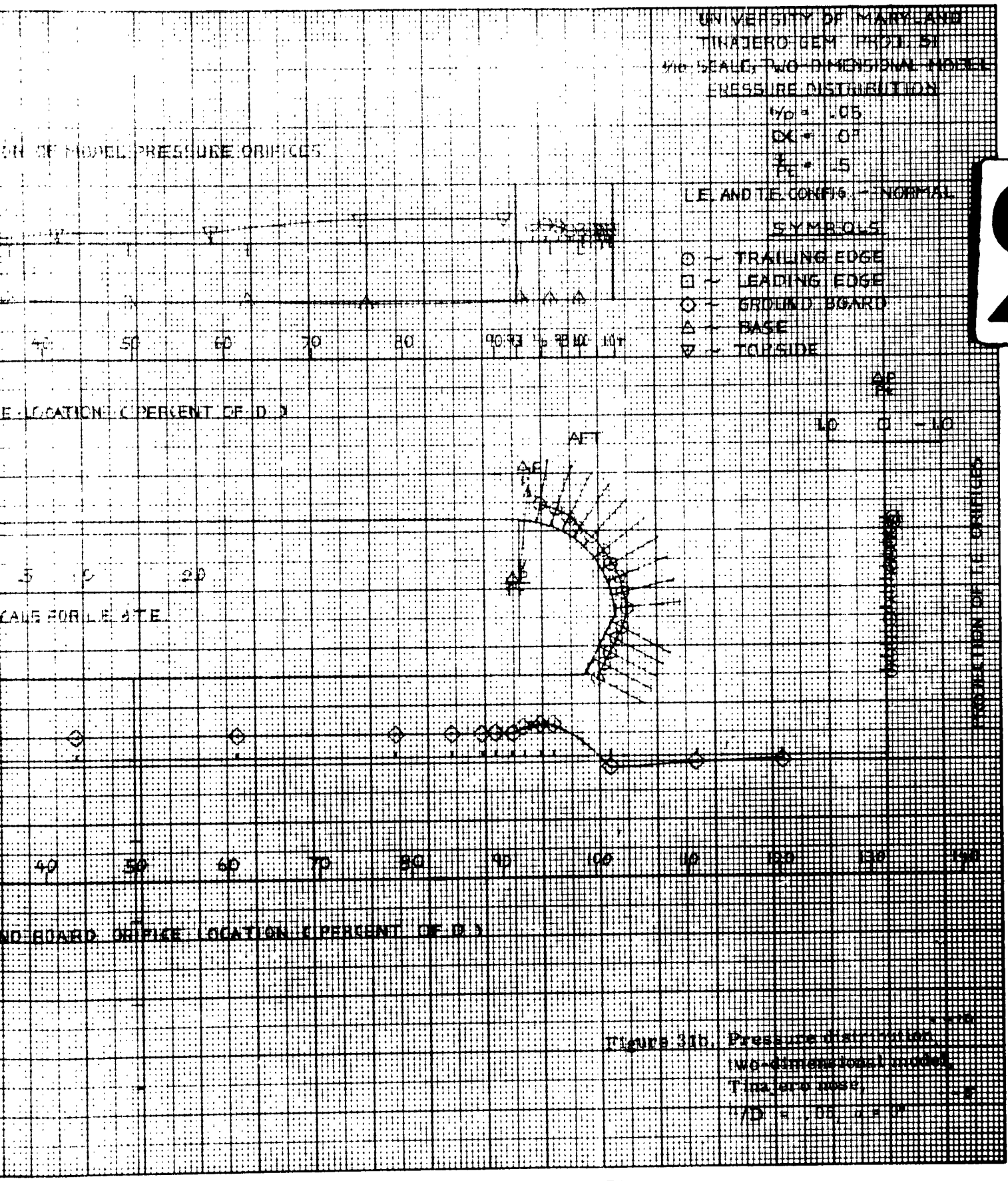


2

Figure 31b. Pressure distribution, two-dimensional model, Tinajero test, $\gamma_D$ = .05

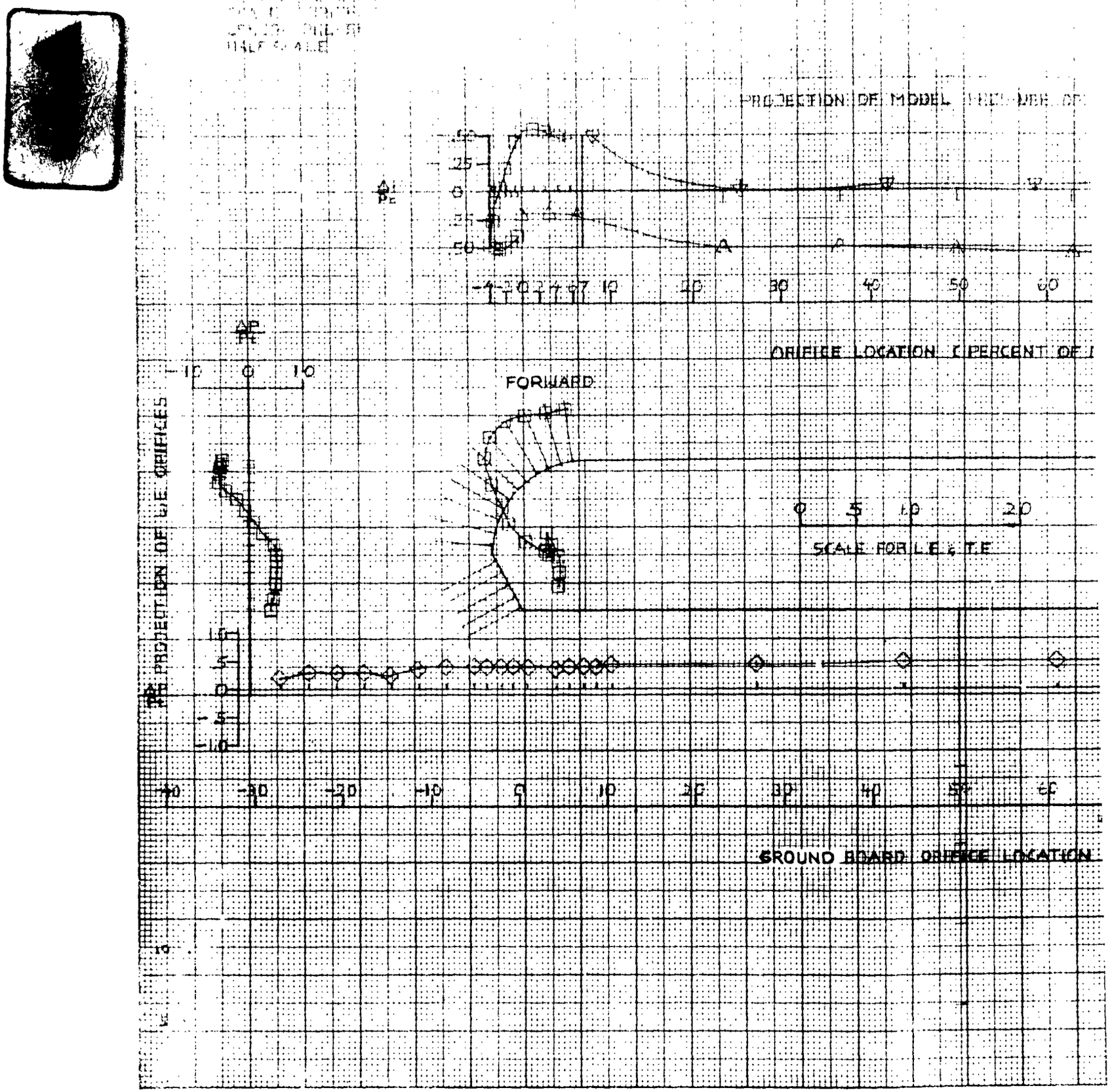
PROJECTION OF MODEL
ORIFICE LOCATION (PERCENT OF
FORWARD
SCALE FOR L.E. & T.E.
PROJECTION OF L.E. ORIFICES
GROUND BOARD ORIFICE LOCATION

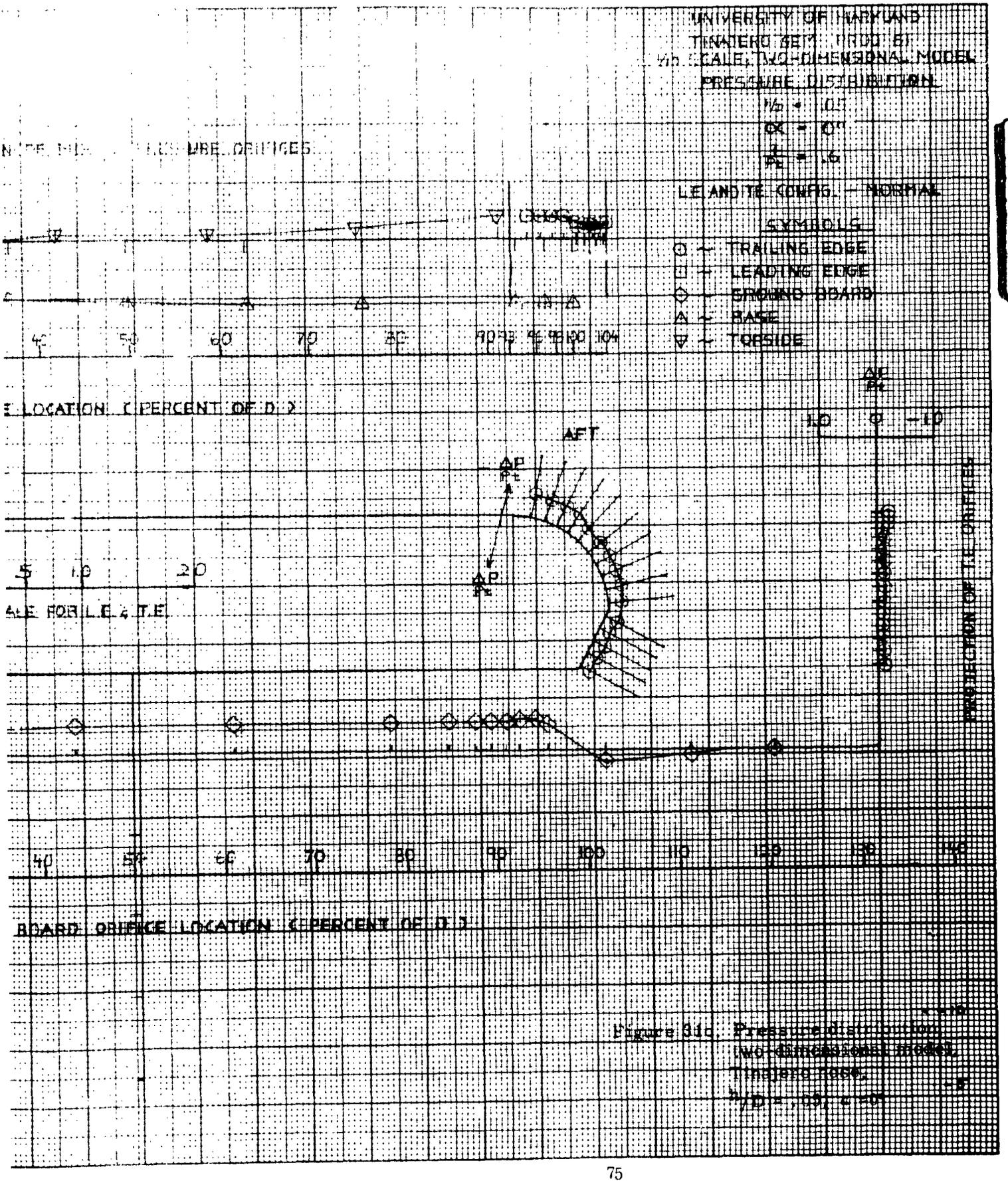


Figure 31c. Pressure distribution, two-dimensional model, Tinajero nose, h/b = .05, α = 10°

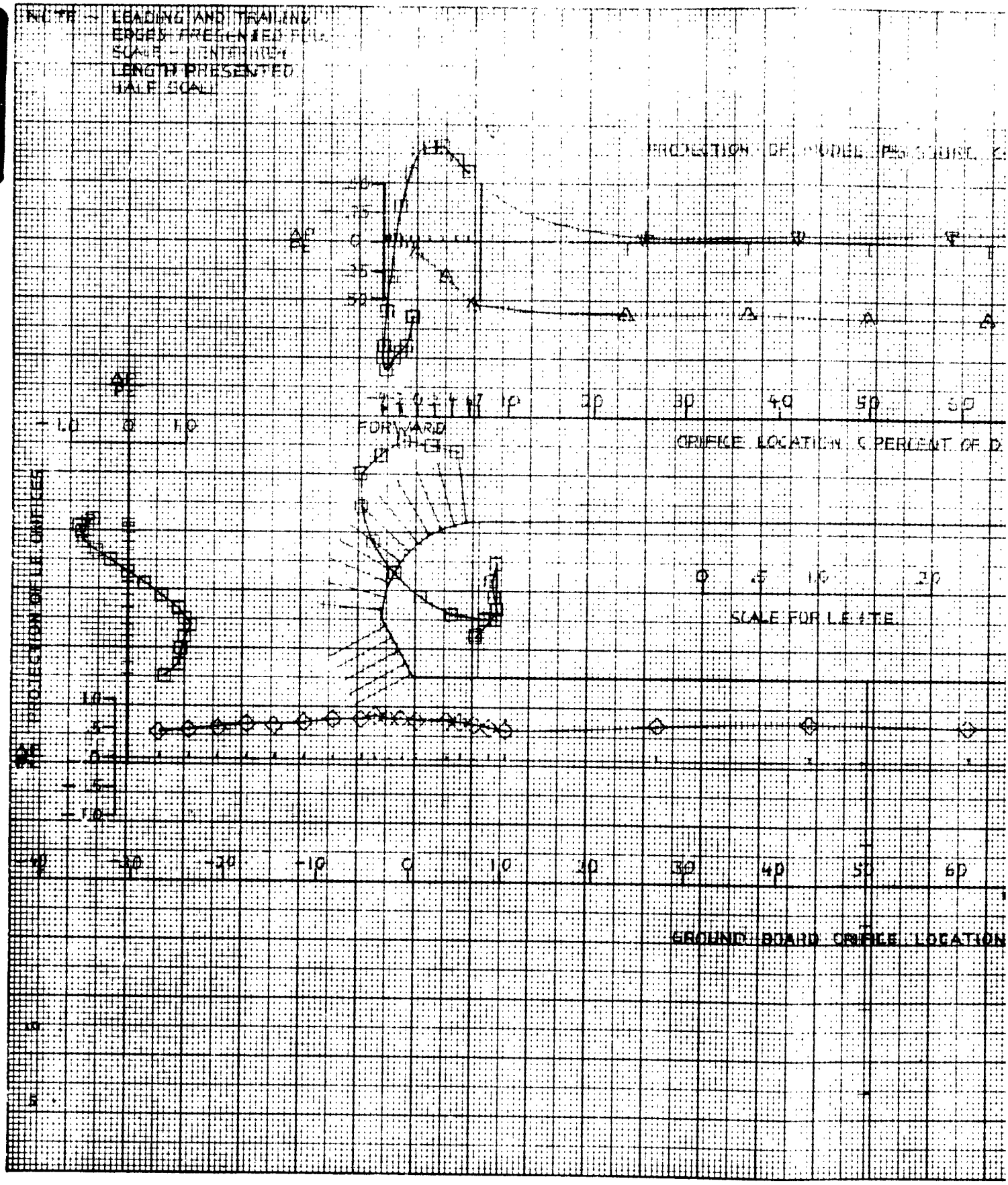
NOTE - LEADING AND TRAILING
EDGES PRESENTED FULL
SCALE - CENTERBOW
LENGTH PRESENTED
HALF SCALE
PROJECTION OF MODEL PRESSURE
FORWARD
ORIFICE LOCATION C PERCENT OF D
SCALE FOR L.E. & T.E.
PROJECTION OF L.E. ORIFICES
GROUND BOARD ORIFICE LOCATION

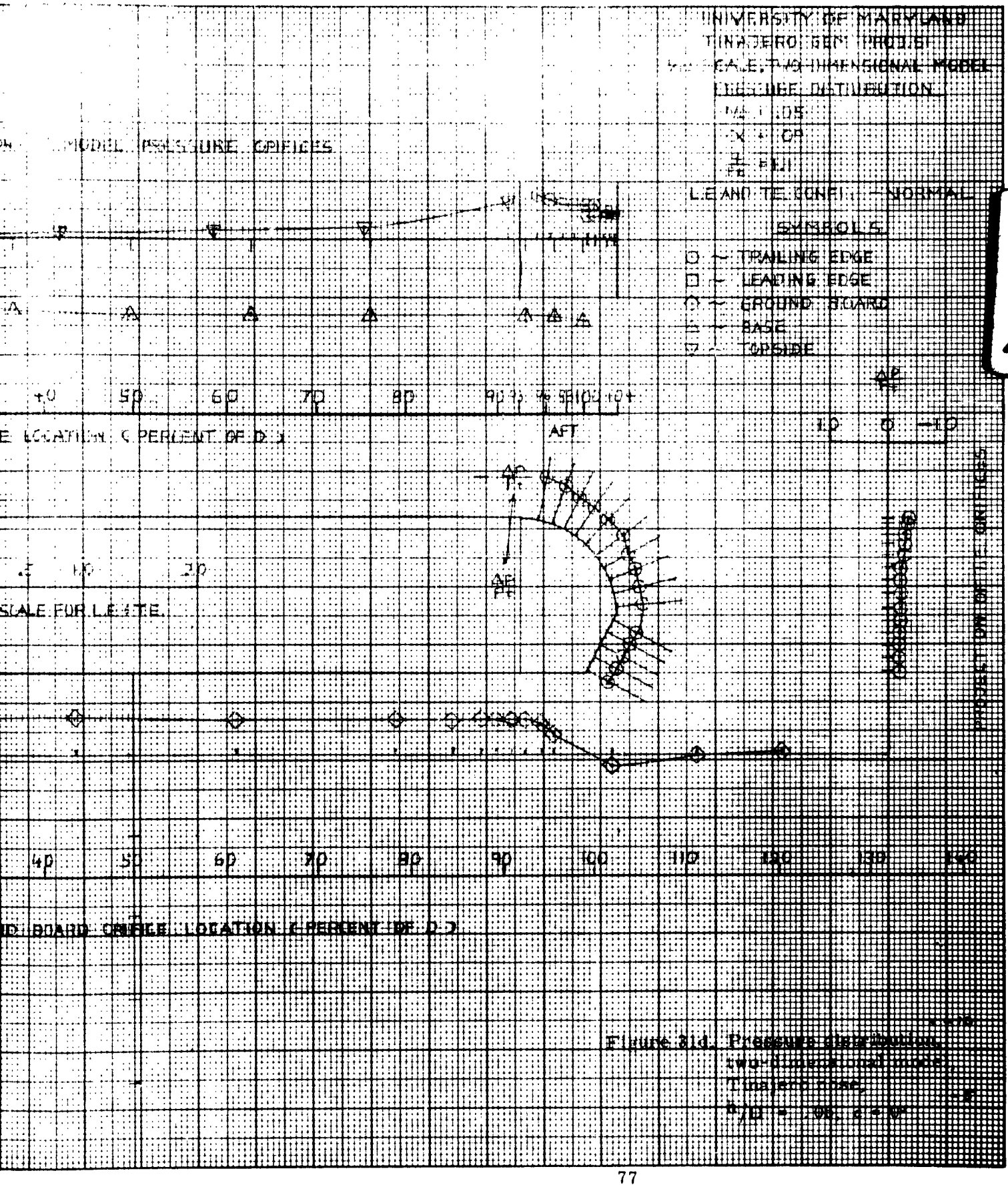


Figure 31d. Pressure distribution, two-dimensional model, Tinajero nose, h/D = .05, α = 0°

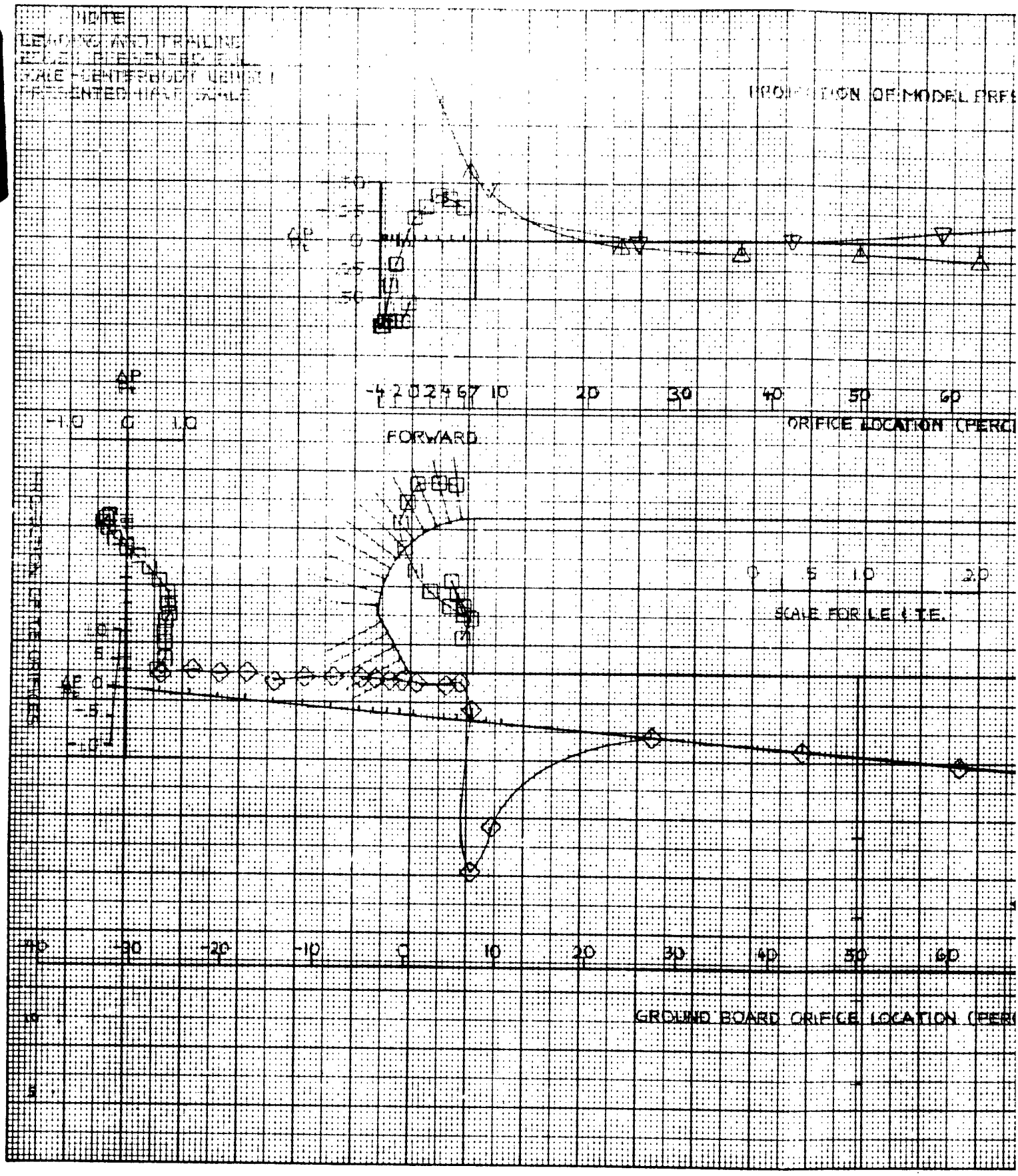
NOTE
PROJECTION OF MODEL PRES
ORIFICE LOCATION (PERC
FORWARD
SCALE FOR LE & TE.
GROUND BOARD ORIFICE LOCATION (PER

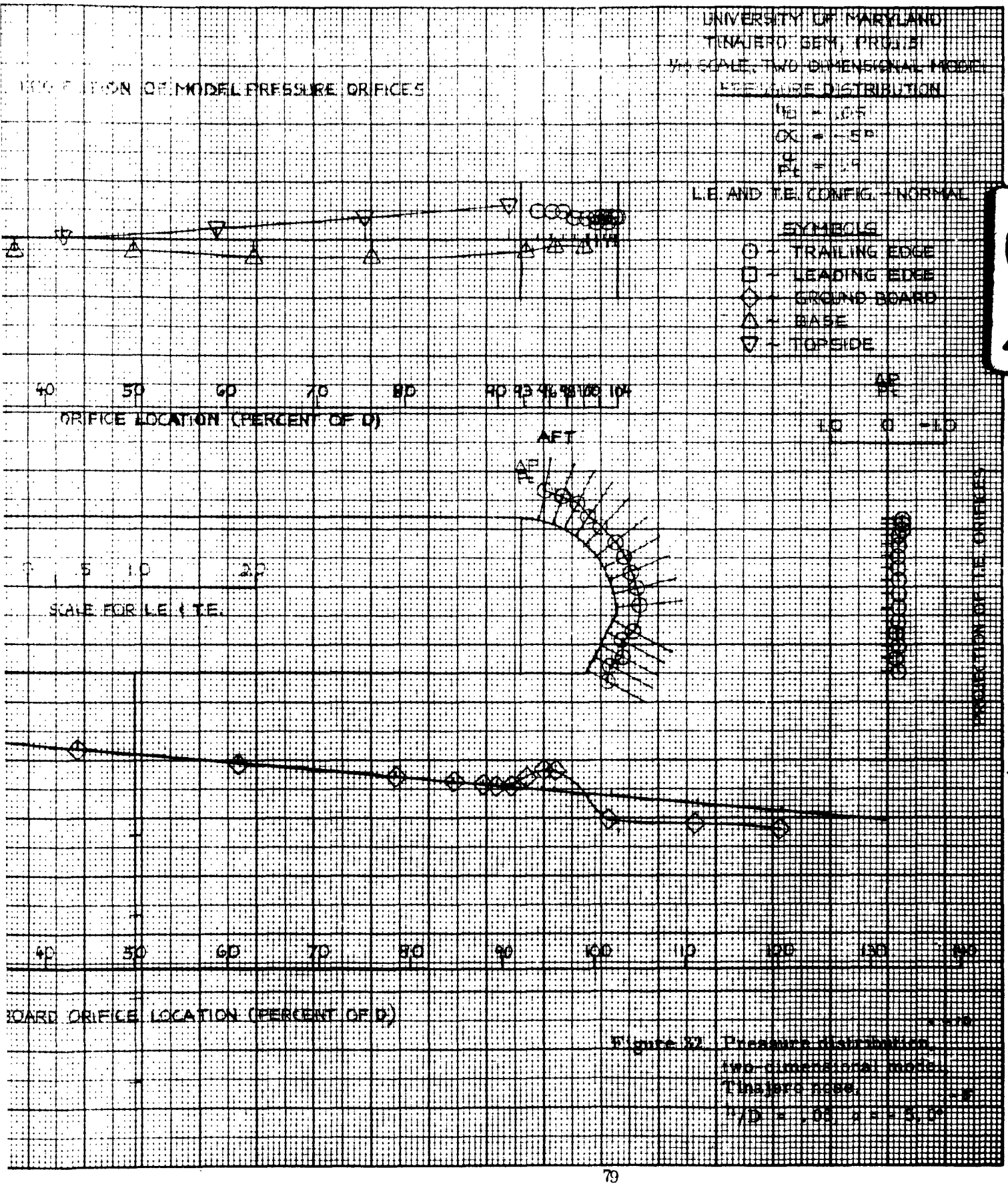


Figure 32. Pressure distribution, two-dimensional model, Tinajero nose.

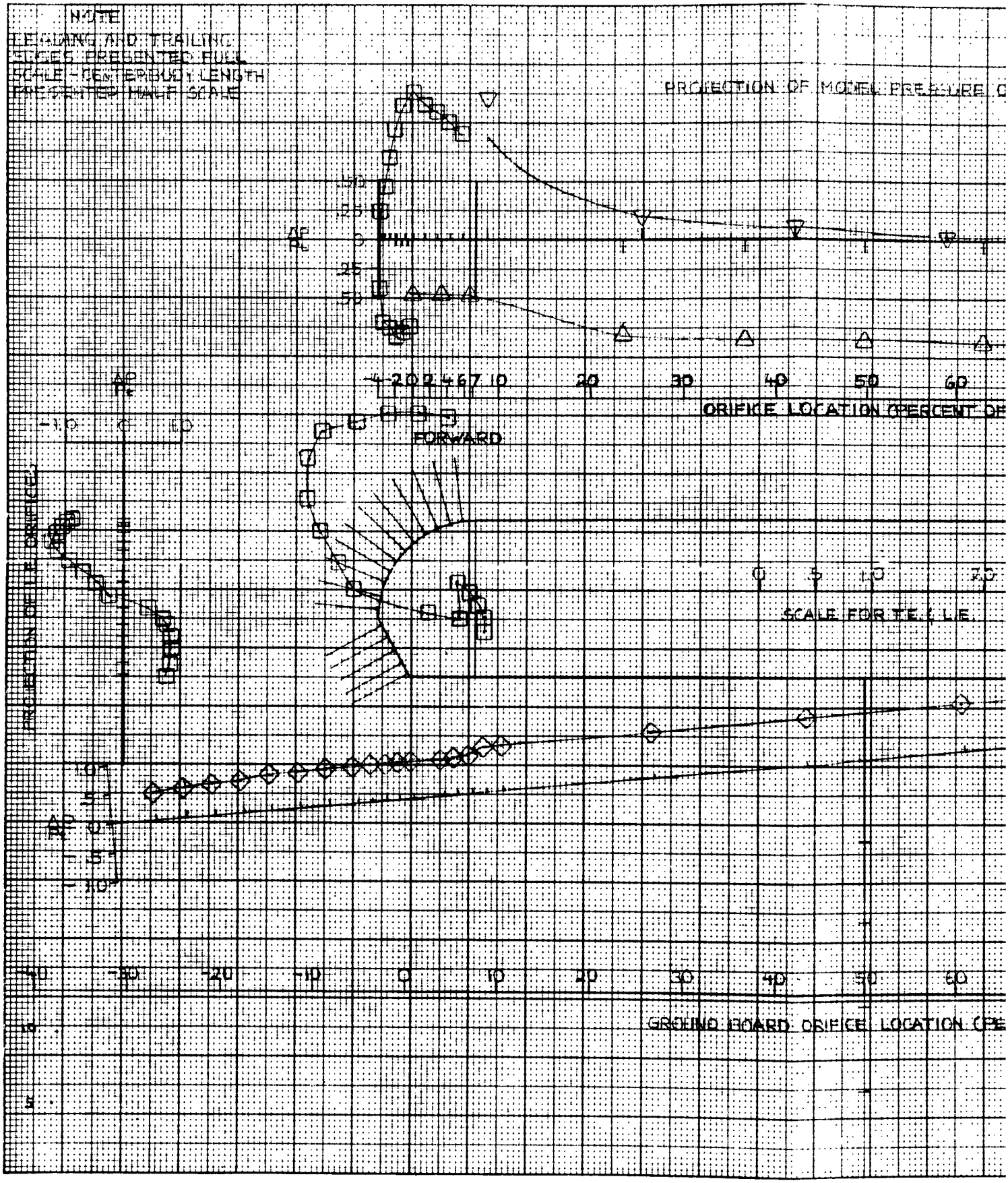
NOTE
LEADING AND TRAILING EDGES PRESENTED FULL SCALE - CENTERBODY LENGTH PRESENTED HALF SCALE
PROJECTION OF MODEL PRESSURE C
ORIFICE LOCATION (PERCENT OF
FORWARD
SCALE FOR T.E. & L.E.
GROUND BOARD ORIFICE LOCATION (PE

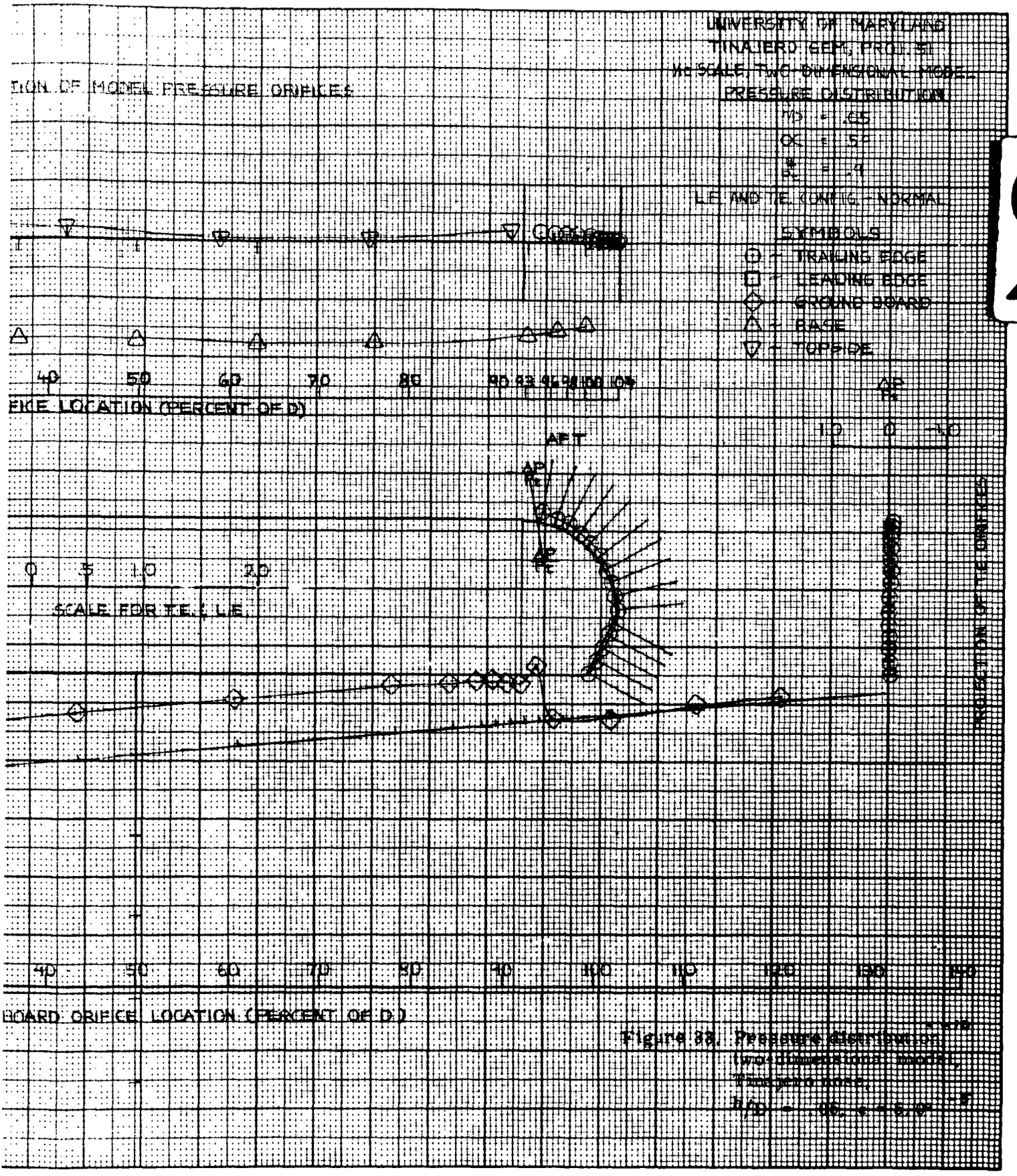


Figure 38. Pressure distribution (two-dimensional model, [illegible]).

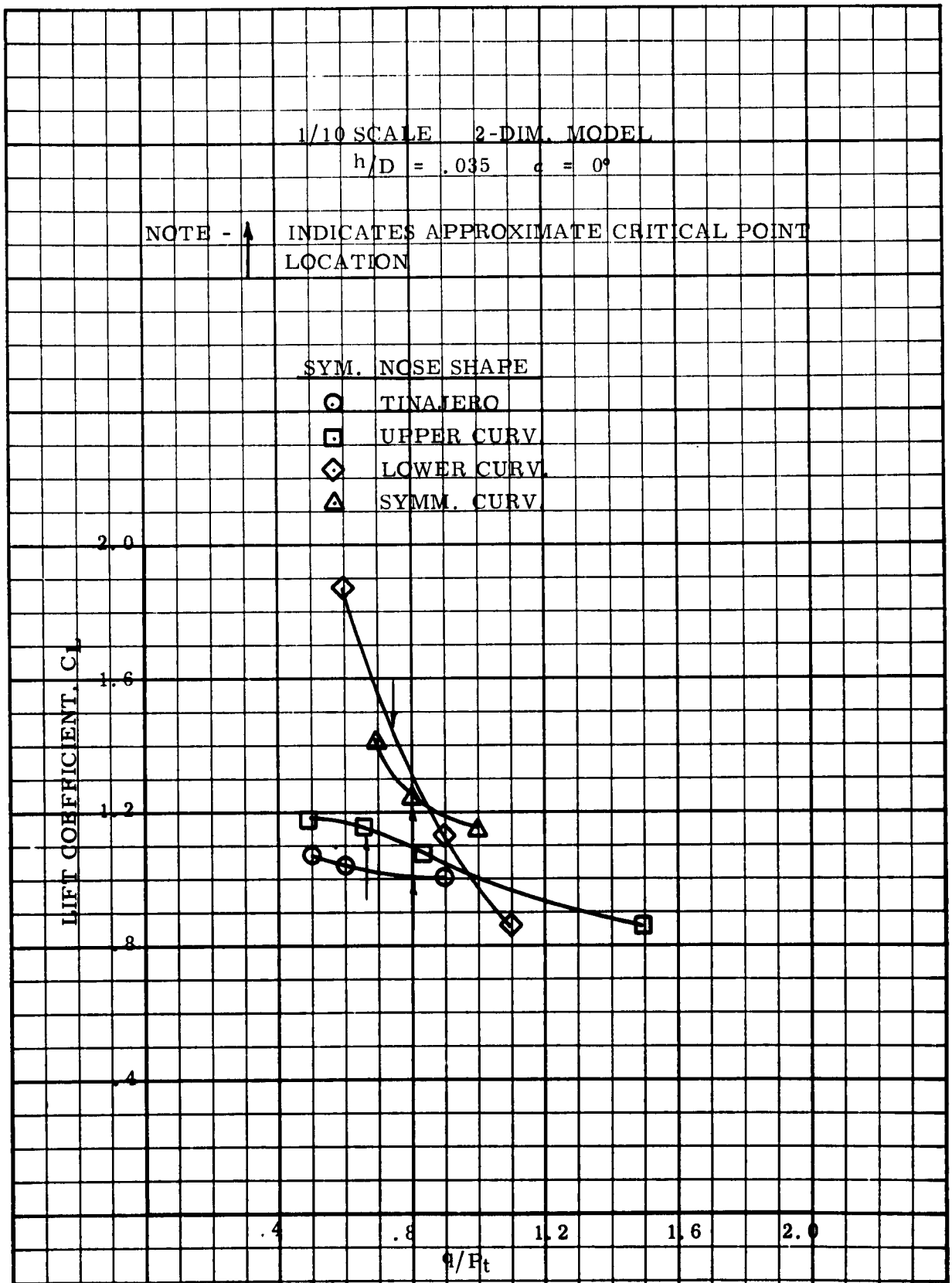


Figure 34. Change of lift coefficient with increasing forward speed. Comparison of nose shapes, $h/D = .035$, $\alpha = 0°$.

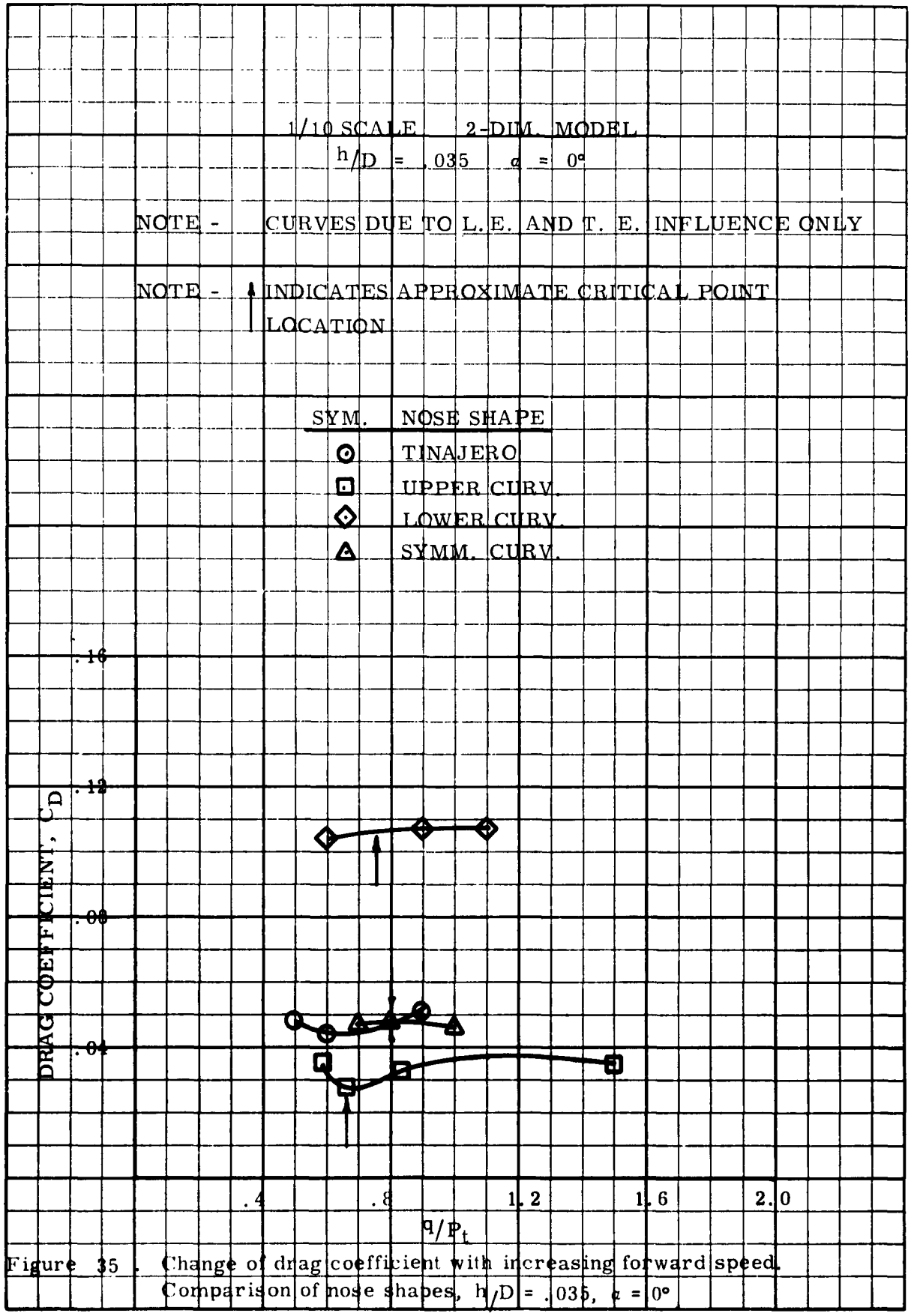


Figure 35. Change of drag coefficient with increasing forward speed. Comparison of nose shapes, h/D = .035, α = 0°

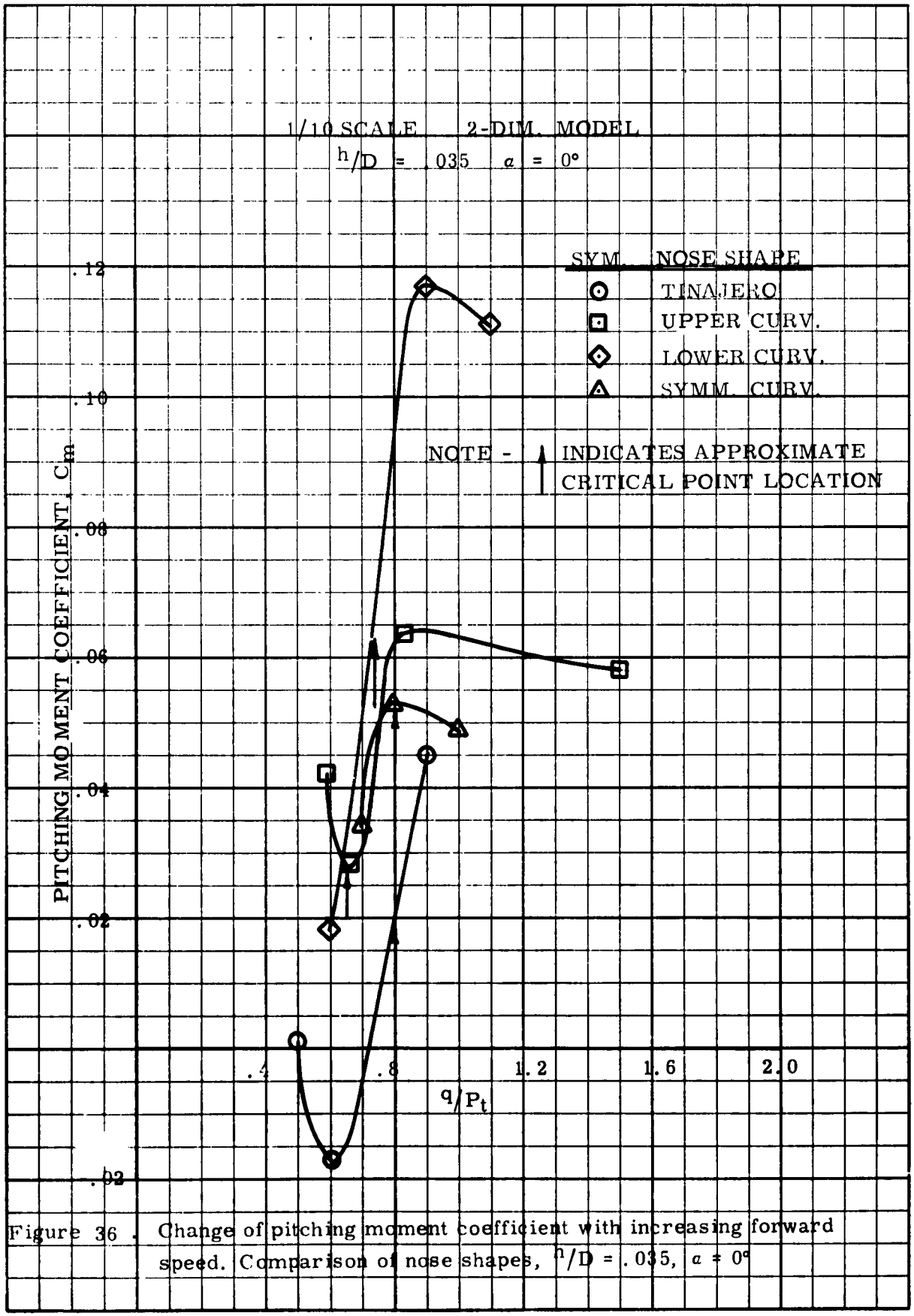


Figure 36. Change of pitching moment coefficient with increasing forward speed. Comparison of nose shapes, $^{h}/D = .035$, $\alpha = 0°$

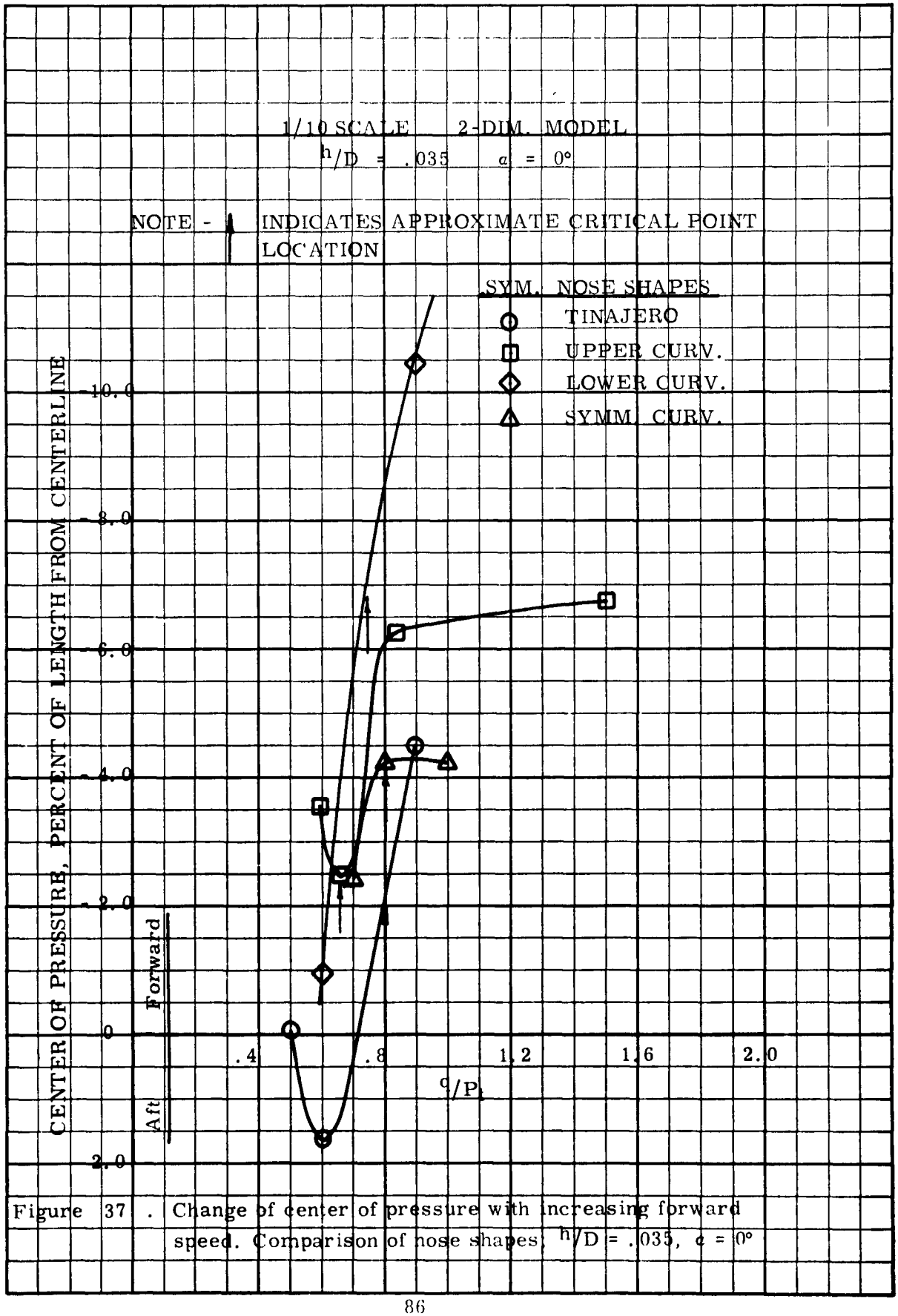


Figure 37 . Change of center of pressure with increasing forward speed. Comparison of nose shapes, h/D = .035, α = 0°

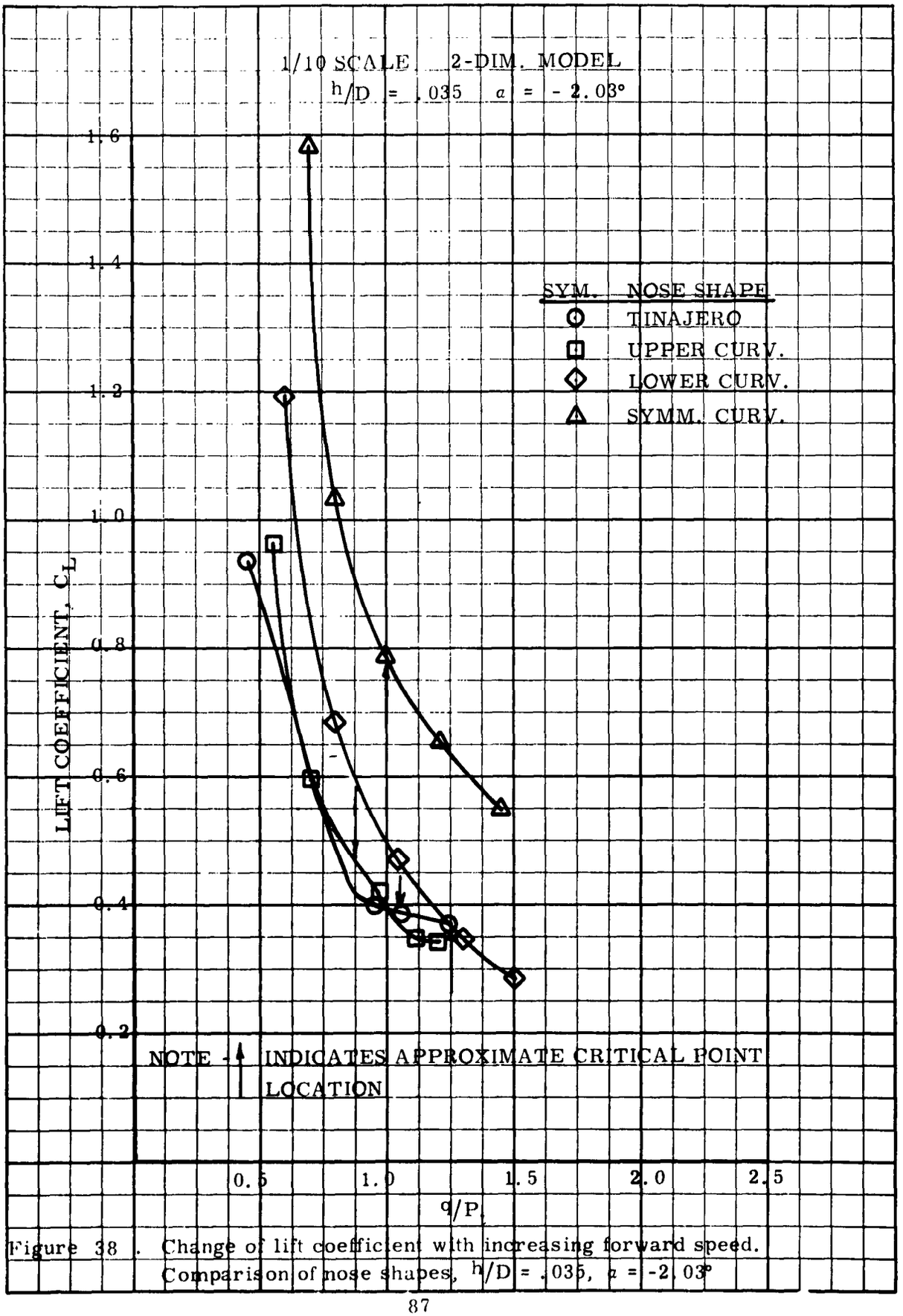


Figure 38 . Change of lift coefficient with increasing forward speed. Comparison of nose shapes, h/D = .035, α = -2.03°

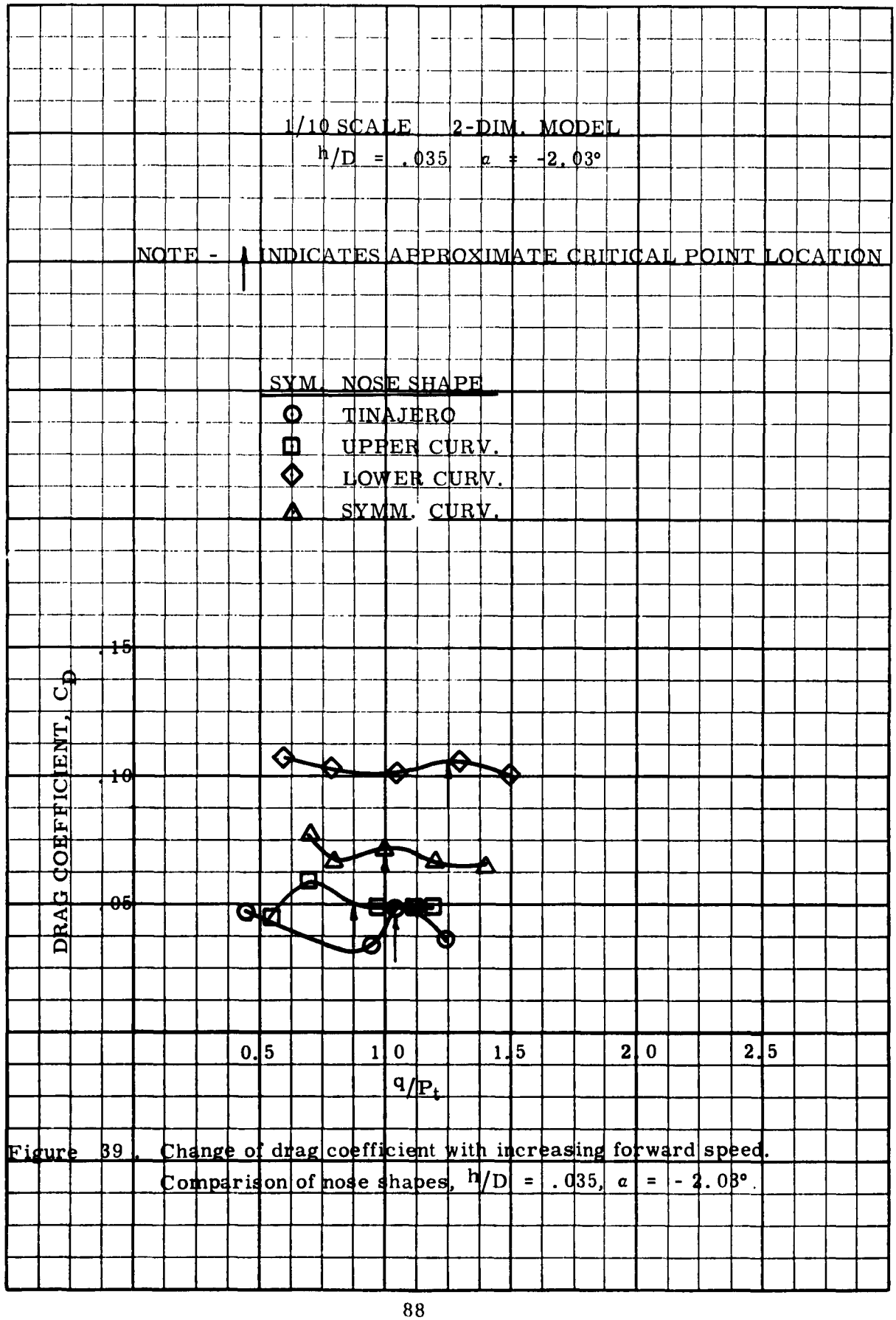


Figure 39. Change of drag coefficient with increasing forward speed. Comparison of nose shapes, $h/D = .035$, $\alpha = -2.03°$.

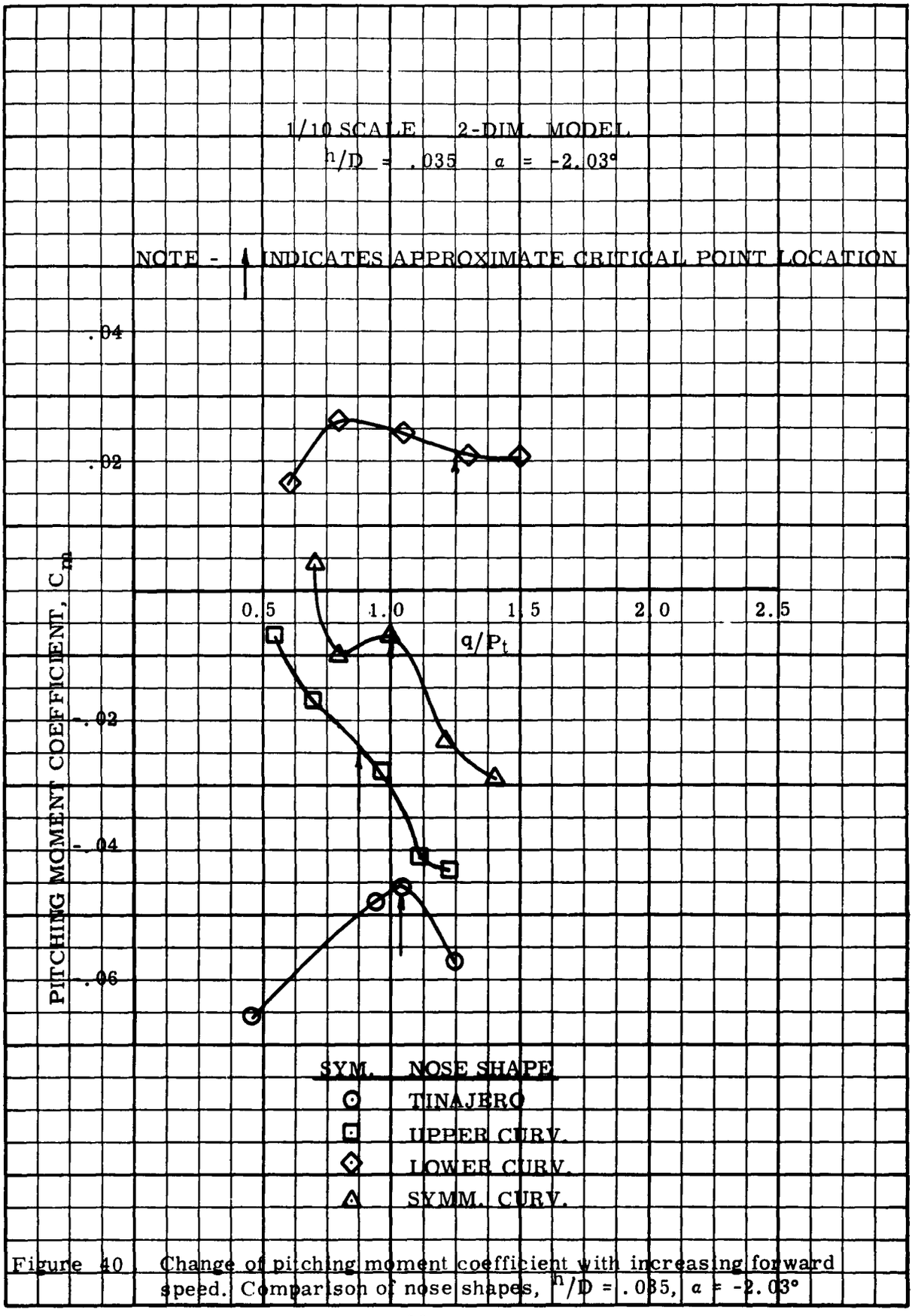


Figure 40 Change of pitching moment coefficient with increasing forward speed. Comparison of nose shapes, $h/D = .035$, $\alpha = -2.03°$

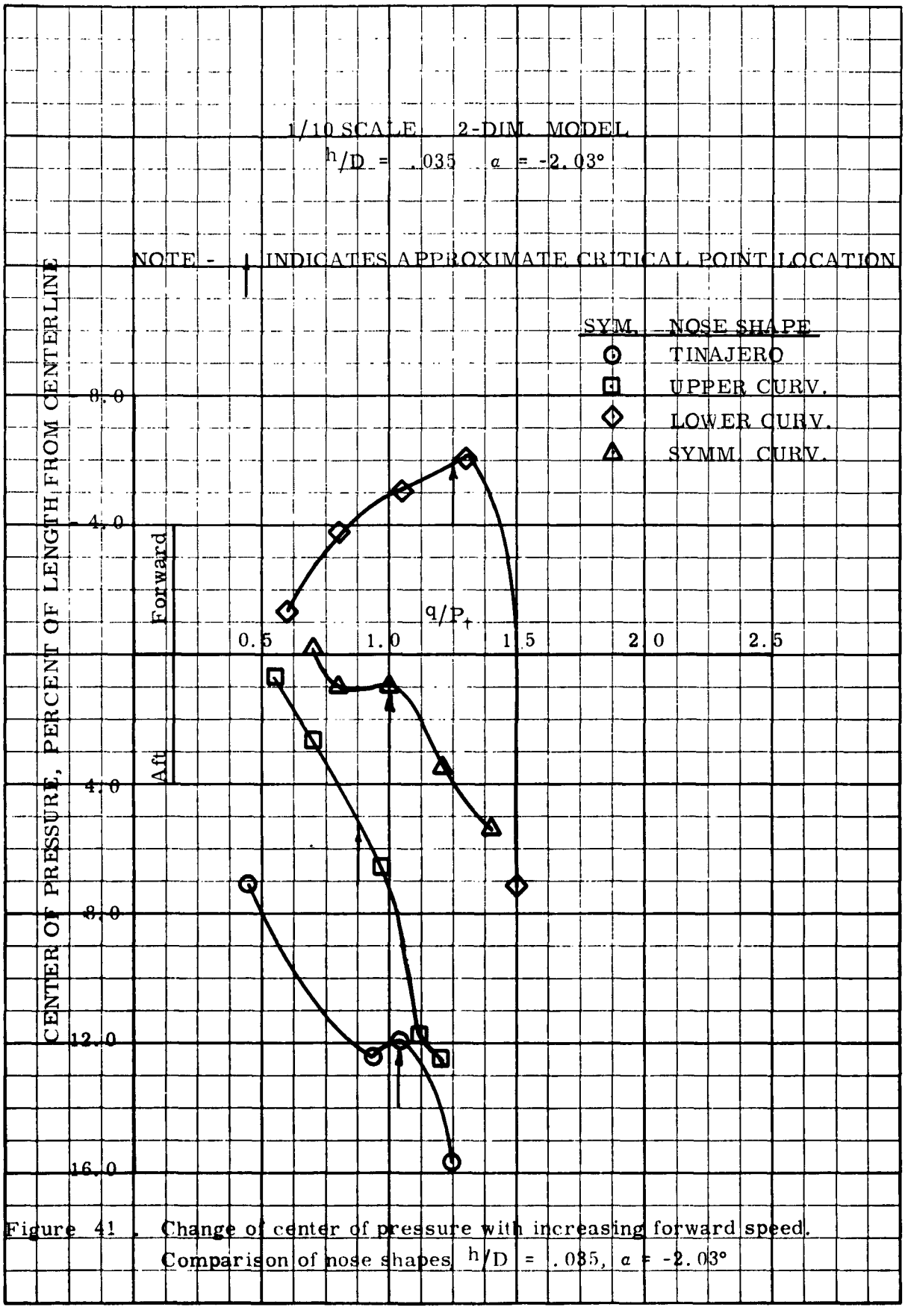


Figure 41. Change of center of pressure with increasing forward speed. Comparison of nose shapes, h/D = .035, α = -2.03°

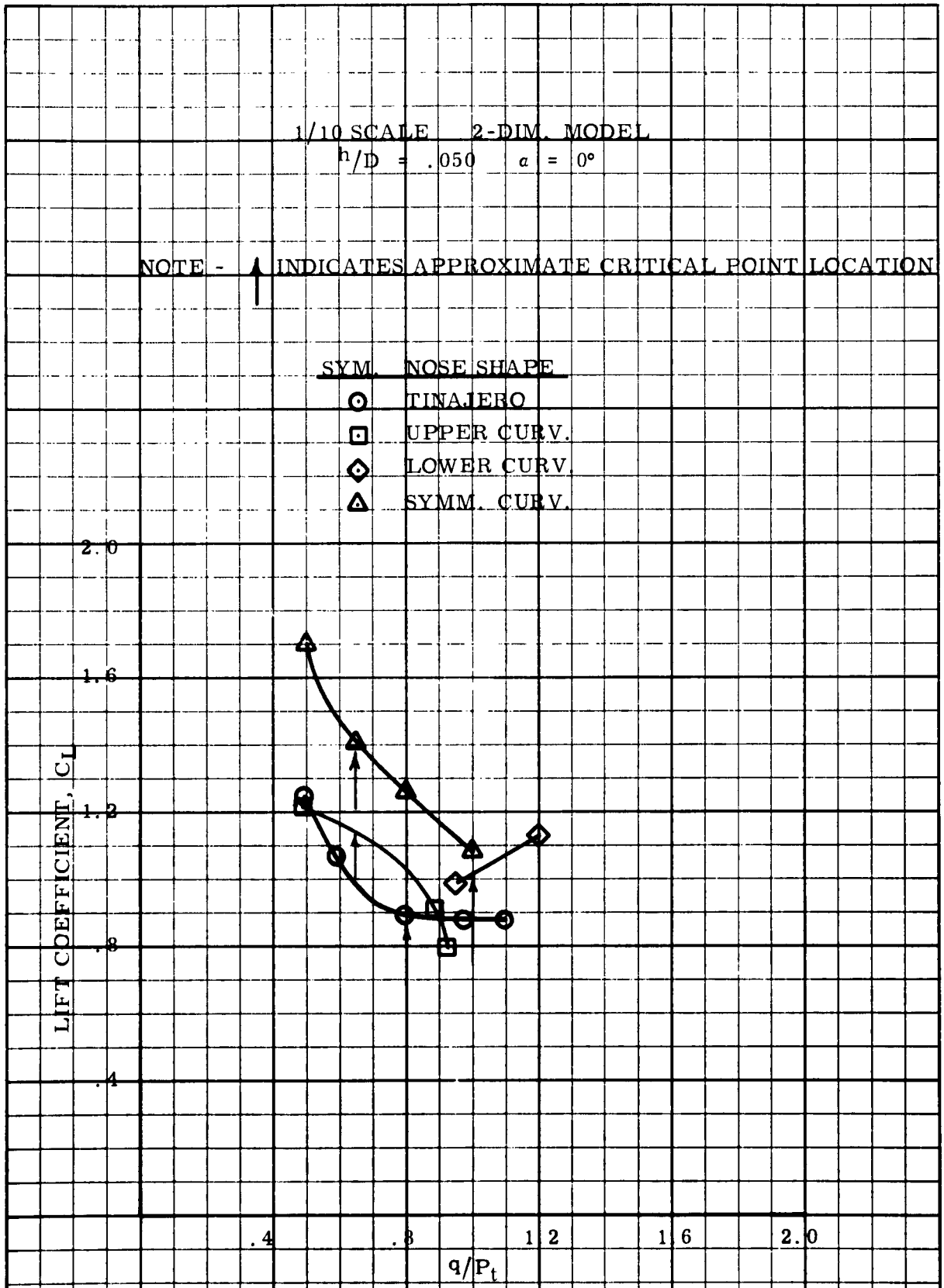


Figure 42 . Change of lift coefficient with increasing forward speed. Comparison of nose shapes, h/D = .050, α = 0°

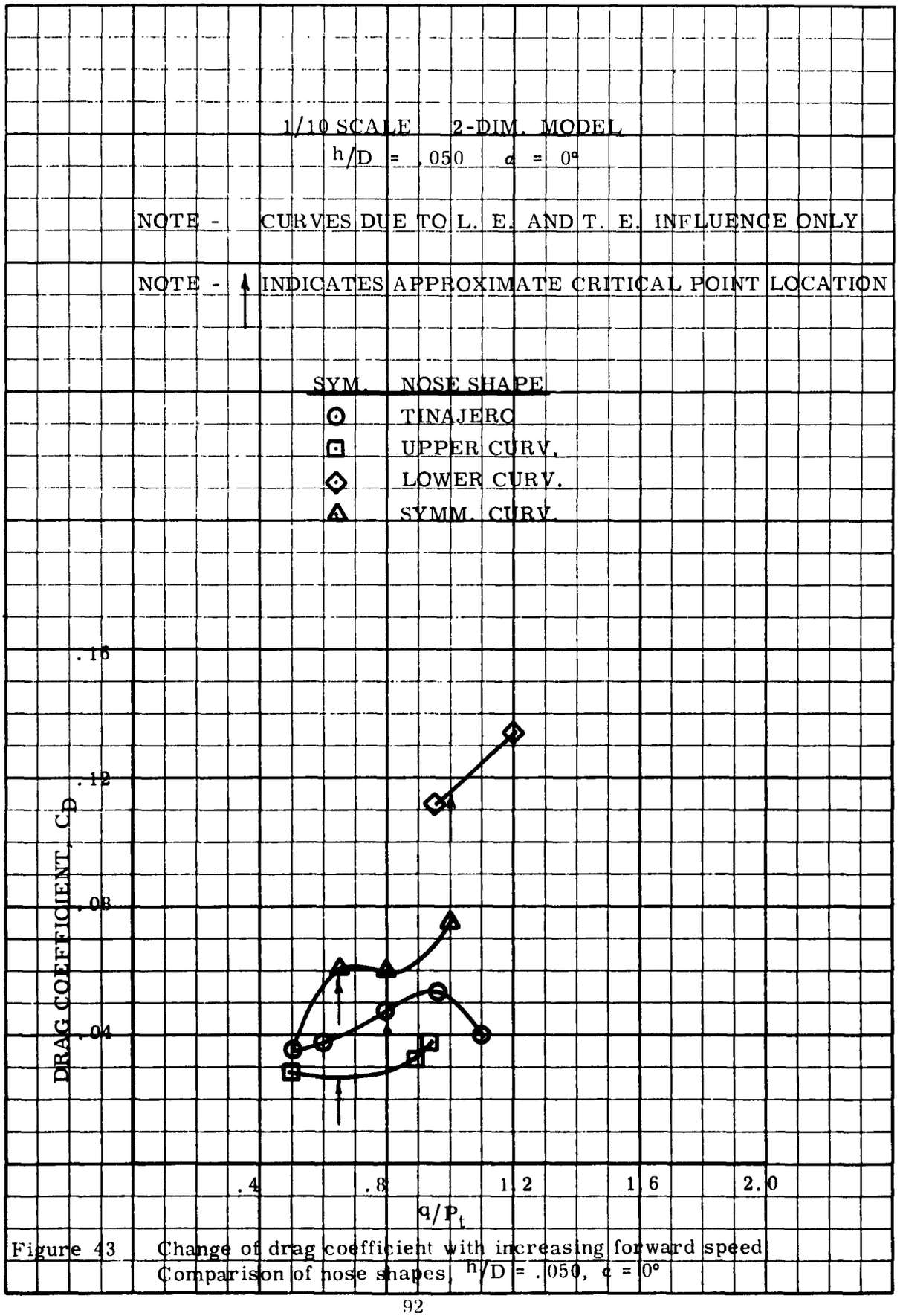


Figure 43 Change of drag coefficient with increasing forward speed. Comparison of nose shapes, $h/D = .050$, $\alpha = 0°$

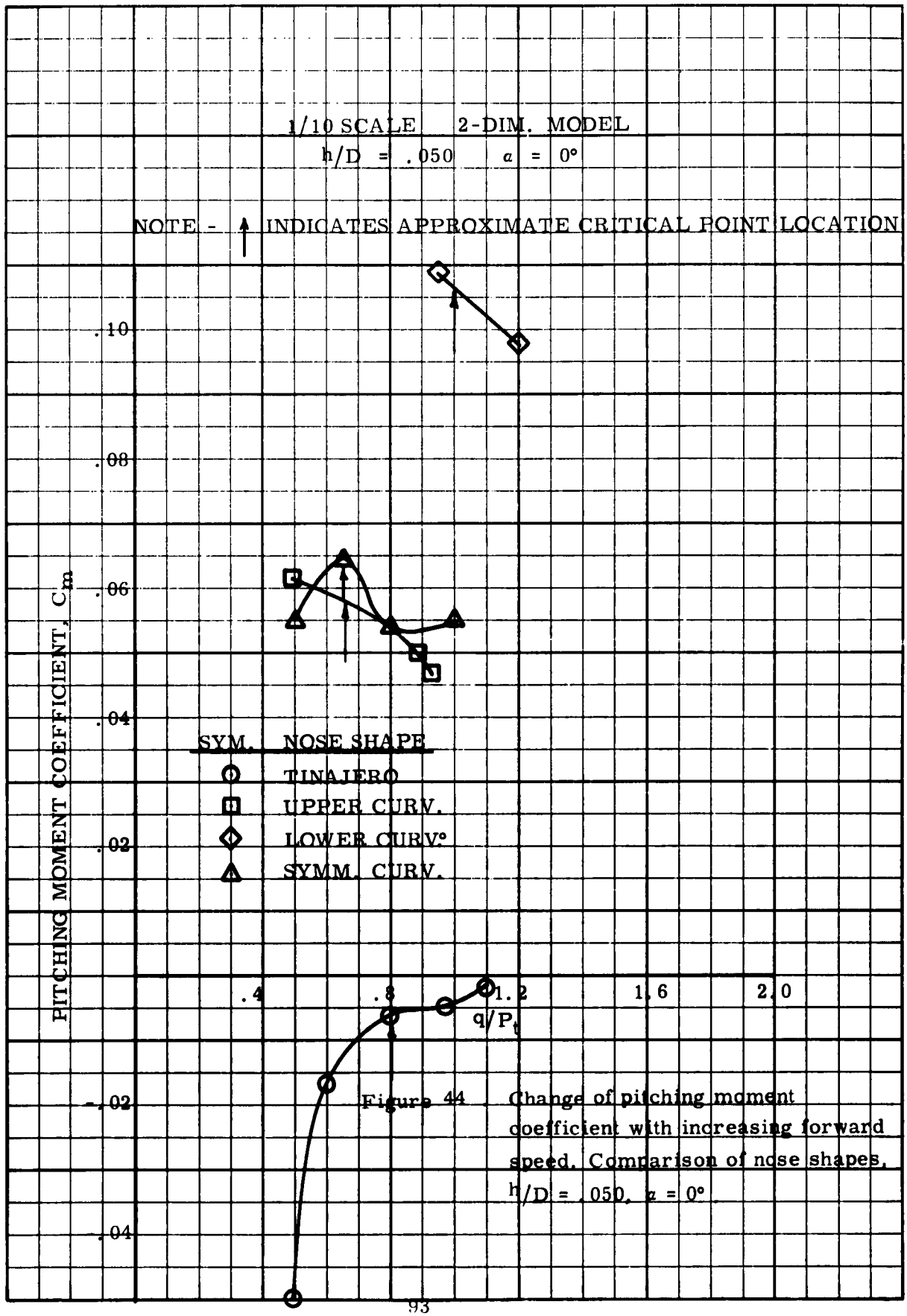


Figure 44. Change of pitching moment coefficient with increasing forward speed. Comparison of nose shapes, h/D = .050, α = 0°.

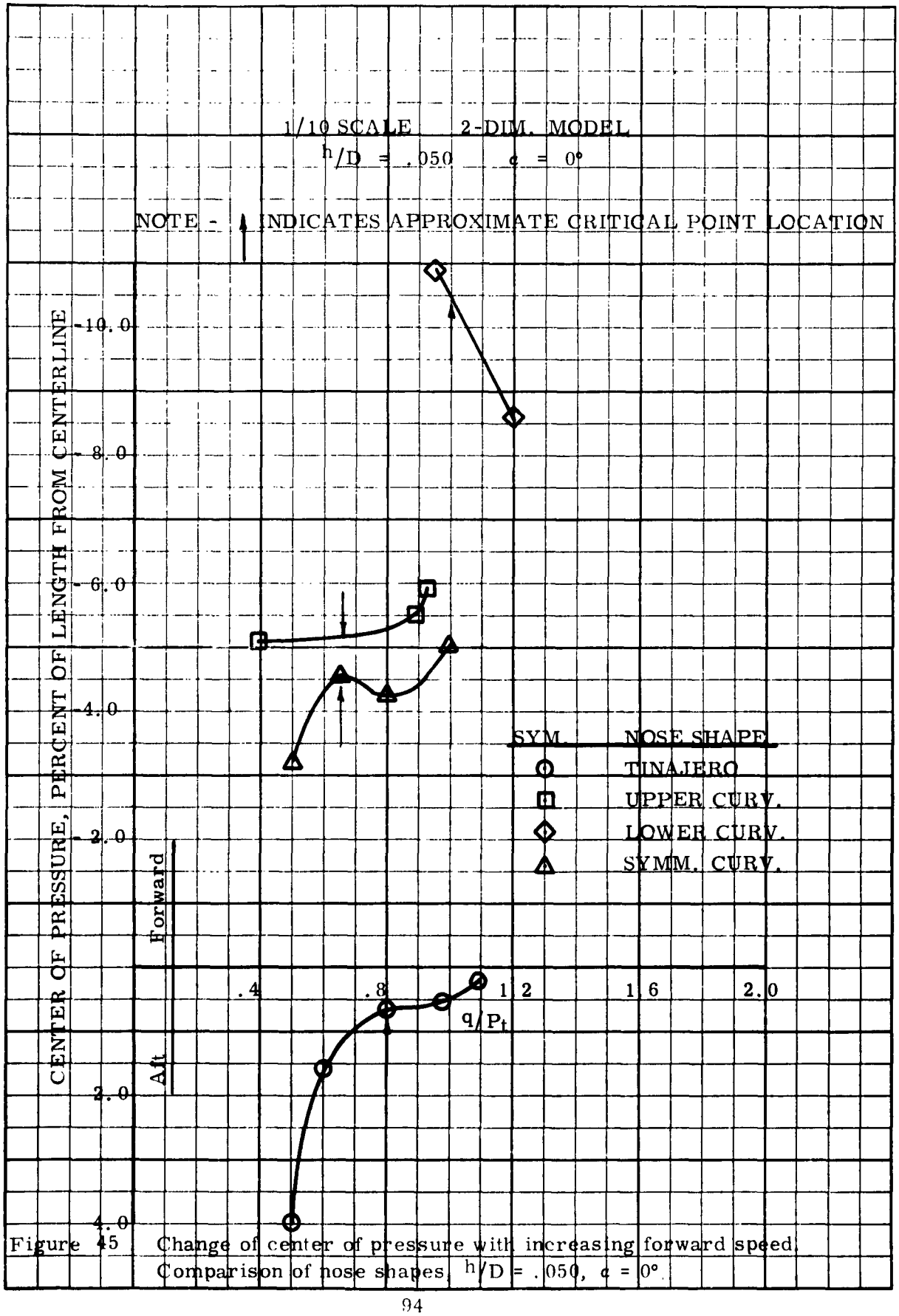


Figure 45 Change of center of pressure with increasing forward speed. Comparison of nose shapes. h/D = .050, α = 0°.

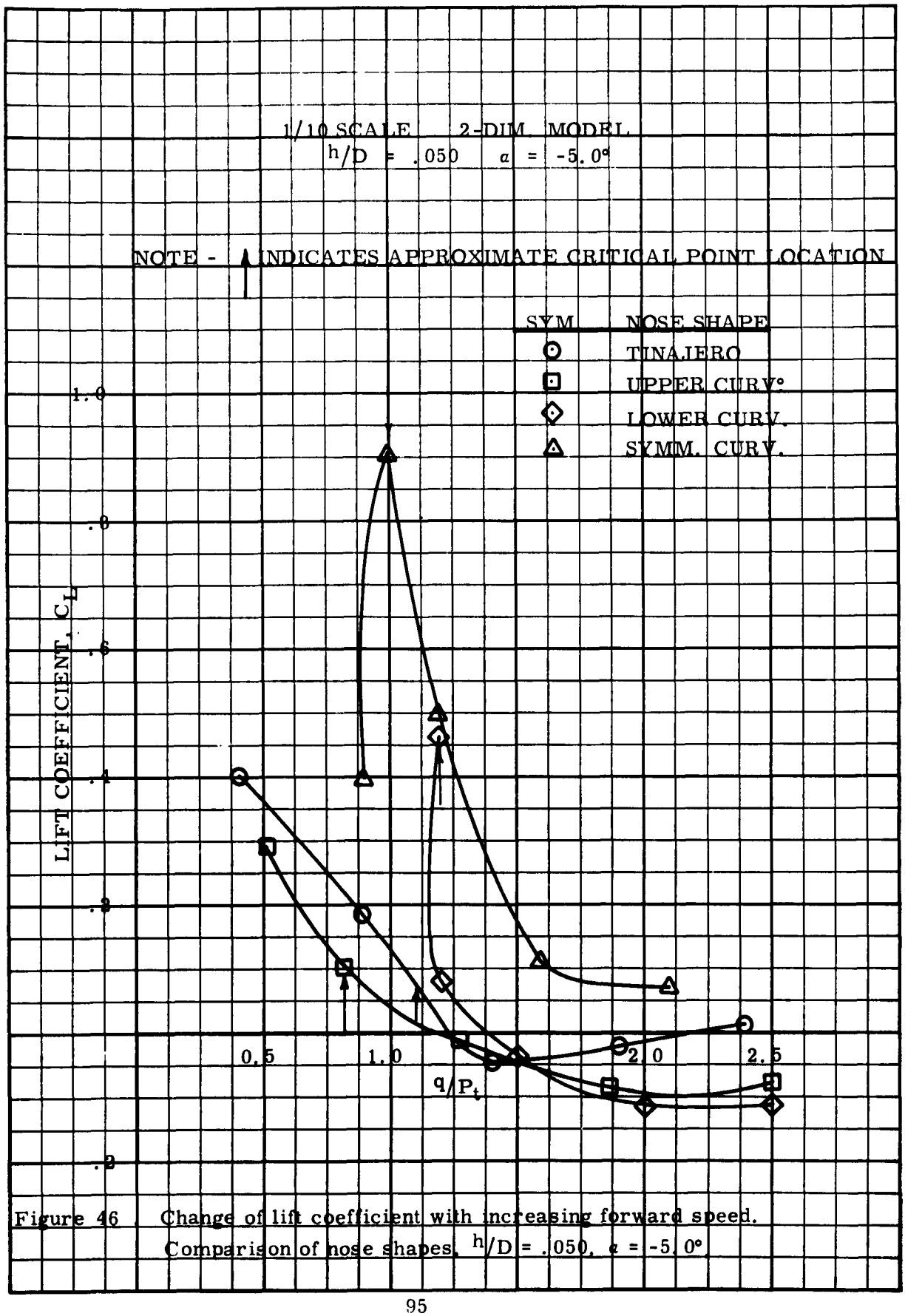


Figure 46 Change of lift coefficient with increasing forward speed. Comparison of nose shapes, $h/D = .050$, $\alpha = -5.0°$

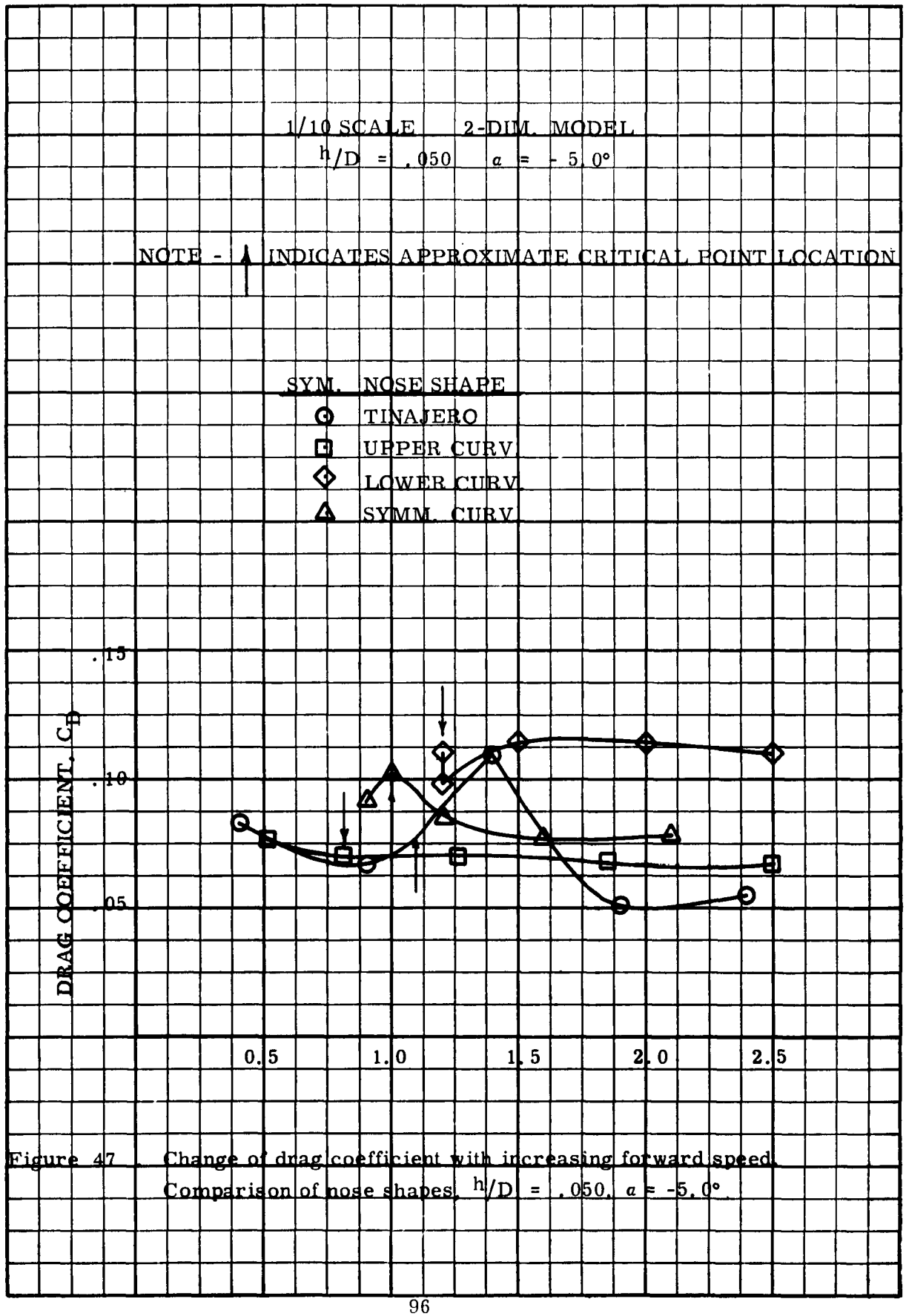


Figure 47 Change of drag coefficient with increasing forward speed. Comparison of nose shapes. $h/D = .050$, $\alpha = -5.0°$.

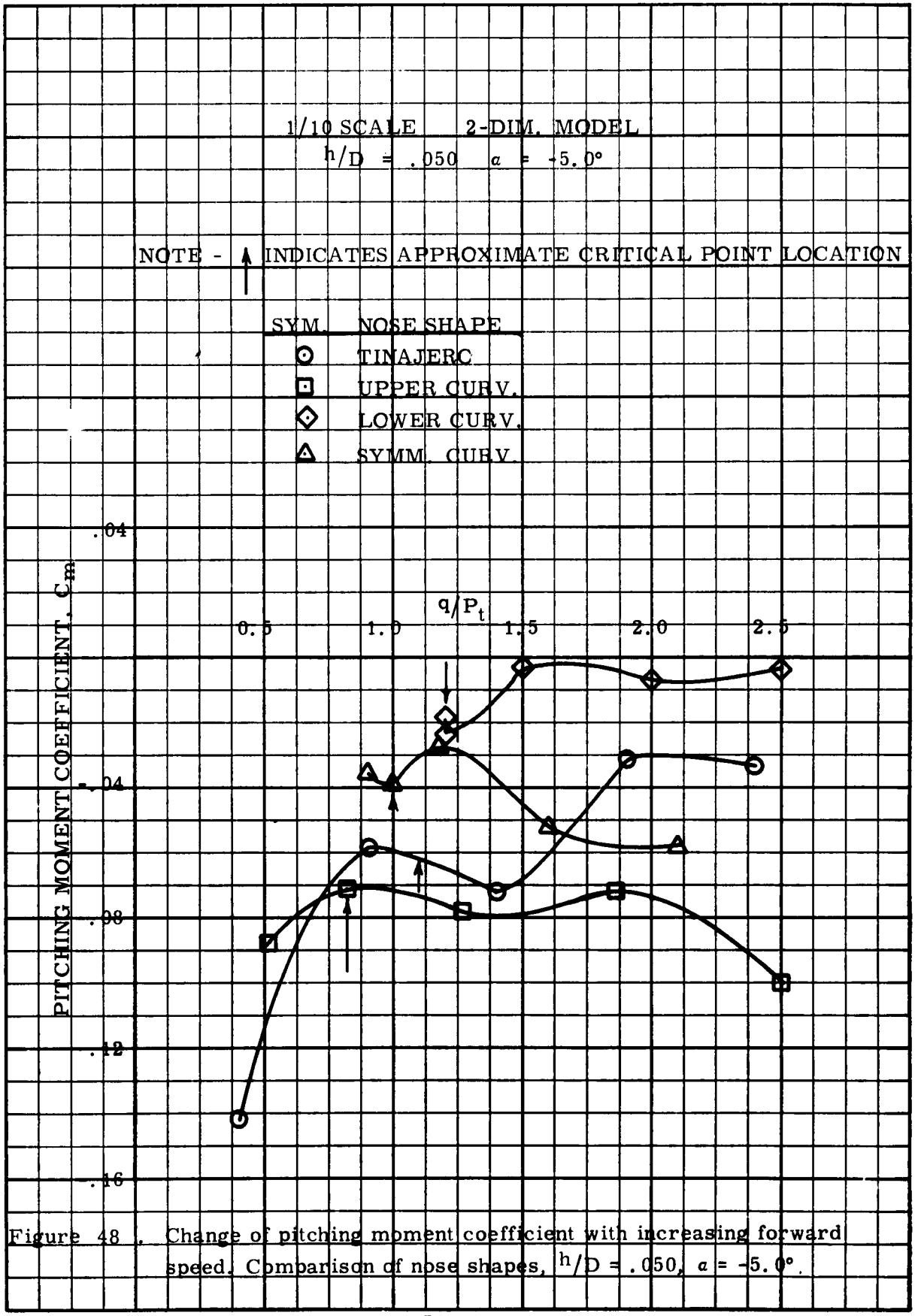


Figure 48 . Change of pitching moment coefficient with increasing forward speed. Comparison of nose shapes, $h/D = .050$, $\alpha = -5.0°$.

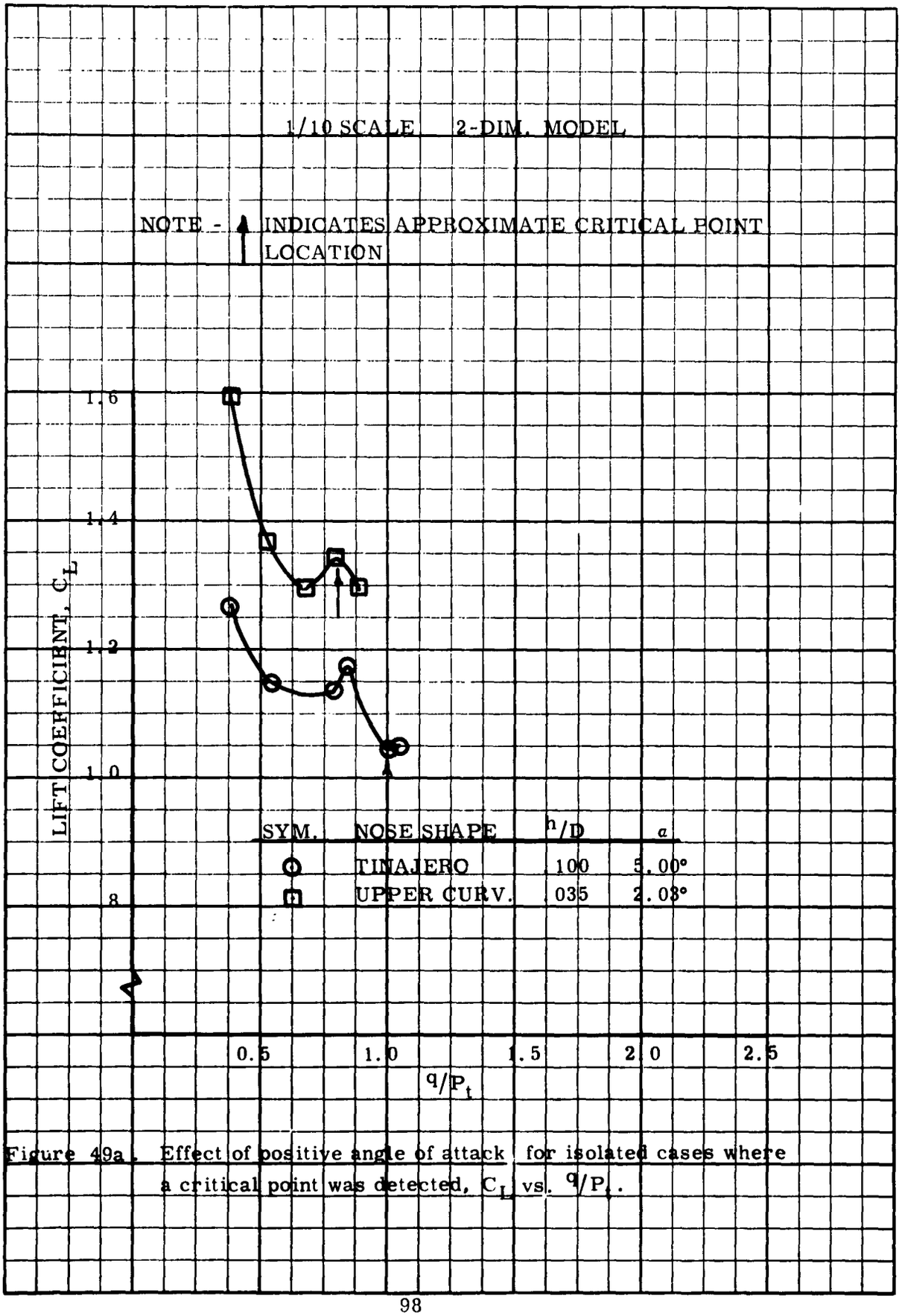


Figure 49a. Effect of positive angle of attack for isolated cases where a critical point was detected, $C_L$ vs. $q/P_t$.

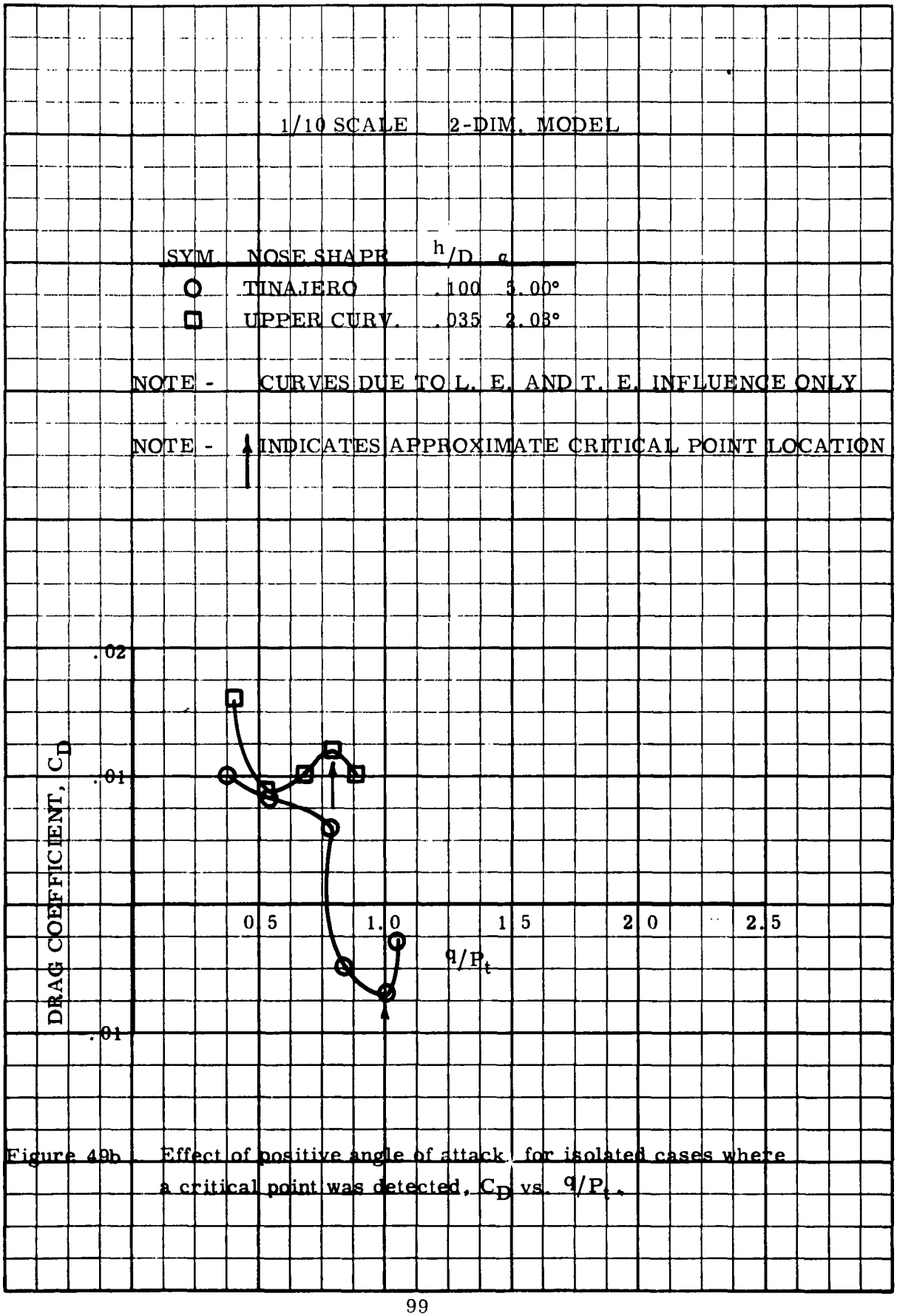


Figure 49b Effect of positive angle of attack for isolated cases where a critical point was detected, $C_D$ vs. $q/P_t$.

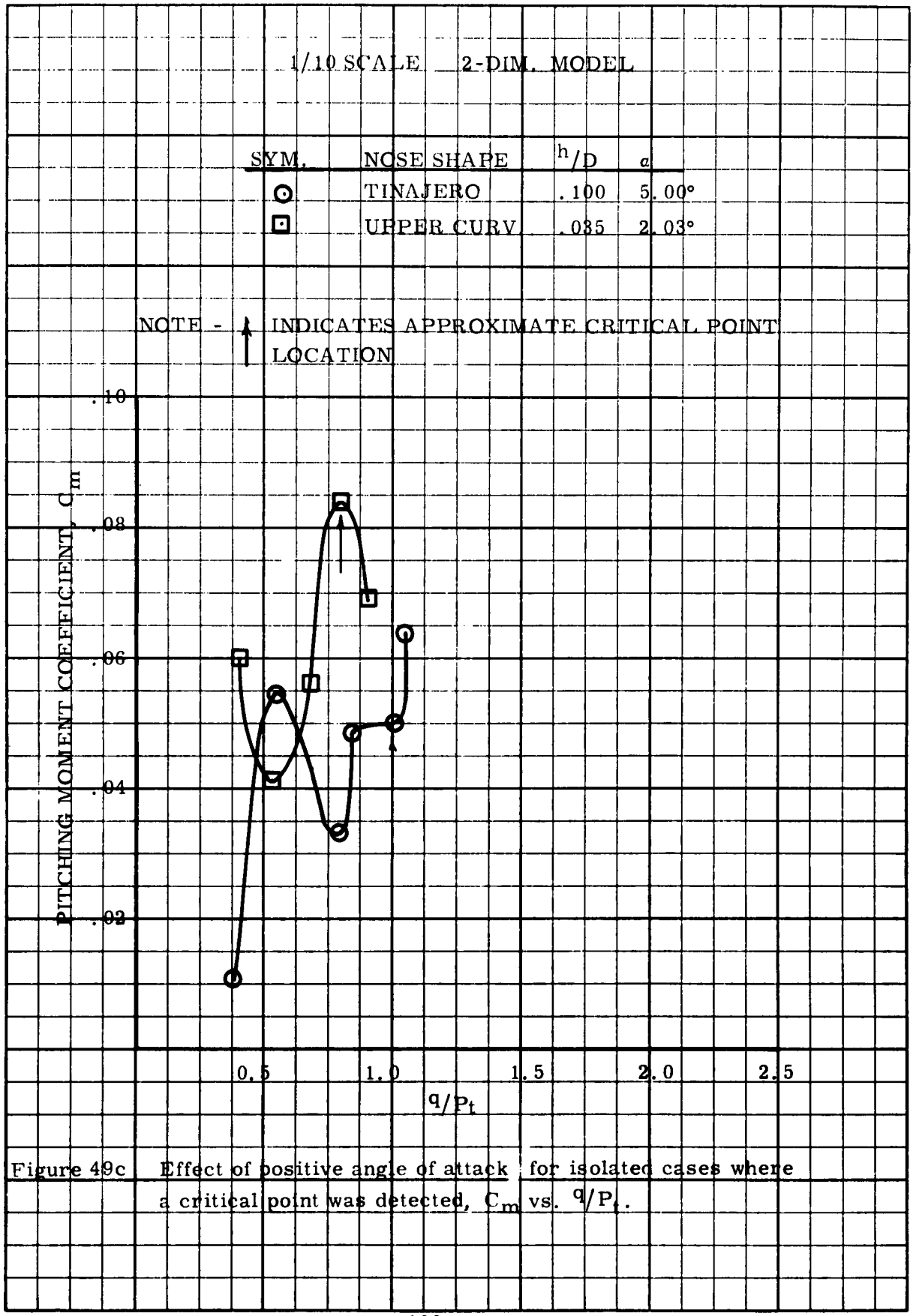


Figure 49c Effect of positive angle of attack for isolated cases where a critical point was detected, $C_m$ vs. $q/P_t$.

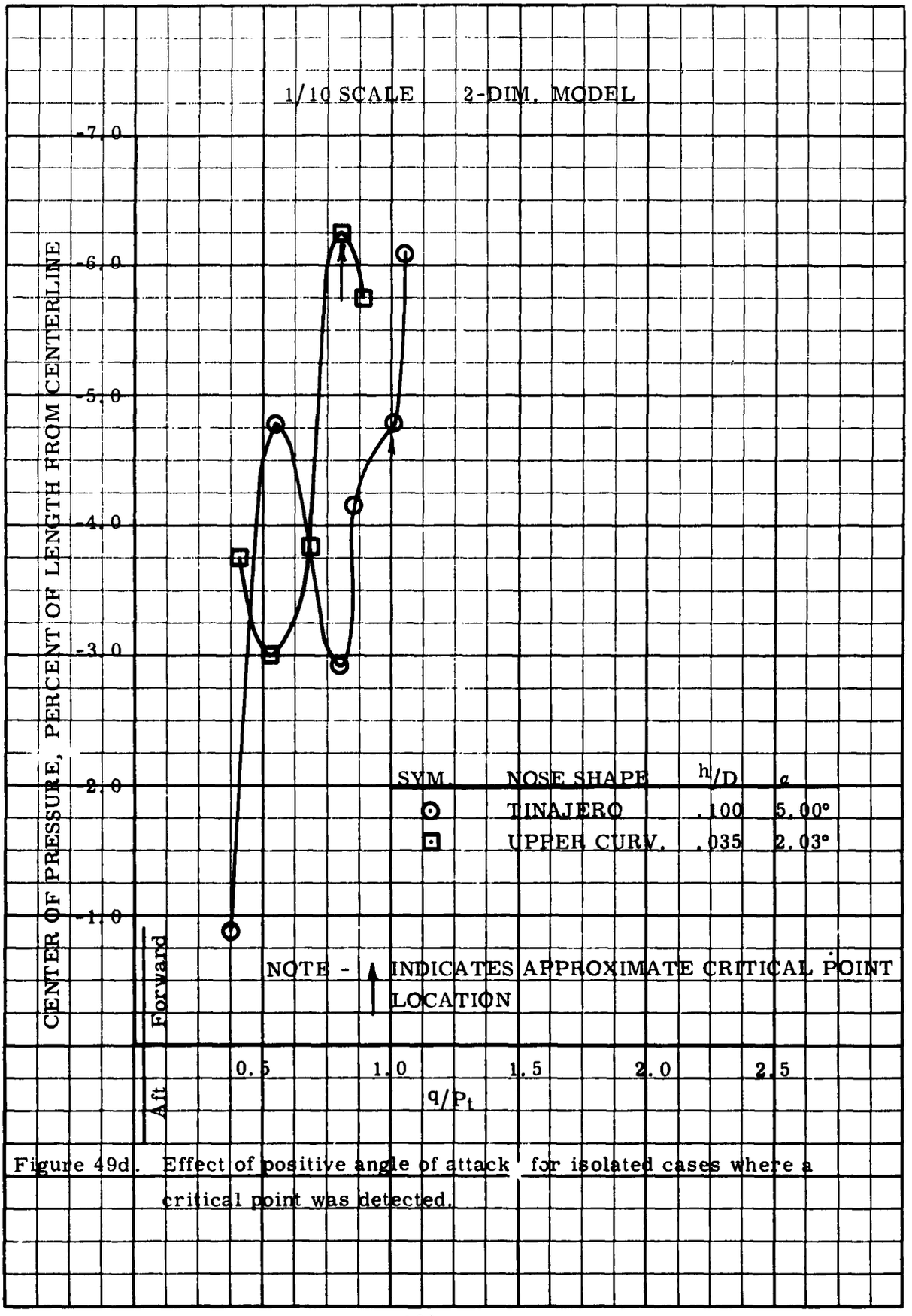


Figure 49d. Effect of positive angle of attack for isolated cases where a critical point was detected.

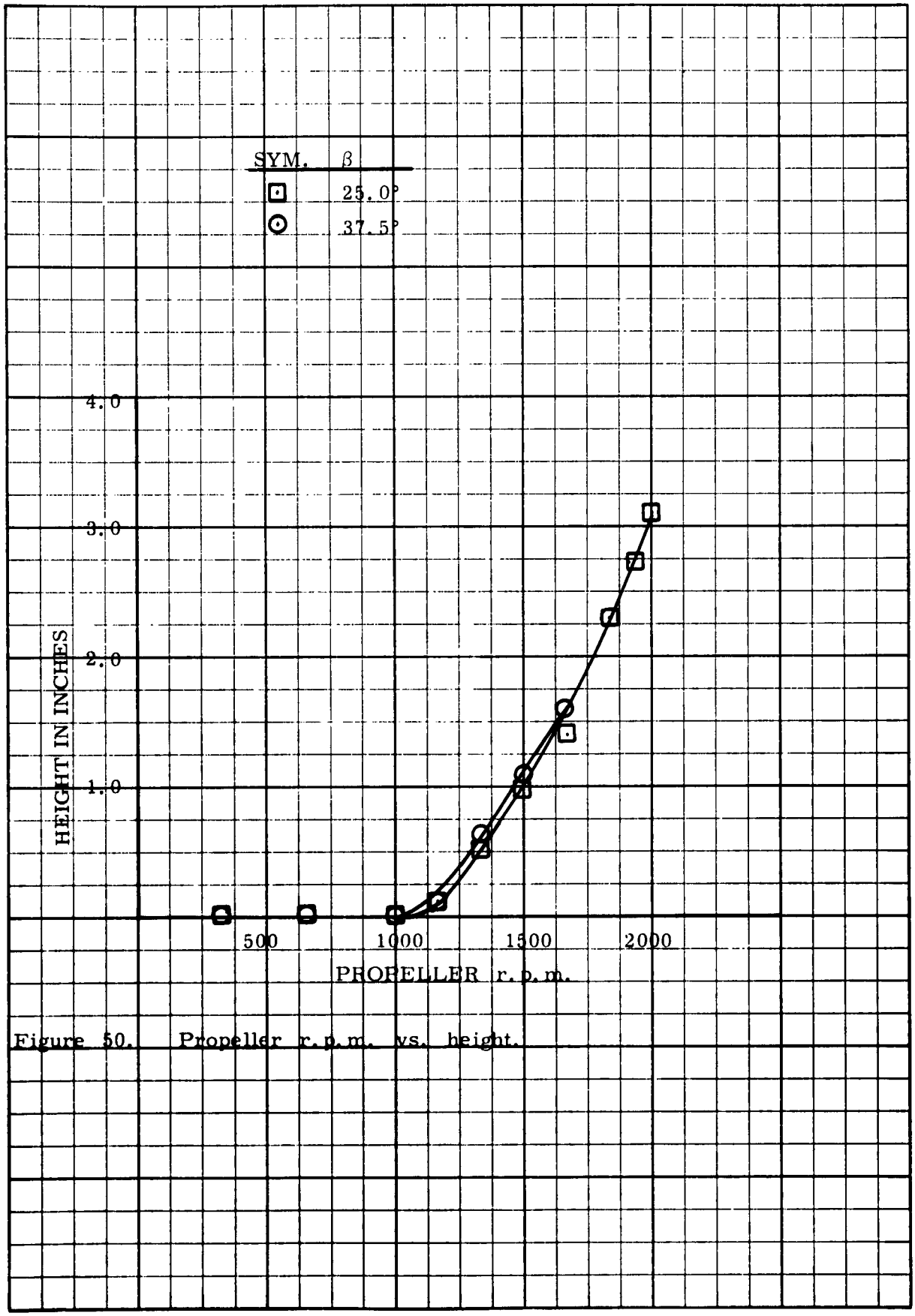


Figure 50. Propeller r.p.m. vs. height.

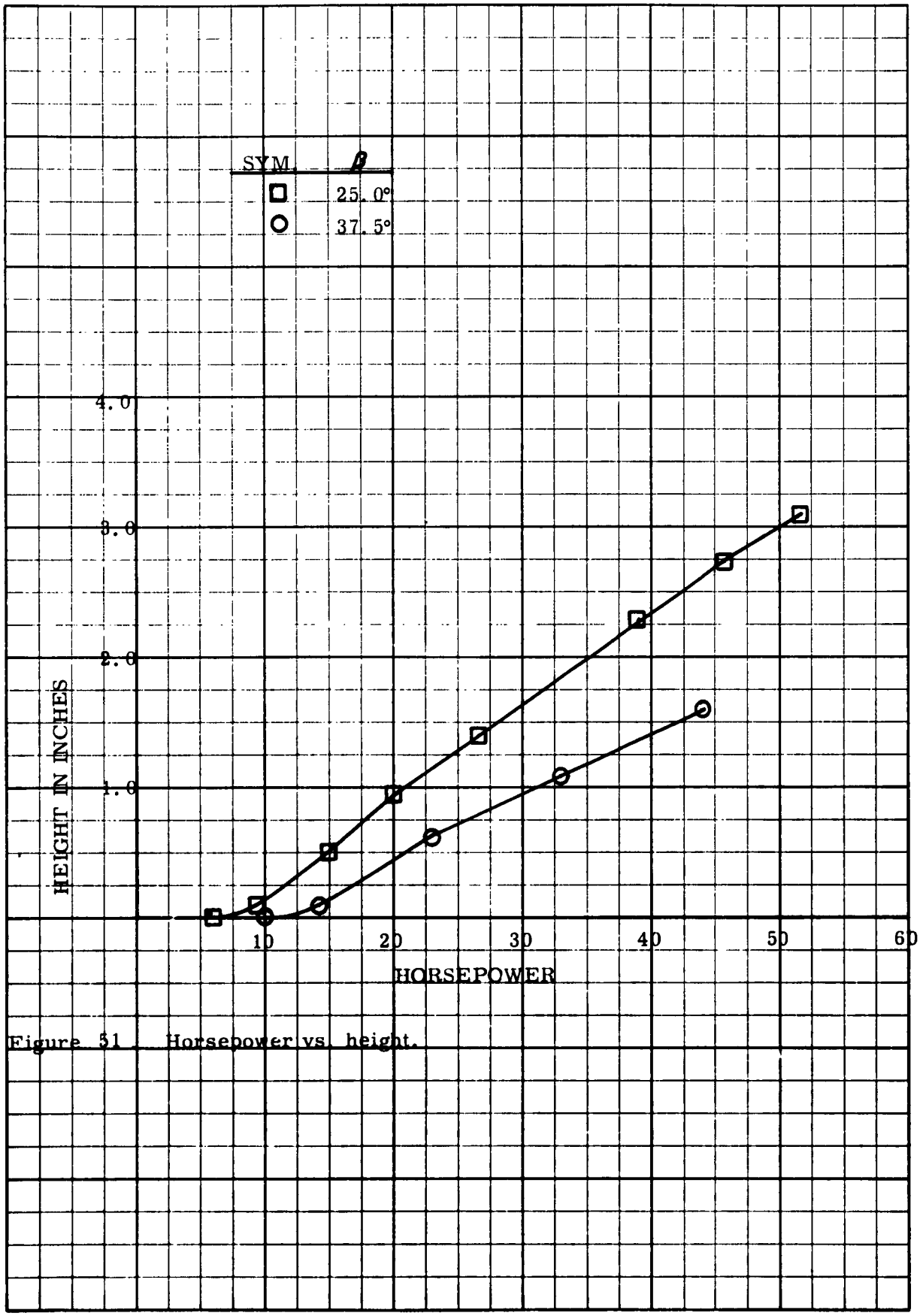


Figure 51. Horsepower vs. height.

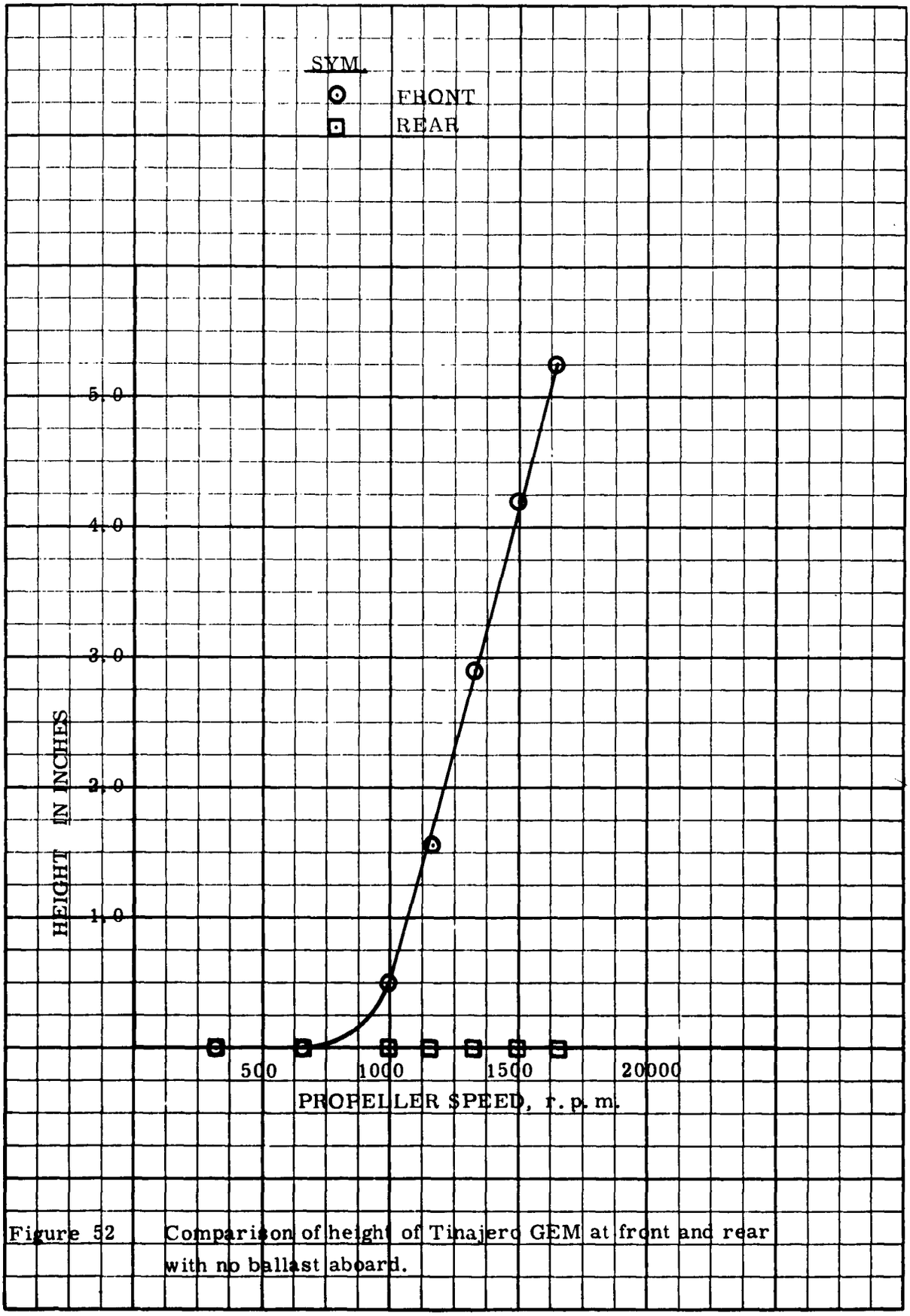


Figure 52 Comparison of height of Tinajero GEM at front and rear with no ballast aboard.

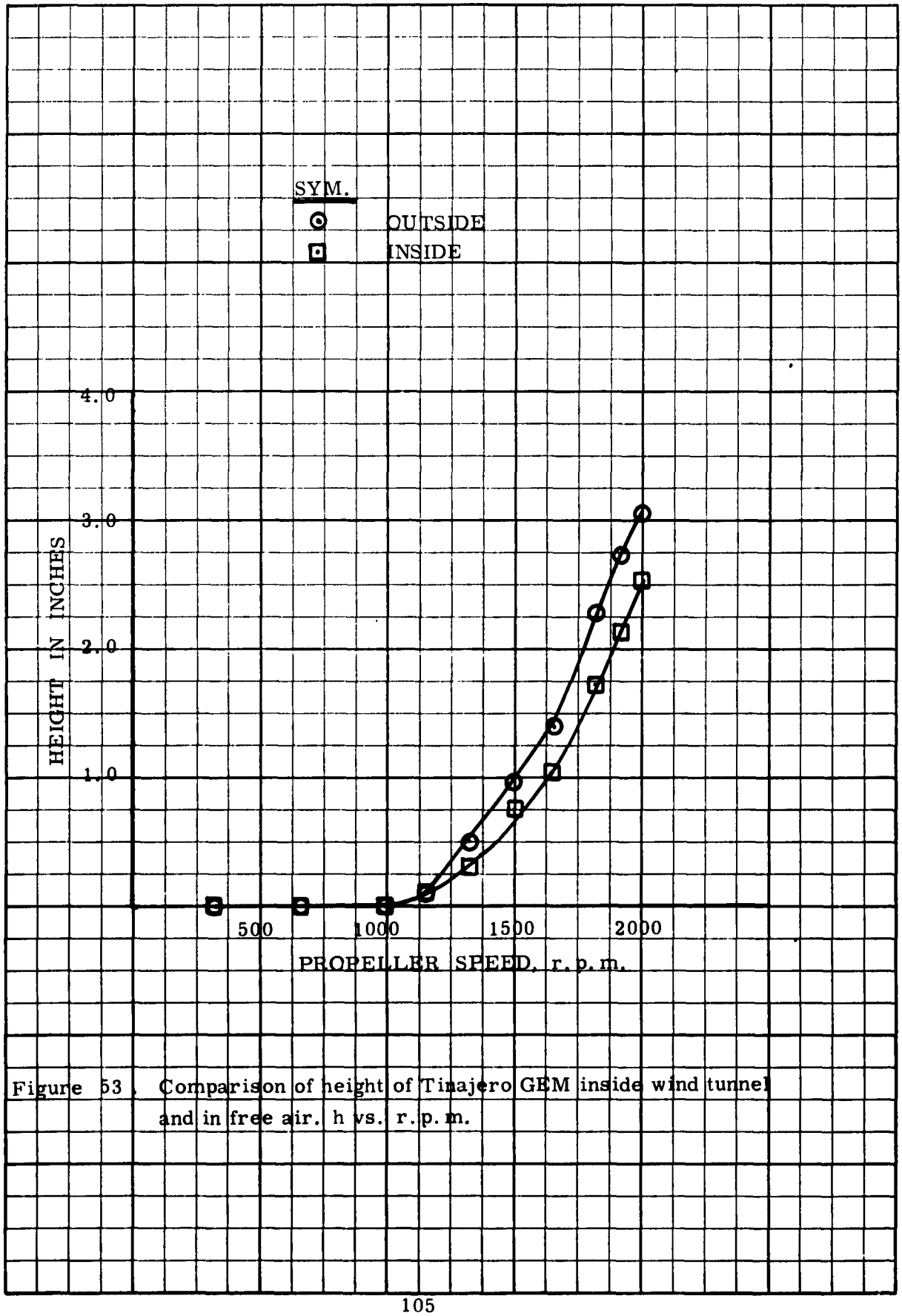


Figure 53. Comparison of height of Tinajero GEM inside wind tunnel and in free air. h vs. r.p.m.

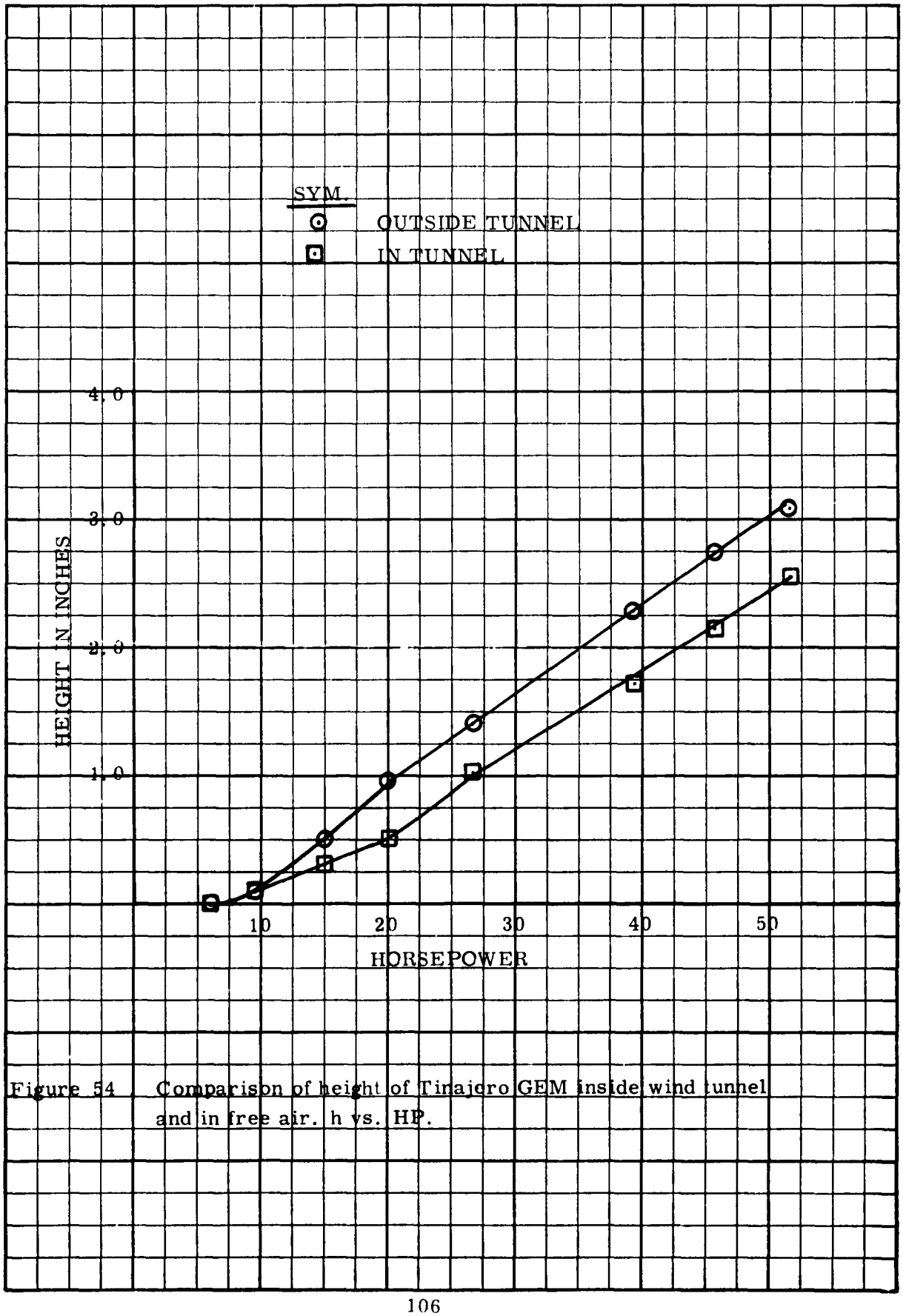


Figure 54. Comparison of height of Tinajero GEM inside wind tunnel and in free air. h vs. HP.

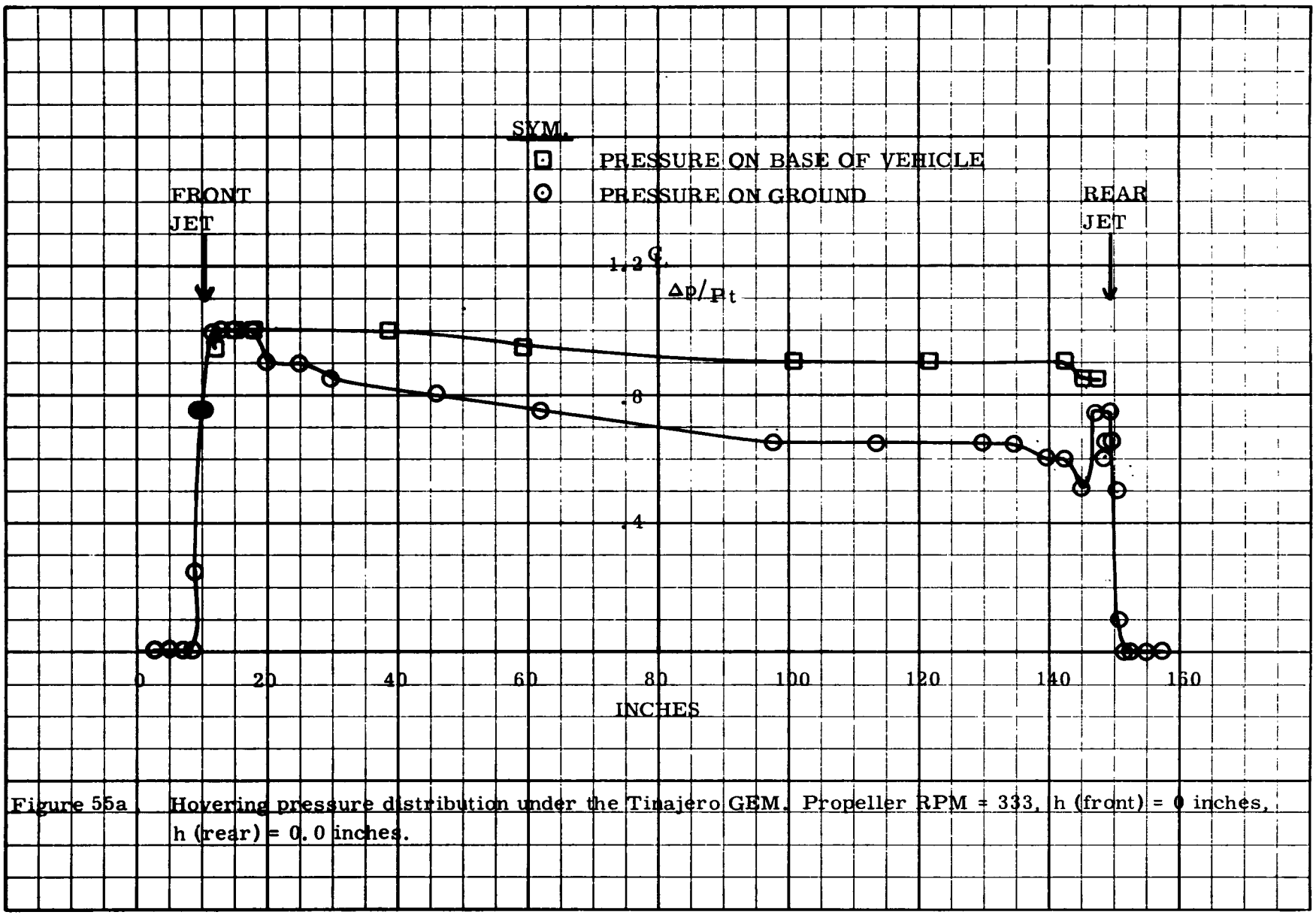


Figure 55a. Hovering pressure distribution under the Tinajero GEM. Propeller RPM = 333, h (front) = 0 inches, h (rear) = 0.0 inches.

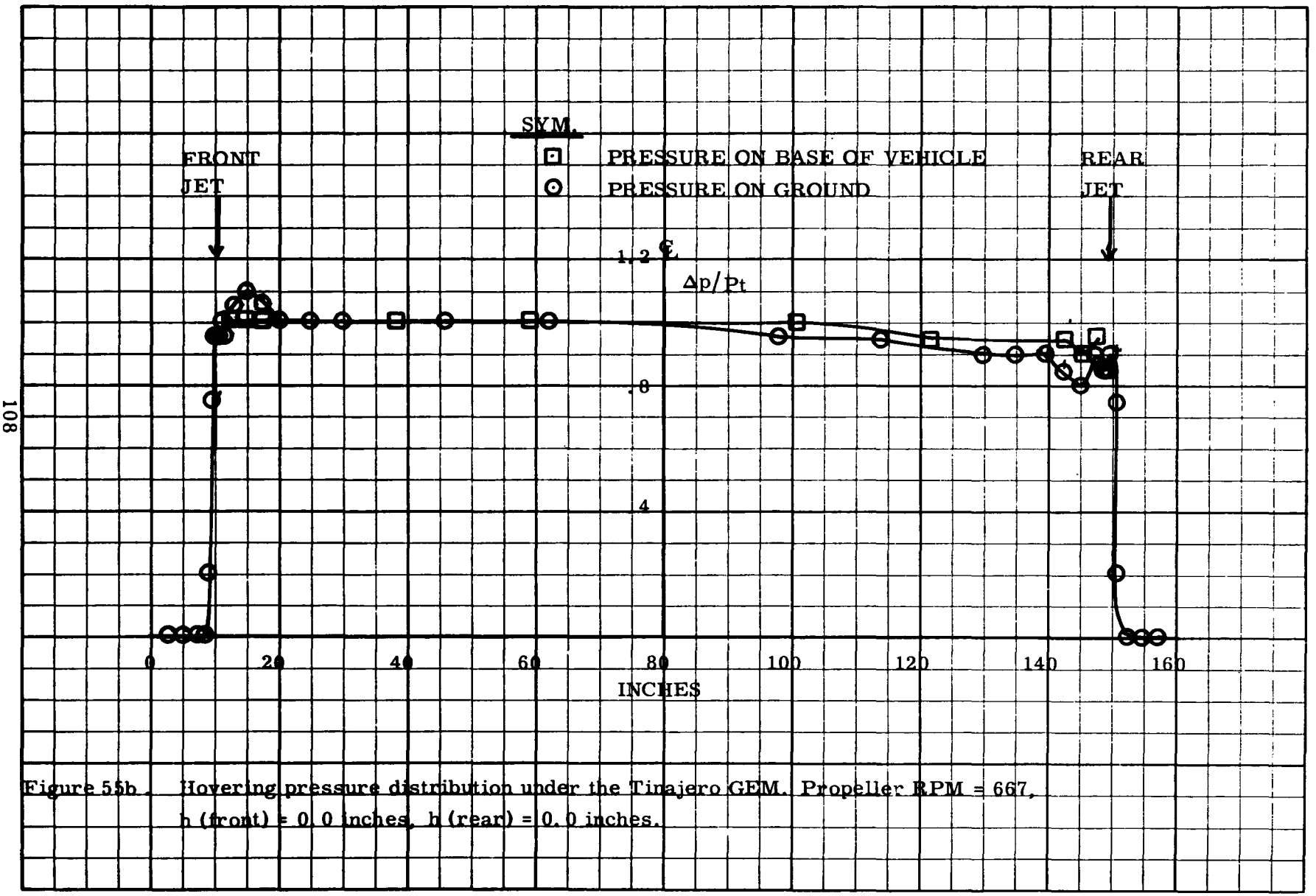


Figure 55b. Hovering pressure distribution under the Tinajero GEM. Propeller RPM = 667, h (front) = 0.0 inches, h (rear) = 0.0 inches.

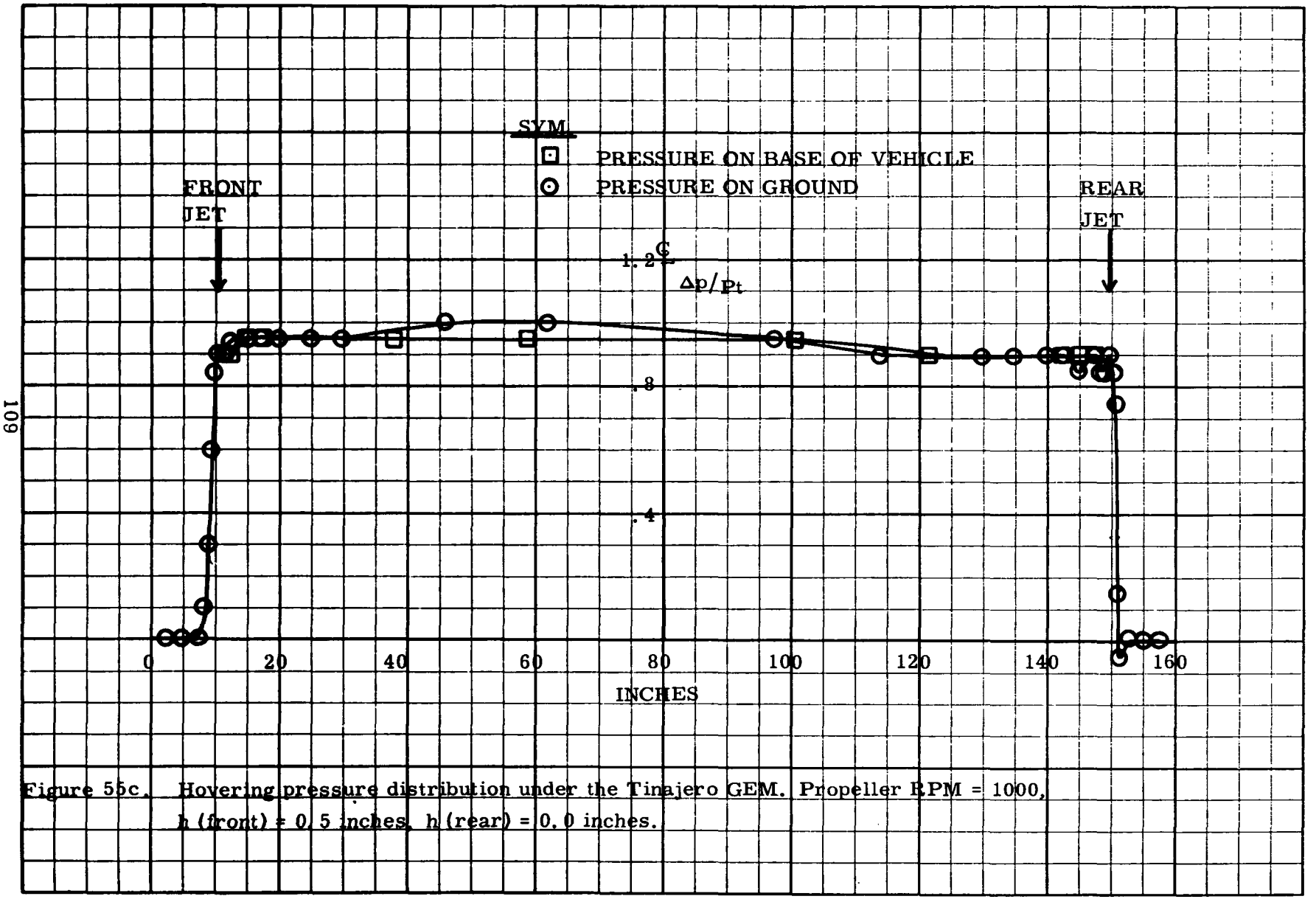


Figure 55c. Hovering pressure distribution under the Tinajero GEM. Propeller RPM = 1000, h (front) = 0.5 inches, h (rear) = 0.0 inches.

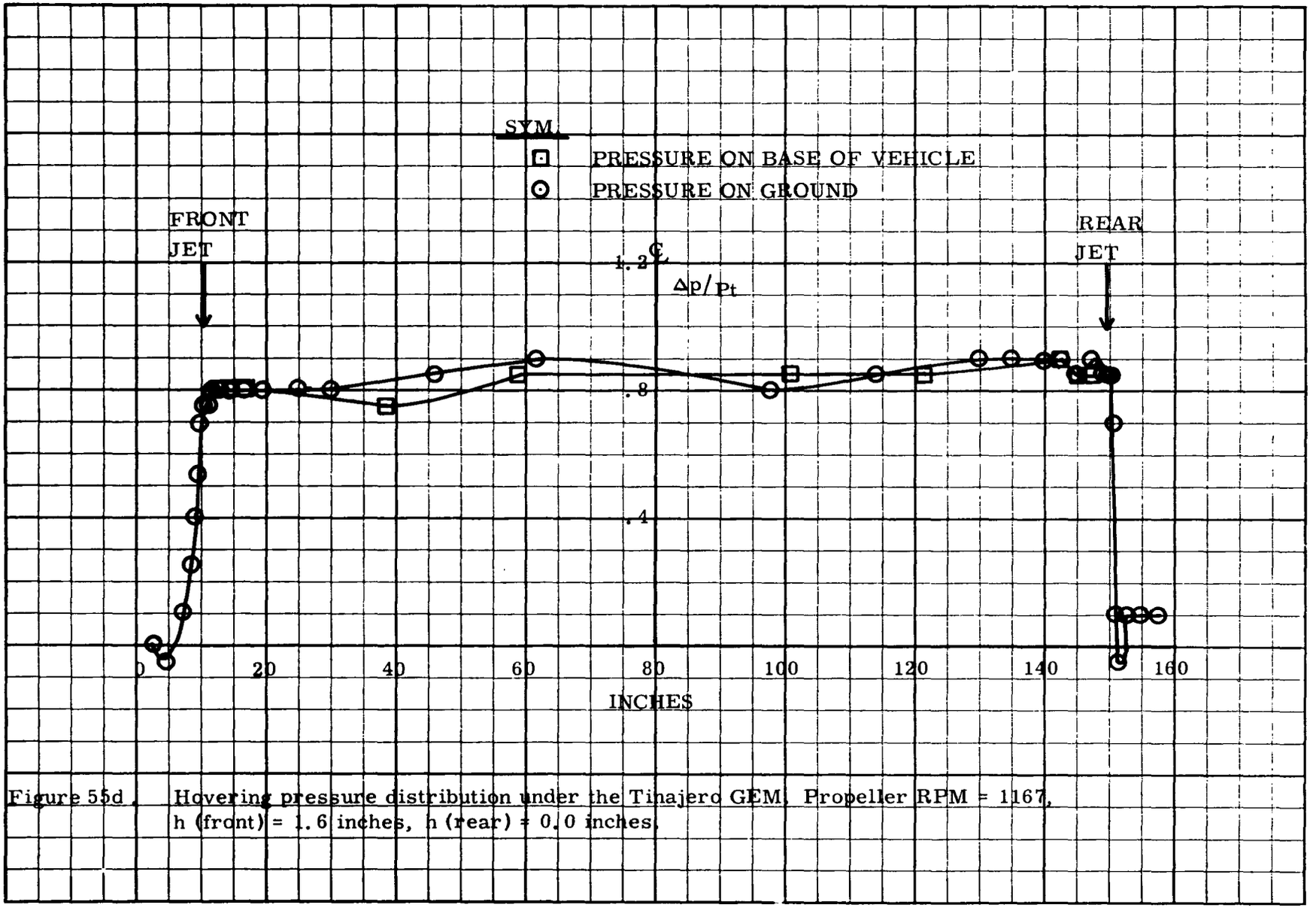


Figure 55d. Hovering pressure distribution under the Tinajero GEM. Propeller RPM = 1167, h (front) = 1.6 inches, h (rear) = 0.0 inches.

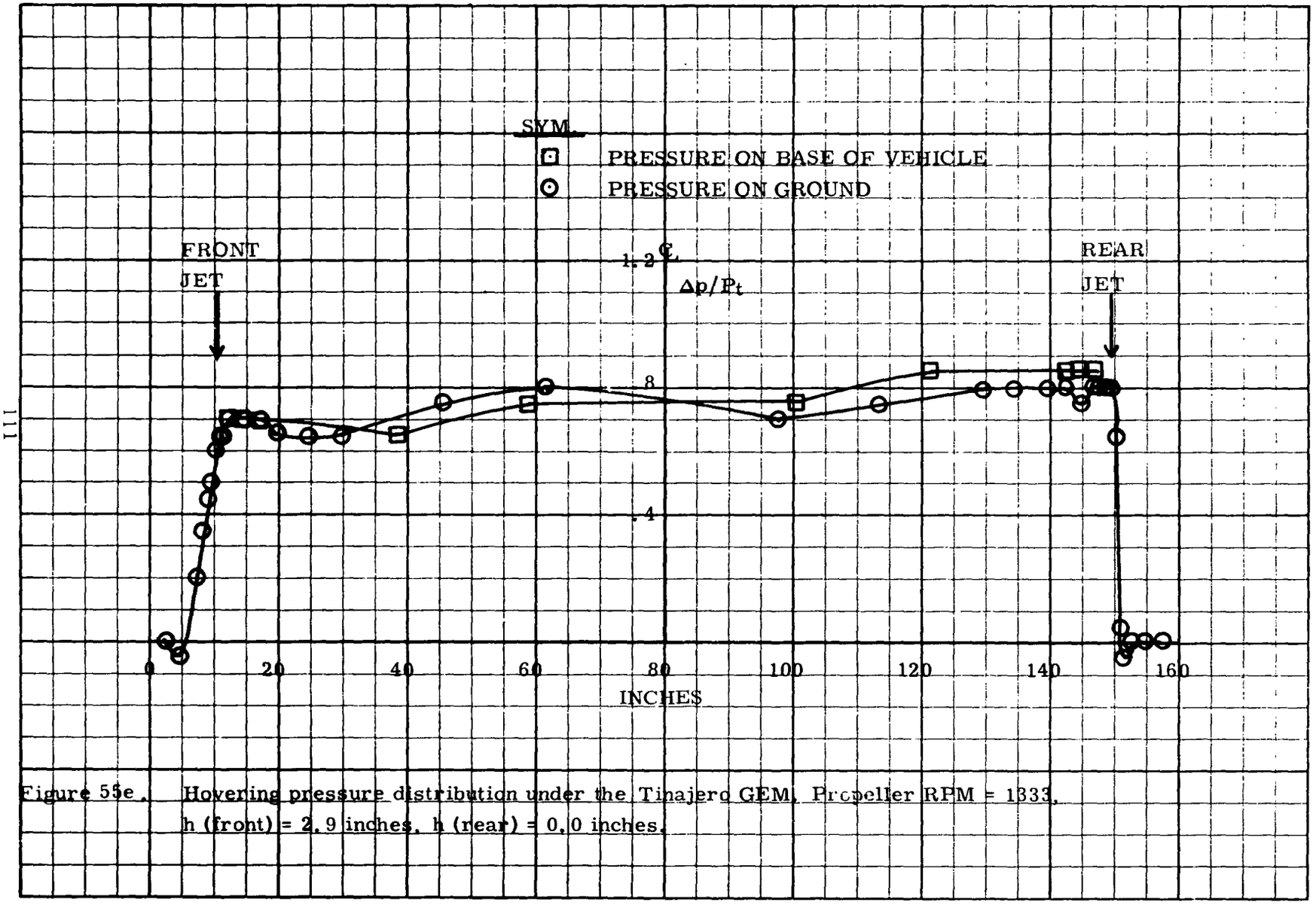


Figure 55e. Hovering pressure distribution under the Tinajero GEM. Propeller RPM = 1333, h (front) = 2.9 inches, h (rear) = 0.0 inches.

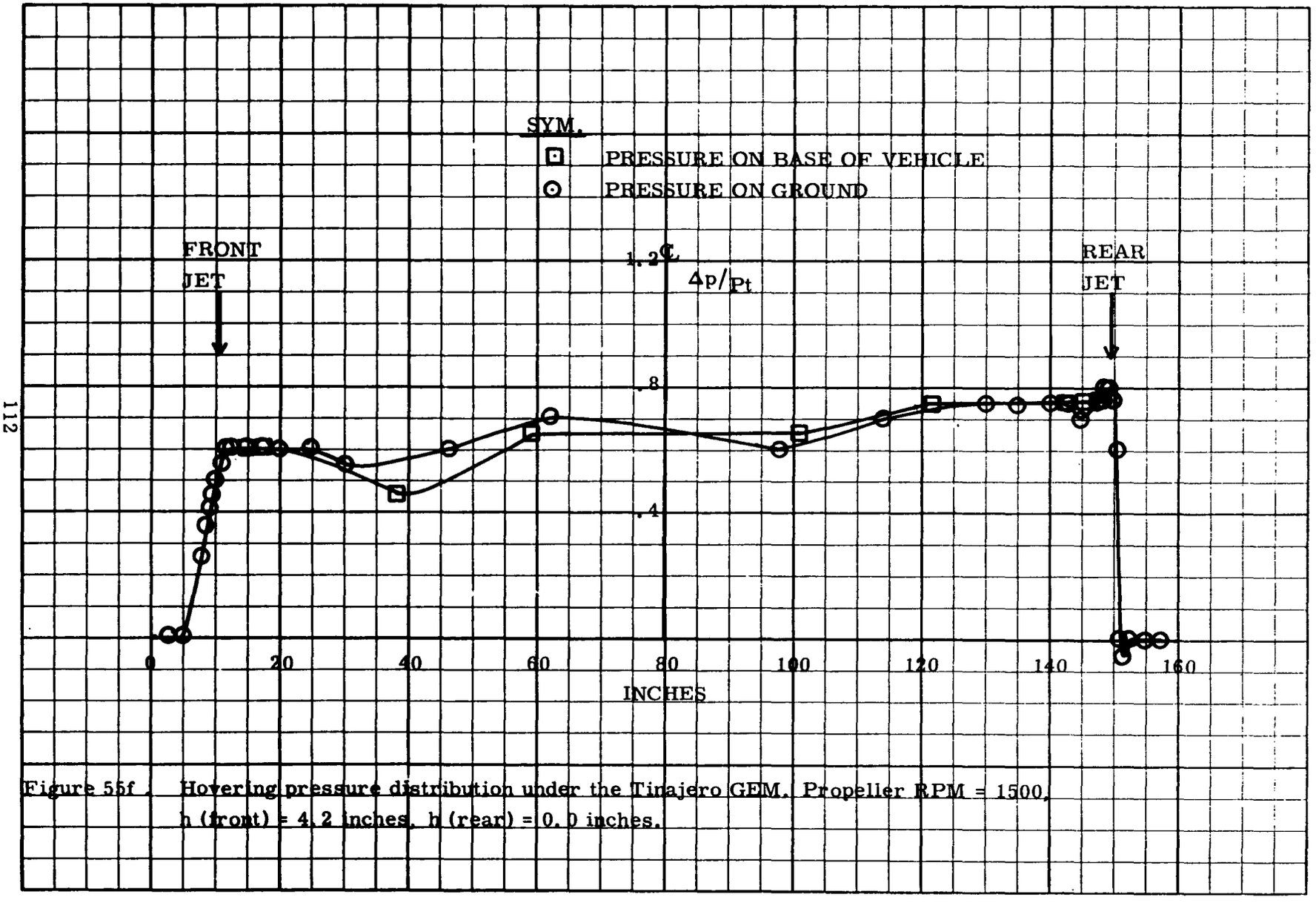


Figure 55f . Hovering pressure distribution under the Tinajero GEM. Propeller RPM = 1500, h (front) = 4.2 inches, h (rear) = 0.0 inches.

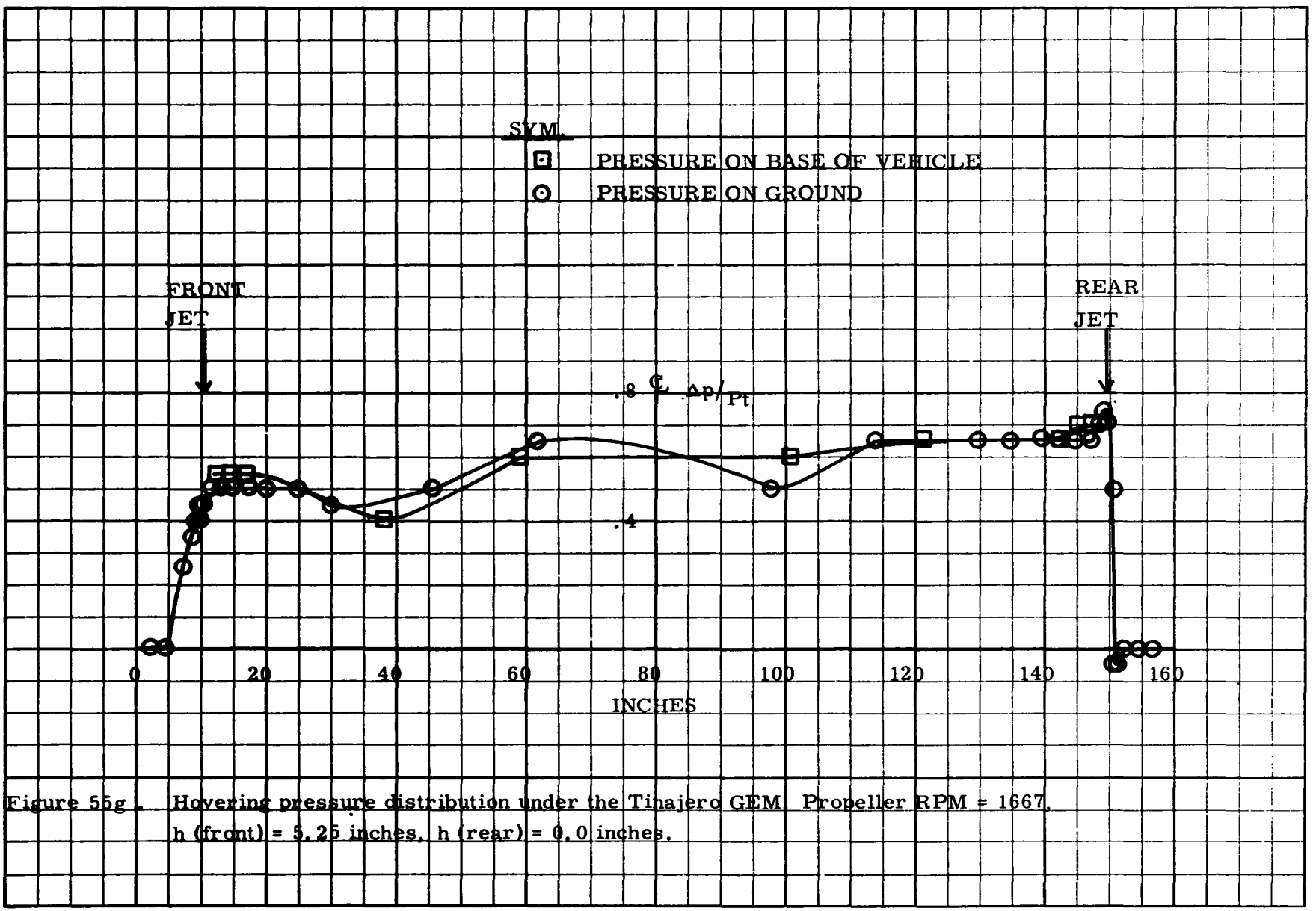


Figure 55g. Hovering pressure distribution under the Tinajero GEM. Propeller RPM = 1667, h (front) = 5.25 inches, h (rear) = 0.0 inches.

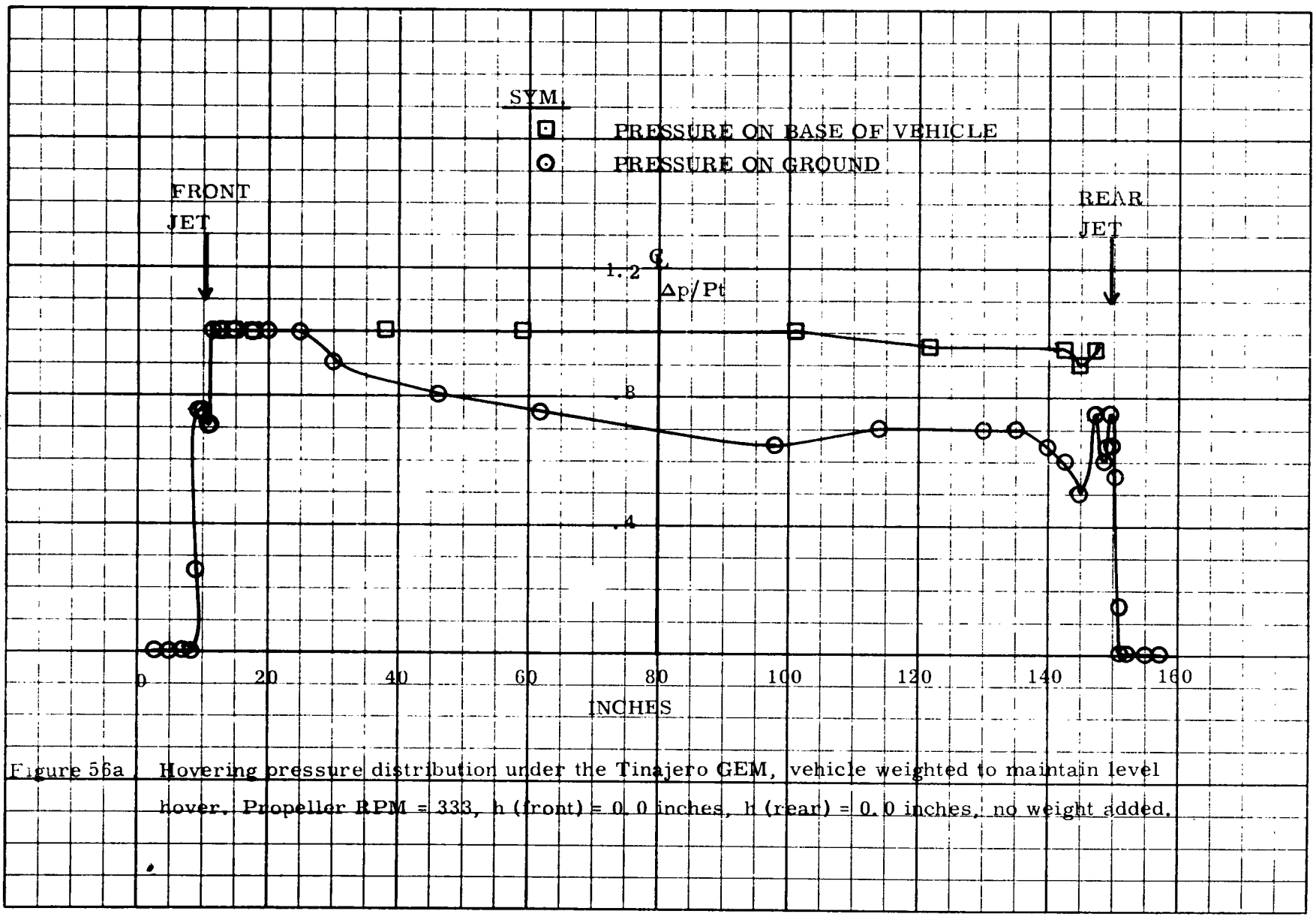


Figure 56a. Hovering pressure distribution under the Tinajero GEM, vehicle weighted to maintain level hover. Propeller RPM = 333, h (front) = 0.0 inches, h (rear) = 0.0 inches, no weight added.

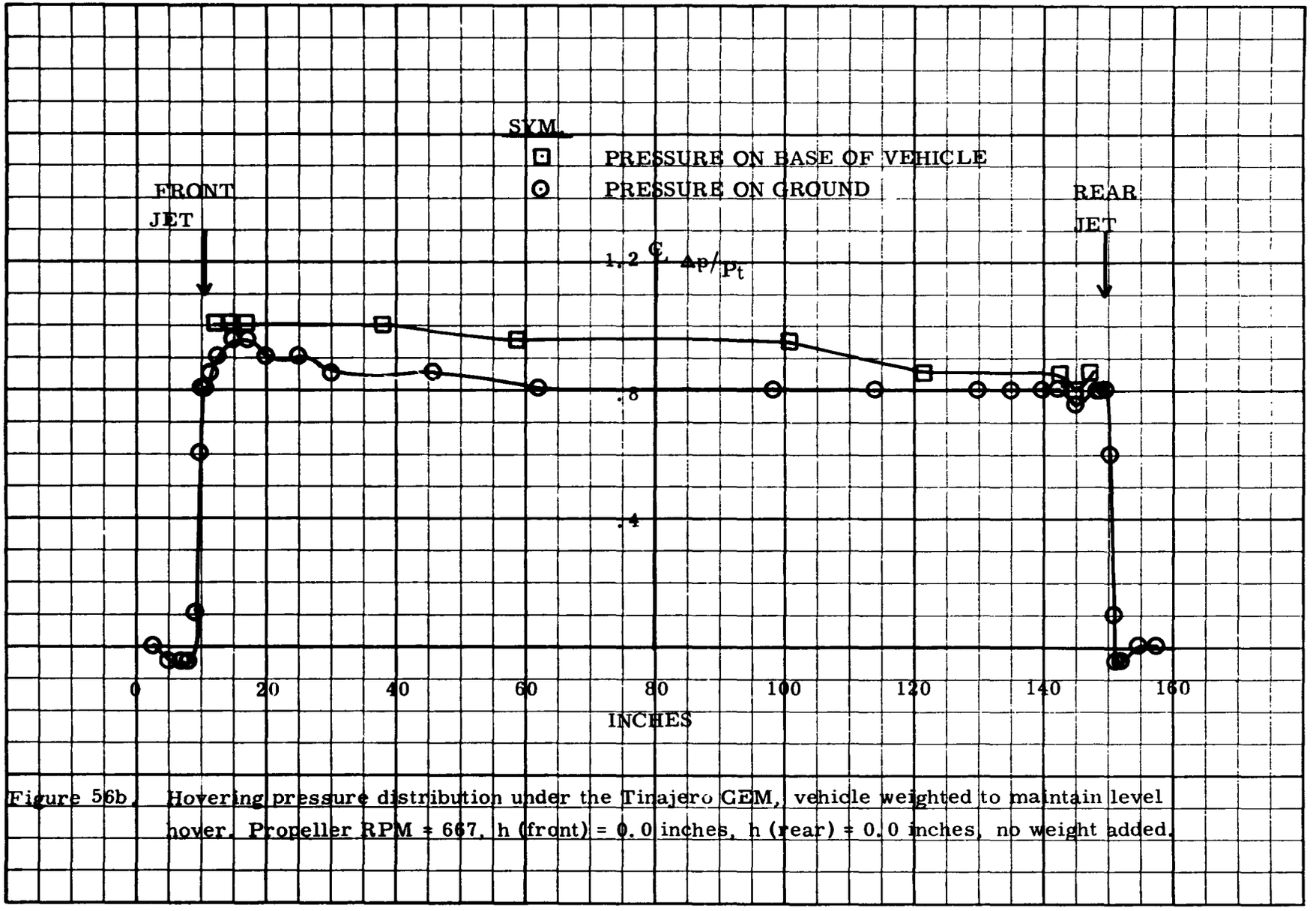


Figure 56b. Hovering pressure distribution under the Tinajero GEM, vehicle weighted to maintain level hover. Propeller RPM = 667, h (front) = 0.0 inches, h (rear) = 0.0 inches, no weight added.

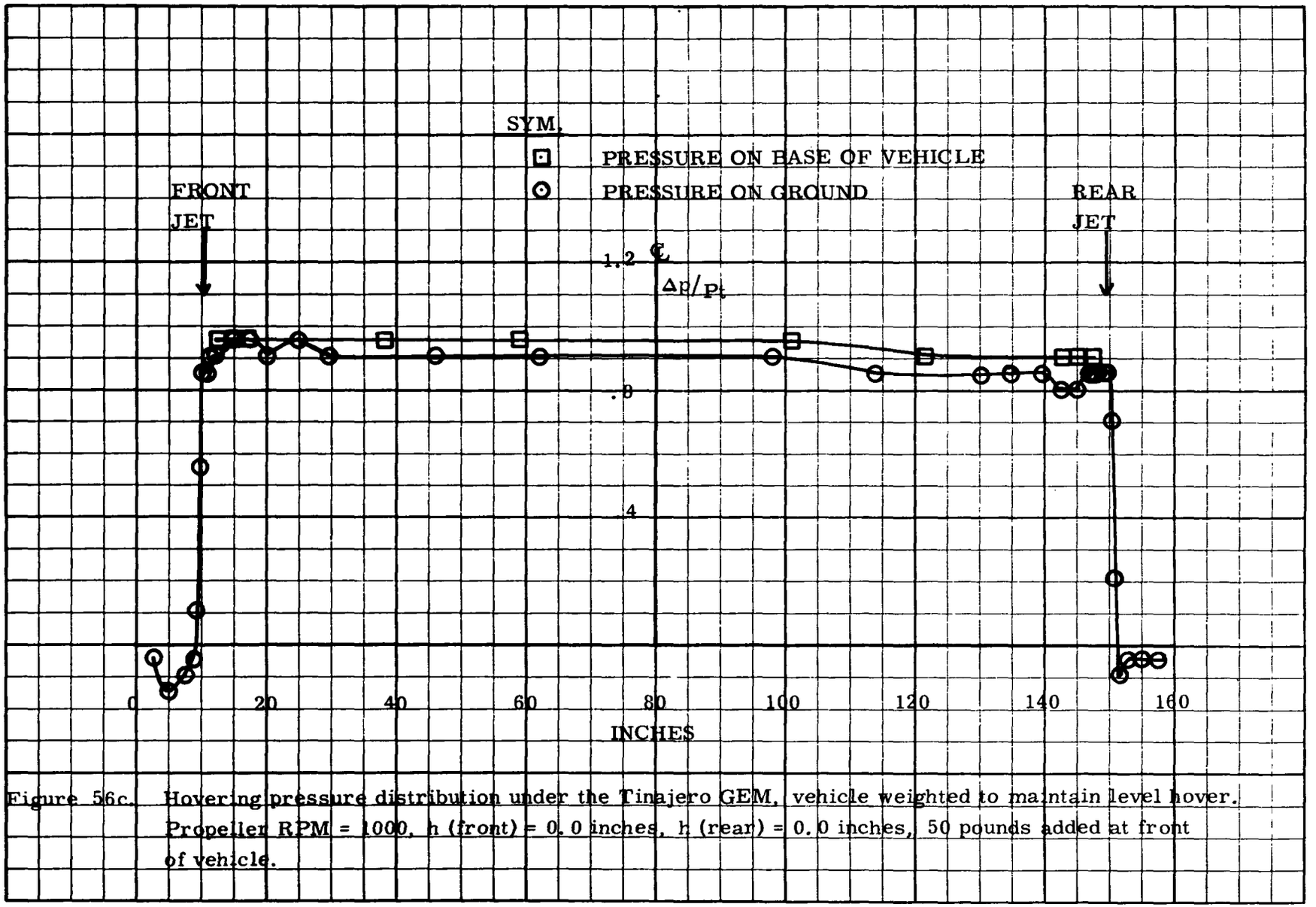


Figure 56c. Hovering pressure distribution under the Tinajero GEM, vehicle weighted to maintain level hover. Propeller RPM = 1000, h (front) = 0.0 inches, h (rear) = 0.0 inches, 50 pounds added at front of vehicle.

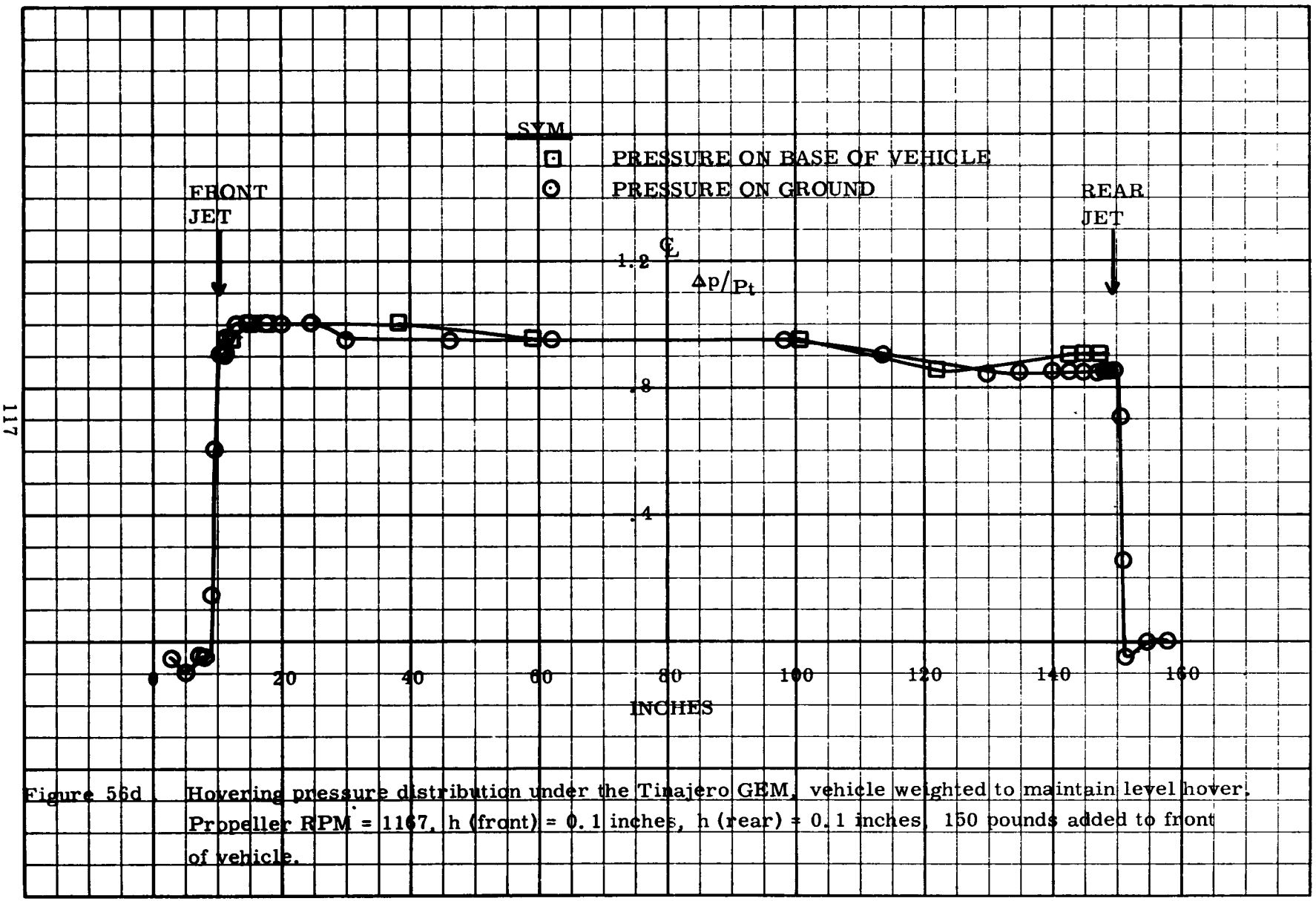


Figure 56d Hovering pressure distribution under the Tinajero GEM, vehicle weighted to maintain level hover. Propeller RPM = 1167, h (front) = 0.1 inches, h (rear) = 0.1 inches, 150 pounds added to front of vehicle.

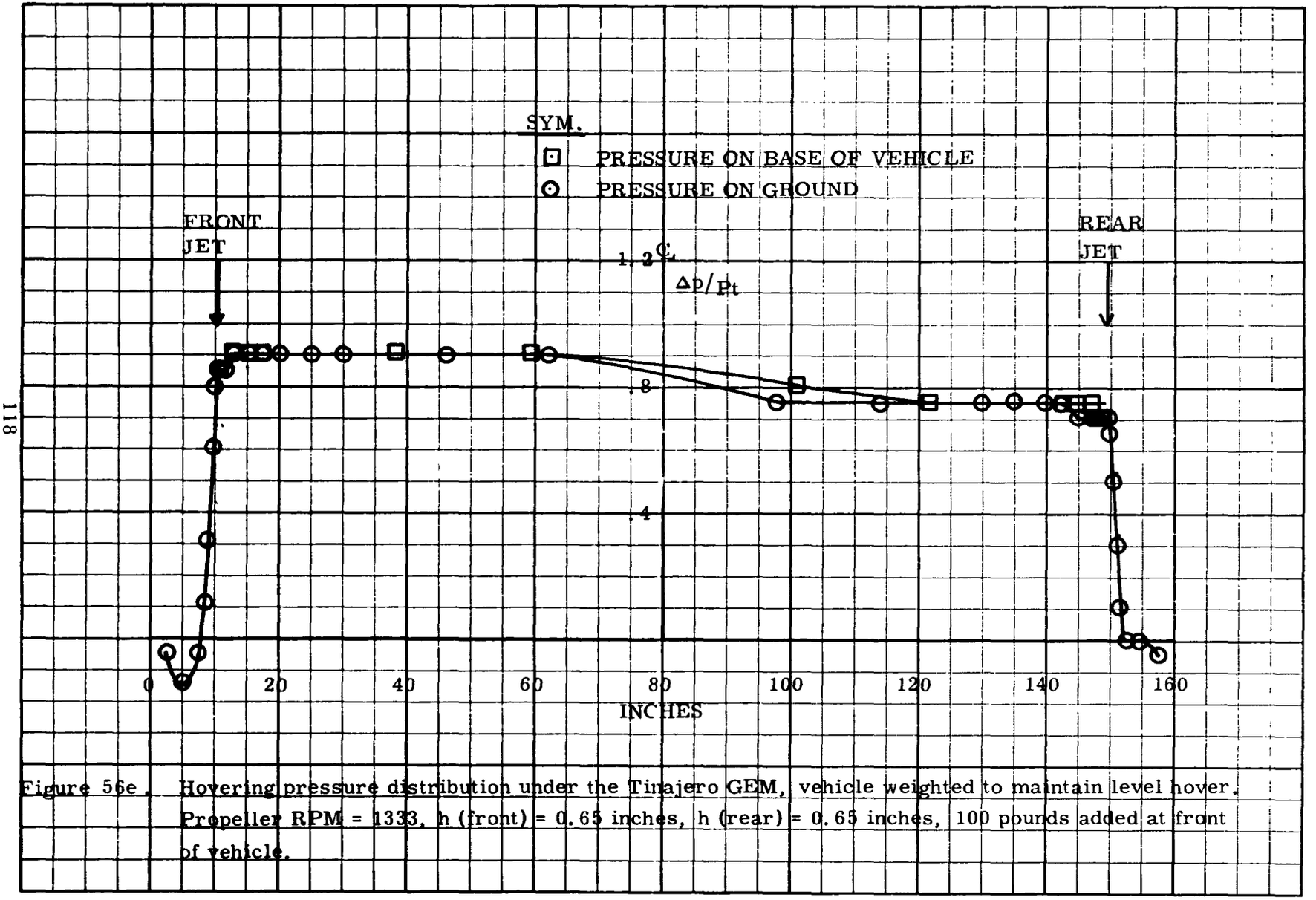


Figure 56e. Hovering pressure distribution under the Tinajero GEM, vehicle weighted to maintain level hover. Propeller RPM = 1333, h (front) = 0.65 inches, h (rear) = 0.65 inches, 100 pounds added at front of vehicle.

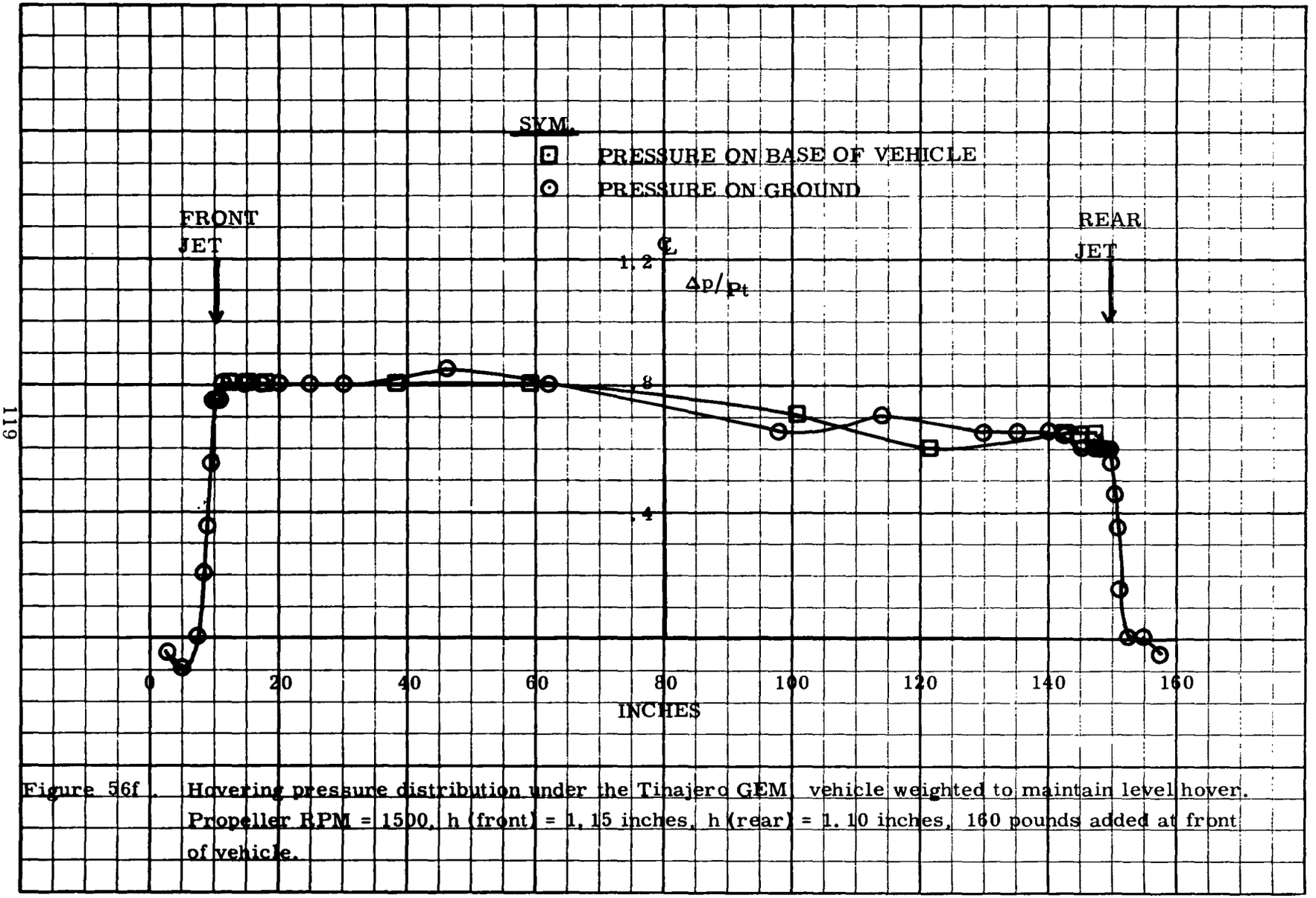


Figure 56f. Hovering pressure distribution under the Tinajero GEM vehicle weighted to maintain level hover. Propeller RPM = 1500, h (front) = 1.15 inches, h (rear) = 1.10 inches, 160 pounds added at front of vehicle.

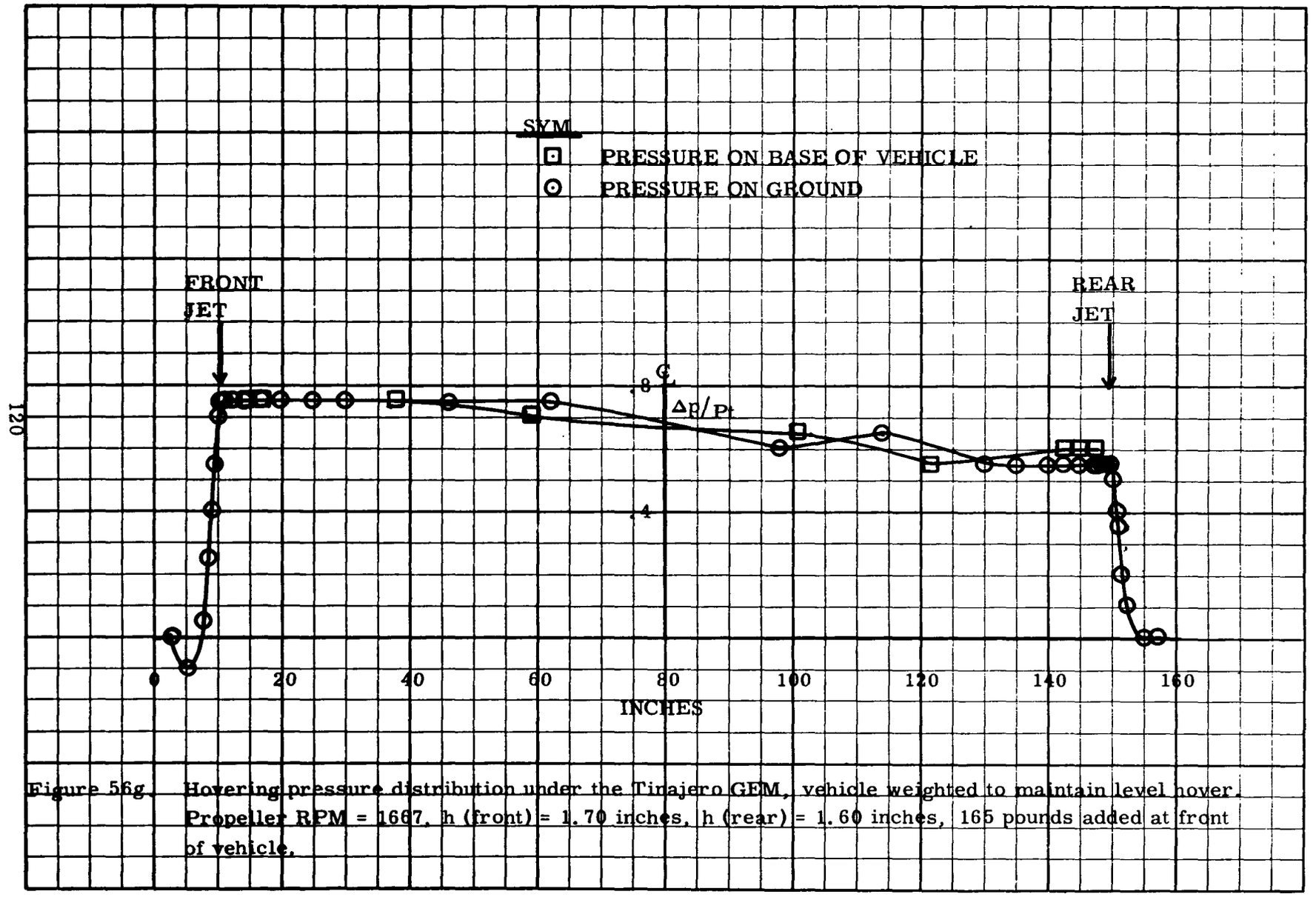


Figure 56g. Hovering pressure distribution under the Tinajero GEM, vehicle weighted to maintain level hover. Propeller RPM = 1667, h (front) = 1.70 inches, h (rear) = 1.60 inches, 165 pounds added at front of vehicle.

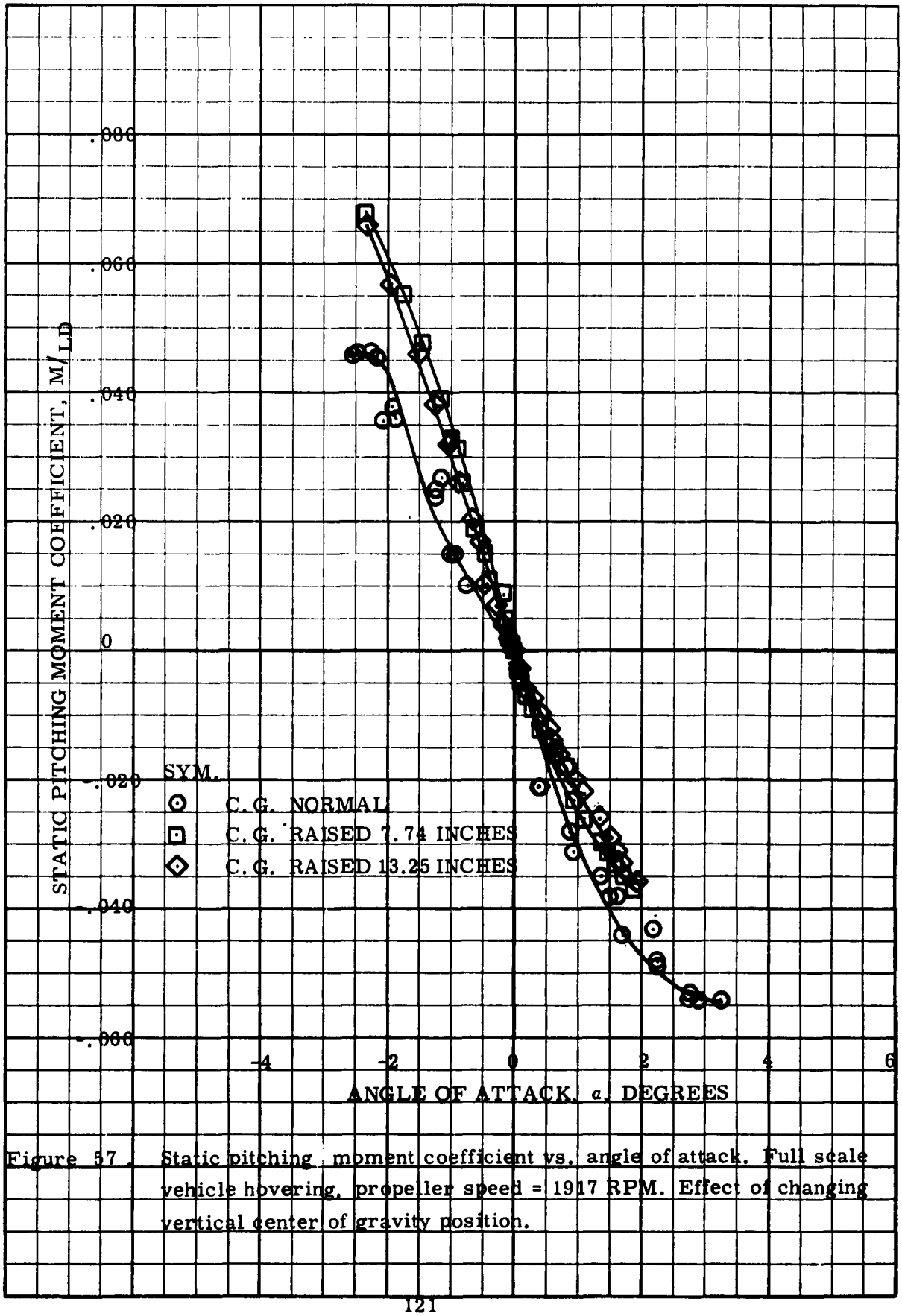


Figure 57. Static pitching moment coefficient vs. angle of attack. Full scale vehicle hovering, propeller speed = 1917 RPM. Effect of changing vertical center of gravity position.

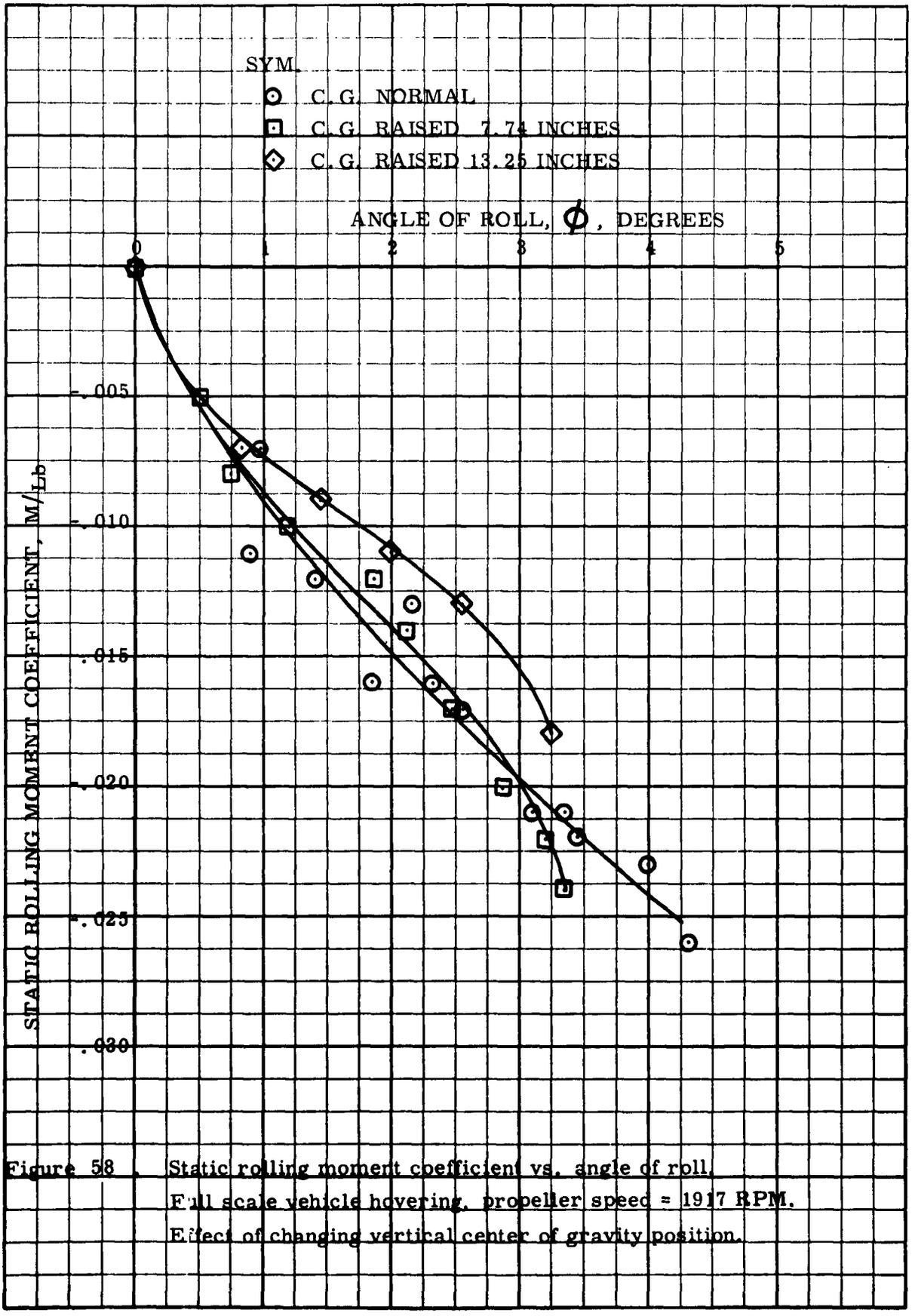


Figure 58. Static rolling moment coefficient vs. angle of roll. Full scale vehicle hovering, propeller speed = 1917 RPM. Effect of changing vertical center of gravity position.

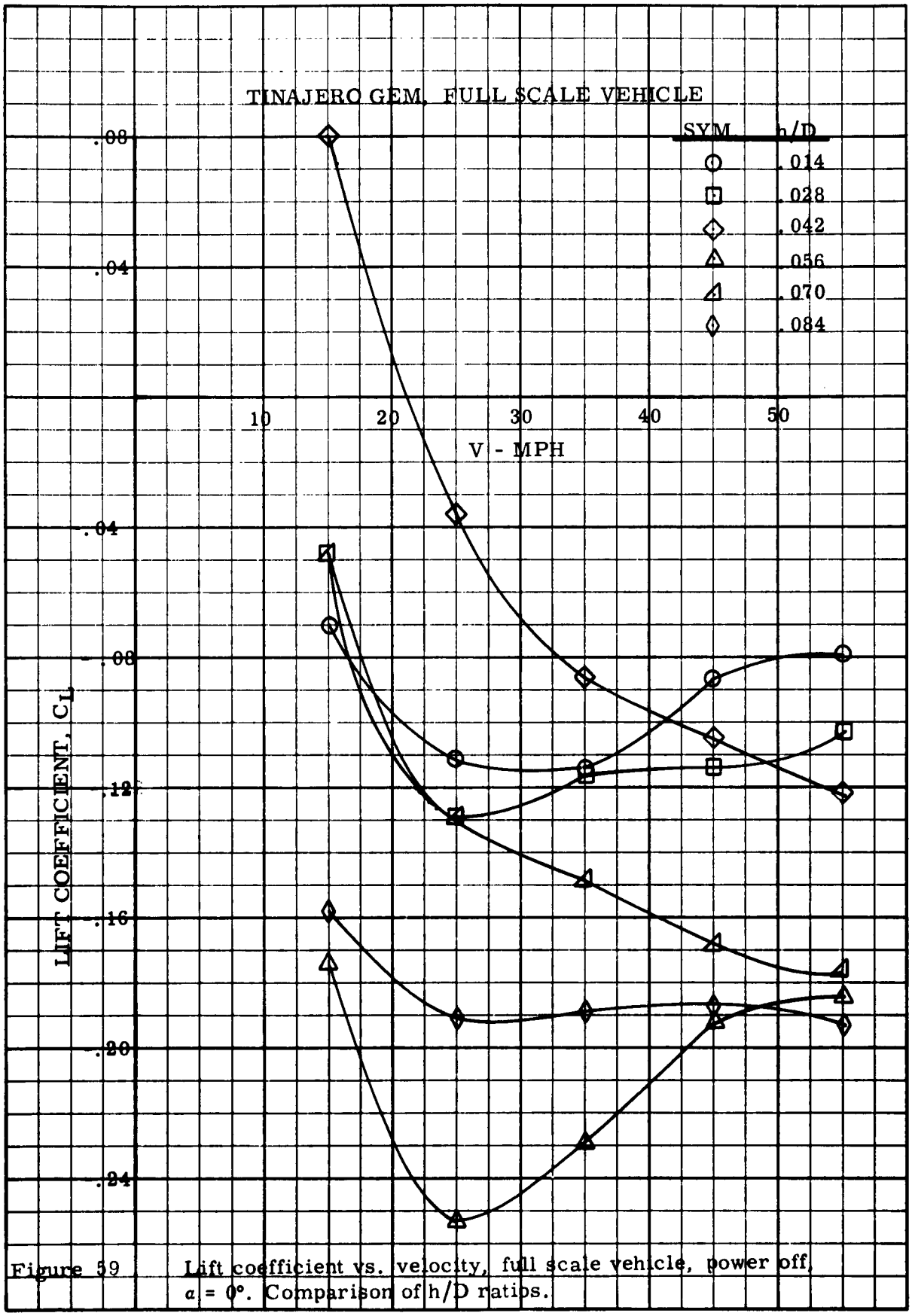


Figure 59 Lift coefficient vs. velocity, full scale vehicle, power off, $\alpha = 0°$. Comparison of h/D ratios.

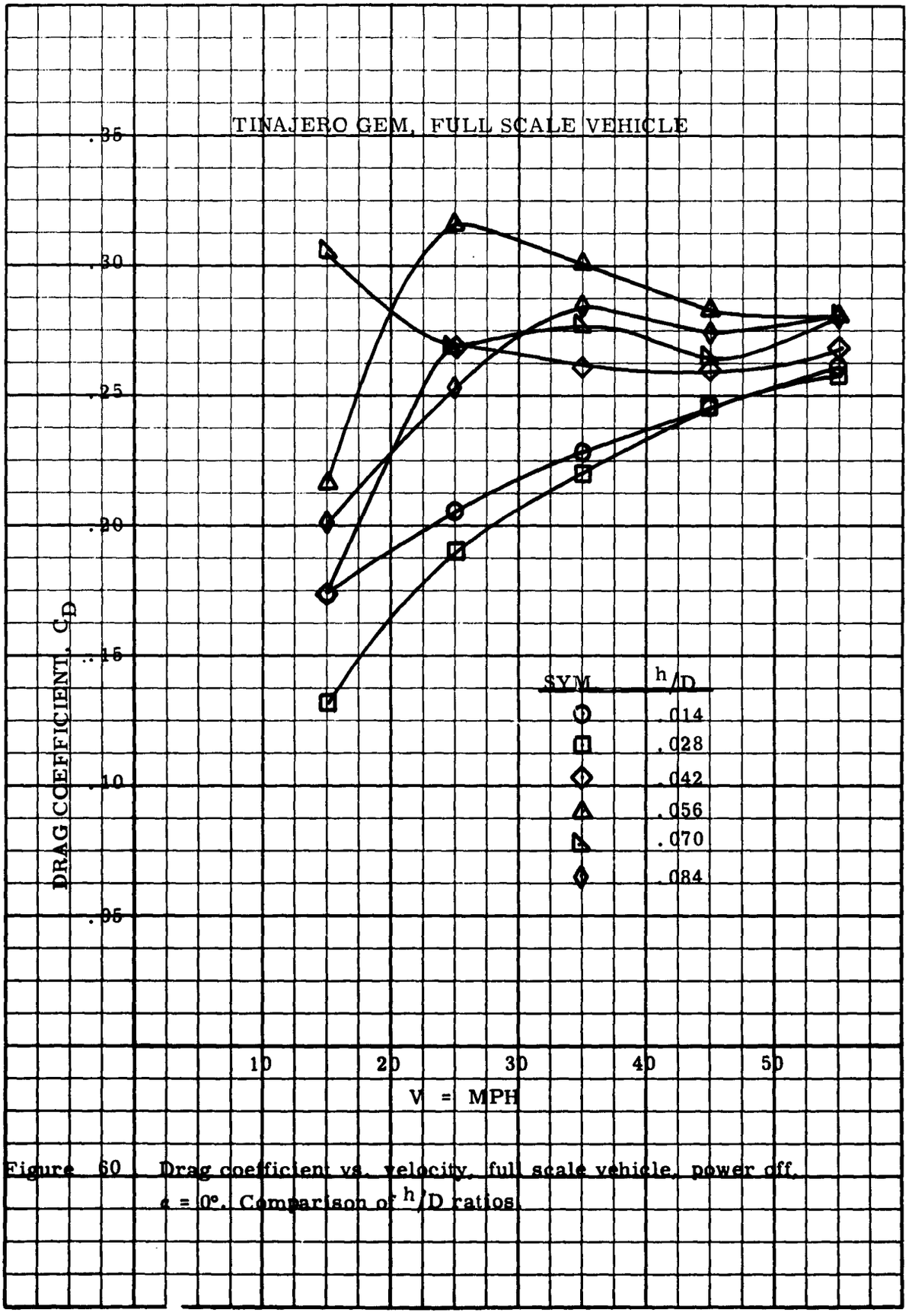


Figure 60. Drag coefficient vs. velocity, full scale vehicle, power off, $\alpha = 0°$. Comparison of $h/D$ ratios.

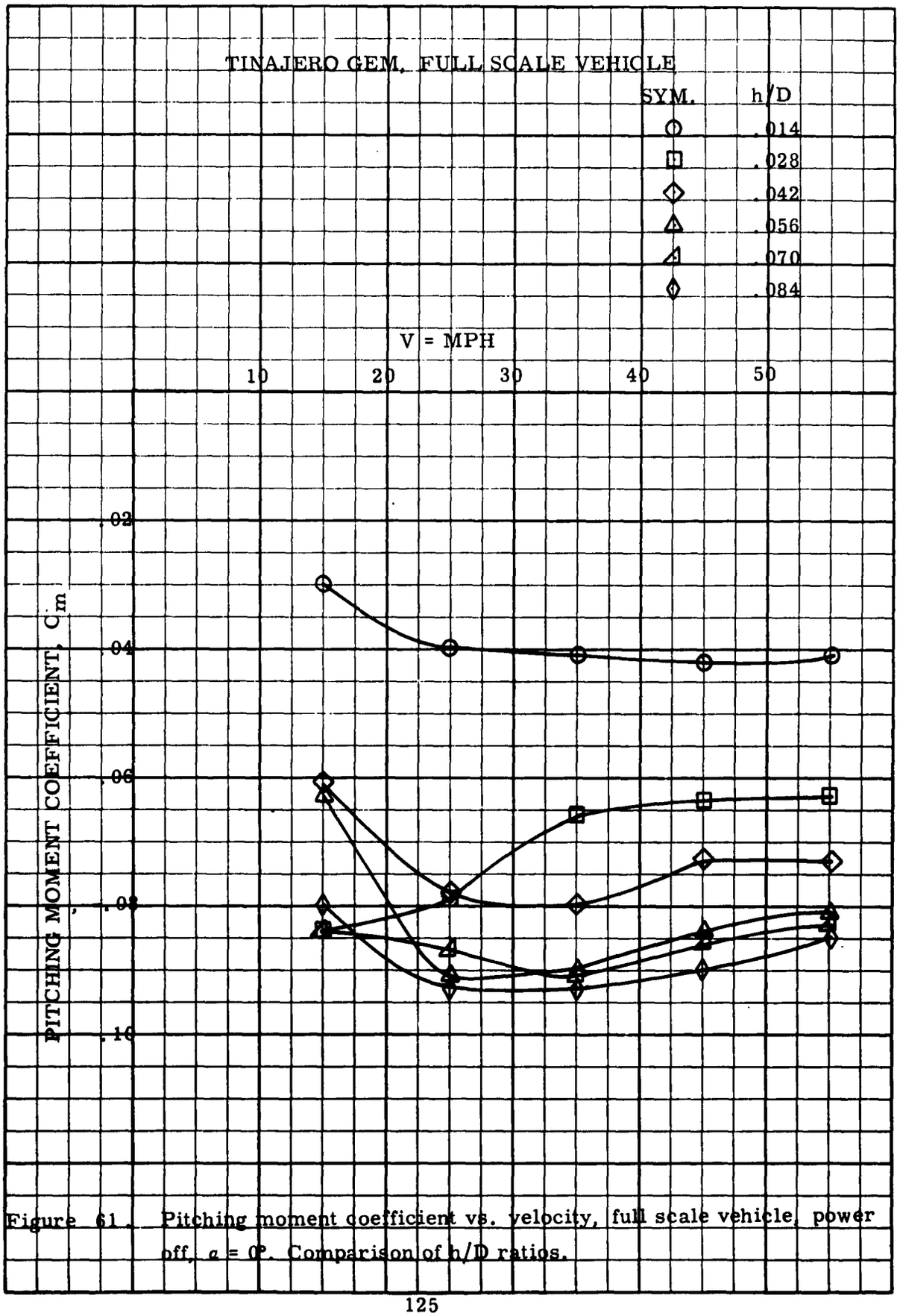


Figure 61. Pitching moment coefficient vs. velocity, full scale vehicle, power off, $\alpha = 0°$. Comparison of h/D ratios.

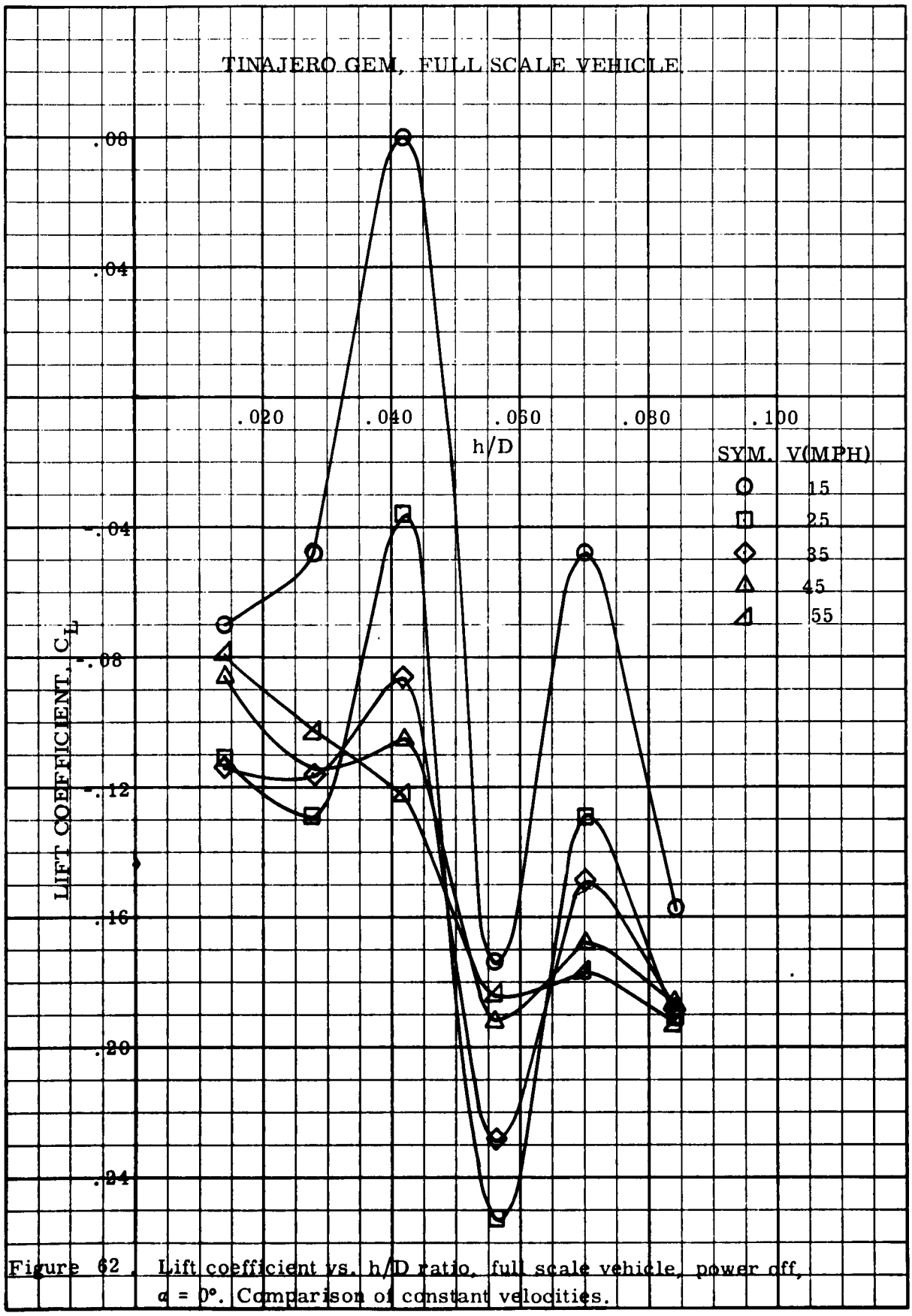


Figure 62. Lift coefficient vs. h/D ratio, full scale vehicle, power off, $\alpha = 0°$. Comparison of constant velocities.

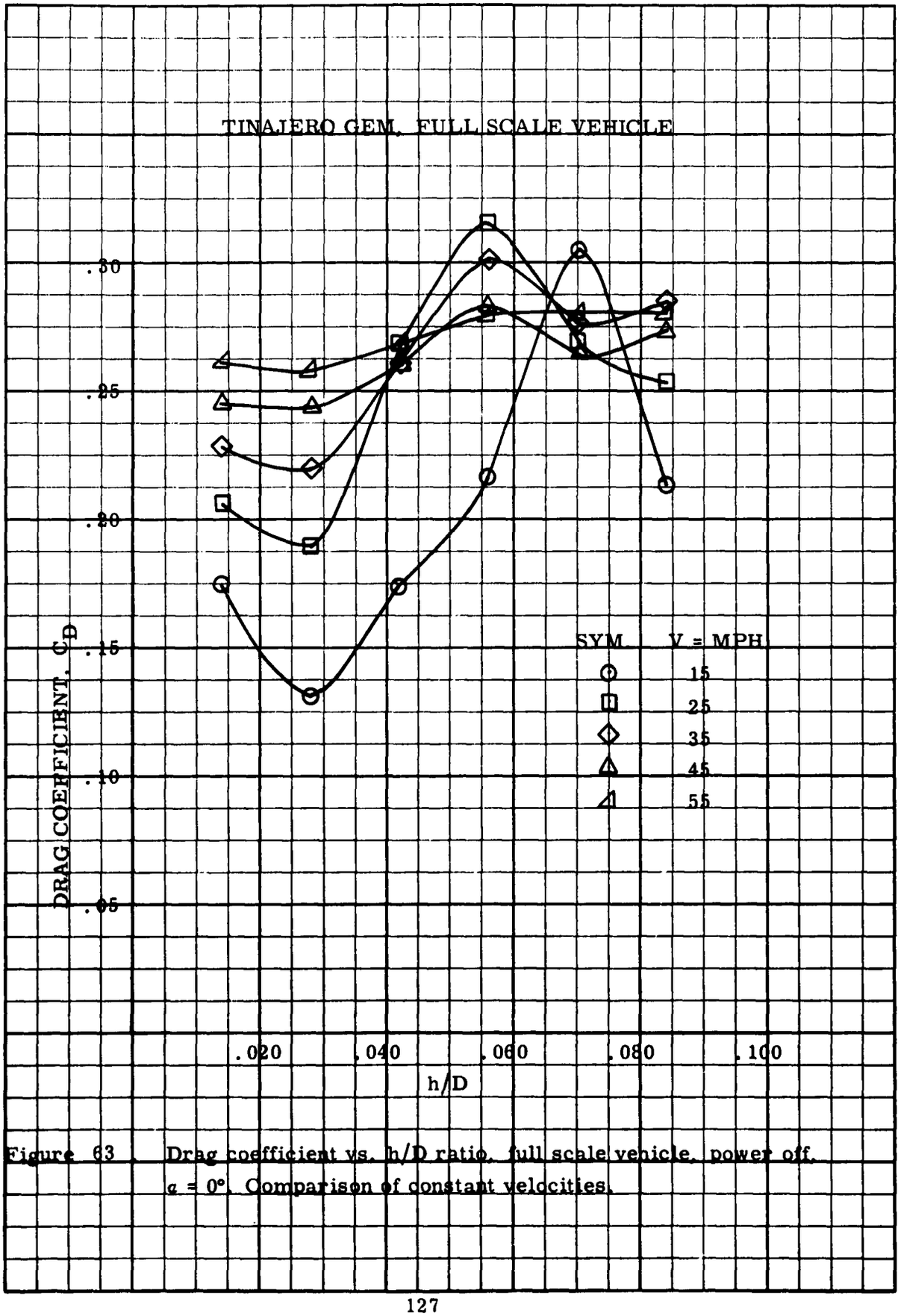


Figure 63. Drag coefficient vs. h/D ratio, full scale vehicle, power off, $\alpha = 0°$, Comparison of constant velocities.

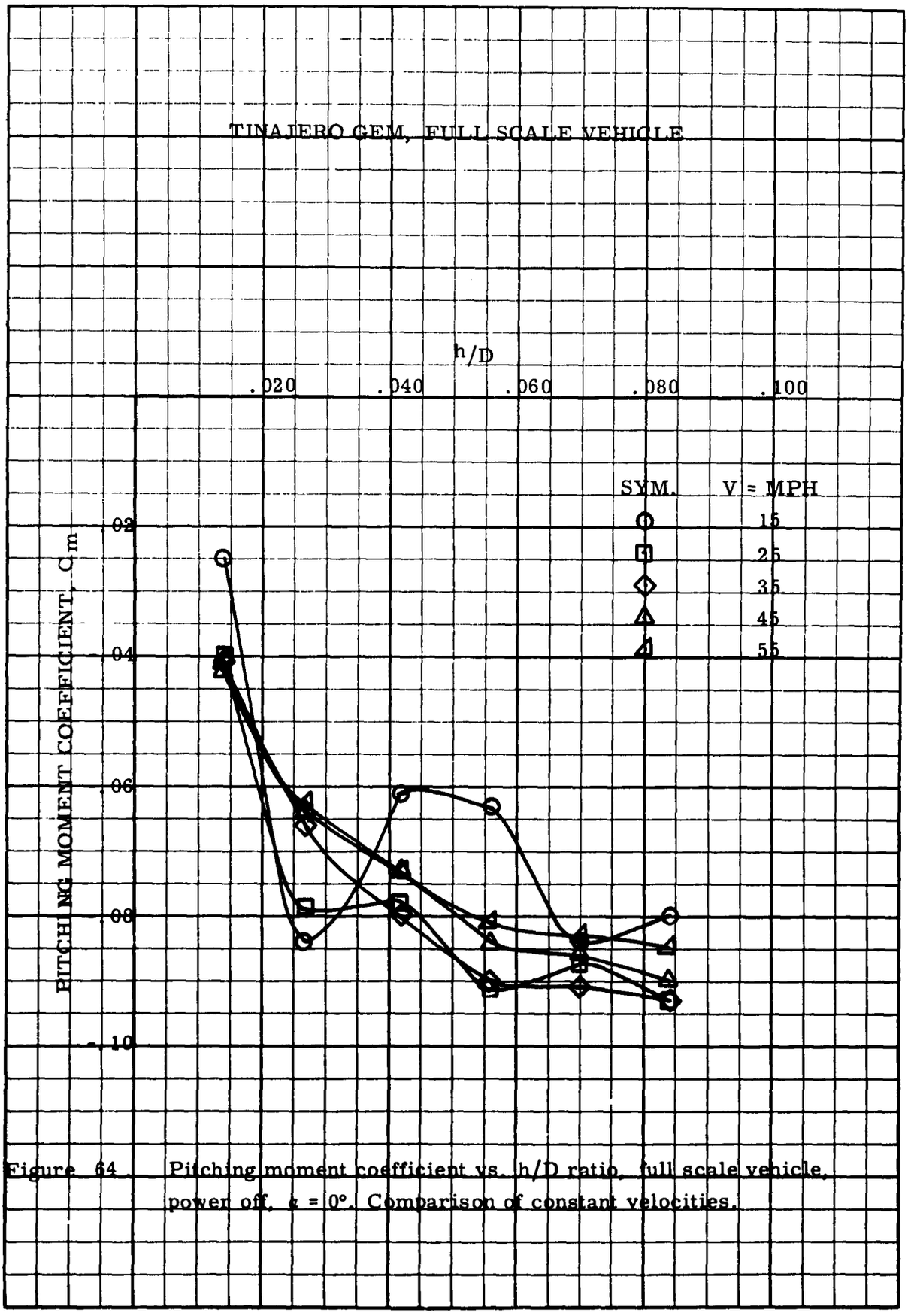


Figure 64. Pitching moment coefficient vs. h/D ratio, full scale vehicle, power off, $\alpha = 0°$. Comparison of constant velocities.

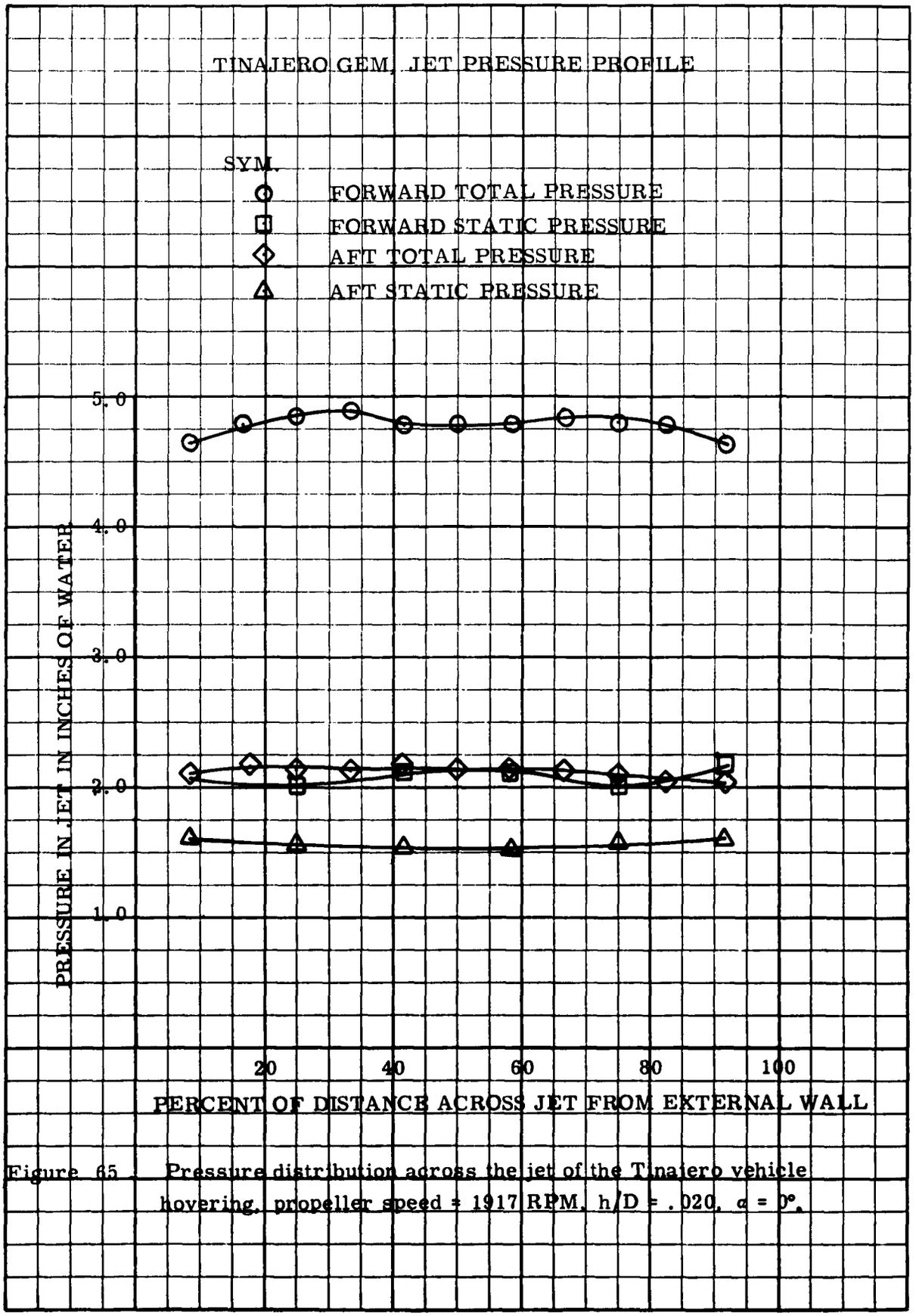


Figure 65. Pressure distribution across the jet of the Tinajero vehicle hovering, propeller speed = 1917 RPM, h/D = .020, $\alpha$ = 0°.

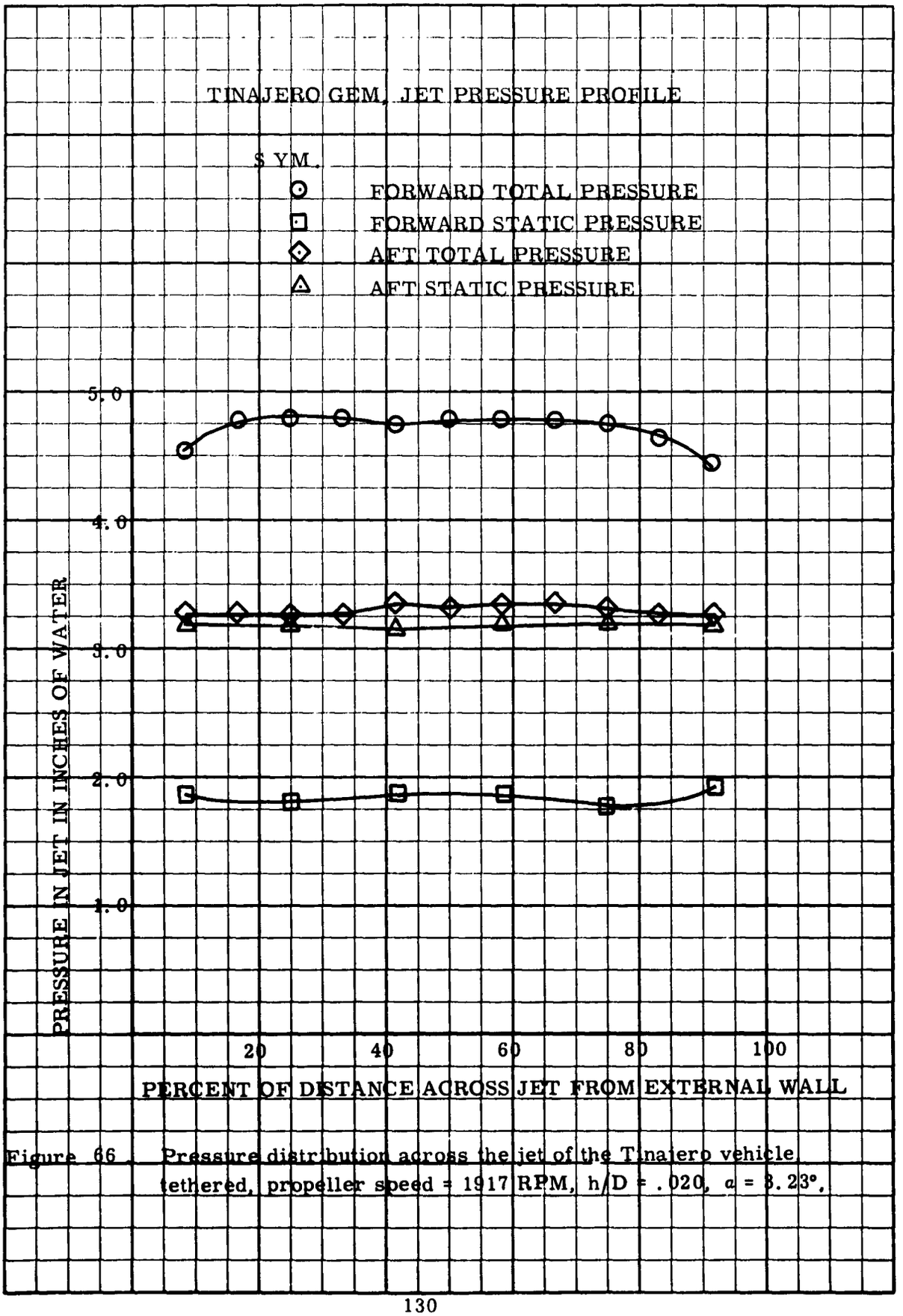


Figure 66. Pressure distribution across the jet of the Tinajero vehicle, tethered, propeller speed = 1917 RPM, h/D = .020, $\alpha$ = 3.23°.

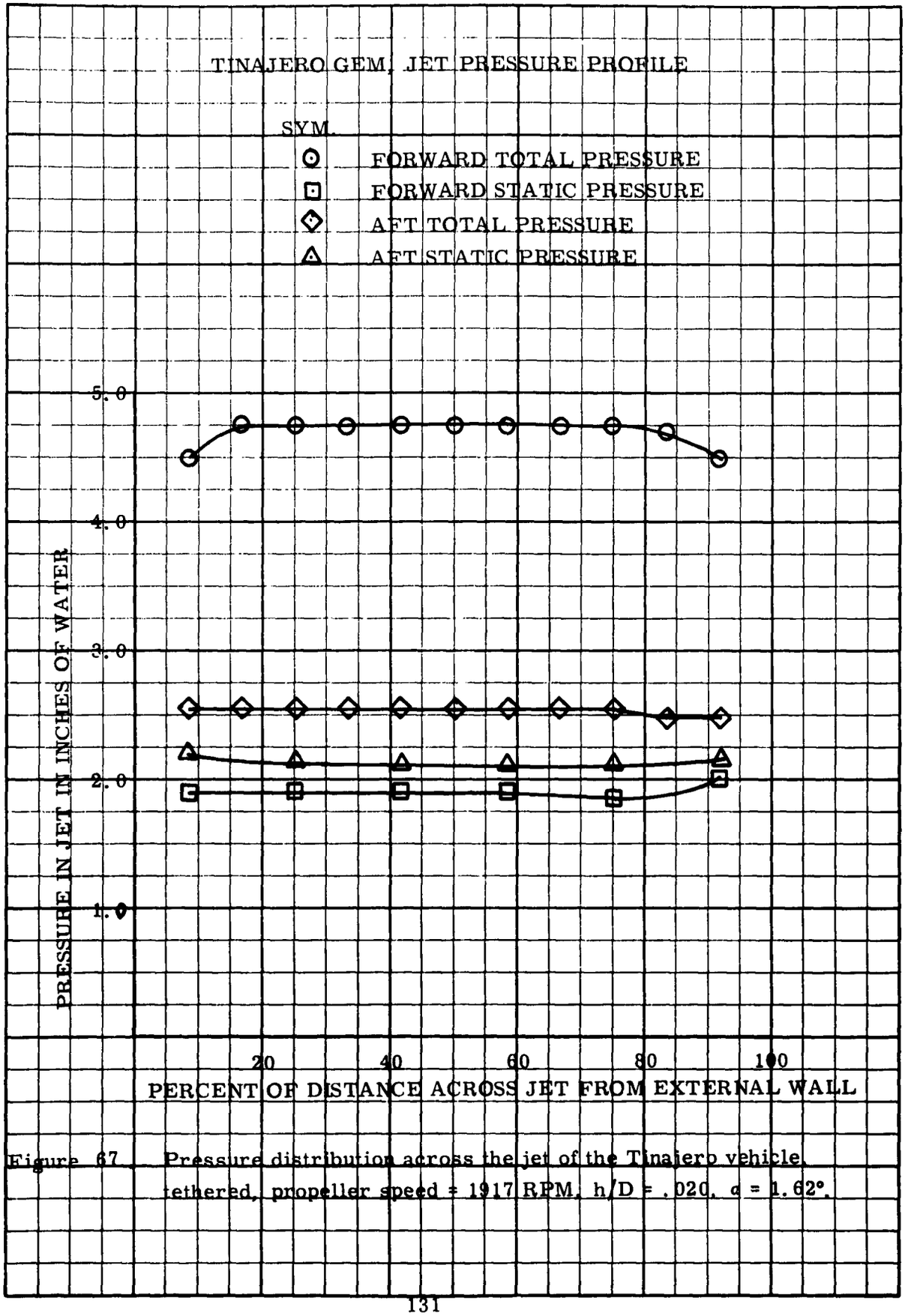


Figure 67. Pressure distribution across the jet of the Tinajero vehicle, tethered, propeller speed = 1917 RPM, h/D = .020, $\alpha$ = 1.62°.

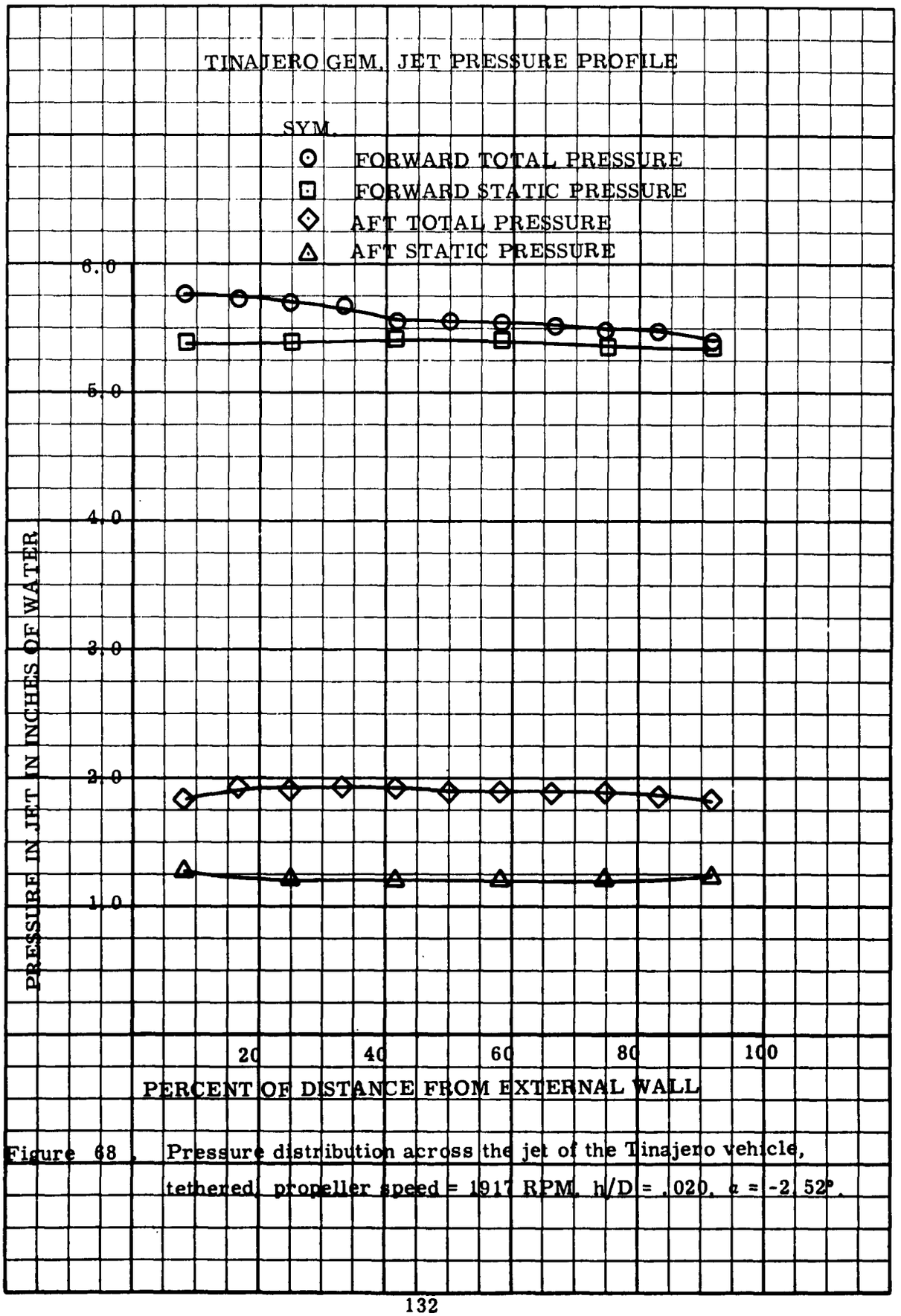


Figure 68. Pressure distribution across the jet of the Tinajero vehicle, tethered, propeller speed = 1917 RPM, h/D = .020, $\alpha$ = -2.52°.

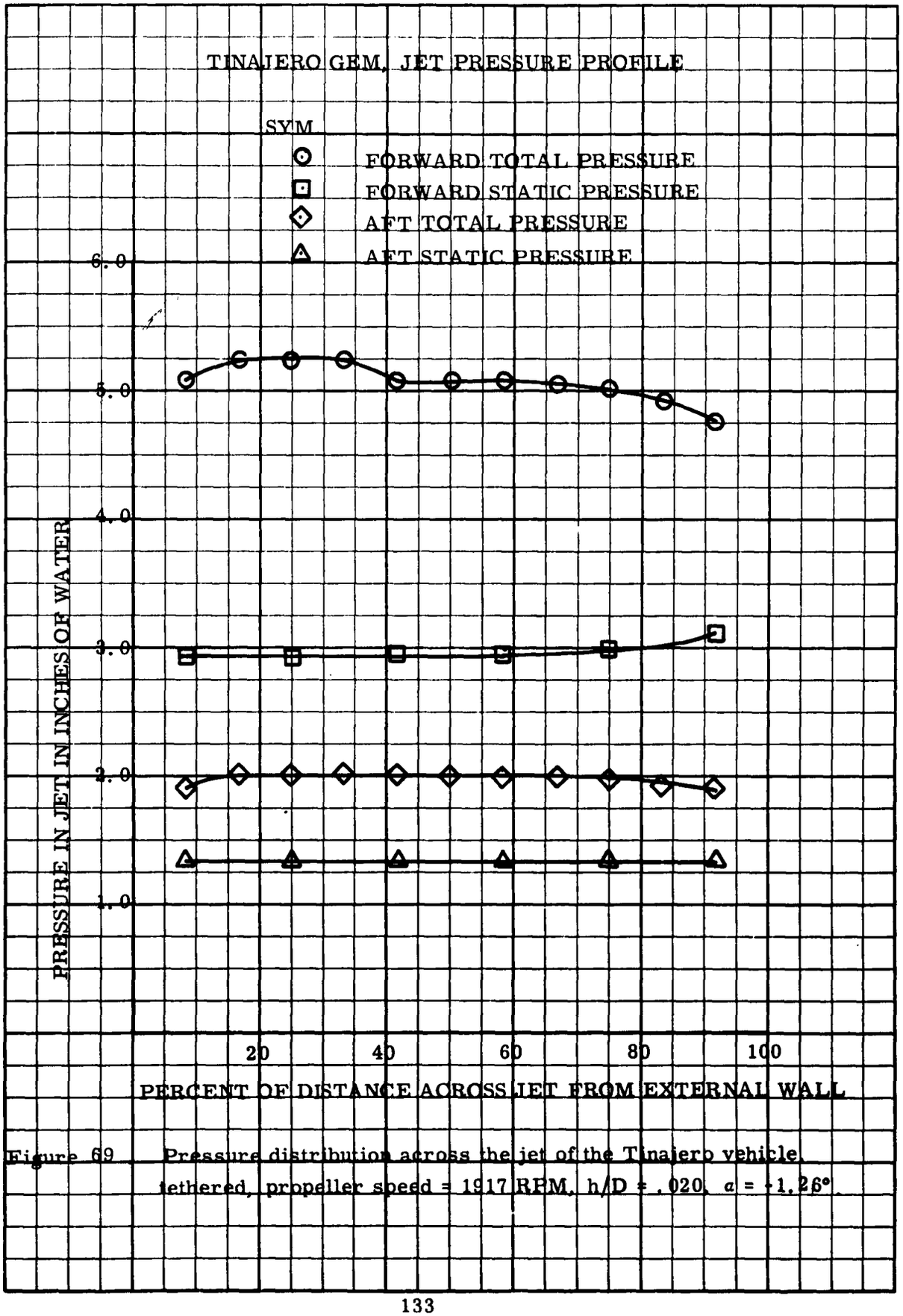


Figure 69 Pressure distribution across the jet of the Tinajero vehicle, tethered, propeller speed = 1917 RPM, h/D = .020, $\alpha$ = +1.26°

# APPENDIX I, INVESTIGATION OF THE PITCH AND ROLL STABILITY OF THE UNIVERSITY OF MARYLAND GROUND EFFECT MACHINE AS WRITTEN BY G. M. LEVIN AND R. E. RYERSON


## SUMMARY

The physical constants of the University of Maryland peripheral jet ground effect machine were obtained. These include the overall dimensions, dimensions of the peripheral jet system, weight, location of the center of gravity, and the moments of inertia about the pitch and roll axes. Curves of static restoring moment as functions of angular displacement in pitch and roll were obtained. The damping moments in pitch and roll were calculated and plotted against angular displacement and angular velocity.


## INTRODUCTION

The quantitative description of the static and dynamic stability of any vehicle is important because the machine and others like it must be designed so that they may be most easily controlled by their operators in all desired operating conditions. Since ground effect machines are still in an early stage of development, comparatively few tests have been made of their stability characteristics.

Contained in this report are scale drawings showing the approximate dimensions of the machine including the peripheral jets and the stability slots on the bottom. The longitudinal and vertical locations of the center of gravity are shown on these drawings. The weight and moments of inertia in pitch and roll of the machine are given.

Curves of dimensionless static restoring moment in pitch and roll were plotted as a function of angular displacement. The moments were made dimensionless by dividing them by the weight of the machine and a characteristic length.

Curves of angular displacement versus time for the freely vibrating machine were obtained. These curves were

expressed as functions $\alpha$ (t) and $\beta$ (t), which were then differentiated to get the angular velocity and angular acceleration.

The residual damping moments were then calculated and plotted against angular displacement and angular velocity to determine how they depend upon these quantities.

## APPARATUS AND TEST PROCEDURE

The ground effect machine under investigation is of the peripheral jet type. It is rectangular in plan form and is 150 inches long, 63.5 inches high, and 79 inches wide. At the present time it is powered by a 100 pound, 100 horsepower, water cooled electric motor. This is soon to be replaced by a 40 horsepower drone engine to allow free flight testing. Air is taken in the machine by a multibladed propeller 42 inches in diameter located in the rear of the machine (Figures 70, 71, 72).

To obtain the weight of the machine, the front was placed on a floor scale and the rear was attached to a scale suspended from the ceiling (Figure 73). The weight of the machine was then the sum of the two weights indicated on the scales.

The longitudinal location of the center of gravity was determined as follows. A knife edge was weighed and placed on a floor scale. The front of the machine was placed on this knife edge. The back of the machine was placed on a second knife edge a known distance from the front knife edge and the whole system was made level by raising or lowering the back knife edge (Figure 74). The weight shown on the front scale was recorded and moments were summed about the rear knife edge to find the longitudinal location of the center of gravity. The vertical location of the center of gravity was obtained by suspending the machine from two points and marking the intersection of the two plumb lines.

The simplified compound pendulum method developed by Gracey (Reference 1) was used to determine the moments of inertia of the machine in pitch and roll.

The machine was suspended from a swinging gear on knife edges and the periods of oscillation measured for each of two suspension lengths about axes of oscillation parallel to the pitch and roll axes of the machine. The differences between the short and long suspension lengths for each axis were measured by measuring from a fixed point on the floor to the bottom of the swinging gear for each suspension length and taking the difference of these values. The swinging gear was weighed. The center of gravity of the swinging gear was found by balancing it in a horizontal position on a knife edge to locate the center of gravity longitudinally, and then suspending it from cables, inclining it to the horizontal, photographing it, and intersecting the plumb line of the cable with a line through the center of gravity perpendicular to the base of the machine. The periods of oscillation of the machine and swinging gear were measured with a Hewlett-Packard electronic counter and the circuit shown in Figure 75. The period of the oscillations was taken as the average of the time for 25 oscillations. The results of the weight, center of gravity, and moment of inertia determinations are shown in Table 4.

To hold the machine stationary except for motion about the axis under investigation the ground effect machine was tethered at the center of gravity. While the machine was hovering its angle of pitch was varied by applying a vertical force through the scale shown in the figure. The point of application of the force was a known distance from the center of gravity of the machine. The angle of pitch was measured with an inclinometer. The same method was used to determine the variation of static restoring moment with roll angle.

To obtain the angular displacement as a function of time the machine was once again tethered at the center of gravity and its free vibration after an initial displacement was photographed with a high speed movie camera at 48 frames per second.

The angular displacement of the machine was measured from reference lines drawn on the side of the machine. The time between each frame was determined from a large electric

clock driven by a syncronous motor. The clock was graduated in 72nds of a second and placed in front of the machine and filmed with the machine. The machine was set in motion by forcing an angular displacement by hand and then letting the motion decay freely. The machine was hovering over a level ground board at the time of the test.

The film was examined in a Bosch and Lomb viewer, designed to measure angles accurately and the angle and time in each frame were recorded.

## RESULTS AND DISCUSSION

The location of the center of gravity is shown in Figure 72. It was experimentally verified that the center of gravity lay in the plane of symmetry. The weight of the ground effect machine is given in Table 4. This weight is estimated to be accurate to within 5 pounds.

The simplified compound pendulum method (Reference 1) consists of measuring the periods of oscillation for two suspension lengths, and then solving the equations for the two suspension lengths simultaneously for one of the suspension lengths. Then this suspension length can be substituted back into one of the equations and the virtual moment of inertia of the machine calculated. The virtual moment of inertia includes the moment of inertia of the machine's structure, the air entrapped within the structure, and the additional moment of inertia, all about the machine's centroidal axis. The virtual moment of inertia is the effective moment of inertia of the machine operating in the atmosphere. The results of the moment of inertia determination are shown in Table 4. As a check of the calculations both $I_{v_s}$ and $I_{v_l}$ for each axis were calculated. These should equal and, in fact, were equal to within 0.0001 per cent or less.

The static restoring moment versus angle of pitch is shown in Figure 76. It should be noted that the curve is nonlinear. The static restoring moment versus roll angle is shown in Figure 77. The curve appears to be linear except for roll angles greater than $\pm$ 3.5° which is approximately the maximum roll angle obtainable.

The variation of pitch angle versus time for the freely vibrating ground effect machine is shown in Figure 78. Free vibration began at the first negative peak. The data points on this figure were put into an IBM 1620 computer and polynomial was calculated by the method of least squares. The curve on Figure 78 is the polynomial

$$\alpha = -0.013908 - 0.27902t + 1.4699t^2 - 2.3358t^3 + 1.4882t^4 - 0.33268t^5.$$

This function was differentiated to get $\dot{\alpha}$ and $\ddot{\alpha}$ as shown

$$\dot{\alpha} = -0.27902 + 2.9398t - 7.0074t^2 + 5.9528t^3 - 1.6634t^4$$

$$\ddot{\alpha} = 2.9398 - 14.0148t + 17.8584t^2 - 6.6536t^3$$

The equation of motion of the freely vibrating ground effect machine was assumed to be of the form:

$$I_p\ddot{\alpha} + M_p + m_p\alpha = 0$$

$$I_r\ddot{\beta} + M_r + m_r\beta = 0$$

where $m_p\alpha$ is the static restoring moment and $M_p$ is the residual damping moment. The subscripts p and r refer to pitch and roll.

At any given time $\alpha$, $\dot{\alpha}$, and $\ddot{\alpha}$ were found from the previous polynomial. The static restoring moment ($m\alpha$) was found from the curve $m\alpha$ versus $\alpha$. By solving the basic equation of motion, a value of the residual damping moment (M) was found at any time (t). It was desired to find upon what quantities this residual damping moment depends and how it depends on these quantities.

In viscous damped systems, the damping moment is directly proportional to velocity. In the case of this ground effect machine this was not found to be true. Figure 79 shows the variation of M with pitching velocity. Analysis of this figure showed that the damping was positive over all but a small portion of the curve. In these small portions the static restoring moment was in the order of ten times the damping moment.

Figure 80 shows the residual damping moment as a function of pitch angle. The residual moment was no obvious function of the angle of pitch or pitching velocity.

Figure 81 shows the rolling angle in free vibration as a function of time. Once again the curve is polynomial computed by the IBM 1620.

The polynomial and its derivatives are:

$$\beta = 0.06092 - 0.0694t^2 + 0.29915t^3$$
$$\dot{\beta} = -0.06924 - 0.63272t + 0.89745t^2$$
$$\ddot{\beta} = -0.63272 + 1.79490t$$

The same method which was used for pitch was used to calculate the residual damping moment in roll. Figure 82 shows the residual damping moment versus rolling velocity, and Figure 83 shows the residual damping moment versus roll angle.

Examination of the curves of pitch and roll angle versus time shows that the absolute values of the trim angles on these curves may be in error by less than 0.17° in pitch and perhaps by as much as 0.5° in roll. This is because the half periods on the pitch and roll curves are not equal or decreasing with time as they should be. In pitch, the possible small error will effect the damping moment no more than 1.1 pound-feet. This is less than 0.5 per cent of the maximum pitch damping moment. In roll, the maximum error in residual damping moment due to the error in the absolute value of the trim angle can be as much as 17 pound-feet. This is approximately 25 per cent of the maximum value of the roll damping moment calculated.

The experiment could be improved by using an accelerometer or gyroscope in the ground effect machine to give continuous outputs of angle versus time. This would eliminate errors in reading the angles from the film. Greater care should be taken to determine the absolute value of the trim angle by recording angular displacements before the machine is initially displaced and long after it appears to return to equilibrium.

Since the machine is not connected to any support other than its air cushion, it is very sensitive to small disturbances and therefore it is felt that the scatter in the data of angular displacement versus time could be reduced by testing the machine indoors or on days of very light or no wind.

# CONCLUSIONS

It is apparent from examining the motion of the machine that it is statically and dynamically stable in pitch and roll and also that both motions are rather heavily damped. This was substantiated by calculations of the residual damping moment, where it was found that the ground effect machine was positively damped for most of its motion. In the brief periods where the machine was negatively damped, the damping moment was small, and therefore the destabilizing effect was small.

The dynamic stability results in pitch are thought to be accurate. However, due to the large possible error in the roll trim angle, the values of the damping moment determined for roll are invalid and should be used only for order of magnitude determinations of the dynamic stability.

The static restoring moment in roll is stabilizing and is linear over approximately $\pm$ 3.5°. The static restoring moment in pitch is stabilizing and is nonlinear.

In addition, it appears that the rate of damping of the pitch displacement is greater at large amplitudes than at small amplitudes.

## SYMBOLS

| | |
|---|---|
| w | Weight of GEM |
| w' | Weight of swinging gear |
| W | Weight of pendulum (w + w') |
| l | Distance from axis of oscillation to center of gravity of GEM (suspension length) |
| l' | Distance from axis of oscillation to center of gravity of swinging gear |
| L | Distance from axis of oscillation to center of gravity of pendulum (pendulum length) |
| $\Delta l$ | Difference between two suspension lengths |
| T | Period of oscillation |
| V | Volume of GEM |
| $\rho$ | Density of air |
| g | acceleration of gravity |
| $M_A$ | Additional mass |
| $I_v$ | Virtual moment of inertia |
| $I_A$ | Additional moment of inertia |
| $I_G$ | Moment of inertia of swinging gear about axis of oscillation |

## SUBSCRIPTS

| | |
|---|---|
| s | Short suspension length |
| l | Long suspension length |

## ANNEX TO APPENDIX I

### Derivation of the Simplified Compound Pendulum Method For a Compound Pendulum Swung at Two Suspension Lengths

$$I_{v_s} = \frac{W_s L_s T_s^2}{4\pi^2} - \left(\frac{w}{g} + V\rho + M_A\right) l_s^2 - I_{G_s} \quad (1)$$

$$I_{v_1} = \frac{W_1 L_1 T_1^2}{4\pi^2} - \left(\frac{w}{g} + V\rho + M_A\right) l_1^2 - I_{G_1} \quad (2)$$

where $\frac{w}{g} - V\rho$ is the true mass of the GEM.

$M_A$ is assumed to be concentrated at the center of gravity of the GEM.

Equations for the determination of $M_A$ based on the projected areas of the machine perpendicular to its motion are in Reference 2.

From the principle of moments, the pendulum length may be expressed in terms of the moments of the GEM and of the swinging gear about the axis of rotation.

$$L = \frac{wl + w'l'}{W} \quad (3)$$

Substituting equation (3) into equations (1) and (2) yields:

$$I_{v_s} = \frac{(wl_s + w's's) T_s^2}{4\pi^2} - \left(\frac{w}{g} + V\rho + M_A\right) l_s^2 - I_{G_s} \quad (4)$$

$$I_{v_1} = \frac{(wl_1 + w'_1 l'_1) T_1^2}{4\pi^2} - \left(\frac{w}{g} + V\rho + M_A\right) l_1^2 - I_{G_1} \quad (5)$$

From the relation $l_1 = l_s + \Delta l$, where $\Delta l$ is the difference between the two suspension lengths, equation (5) may be written:

$$I_{v_1} = \frac{((l_s + \Delta l) w + w'_1 l'_1) T_1^2}{4\pi^2} - \left(\frac{w}{g} + V\rho + M_A\right) (l_s + \Delta l)^2 - I_{G_1} \quad (6)$$

The moment of inertia of the machine about its body axes is the same for both suspension lengths. Therefore equations (4) and (6) may be solved simultaneously for the suspension length:

$$l_s = \frac{T_s^2 w'_s l'_s - T_1^2(w\Delta l + w'_1 l'_1) + 4\pi^2((\frac{w}{g} + V\rho + M_A)(\Delta l)^2 + I_{G_1} - I_{G_s}}{w(T_1^2 - T_s^2) - 8\pi^2 \Delta l (\frac{w}{g} + V\rho + M_A)} \quad (7)$$

From the value of $l_s$ found from equation (7) and with the value of l' found by measurement, the short suspension length ($L_s$) may be calculated from equation (3). Then from equation (1) the virtual moment of inertia may be found.

Sample Calculations about Pitch Axis

Substituting into equation (7):

$T_s^2 w'_s l'_s = (3.00536)^2(72.6)(78.21) = 51,285.184623$

$T_1^2 = 10.32106$

$w\Delta l = (703.2)(19.1) = 13,431.12$

$w'_1 l'_1 = (72.6)(97.31) = 7064.706$

$4\pi^2 = 39.47836$

$I_{G_1} = 347.864022 + \frac{72.6}{(32.174)(12)}(97.31)^2 = 2,308.14469$

$I_{G_s} = 347.864022 + (0.197235)(78.5462)^2 = 1216.842420$

$\Delta l^2 = 364.81$

$w(T_1^2 - T_s^2) = 703.2(10.321056 - 9.032189) = 906.123374$

$8\pi^2\Delta l = 2(39.47836)(19.1) = 1508.073352$

$T_1^2(w\Delta l + w'_1 l'_1) = 211,538.649896$

$I_{G_1} - I_{G_s} = 743.438244$

$\frac{w}{g} + V\rho = 1.82135 + \frac{(246,437.3)(0.00230)}{(1728)(12)} = 1.84868$

$$M_A = \frac{\pi \rho}{4} K \bar{c}^2 b$$

where:

$\bar{c}$ = average chord of projected area of machine perpendicular to its motion

b = span of projected area of machine perpendicular to its motion

K is defined in Reference 2

$$M_A = \frac{\pi}{4}(1.108 \times 10^{-7})(0.56)(62.5)^2(58) = 0.01104$$

$l_s$ = 54.850078 (7)

$$L_s = \frac{(703.2)(54.850078)+(72.6)(78.21)}{775.8} = 57.036118 \quad (3)$$

$$I_{v_s} = \frac{(775.8)(57.036118)(9.032188)}{39.47836} - (1.85972)(54.850078)^2$$

$$- 1564.706446 = 2963.836331 \text{ lb. sec.}^2 \text{ in.} \quad (1)$$

$I_{v_s}$ = 246.986360 slug-ft.$^2$

$$I_{v_1} = (775.8)(57.036118+19.1)(10.32106)-(1.85972)(l_s+\Delta 1)^2$$

$$- 2308.14469 = 2963.841095 \text{ lb. sec.}^2 \text{ in.} \quad (2)$$

$I_{v_1}$ = 246.986757 slug-ft.$^2$

Deviation between $I_{v_s}$ and $I_{v_1}$ equals 0.0001 per cent.

## REFERENCES


1. Gracey, William, The Experimental Determination of the Moments of Inertia of Airplanes by a Simplified Compound Pendulum Method, NACA TN No. 1629.

2. Malvestuto, Frank S., Jr., and Gale, Lawrence J., Formulas for Additional Mass Corrections to the Moments of Inertia of Airplanes, NACA TN No. 1187, 1947.

3. Shantz, Irving, and Groves, Robert T., Dynamic and Static Stability Measurements of the Basic Finner at Supersonic Speeds, NAVORD Report No. 4516, September 1960.

4. Eames, Michael C., "Fundamentals of the Stability of Peripheral Jet Vehicles" Vol. 1 Elementary Principles, Systems Engineering Division, Pneumodynamics Corporation.

5. Foltz, Claude A., Ground Effect Machine Investigations at the University of Wichita: Final Report Summarizing the Test Program and Data Obtained, May 1961.

TABLE 4

SUMMARY OF MEASURED PHYSICAL CHARACTERISTICS

| | | |
|---|---|---|
| Weight of GEM | - | 703.2 lb. |
| Longitudinal CG location | - | 60.2 inches from rear peripheral jet |
| Moment of inertia in roll | - | 122.45 slug-ft.$^2$ |
| Moment of inertia in pitch | - | 246.98 slug-ft.$^2$ |

Dimensions in inches

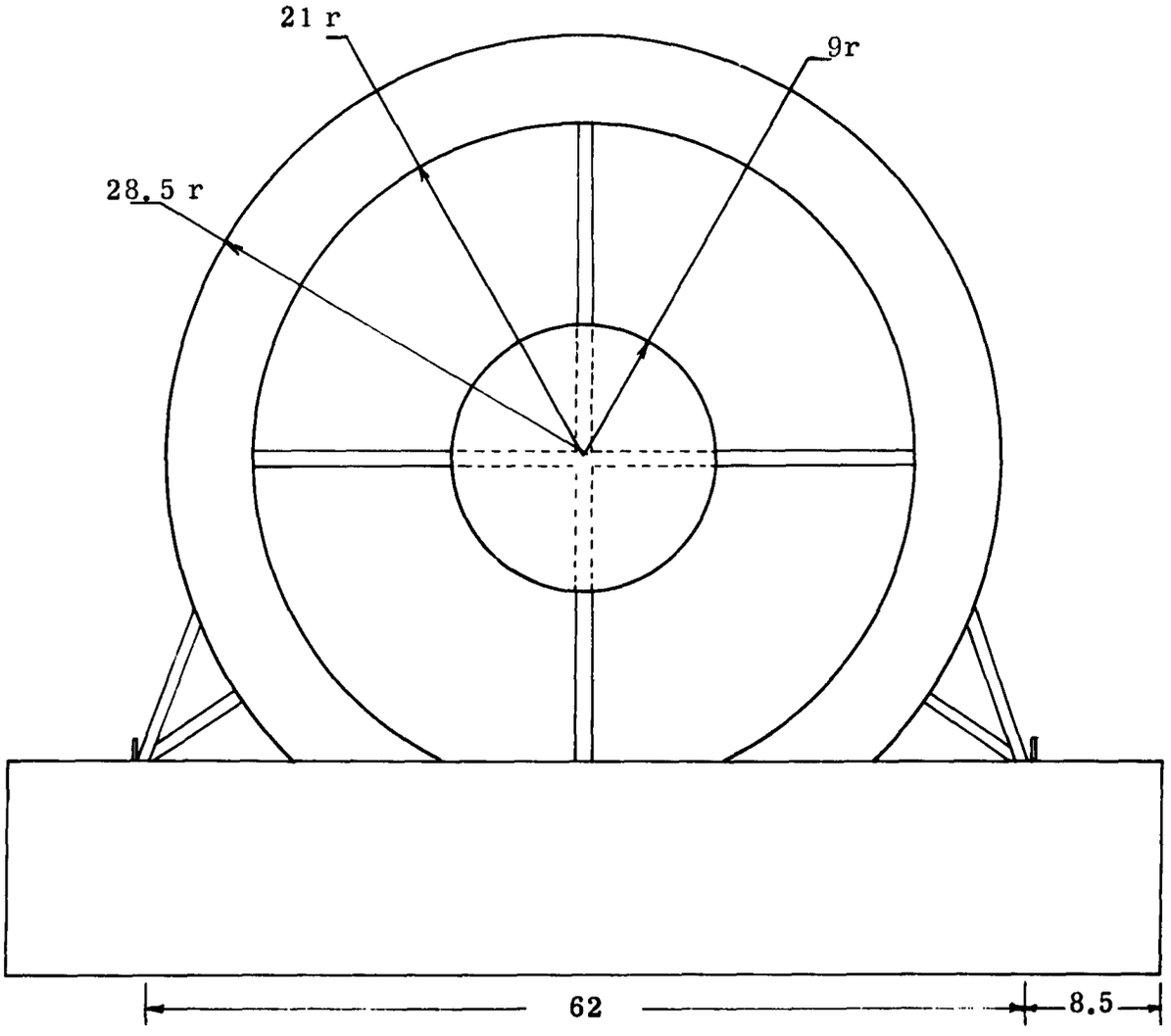


Figure 70. Rear view of GEM.

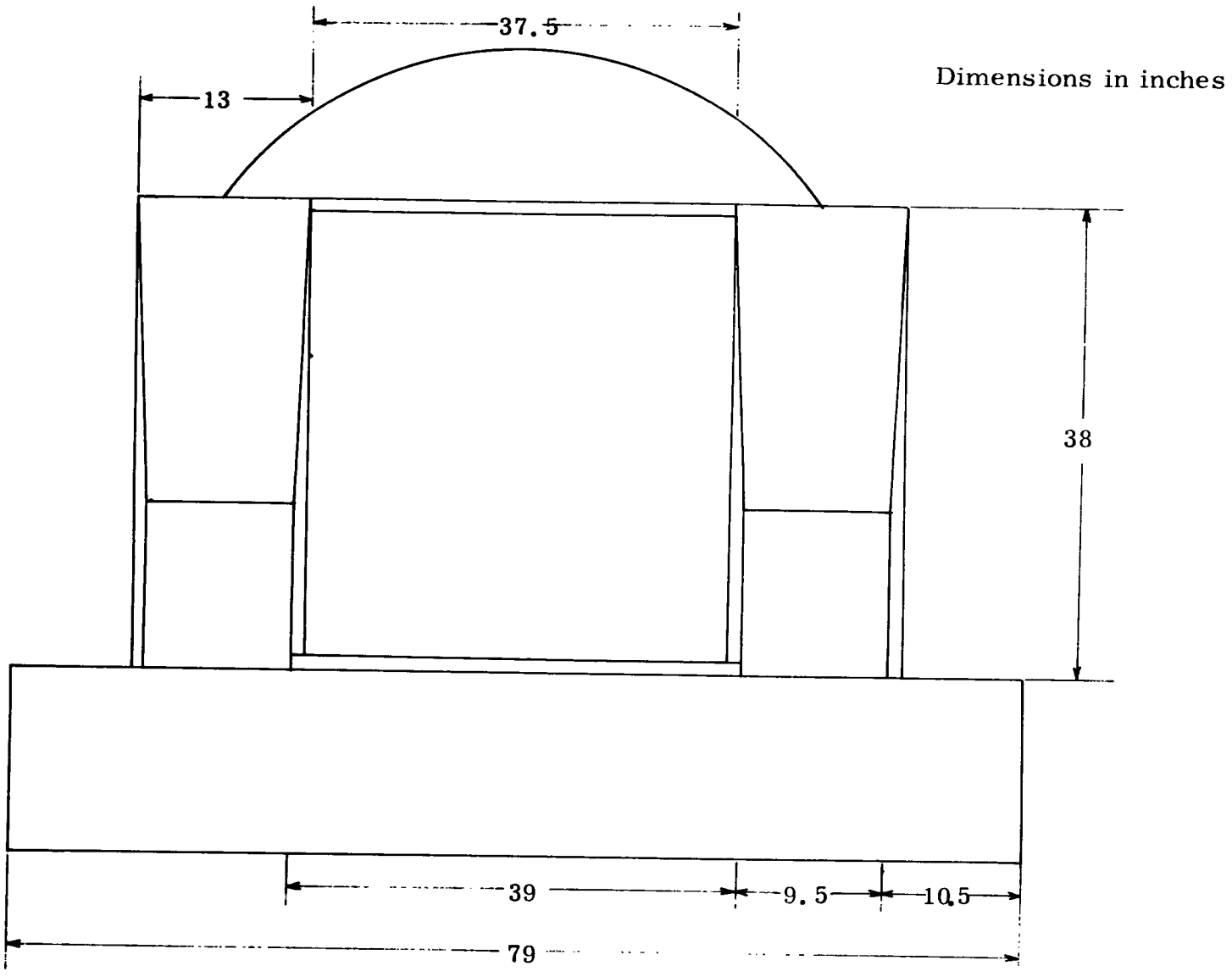


**Figure 71 . Front view of GEM.**

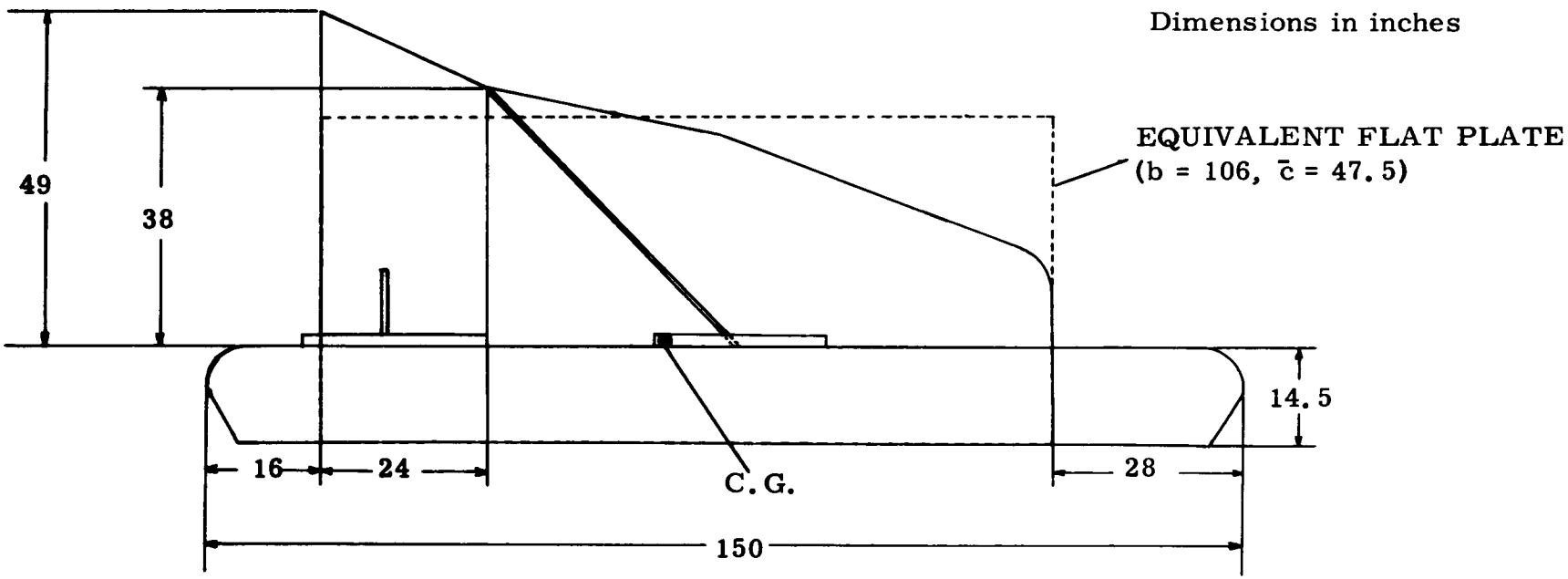


**Figure 72. Side view of GEM.**

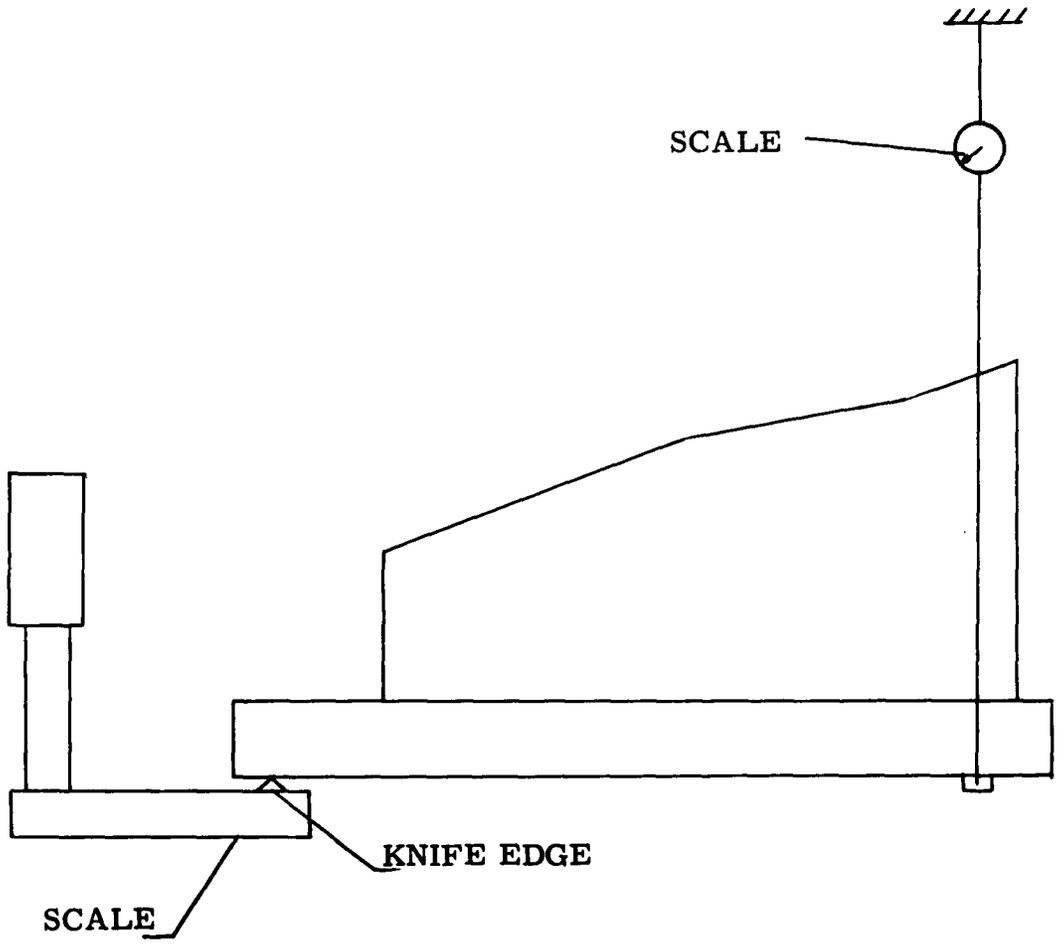


Figure 73 . Apparatus for weighing GEM.

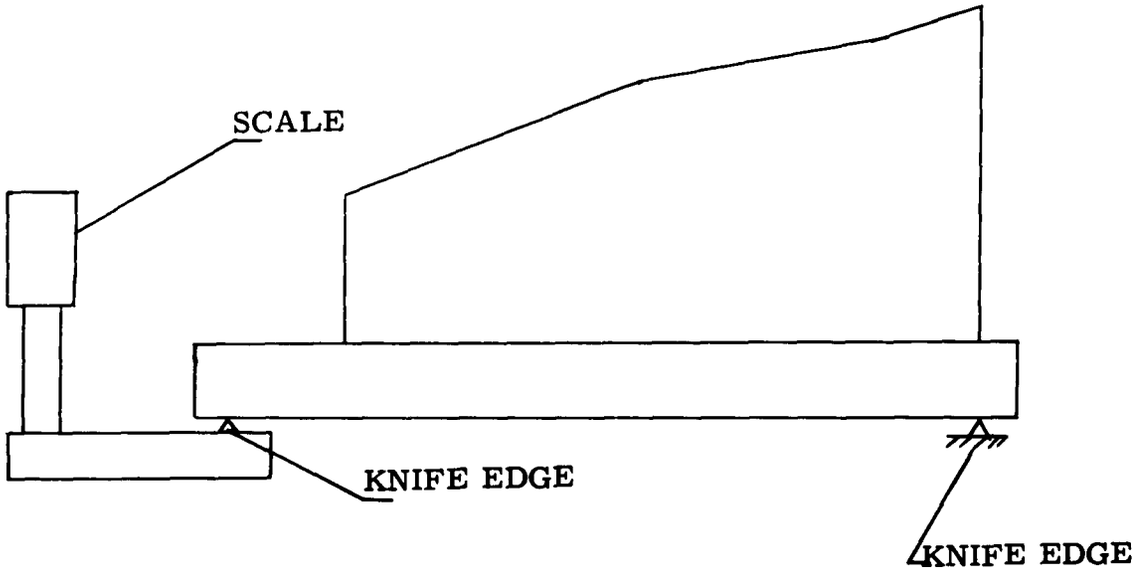


Figure 74 . Apparatus for determining longitudinal C.G. location.

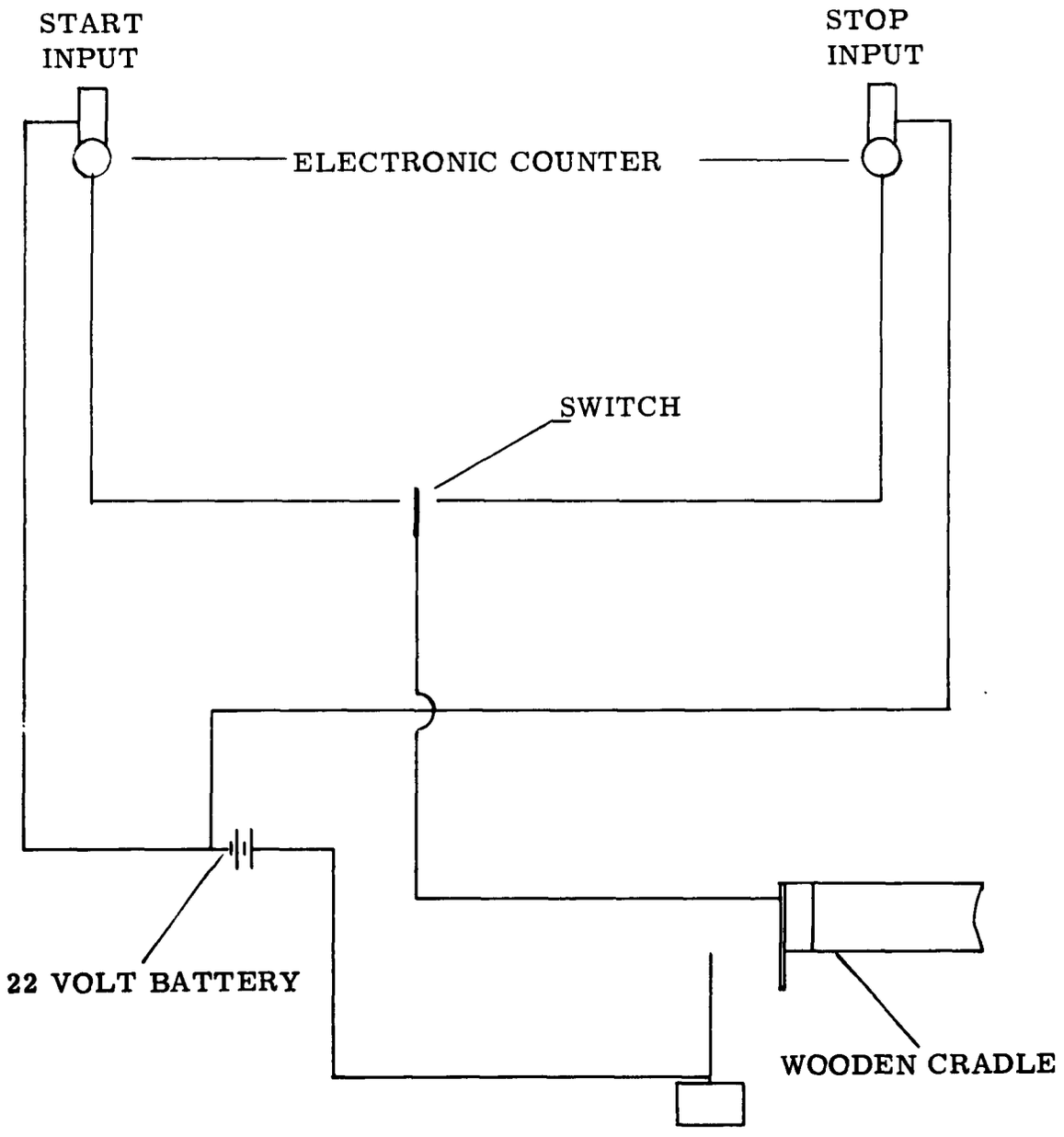


Figure 75. Circuit for determining period of oscillation.

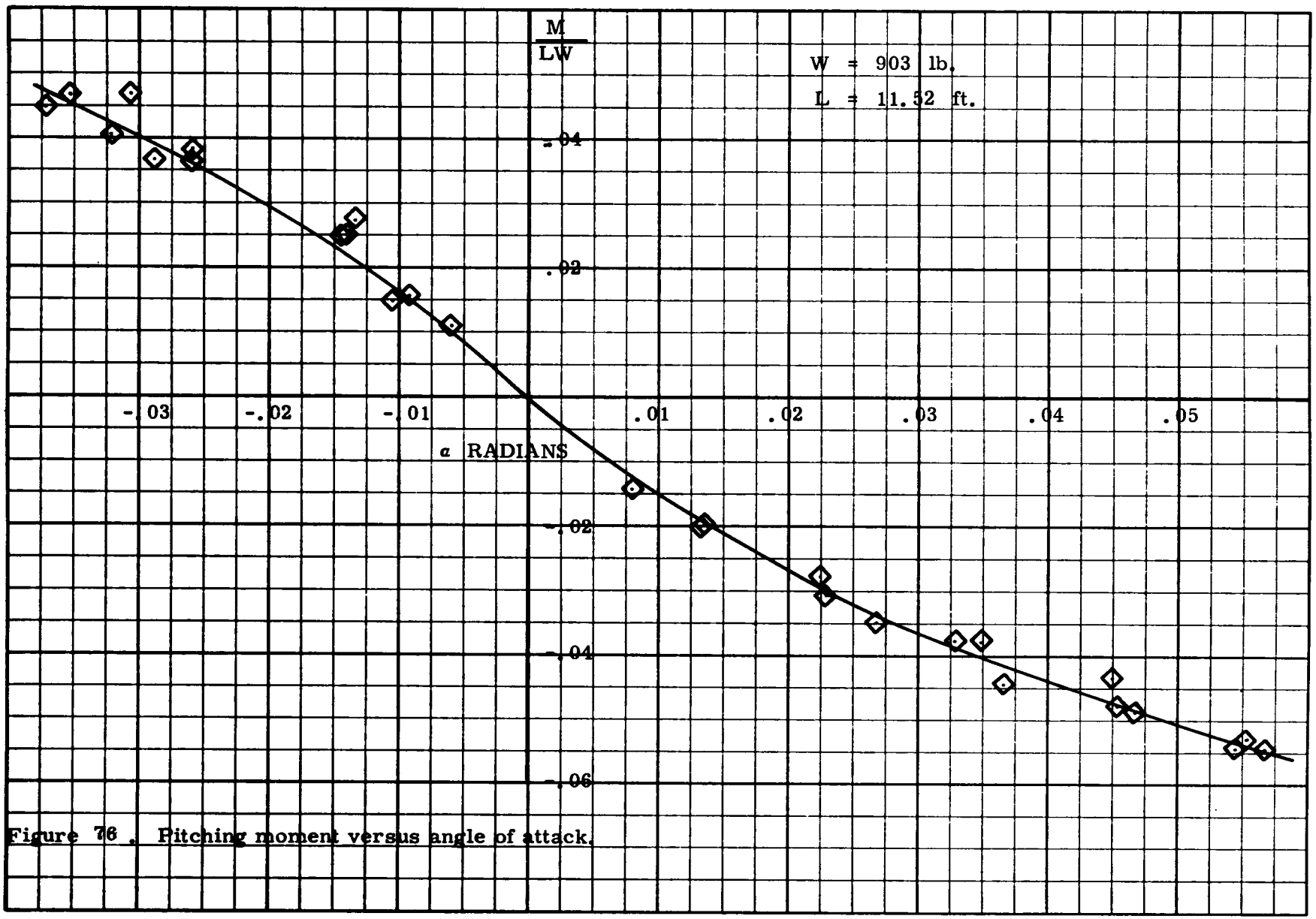


Figure 76. Pitching moment versus angle of attack.

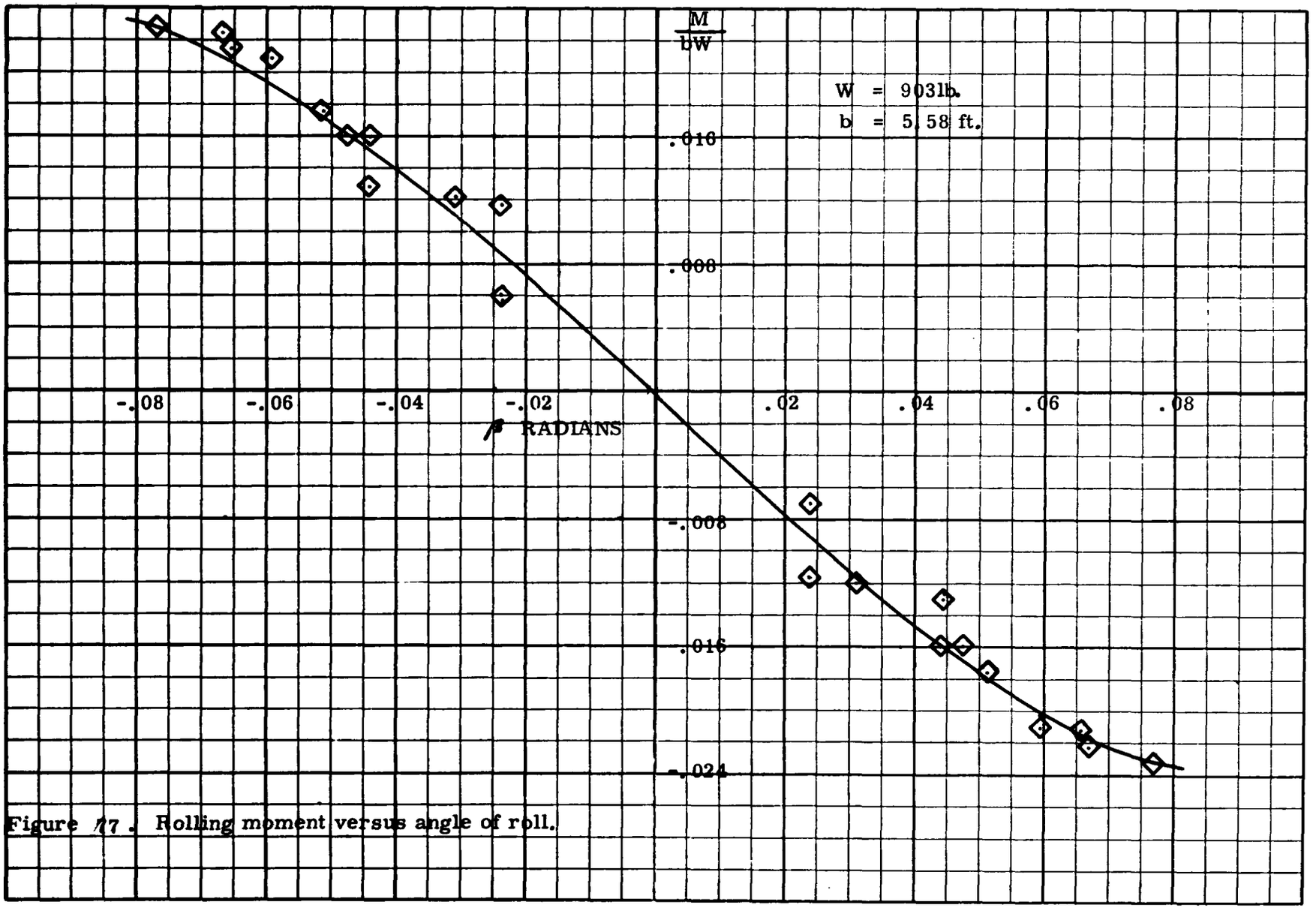


Figure 17. Rolling moment versus angle of roll.

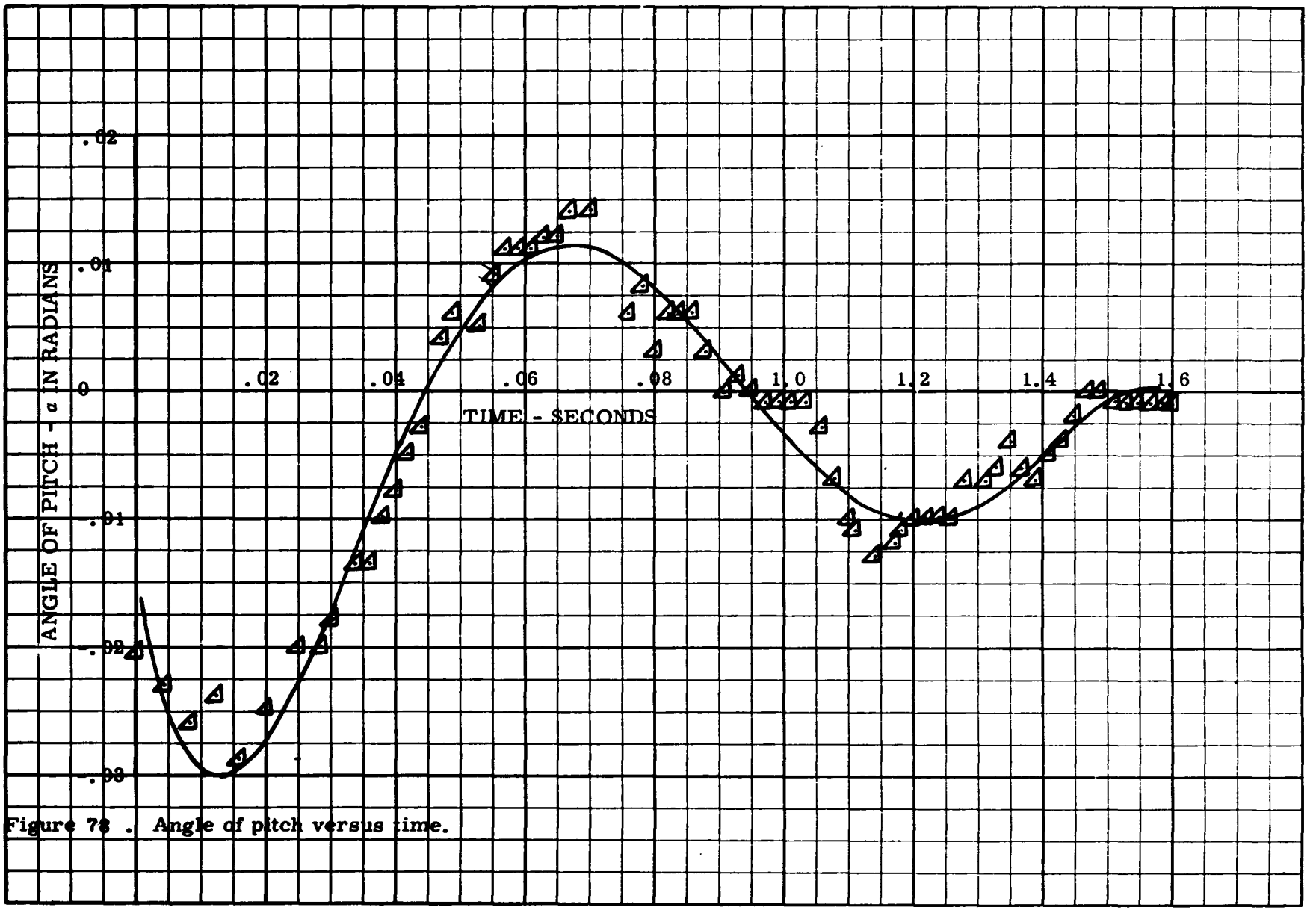


Figure 78 . Angle of pitch versus time.

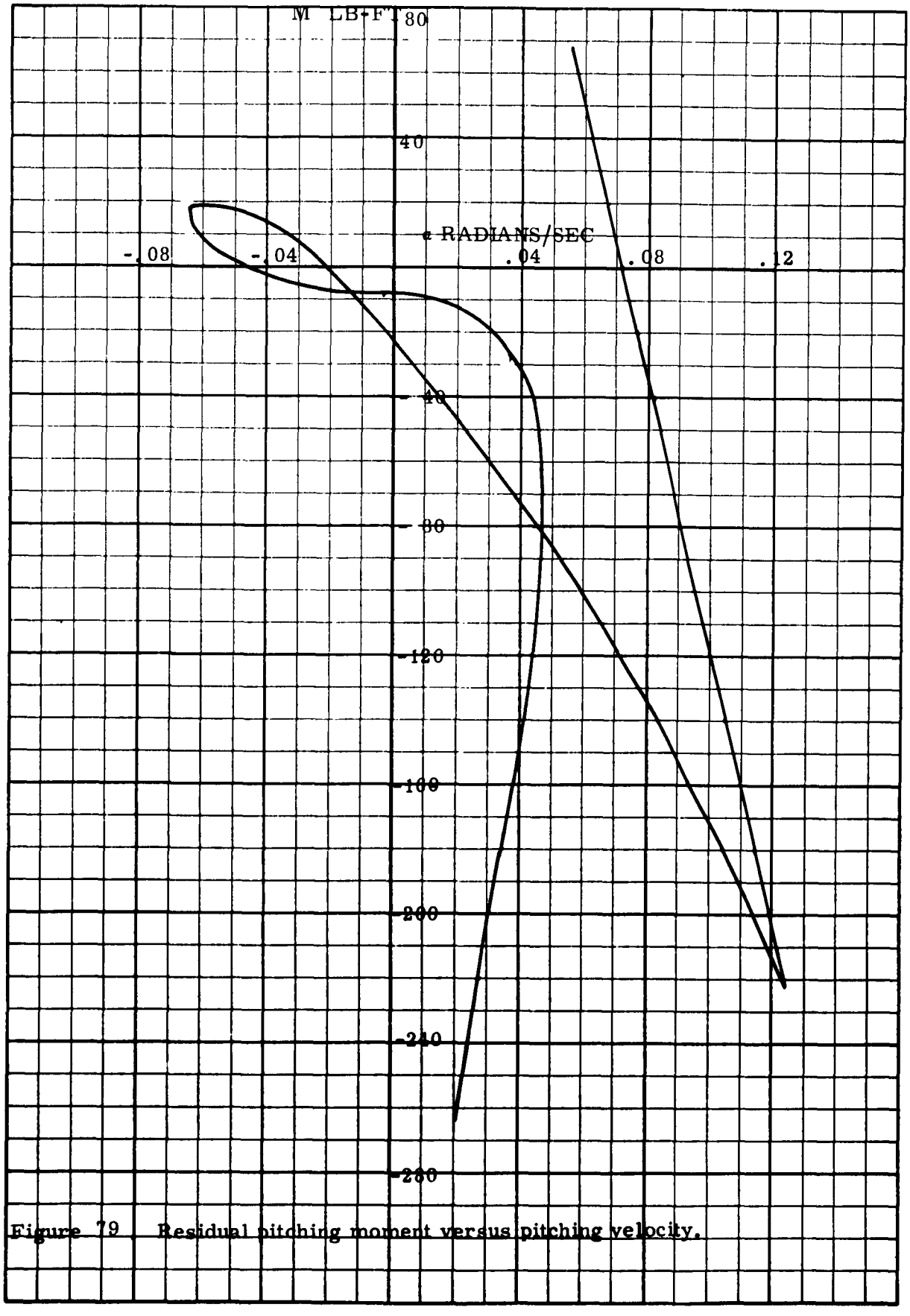


Figure 79 Residual pitching moment versus pitching velocity.

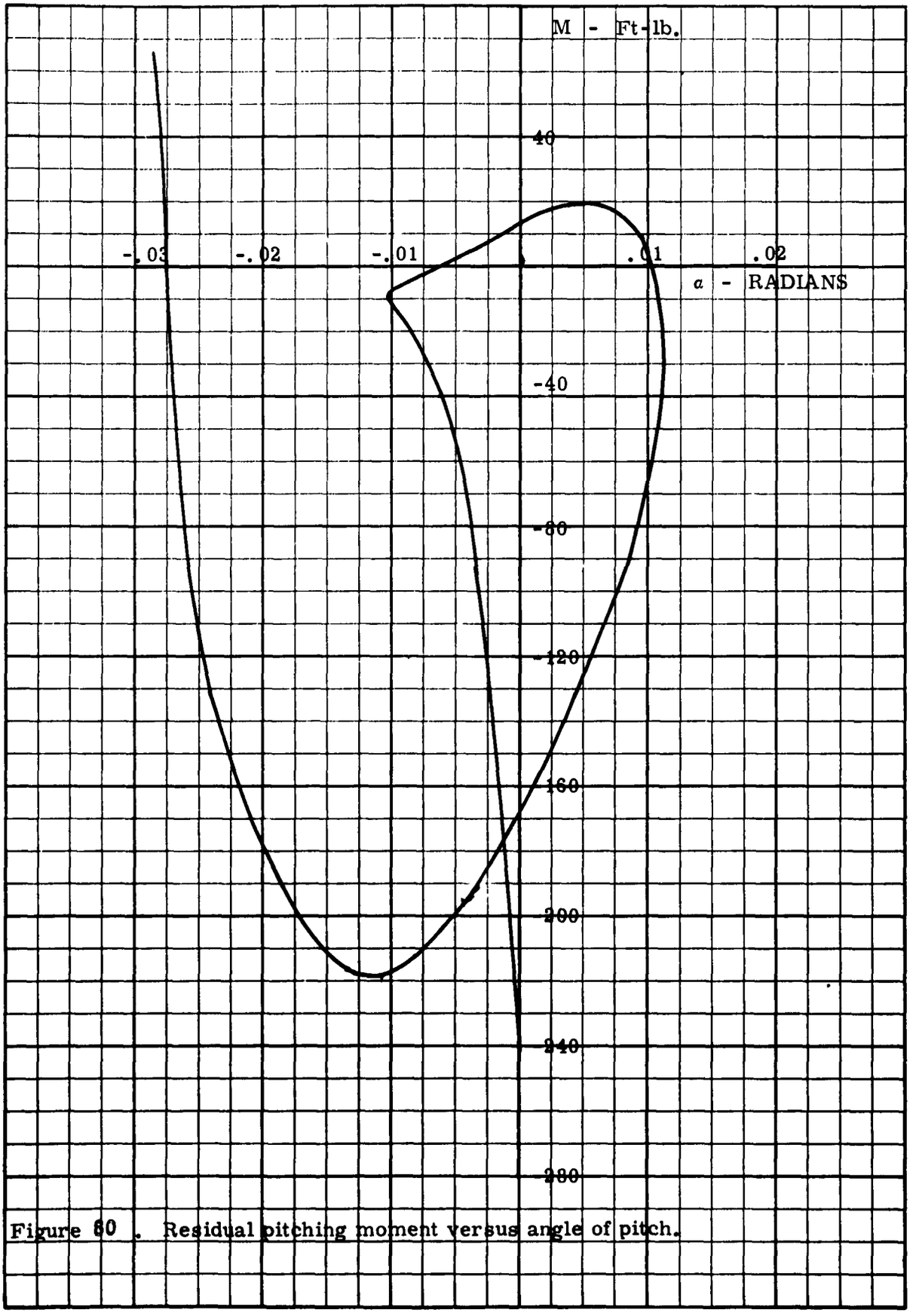


Figure 60. Residual pitching moment versus angle of pitch.

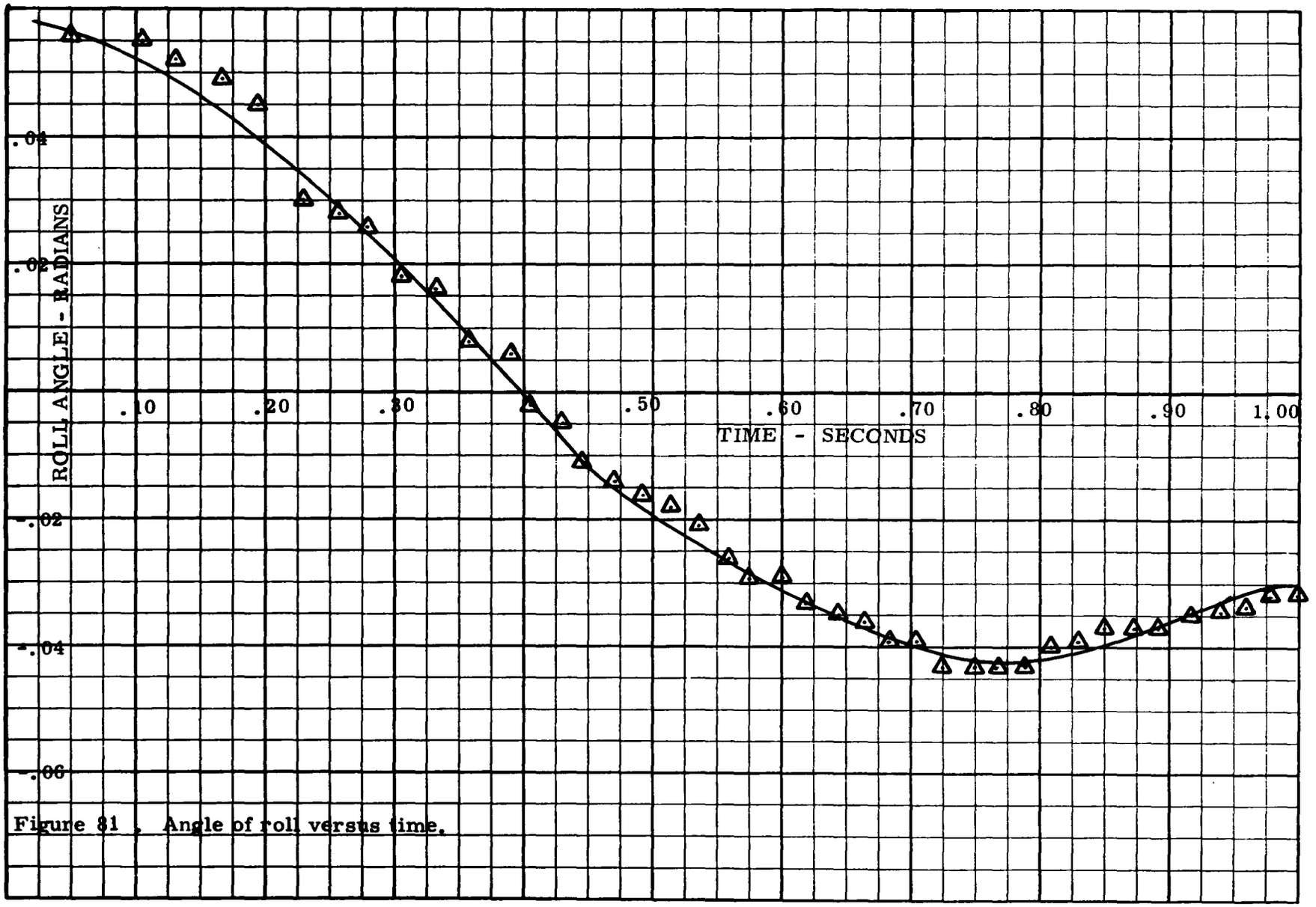


Figure 81 . Angle of roll versus time.

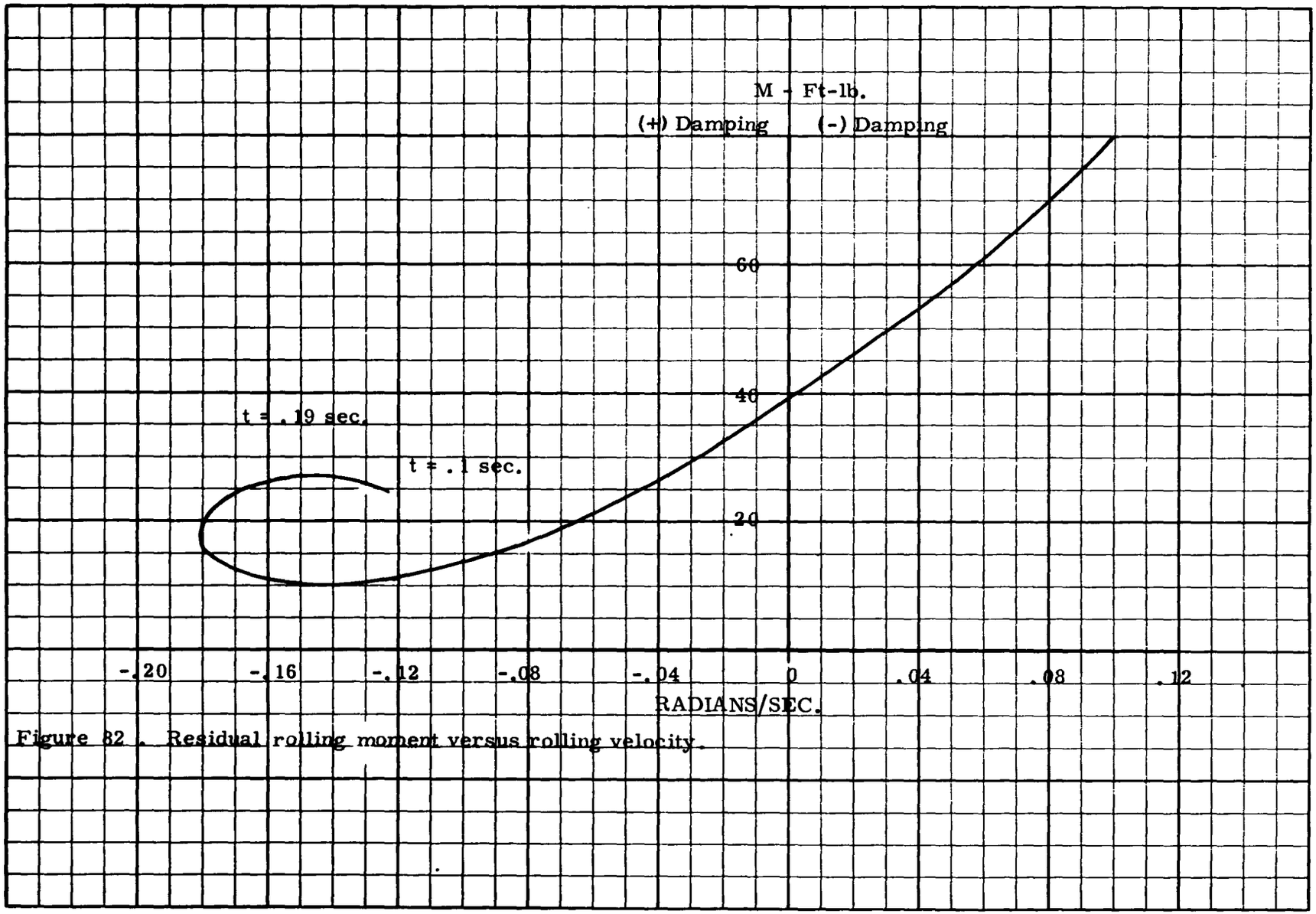


Figure 82. Residual rolling moment versus rolling velocity.

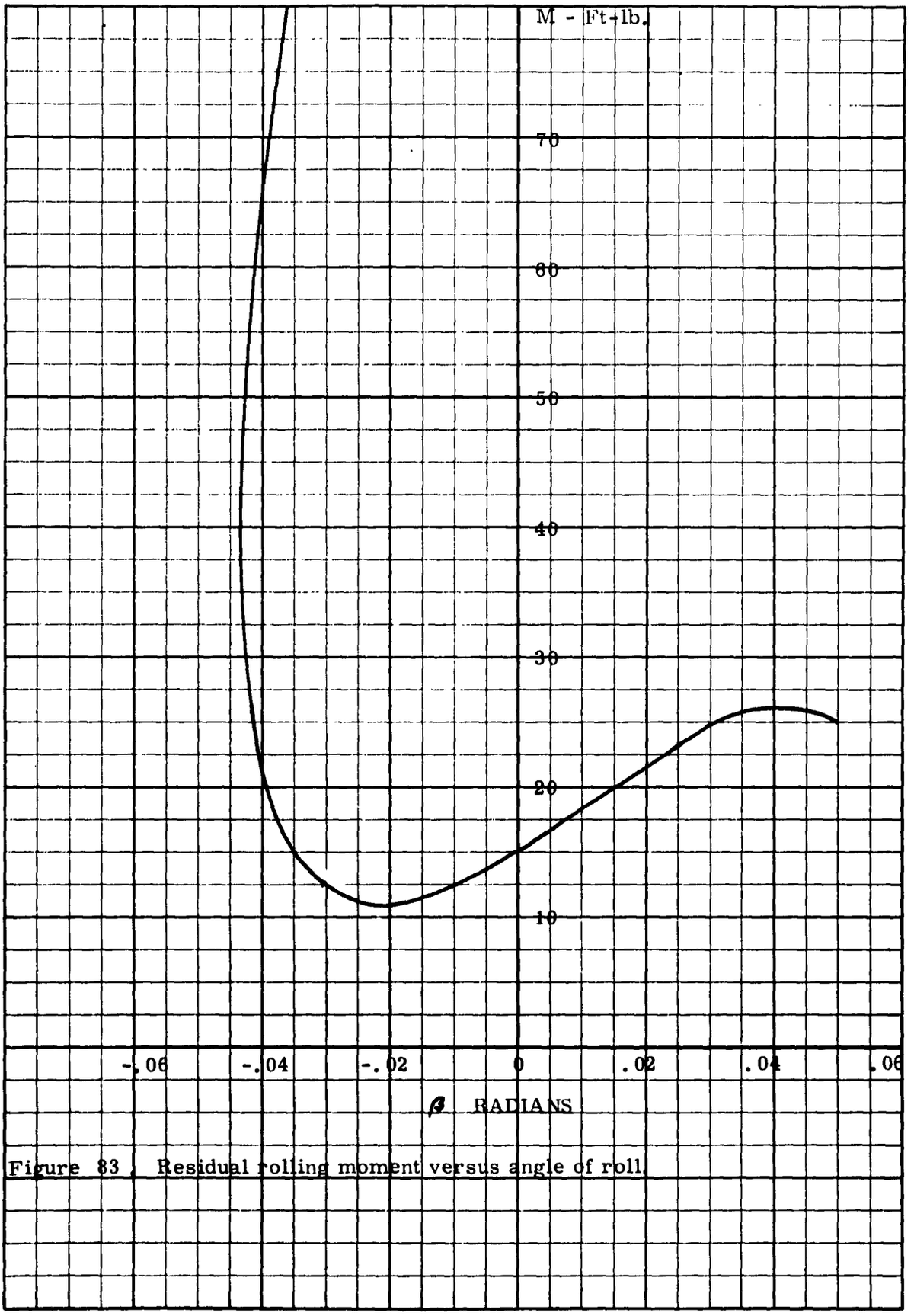


Figure 83. Residual rolling moment versus angle of roll.

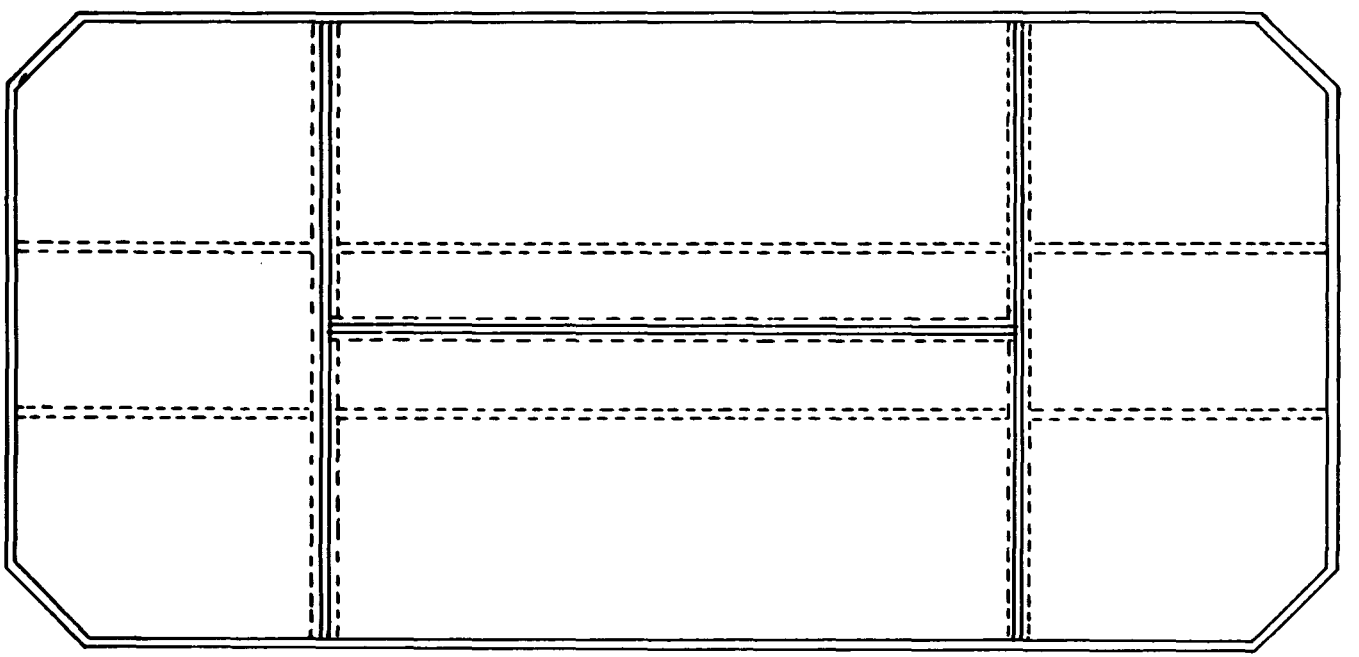

**Figure 84 . Peripheral jets and stability slots - Scale 1/20**

## APPENDIX II, TEST PROGRAM - TWO-DIMENSIONAL PRESSURE DISTRIBUTION

| Model | h/D | $\alpha$ (deg.) | $q/P_t$ | Wind on only | Air on only | Wind and air on |
|---|---|---|---|---|---|---|
| TINA-JERO | .022 | 0 | - | x | - | - |
| | | | - | x | - | - |
| | | | 0.35 | - | - | x |
| | | | 0.40 | - | - | x |
| | | | 0.75 | - | - | x |
| | | | 0.80 | - | - | x |
| | | | 0 | - | x | - |
| | | 1.18 | - | x | - | - |
| | | | - | x | - | - |
| | | | 0.40 | - | - | x |
| | | | 0.40 | - | - | x |
| | | | 0.60 | - | - | x |
| | | | 0.70 | - | - | x |
| | | | 0.85 | - | - | x |
| | | | 0 | - | x | - |
| | | 2.36 | - | x | - | - |
| | | | - | x | - | - |
| | | | 0.25 | - | - | x |
| | | | 0.45 | - | - | x |
| | | | 0.65 | - | - | x |
| | | | 0.70 | - | - | x |
| | | | 0 | - | x | - |
| | | -1.18 | - | x | - | - |
| | | | - | x | - | - |
| | | | 0.30 | - | - | x |
| | | | 0.95 | - | - | x |
| | | | 0 | - | x | - |
| | | -2.36 | - | x | - | - |
| | | | - | x | - | - |
| | | | 0.25 | - | - | x |
| | | | 0.85 | - | - | x |
| | | | 0 | - | x | - |
| | .035 | 0 | - | x | - | - |
| | | | - | x | - | - |
| | | | 0.35 | - | - | x |
| | | | 0.35 | - | - | x |
| | | | 0.50 | - | - | x |
| | | | 0.60 | - | - | x |
| | | | 0.90 | - | - | x |
| | | | 0 | - | x | - |

| Model | h/D | $\alpha$ (deg.) | $q/P_t$ | Wind on only | Air on only | Wind and air on |
|---|---|---|---|---|---|---|
| TINA-JERO | .035 | 0 | 0 | - | x | - |
| | | 2.03 | - | x | - | - |
| | | | - | x | - | - |
| | | | 0.45 | - | - | x |
| | | | 0.90 | - | - | x |
| | | | 0 | - | x | - |
| | | 4.07 | - | x | - | - |
| | | | - | x | - | - |
| | | | 0.40 | - | - | x |
| | | | 0.80 | - | - | x |
| | | | 0 | - | x | - |
| | | -2.03 | - | x | - | - |
| | | | - | x | - | - |
| | | | 0.45 | - | - | x |
| | | | 0.95 | - | - | x |
| | | | 1.05 | - | - | x |
| | | | 1.25 | - | - | x |
| | | | 0 | - | x | - |
| | | | - | x | - | - |
| | | -4.07 | - | x | - | - |
| | | | 0.10 | - | - | x |
| | | | 0.20 | - | - | x |
| | | | 0.25 | - | - | x |
| | | | 0.50 | - | - | x |
| | | | 0 | - | x | - |
| | .050 | 0 | - | x | - | - |
| | | | - | x | - | - |
| | | | 0.50 | - | - | x |
| | | | 0.60 | - | - | x |
| | | | 0.80 | - | - | x |
| | | | 0.98 | - | - | x |
| | | | 1.10 | - | - | x |
| | | | 0 | - | x | - |
| | | 5.0 | - | x | - | - |
| | | | - | x | - | - |
| | | | 0.40 | - | - | x |
| | | | 0.60 | - | - | x |
| | | | 0.70 | - | - | x |
| | | | 0.80 | - | - | x |
| | | | 0.85 | - | - | x |
| | | | 0.90 | - | - | x |
| | | | 0 | - | x | - |
| | | -5.0 | - | x | - | - |

| Model | h/D | $\alpha$ (deg.) | $q/P_t$ | Wind on only | Air on only | Wind and air on |
|---|---|---|---|---|---|---|
| TINA-JERO | .050 | -5.0 | - | x | - | - |
| | | | 0.40 | - | - | x |
| | | | 0.90 | - | - | x |
| | | | 1.40 | - | - | x |
| | | | 1.90 | - | - | x |
| | | | 2.20 | - | - | x |
| | | | 0 | - | x | - |
| | .100 | 0 | - | x | - | - |
| | | | - | x | - | - |
| | | | 0.34 | - | - | x |
| | | | 0.63 | - | - | x |
| | | | 0.95 | - | - | x |
| | | | 1.17 | - | - | x |
| | | | 1.40 | - | - | x |
| | | | 0 | - | x | - |
| | | -5.0 | - | x | - | - |
| | | | - | x | - | - |
| | | | 0.38 | - | - | x |
| | | | 0.55 | - | - | x |
| | | | 0.80 | - | - | x |
| | | | 0.85 | - | - | x |
| | | | 1.02 | - | - | x |
| | | | 1.05 | - | - | x |
| | | | 0 | - | x | - |
| | | 10.0 | - | x | - | - |
| | | | - | x | - | - |
| | | | 0.40 | - | - | x |
| | | | 0.70 | - | - | x |
| | | | 0.85 | - | - | x |
| | | | 0.90 | - | - | x |
| | | | 0.95 | - | - | x |
| | | | 0.98 | - | - | x |
| | | | 0 | - | x | - |
| | | -5.0 | - | x | - | - |
| | | | - | x | - | - |
| | | | 0.40 | - | - | x |
| | | | 1.30 | - | - | x |
| | | | 2.50 | - | - | x |
| | | | 5.75 | - | - | x |
| | | | 0 | - | x | - |
| | | -10.0 | - | x | - | - |
| | | | - | x | - | - |

| Model | h/D | $\alpha$ (deg.) | $q/P_t$ | Wind on only | Air on only | Wind and air on |
|---|---|---|---|---|---|---|
| TINA-JERO | .100 | -10.0 | 0.40 | - | - | x |
| | | | 1.30 | - | - | x |
| | | | 2.40 | - | - | x |
| | | | 4.30 | - | - | x |
| | | | 0 | - | x | - |
| | .150 | 0 | - | x | - | - |
| | | | - | x | - | - |
| | | | 0.40 | - | - | x |
| | | | 0.60 | - | - | x |
| | | | 0.90 | - | - | x |
| | | | 1.20 | - | - | x |
| | | | 1.35 | - | - | x |
| | | | 0 | - | x | - |
| | | -5.0 | - | x | - | - |
| | | | - | x | - | - |
| | | | 0.40 | - | - | x |
| | | | 0.50 | - | - | x |
| | | | 0.70 | - | - | x |
| | | | 0.80 | - | - | x |
| | | | 0.85 | - | - | x |
| | | | 0 | - | x | - |
| | | 10.0 | - | x | - | - |
| | | | - | x | - | - |
| | | | 0.40 | - | - | x |
| | | | 0.60 | - | - | x |
| | | | 0.70 | - | - | x |
| | | | 0.75 | - | - | x |
| | | | 0.80 | - | - | x |
| | | | 0.87 | - | - | x |
| | | | 0 | - | x | - |
| | | -5.0 | - | x | - | - |
| | | | - | x | - | - |
| | | | 0.40 | - | - | x |
| | | | 1.30 | - | - | x |
| | | | 4.00 | - | - | x |
| | | | 3.75 | - | - | x |
| | | | 4.50 | - | - | x |
| | | | 0 | - | x | - |
| | | -10.0 | - | x | - | - |
| | | | - | x | - | - |
| | | | 0.60 | - | - | x |
| | | | 2.50 | - | - | x |

| Model | h/D | $\alpha$ (deg.) | $q/P_t$ | Wind on only | Air on only | Wind and air on |
|---|---|---|---|---|---|---|
| TINA-JERO | .150 | -10.0 | 5.00 | - | - | x |
| | | | * | - | - | x |
| | | | 0 | - | x | - |
| | .200 | 0 | - | x | - | - |
| | | | - | x | - | - |
| | | | 0.40 | - | - | x |
| | | | 0.70 | - | - | x |
| | | | 1.00 | - | - | x |
| | | | 1.20 | - | - | x |
| | | | 1.45 | - | - | x |
| | | | 0 | - | x | - |
| | | 5.0 | - | x | - | - |
| | | | 0 | x | - | - |
| | | | 0.45 | - | - | x |
| | | | 0.60 | - | - | x |
| | | | 0.75 | - | - | x |
| | | | 0.87 | - | - | x |
| | | | 0.91 | - | - | x |
| | | | 0.95 | - | - | x |
| | | | 0 | - | x | - |
| | | 10.0 | - | x | - | - |
| | | | - | x | - | - |
| | | | 0.40 | - | - | x |
| | | | 0.62 | - | - | x |
| | | | 0.70 | - | - | x |
| | | | 0.80 | - | - | x |
| | | | 0.85 | - | - | x |
| | | | 0.90 | - | - | x |
| | | | 0 | - | x | - |
| | .200 | -5.0 | - | x | - | - |
| | | | - | x | - | - |
| | | | 0.50 | - | - | x |
| | | | 1.30 | - | - | x |
| | | | 3.50 | - | - | x |
| | | | 6.80 | - | - | x |
| | | | 17.50 | - | - | x |
| | | | 0 | - | x | - |
| | | -10.0 | - | x | - | - |
| | | | - | x | - | - |
| | | | 1.90 | - | - | x |
| | | | 5.00 | - | - | x |
| | | | * | - | - | x |

| Model | h/D | $\alpha$ (deg.) | $q/P_t$ | Wind on only | Air on only | Wind and air on |
|---|---|---|---|---|---|---|
| TINA- | .200 | -10.0 | 0 | - | x | - |
| JERO | .250 | 0 | - | x | - | - |
| | | | - | x | - | - |
| | | | 0.40 | - | - | x |
| | | | 0.77 | - | - | x |
| | | | 1.10 | - | - | x |
| | | | 1.40 | - | - | x |
| | | | 1.70 | - | - | x |
| | | | 0 | - | x | - |
| | | 5.0 | - | x | - | - |
| | | | - | x | - | - |
| | | | 0.40 | - | - | x |
| | | | 0.55 | - | - | x |
| | | | 0.70 | - | - | x |
| | | | 0.76 | - | - | x |
| | | | 0.80 | - | - | x |
| | | | 0.83 | - | - | x |
| | | | 0 | - | x | - |
| | | 10.0 | - | x | - | - |
| | | | - | x | - | - |
| | | | 0.40 | - | - | x |
| | | | 0.60 | - | - | x |
| | | | 0.70 | - | - | x |
| | | | 0.80 | - | - | x |
| | | | 0.85 | - | - | x |
| | | | 0.90 | - | - | x |
| | | | 0 | - | x | - |
| | | -5.0 | - | x | - | - |
| | | | - | x | - | - |
| | | | 0.40 | - | - | x |
| | | | 1.50 | - | - | x |
| | | | 3.00 | - | - | x |
| | | | 15.00 | - | - | x |
| | | | 0 | - | x | - |
| | | -10.0 | - | x | - | - |
| | | | - | x | - | - |
| | | | 0.40 | - | - | x |
| | | | 0.70 | - | - | x |
| | | | 3.40 | - | - | x |
| | | | * | - | - | x |
| | | | 0 | - | x | - |
| | .300 | 0 | - | x | - | - |

| Model | h/D | $\alpha$ (deg.) | $q/P_t$ | Wind on only | Air on only | Wind and air on |
|---|---|---|---|---|---|---|
| TINA- | .300 | 0 | - | x | - | - |
| JERO | | | 0.50 | - | - | x |
| | | | 0.81 | - | - | x |
| | | | 1.10 | - | - | x |
| | | | 1.40 | - | - | x |
| | | | 1.72 | - | - | x |
| | | 0 | 0 | - | x | - |
| | | 5.0 | - | x | - | - |
| | | | - | x | - | - |
| | | | 0.40 | - | - | x |
| | | | 0.60 | - | - | x |
| | | | 0.75 | - | - | x |
| | | | 0.80 | - | - | x |
| | | | 0.93 | - | - | x |
| | | | 0 | - | x | - |
| | | 10.0 | - | x | - | - |
| | | | - | x | - | - |
| | | | 0.40 | - | - | x |
| | | | 0.60 | - | - | x |
| | | | 0.70 | - | - | x |
| | | | 0.80 | - | - | x |
| | | | 0.88 | - | - | x |
| | | | 0.92 | - | - | x |
| | | | 0 | - | x | - |
| | | -5.0 | - | x | - | - |
| | | | - | x | - | - |
| | | | 0.35 | - | - | x |
| | | | 0.60 | - | - | x |
| | | | 1.60 | - | - | x |
| | | | 3.00 | - | - | x |
| | | | 9.50 | - | - | x |
| | | | 0 | - | x | - |
| | | -10.0 | - | x | - | - |
| | | | - | x | - | - |
| | | | 0.50 | - | - | x |
| | | | 2.75 | - | - | x |
| | | | * | - | - | x |
| | | | * | - | - | x |
| | | | 0 | - | x | - |
| UPPER | .022 | 0 | - | x | - | - |
| CURV. | | | - | x | - | - |
| | | | 0.80 | - | - | x |

| Model | h/D | $\alpha$ (deg.) | $q/P_t$ | Wind on only | Air on only | Wind and air on |
|---|---|---|---|---|---|---|
| UPPER CURV. | .022 | 0 | 1.05 | - | - | x |
| | | | 1.40 | - | - | x |
| | | | 1.50 | - | - | x |
| | | | 1.70 | - | - | x |
| | | | 1.70 | - | - | x |
| | | | 0 | - | x | - |
| | | 1.18 | - | x | - | - |
| | .022 | 1.18 | - | x | - | - |
| | | | 1.25 | - | - | x |
| | | | 1.40 | - | - | x |
| | | | 1.60 | - | - | x |
| | | | 1.70 | - | - | x |
| | | | 1.65 | - | - | x |
| | | | 0 | - | x | - |
| | | 2.36 | - | x | - | - |
| | | | - | x | - | - |
| | | | 1.00 | - | - | x |
| | | | 1.15 | - | - | x |
| | | | 1.13 | - | - | x |
| | | | 1.40 | - | - | x |
| | | | 1.45 | - | - | x |
| | | | 1.50 | - | - | x |
| | | | 0 | - | x | - |
| | | -1.18 | - | x | - | - |
| | | | - | x | - | - |
| | | | 1.30 | - | - | x |
| | | | 1.50 | - | - | x |
| | | | 1.60 | - | - | x |
| | | | 1.90 | - | - | x |
| | | | 1.90 | - | - | x |
| | | | 0 | - | x | - |
| | | -2.36 | - | x | - | - |
| | | | - | x | - | - |
| | | | 0.80 | - | - | x |
| | | | 1.05 | - | - | x |
| | | | 1.40 | - | - | x |
| | | | 1.50 | - | - | x |
| | | | 1.65 | - | - | x |
| | | | 1.70 | - | - | x |
| | | | 0 | - | x | - |
| | .035 | 0 | - | x | - | - |
| | | | - | x | - | - |

| Model | h/D | $\alpha$ (deg.) | $q/P_t$ | Wind on only | Air on only | Wind and air on |
|---|---|---|---|---|---|---|
| UPPER CURV. | .035 | 0 | 1.45 | - | - | x |
| | | | 1.50 | - | - | x |
| | | | 1.60 | - | - | x |
| | | | 1.60 | - | - | x |
| | | | 1.70 | - | - | x |
| | | | 0 | - | x | - |
| | .035 | 2.03 | - | x | - | - |
| | | | - | x | - | - |
| | .035 | 2.03 | 1.30 | - | - | x |
| | | | 1.40 | - | - | x |
| | | | 1.50 | - | - | x |
| | | | 1.60 | - | - | x |
| | | | 1.60 | - | - | x |
| | | 4.07 | 0 | - | x | - |
| | | | - | x | - | - |
| | | | - | x | - | - |
| | | | 1.40 | - | - | x |
| | | | 1.50 | - | - | x |
| | | | 1.50 | - | - | x |
| | | | 1.60 | - | - | x |
| | | | 1.60 | - | - | x |
| | | | 0 | - | x | - |
| | | -2.03 | - | x | - | - |
| | | | - | x | - | - |
| | | | 1.50 | - | - | x |
| | | | 2.00 | - | - | x |
| | | | 2.00 | - | - | x |
| | | | 2.00 | - | - | x |
| | | | 2.25 | - | - | x |
| | | | 0 | - | x | - |
| | | -4.07 | - | x | - | - |
| | | | - | x | - | - |
| | | | 1.25 | - | - | x |
| | | | 1.50 | - | - | x |
| | | | 2.00 | - | - | x |
| | | | 2.00 | - | - | x |
| | | | 2.20 | - | - | x |
| | | | 0 | - | x | - |
| | .050 | 0 | - | x | - | - |
| | | | - | x | - | - |
| | | | 1.40 | - | - | x |
| | | | 1.60 | - | - | x |

| Model | h/D | $\alpha$ (deg.) | $q/P_t$ | Wind on only | Air on only | Wind and air on |
|---|---|---|---|---|---|---|
| UPPER CURV. | .050 | 0 | 1.60 | - | - | x |
| | | | 0 | - | x | - |
| | .050 | -5.0 | - | x | - | - |
| | | | - | x | - | - |
| | | | 1.75 | - | - | x |
| | | | 2.00 | - | - | x |
| | | | 2.30 | - | - | x |
| | | | 2.50 | - | - | x |
| | | | 2.75 | - | - | x |
| | | | 0 | - | x | - |
| | .100 | 0 | - | x | - | - |
| | | | - | x | - | - |
| | | | 1.10 | - | - | x |
| | | | 1.50 | - | - | x |
| | | | 1.60 | - | - | x |
| | | | 1.70 | - | - | x |
| | | | 1.75 | - | - | x |
| | | | 0 | - | x | - |
| | | 5.0 | - | x | - | - |
| | | | - | x | - | - |
| | | | 1.25 | - | - | x |
| | | | 1.50 | - | - | x |
| | | | 1.60 | - | - | x |
| | | | 1.60 | - | - | x |
| | | | 1.60 | - | - | x |
| | | | 0 | - | x | - |
| | | 10.0 | - | x | - | - |
| | | | - | x | - | - |
| | | | 1.15 | - | - | x |
| | | | 1.35 | - | - | x |
| | | | 1.40 | - | - | x |
| | | | 1.40 | - | - | x |
| | | | 1.40 | - | - | x |
| | | | 1.40 | - | - | x |
| | | | 0 | - | x | - |
| | | -5.0 | - | x | - | - |
| | | | - | x | - | - |
| | | | 1.80 | - | - | x |
| | | | 2.40 | - | - | x |
| | | | 3.20 | - | - | x |
| | | | 3.80 | - | - | x |
| | | | 5.10 | - | - | x |

| Model | h/D | $\alpha$ (deg.) | $q/P_t$ | Wind on only | Air on only | Wind and air on |
|---|---|---|---|---|---|---|
| UPPER CURV. | .100 | -5.0 | 0 | - | x | - |
| | | -10.0 | - | x | - | - |
| | | | - | x | - | - |
| | .100 | -10.0 | 3.20 | - | - | x |
| | | | 4.00 | - | - | x |
| | | | 4.00 | - | - | x |
| | | | 4.80 | - | - | x |
| | | | 0 | - | x | - |
| | .150 | 0 | - | x | - | - |
| | | | - | x | - | - |
| | | | 1.50 | - | - | x |
| | | | 1.80 | - | - | x |
| | | | 2.00 | - | - | x |
| | | | 2.00 | - | - | x |
| | | | 2.20 | - | - | x |
| | | | 2.25 | - | - | x |
| | | | 0 | - | x | - |
| | | 5.0 | - | x | - | - |
| | | | - | x | - | - |
| | | | 1.25 | - | - | x |
| | | | 1.60 | - | - | x |
| | | | 1.60 | - | - | x |
| | | | 1.60 | - | - | x |
| | | | 1.62 | - | - | x |
| | | | 1.65 | - | - | x |
| | | | 0 | - | x | - |
| | | 10.0 | - | x | - | - |
| | | | - | x | - | - |
| | | | 1.25 | - | - | x |
| | | | 1.25 | - | - | x |
| | | | 1.25 | - | - | x |
| | | | 1.30 | - | - | x |
| | | | 1.30 | - | - | x |
| | | | 1.50 | - | - | x |
| | | | 0 | - | x | - |
| | | -5.0 | - | x | - | - |
| | | | - | x | - | - |
| | | | 2.50 | - | - | x |
| | | | 3.80 | - | - | x |
| | | | 5.00 | - | - | x |
| | | | 6.50 | - | - | x |
| | | | 0 | - | x | - |
| | | -10.0 | - | x | - | - |

| Model | h/D | $\alpha$ (deg.) | $q/P_t$ | Wind on only | Air on only | Wind and air on |
|---|---|---|---|---|---|---|
| UPPER CURV. | .150 | -10.0 | - | x | - | - |
| | | | 3.50 | - | - | x |
| | | | 5.50 | - | - | x |
| | .150 | -10.0 | 7.50 | - | - | x |
| | | | 0 | - | x | - |
| | .200 | 0 | - | x | - | - |
| | | | - | x | - | - |
| | | | 1.80 | - | - | x |
| | | | 1.80 | - | - | x |
| | | | 2.00 | - | - | x |
| | | | 2.00 | - | - | x |
| | | | 0 | - | x | - |
| | .200 | 5.0 | - | x | - | - |
| | | | - | x | - | - |
| | | | 1.20 | - | - | x |
| | | | 1.40 | - | - | x |
| | | | 1.43 | - | - | x |
| | | | 1.50 | - | - | x |
| | | | 0 | - | x | - |
| | | 10.0 | - | x | - | - |
| | | | - | x | - | - |
| | | | 1.60 | - | - | x |
| | | | 1.80 | - | - | x |
| | | | 1.80 | - | - | x |
| | | | 1.90 | - | - | x |
| | | | 2.00 | - | - | x |
| | | | 0 | - | x | - |
| | | -5.0 | - | x | - | - |
| | | | - | x | - | - |
| | | | 2.00 | - | - | x |
| | | | 3.00 | - | - | x |
| | | | 3.25 | - | - | x |
| | | | 3.50 | - | - | x |
| | | | 0 | - | x | - |
| | | -10.0 | - | x | - | - |
| | | | - | x | - | - |
| | | | 3.80 | - | - | x |
| | | | 5.00 | - | - | x |
| | | | 5.50 | - | - | x |
| | | | 6.00 | - | - | x |
| | | | 0 | - | x | - |
| | .250 | 0 | - | x | - | - |

| Model | h/D | $\alpha$ (deg.) | $q/P_t$ | Wind on only | Air on only | Wind and air on |
|---|---|---|---|---|---|---|
| UPPER CURV. | .250 | 0 | - | x | - | - |
| | | | 2.00 | - | - | x |
| | | | 2.25 | - | - | x |
| | | | 2.40 | - | - | x |
| | | | 2.50 | - | - | x |
| | | | 0 | - | x | - |
| | | 5.0 | - | x | - | - |
| | | | - | x | - | - |
| | .250 | 5.0 | 1.75 | - | - | x |
| | | | 1.90 | - | - | x |
| | | | 2.00 | - | - | x |
| | | | 2.00 | - | - | x |
| | | | 0 | - | x | - |
| | | 10.0 | - | x | - | - |
| | | | - | x | - | - |
| | | | 1.10 | - | - | x |
| | | | 1.25 | - | - | x |
| | | | 1.40 | - | - | x |
| | | | 1.40 | - | - | x |
| | | | 1.50 | - | - | x |
| | | | 0 | - | x | - |
| | .250 | -5.0 | - | x | - | - |
| | | | - | x | - | - |
| | | | 2.00 | - | - | x |
| | | | 3.30 | - | - | x |
| | | | 3.50 | - | - | x |
| | | | 3.70 | - | - | x |
| | | | 0 | - | x | - |
| | | -10.0 | - | x | - | - |
| | | | - | x | - | - |
| | | | 3.50 | - | - | x |
| | | | 5.50 | - | - | x |
| | | | 5.80 | - | - | x |
| | | | 0 | - | x | - |
| | .300 | 0 | - | x | - | - |
| | | | - | x | - | - |
| | | | 1.50 | - | - | x |
| | | | 1.70 | - | - | x |
| | | | 1.90 | - | - | x |
| | | | 2.00 | - | - | x |
| | | | 0 | - | x | - |
| | | 5.0 | - | x | - | - |

| Model | h/D | $\alpha$ (deg.) | $q/P_t$ | Wind on only | Air on only | Wind and air on |
|---|---|---|---|---|---|---|
| UPPER CURV. | .300 | 5.0 | - | x | - | - |
| | | | 1.15 | - | - | x |
| | | | 1.40 | - | - | x |
| | | | 1.45 | - | - | x |
| | | | 1.50 | - | - | x |
| | | | 0 | - | x | - |
| | | 10.0 | - | x | - | - |
| | | | - | x | - | - |
| | | | 1.20 | - | - | x |
| | | | 1.40 | - | - | x |
| | | | 1.50 | - | - | x |
| | | | 1.50 | - | - | x |
| | .300 | 10.0 | 0 | - | x | - |
| | | -5.0 | - | x | - | - |
| | | | - | x | - | - |
| | | | 2.00 | - | - | x |
| | | | 3.00 | - | - | x |
| | | | 3.15 | - | - | x |
| | | | 3.30 | - | - | x |
| | | | 0 | - | x | - |
| | | -10.0 | - | x | - | - |
| | | | - | x | - | - |
| | | | 2.10 | - | - | x |
| | | | 3.00 | - | - | x |
| | | | 3.50 | - | - | x |
| | | | 3.50 | - | - | x |
| | | | 0 | - | x | - |
| LOWER CURV. | .022 | 0 | - | x | - | - |
| | | | - | x | - | - |
| | | | 0.50 | - | - | x |
| | | | 0.55 | - | - | x |
| | | | 0.70 | - | - | x |
| | | | 0.83 | - | - | x |
| | | | 0.95 | - | - | x |
| | | | 0 | - | x | - |
| | | 1.18 | - | x | - | - |
| | | | - | x | - | - |
| | | | 0.40 | - | - | x |
| | | | 0.50 | - | - | x |
| | | | 0.63 | - | - | x |
| | | | 0.73 | - | - | x |
| | | | 0.85 | - | - | x |

| Model | h/D | $\alpha$ (deg.) | $q/P_t$ | Wind on only | Air on only | Wind and air on |
|---|---|---|---|---|---|---|
| LOWER CURV. | .022 | 1.18 | 0 | - | x | - |
| | | 2.36 | - | x | - | - |
| | | | - | x | - | - |
| | | | 0.25 | - | - | x |
| | | | 0.30 | - | - | x |
| | | | 0.40 | - | - | x |
| | | | 0.50 | - | - | x |
| | | | 0.55 | - | - | x |
| | | | 0.65 | - | - | x |
| | | | 0 | - | x | - |
| | | -1.18 | - | x | - | - |
| | | | - | x | - | - |
| | | | 0.50 | - | - | x |
| | | | 0.65 | - | - | x |
| | | | 0.90 | - | - | x |
| | | | 1.05 | - | - | x |
| | | | 1.15 | - | - | x |
| | | | 0 | - | x | - |
| | .022 | -2.36 | - | x | - | - |
| | | | - | x | - | - |
| | | | 0.15 | - | - | x |
| | | | 0.20 | - | - | x |
| | | | 0.25 | - | - | x |
| | | | 0.33 | - | - | x |
| | | | 0.39 | - | - | x |
| | | | 0 | - | x | - |
| | .035 | 0 | - | x | - | - |
| | | | - | x | - | - |
| | | | 0.60 | - | - | x |
| | | | 0.65 | - | - | x |
| | | | 0.80 | - | - | x |
| | | | 0.90 | - | - | x |
| | | | 1.00 | - | - | x |
| | | | 1.10 | - | - | x |
| | | | 0 | - | x | - |
| | .035 | 2.03 | - | x | - | - |
| | | | - | x | - | - |
| | | | 0.40 | - | - | x |
| | | | 0.55 | - | - | x |
| | | | 0.70 | - | - | x |
| | | | 0.80 | - | - | x |
| | | | 0.85 | - | - | x |
| | | | 0.90 | - | - | x |

| Model | h/D | $\alpha$ (deg.) | $q/P_t$ | Wind on only | Air on only | Wind and air on |
|---|---|---|---|---|---|---|
| LOWER CURV. | .035 | 2.03 | 0 | - | x | - |
| | | 4.07 | - | x | - | - |
| | | | - | x | - | - |
| | | | 0.20 | - | - | x |
| | | | 0.35 | - | - | x |
| | | | 0.45 | - | - | x |
| | | | 0.55 | - | - | x |
| | | | 0.60 | - | - | x |
| | | | 0.70 | - | - | x |
| | | | 0 | - | x | - |
| | | -2.03 | - | x | - | - |
| | | | - | x | - | - |
| | | | 0.60 | - | - | x |
| | | | 0.80 | - | - | x |
| | | | 1.05 | - | - | x |
| | | | 1.30 | - | - | x |
| | | | 1.50 | - | - | x |
| | | | 0 | - | x | - |
| | | -4.07 | - | x | - | - |
| | | | - | x | - | - |
| | | | 0.17 | - | - | x |
| | | | 0.32 | - | - | x |
| | | | 0.45 | - | - | x |
| | | | 0.55 | - | - | x |
| | .035 | -4.07 | 0.75 | - | - | x |
| | | | 0 | - | x | - |
| | .050 | 0 | - | x | - | - |
| | | | - | x | - | - |
| | | | 0.75 | - | - | x |
| | | | 0.90 | - | - | x |
| | | | 0.95 | - | - | x |
| | | | 1.10 | - | - | x |
| | | | 1.10 | - | - | x |
| | | | 1.50 | - | - | x |
| | | | 0 | - | x | - |
| | | 5.0 | - | x | - | - |
| | | | - | x | - | - |
| | | | 0.55 | - | - | x |
| | | | 0.65 | - | - | x |
| | | | 0.75 | - | - | x |
| | | | 0.80 | - | - | x |
| | | | 0.85 | - | - | x |

| Model | h/D | $\alpha$ (deg.) | $q/P_t$ | Wind on only | Air on only | Wind and air on |
|---|---|---|---|---|---|---|
| LOWER CURV. | .050 | 5.0 | 0.95 | - | - | x |
| | | | 0 | - | x | - |
| | .050 | -5.0 | - | x | - | - |
| | | | - | x | - | - |
| | | | 1.20 | - | - | x |
| | | | 1.20 | - | - | x |
| | | | 1.50 | - | - | x |
| | | | 2.00 | - | - | x |
| | | | 2.50 | - | - | x |
| | | | 0 | - | x | - |
| | .100 | 0 | - | x | - | - |
| | | | - | x | - | - |
| | | | 0.90 | - | - | x |
| | | | 1.02 | - | - | x |
| | | | 1.20 | - | - | x |
| | | | 1.20 | - | - | x |
| | | | 1.31 | - | - | x |
| | | | 0 | - | x | - |
| | | 5.0 | - | x | - | - |
| | | | - | x | - | - |
| | | | 0.80 | - | - | x |
| | | | 0.80 | - | - | x |
| | | | 0.85 | - | - | x |
| | | | 0.90 | - | - | x |
| | | | 0.95 | - | - | x |
| | | | 0 | - | x | - |
| | .100 | 10.0 | - | x | - | - |
| | | | - | x | - | - |
| | | | 0.60 | - | - | x |
| | | | 0.69 | - | - | x |
| | | | 0.79 | - | - | x |
| | | | 0.80 | - | - | x |
| | | | 0.85 | - | - | x |
| | | | 0.92 | - | - | x |
| | | | 0 | - | x | - |
| | | -5.0 | - | x | - | - |
| | | | - | x | - | - |
| | | | 1.75 | - | - | x |
| | | | 2.70 | - | - | x |
| | | | 4.50 | - | - | x |
| | | | 14.50 | - | - | x |
| | | | * | - | - | x |

| Model | h/D | $\alpha$ (deg.) | $q/P_t$ | Wind on only | Air on only | Wind and air on |
|---|---|---|---|---|---|---|
| LOWER CURV. | .100 | -5.0 | 0 | - | x | - |
| | | -10.0 | - | x | - | - |
| | | | - | x | - | - |
| | | | 0.85 | - | - | x |
| | | | 1.75 | - | - | x |
| | | | 3.50 | - | - | x |
| | | | 7.50 | - | - | x |
| | | | 0 | - | x | - |
| | .150 | 0 | - | x | - | - |
| | | | - | x | - | - |
| | | | 0.60 | - | - | x |
| | | | 0.81 | - | - | x |
| | | | 1.10 | - | - | x |
| | | | 1.30 | - | - | x |
| | | | 1.50 | - | - | x |
| | | | 1.65 | - | - | x |
| | | | 0 | - | x | - |
| | | 5.0 | - | x | - | - |
| | | | - | x | - | - |
| | | | 0.32 | - | - | x |
| | | | 0.70 | - | - | x |
| | | | 0.80 | - | - | x |
| | | | 0.87 | - | - | x |
| | | | 0.90 | - | - | x |
| | | | 0.95 | - | - | x |
| | | | 0 | - | x | - |
| | | 10.0 | - | x | - | - |
| | | | - | x | - | - |
| | | | 0.40 | - | - | x |
| | | | 0.65 | - | - | x |
| | | | 0.75 | - | - | x |
| | | | 0.80 | - | - | x |
| | .150 | 10.0 | 0.85 | - | - | x |
| | | | 0.90 | - | - | x |
| | | | 0 | - | x | - |
| | | -5.0 | - | x | - | - |
| | | | - | x | - | - |
| | | | 1.20 | - | - | x |
| | | | 2.20 | - | - | x |
| | | | 4.20 | - | - | x |
| | | | 14.00 | - | - | x |
| | | | 16.80 | - | - | x |

| Model | h/D | $\alpha$ (deg.) | $q/P_t$ | Wind on only | Air on only | Wind and air on |
|---|---|---|---|---|---|---|
| LOWER CURV. | .150 | -5.0 | 0 | - | x | - |
| | | -10.0 | - | x | - | - |
| | | | - | x | - | - |
| | | | 2.00 | - | - | x |
| | | | 6.00 | - | - | x |
| | | | * | - | - | x |
| | | | * | - | - | x |
| | | | 0 | - | x | - |
| | .200 | 0 | - | x | - | - |
| | | | - | x | - | - |
| | | | 2.10 | - | - | x |
| | | | 1.21 | - | - | x |
| | | | 1.40 | - | - | x |
| | | | 1.70 | - | - | x |
| | | | 2.22 | - | - | x |
| | | | 0 | - | x | - |
| | .200 | 5.0 | - | x | - | - |
| | | | - | x | - | - |
| | | | 0.90 | - | - | x |
| | | | 0.95 | - | - | x |
| | | | 0.98 | - | - | x |
| | | | 1.00 | - | - | x |
| | | | 1.05 | - | - | x |
| | | | 0 | - | x | - |
| | | 10.0 | - | x | - | - |
| | | | - | x | - | - |
| | | | 0.80 | - | - | x |
| | | | 0.87 | - | - | x |
| | | | 0.94 | - | - | x |
| | | | 0.98 | - | - | x |
| | | | 1.00 | - | - | x |
| | | | 0 | - | x | - |
| | | -5.0 | - | x | - | - |
| | | | - | x | - | - |
| | | | 1.10 | - | - | x |
| | | | 3.20 | - | - | x |
| | .200 | -5.0 | 8.50 | - | - | x |
| | | | * | - | - | x |
| | | | 0 | - | x | - |
| | | -10.0 | - | x | - | - |
| | | | - | x | - | - |
| | | | * | - | - | x |

| Model | h/D | $\alpha$ (deg.) | $q/P_t$ | Wind on only | Air on only | Wind and air on |
|---|---|---|---|---|---|---|
| LOWER CURV. | .200 | -10.0 | * | - | - | x |
| | | | * | - | - | x |
| | | | * | - | - | x |
| | | | 0 | - | x | - |
| | .250 | 0 | - | x | - | - |
| | | | - | x | - | - |
| | | | 1.02 | - | - | x |
| | | | 1.20 | - | - | x |
| | | | 1.41 | - | - | x |
| | | | 1.90 | - | - | x |
| | | | 2.20 | - | - | x |
| | | | 0 | - | x | - |
| | | 5.0 | - | x | - | - |
| | | | - | x | - | - |
| | | | 0.70 | - | - | x |
| | | | 0.70 | - | - | x |
| | | | 0.84 | - | - | x |
| | | | 1.00 | - | - | x |
| | | | 1.05 | - | - | x |
| | | | 1.10 | - | - | x |
| | | | 0 | - | x | - |
| | .250 | 10.0 | - | x | - | - |
| | | | - | x | - | - |
| | | | 0.57 | - | - | x |
| | | | 0.70 | - | - | x |
| | | | 0.80 | - | - | x |
| | | | 0.85 | - | - | x |
| | | | 0.93 | - | - | x |
| | | | 1.00 | - | - | x |
| | | | 0 | - | x | - |
| | | -5.0 | - | x | - | - |
| | | | - | x | - | - |
| | | | 1.05 | - | - | x |
| | | | 1.90 | - | - | x |
| | | | 5.30 | - | - | x |
| | | | * | - | - | x |
| | | | 0 | - | x | - |
| | | -10.0 | - | x | - | - |
| | | | - | x | - | - |
| | | | 0.75 | - | - | x |
| | .250 | -10.0 | 1.80 | - | - | x |
| | | | 5.20 | - | - | x |

| Model | h/D | $\alpha$ (deg.) | $q/P_t$ | Wind on only | Air on only | Wind and air on |
|---|---|---|---|---|---|---|
| LOWER CURV. | .250 | -10.0 | * | - | - | x |
| | | | 0 | - | x | - |
| | .300 | 0 | - | x | - | - |
| | | | - | x | - | - |
| | | | 1.20 | - | - | x |
| | | | 1.30 | - | - | x |
| | | | 1.50 | - | - | x |
| | | | 1.80 | - | - | x |
| | | | 2.20 | - | - | x |
| | | | 0 | - | x | - |
| | | 5.0 | - | x | - | - |
| | | | - | x | - | - |
| | | | 0.60 | - | - | x |
| | | | 0.80 | - | - | x |
| | | | 0.92 | - | - | x |
| | | | 1.00 | - | - | x |
| | | | 1,10 | - | - | x |
| | | | 1.20 | - | - | x |
| | | | 0 | - | x | - |
| | | 10.0 | - | x | - | - |
| | | | - | x | - | - |
| | | | 0.42 | - | - | x |
| | | | 0.63 | - | - | x |
| | | | 0.75 | - | - | x |
| | | | 0.85 | - | - | x |
| | | | 0.90 | - | - | x |
| | | | 0.98 | - | - | x |
| | | | 0 | - | x | - |
| | | -5.0 | - | x | - | - |
| | | | - | x | - | - |
| | | | 3.50 | - | - | x |
| | | | 5.20 | - | - | x |
| | | | 7.10 | - | - | x |
| | | | 16.50 | - | - | x |
| | | | * | - | - | x |
| | | | 0 | - | x | - |
| | | -10.0 | - | x | - | - |
| | | | - | x | - | - |
| | | | * | - | - | x |
| | | | * | - | - | x |
| | | | * | - | - | x |
| | | | * | - | - | x |
| | | | 0 | - | x | - |

| Model | h/D | $\alpha$ (deg.) | $q/P_t$ | Wind on only | Air on only | Wind and air on |
|---|---|---|---|---|---|---|
| SYMM. | .022 | 0 | - | x | - | - |
| CURV. | | | - | x | - | - |
| | | | 0.35 | - | - | x |
| | | | 0.60 | - | - | x |
| | | | 0.75 | - | - | x |
| | | | 0.90 | - | - | x |
| | | | 1.00 | - | - | x |
| | | | 0 | - | x | - |
| | | 1.18 | - | x | - | - |
| | | | - | x | - | - |
| | | | 0.40 | - | - | x |
| | | | 0.60 | - | - | x |
| | | | 0.72 | - | - | x |
| | | | 0.82 | - | - | x |
| | | | 0.93 | - | - | x |
| | | | 0 | - | x | - |
| | | 2.36 | - | x | - | - |
| | | | - | x | - | - |
| | | | 0.21 | - | - | x |
| | | | 0.28 | - | - | x |
| | | | 0.40 | - | - | x |
| | | | 0.46 | - | - | x |
| | | | 0.57 | - | - | x |
| | | | 0 | - | x | - |
| | | -1.18 | - | x | - | - |
| | | | - | x | - | - |
| | | | 0.40 | - | - | x |
| | | | 0.62 | - | - | x |
| | | | 0.80 | - | - | x |
| | | | 0.93 | - | - | x |
| | | | 1.05 | - | - | x |
| | | | 0 | - | x | - |
| | | -2.36 | - | x | - | - |
| | | | - | x | - | - |
| | | | 0.10 | - | - | x |
| | | | 0.13 | - | - | x |
| | | | 0.21 | - | - | x |
| | | | 0.37 | - | - | x |
| | | | 0 | - | x | - |
| | .035 | 0 | - | x | - | - |
| | | | - | x | - | - |
| | | | 0.45 | - | - | x |

| Model | h/D | $\alpha$ (deg.) | $q/P_t$ | Wind on only | Air on only | Wind and air on |
|---|---|---|---|---|---|---|
| SYMM. | .035 | 0 | 0.70 | - | - | x |
| CURV. | | | 0.80 | - | - | x |
| | | | 0.90 | - | - | x |
| | | | 1.00 | - | - | x |
| | | | 0 | - | x | - |
| | .035 | 2.03 | - | x | - | - |
| | | | - | x | - | - |
| | | | 0.70 | - | - | x |
| | | | 0.80 | - | - | x |
| | | | 1.00 | - | - | x |
| | | | 1.20 | - | - | x |
| | | | 1.40 | - | - | x |
| | | | 0 | - | x | - |
| | | 4.07 | - | x | - | - |
| | | | - | x | - | - |
| | | | 0.25 | - | - | x |
| | | | 0.33 | - | - | x |
| | | | 0.45 | - | - | x |
| | | | 0.55 | - | - | x |
| | | | 0.65 | - | - | x |
| | | | 0 | - | x | - |
| | | -2.03 | - | x | - | - |
| | | | - | x | - | - |
| | | | 0.70 | - | - | x |
| | | | 0.80 | - | - | x |
| | | | 1.00 | - | - | x |
| | | | 1.20 | - | - | x |
| | | | 1.40 | - | - | x |
| | | | 0 | - | x | - |
| | | -4.07 | - | x | - | - |
| | | | - | x | - | - |
| | | | 0.10 | - | - | x |
| | | | 0.17 | - | - | x |
| | | | 0.27 | - | - | x |
| | | | 0.37 | - | - | x |
| | | | 0.47 | - | - | x |
| | | | 0 | - | x | - |
| | .050 | 0 | - | x | - | - |
| | | | - | x | - | - |
| | | | 0.50 | - | - | x |
| | | | 0.65 | - | - | x |
| | | | 0.80 | - | - | x |

| Model | h/D | $\alpha$ (deg.) | $q/P_t$ | Wind on only | Air on only | Wind and air on |
|---|---|---|---|---|---|---|
| SYMM. | .050 | 0 | 0.90 | - | - | x |
| CURV. | | | 1.00 | - | - | x |
| | | | 1.03 | - | - | x |
| | | | 0 | - | x | - |
| | | 5.0 | - | x | - | - |
| | | | - | x | - | - |
| | | | 0.6 | - | - | x |
| | .050 | 5.0 | 0.80 | - | - | x |
| | | | 0.88 | - | - | x |
| | | | 0.90 | - | - | x |
| | | | 0.95 | - | - | x |
| | | | 0.99 | - | - | x |
| | | | 0 | - | x | - |
| | .050 | -5.0 | - | x | - | - |
| | | | - | x | - | - |
| | | | 0.90 | - | - | x |
| | | | 1.00 | - | - | x |
| | | | 1.20 | - | - | x |
| | | | 1.60 | - | - | x |
| | | | 2.10 | - | - | x |
| | | | 0 | - | x | - |
| | .100 | 0 | - | x | - | - |
| | | | - | x | - | - |
| | | | 0.80 | - | - | x |
| | | | 0.87 | - | - | x |
| | | | 1.00 | - | - | x |
| | | | 1.00 | - | - | x |
| | | | 1.70 | - | - | x |
| | | | 0 | - | x | - |
| | | 5.0 | - | x | - | - |
| | | | - | x | - | - |
| | | | 0.65 | - | - | x |
| | | | 0.70 | - | - | x |
| | | | 0.80 | - | - | x |
| | | | 0.90 | - | - | x |
| | | | 0.95 | - | - | x |
| | | | 0.96 | - | - | x |
| | | | 0 | - | x | - |
| | | 10.0 | - | x | - | - |
| | | | - | x | - | - |
| | | | 0.70 | - | - | x |
| | | | 0.75 | - | - | x |
| | | | 0.82 | - | - | x |

| Model | h/D | $\alpha$ (deg.) | $q/P_t$ | Wind on only | Air on only | Wind and air on |
|---|---|---|---|---|---|---|
| SYMM. CURV. | .100 | 10.0 | 0.95 | - | - | x |
| | | | 0.99 | - | - | x |
| | | | 1.00 | - | - | x |
| | | | 0 | - | x | - |
| | | -5.0 | - | x | - | - |
| | | | - | x | - | - |
| | | | 0.80 | - | - | x |
| | | | 1.40 | - | - | x |
| | | | 2.70 | - | - | x |
| | | | 7.50 | - | - | x |
| | .100 | -5.0 | * | - | - | x |
| | | | 0 | - | x | - |
| | | -10.0 | - | x | - | - |
| | | | - | x | - | - |
| | | | 3.00 | - | - | x |
| | | | 4.70 | - | - | x |
| | | | 16.50 | - | - | x |
| | | | * | - | - | x |
| | | | 0 | - | x | - |
| | .150 | 0 | - | x | - | - |
| | | | - | x | - | - |
| | | | 0.40 | - | - | x |
| | | | 0.75 | - | - | x |
| | | | 0.95 | - | - | x |
| | | | 1.10 | - | - | x |
| | | | 1.23 | - | - | x |
| | | | 0 | - | x | - |
| | | 5.0 | - | x | - | - |
| | | | - | x | - | - |
| | | | 0.60 | - | - | x |
| | | | 0.70 | - | - | x |
| | | | 0.84 | - | - | x |
| | | | 0.92 | - | - | x |
| | | | 1.00 | - | - | x |
| | | | 0 | - | x | - |
| | | 10.0 | - | x | - | - |
| | | | - | x | - | - |
| | | | 0.42 | - | - | x |
| | | | 0.70 | - | - | x |
| | | | 0.89 | - | - | x |
| | | | 0.93 | - | - | x |
| | | | 0.93 | - | - | x |

| Model | h/D | $\alpha$ (deg.) | $q/P_t$ | Wind on only | Air on only | Wind and air on |
|---|---|---|---|---|---|---|
| SYMM. | .150 | 10.0 | 0.98 | - | - | x |
| CURV. | | | 0 | - | x | - |
| | | -5.0 | - | x | - | - |
| | | | - | x | - | - |
| | | | 1.10 | - | - | x |
| | | | 1.40 | - | - | x |
| | | | 2.35 | - | - | x |
| | | | 4.27 | - | - | x |
| | | | 0 | - | x | - |
| | | -10.0 | - | x | - | - |
| | | | - | x | - | - |
| | | | 2.0 | - | - | x |
| | .150 | -10.0 | * | - | - | x |
| | | | * | - | - | x |
| | | | * | - | - | x |
| | | | 0 | - | x | - |
| | .200 | 0 | - | x | - | - |
| | | | - | x | - | - |
| | | | 0.60 | - | - | x |
| | | | 0.80 | - | - | x |
| | | | 1.00 | - | - | x |
| | | | 1.30 | - | - | x |
| | | | 0 | - | x | - |
| | .200 | 5.0 | - | x | - | - |
| | | | - | x | - | - |
| | | | 0.80 | - | - | x |
| | | | 0.90 | - | - | x |
| | | | 0.93 | - | - | x |
| | | | 1.00 | - | - | x |
| | | | 1.00 | - | - | x |
| | | | 1.10 | - | - | x |
| | | | 0 | - | x | - |
| | | 10.0 | - | x | - | - |
| | | | - | x | - | - |
| | | | 0.42 | - | - | x |
| | | | 0.70 | - | - | x |
| | | | 0.81 | - | - | x |
| | | | 0.90 | - | - | x |
| | | | 0.92 | - | - | x |
| | | | 0.95 | - | - | x |
| | | | 0 | - | x | - |
| | | -5.0 | - | x | - | - |
| | | | - | x | - | - |

| Model | h/D | $\alpha$ (deg.) | $q/P_t$ | Wind on only | Air on only | Wind and air on |
|---|---|---|---|---|---|---|
| SYMM. CURV. | .200 | -5.0 | 0.85 | - | - | x |
| | | | 1.75 | - | - | x |
| | | | 2.75 | - | - | x |
| | | | 5.00 | - | - | x |
| | | | 8.50 | - | - | x |
| | | | 0 | - | x | - |
| | | -10.0 | - | x | - | - |
| | | | - | x | - | - |
| | | | * | - | - | x |
| | | | * | - | - | x |
| | | | * | - | - | x |
| | | | * | - | - | x |
| | | | 0 | - | x | - |
| | .250 | 0 | - | x | - | - |
| | | | - | x | - | - |
| | | | 100 | - | - | x |
| | | | 1.13 | - | - | x |
| | | | 1.30 | - | - | x |
| | | | 1.38 | - | - | x |
| | | | 1.54 | - | - | x |
| | | | 0 | - | x | - |
| | | 5.0 | - | x | - | - |
| | | | - | x | - | - |
| | | | 0.70 | - | - | x |
| | | | 0.80 | - | - | x |
| | | | 0.87 | - | - | x |
| | | | 0.97 | - | - | x |
| | | | 1.07 | - | - | x |
| | | | 0 | - | x | - |
| | .250 | 10.0 | - | x | - | - |
| | | | - | x | - | - |
| | | | 0.50 | - | - | x |
| | | | 0.70 | - | - | x |
| | | | 0.80 | - | - | x |
| | | | 0.93 | - | - | x |
| | | | 0.95 | - | - | x |
| | | | 0.95 | - | - | x |
| | | | 0 | - | x | - |
| | | -5.0 | - | x | - | - |
| | | | - | x | - | - |
| | | | 2.00 | - | - | x |
| | | | 3.60 | - | - | x |

| Model | h/D | $\alpha$ (deg.) | $q/P_t$ | Wind on only | Air on only | Wind and air on |
|---|---|---|---|---|---|---|
| SYMM. | .250 | -5.0 | 5.50 | - | - | x |
| CURV. | | | * | - | - | x |
| | | | 0 | - | x | - |
| | | -10.0 | - | x | - | - |
| | | | - | x | - | - |
| | | | * | - | - | x |
| | | | * | - | - | x |
| | | | * | - | - | x |
| | | | * | - | - | x |
| | | | 0 | - | x | - |
| | .300 | 0 | - | x | - | - |
| | | | - | x | - | - |
| | | | 1.10 | - | - | x |
| | | | 1.20 | - | - | x |
| | | | 1.50 | - | - | x |
| | | | 1.50 | - | - | x |
| | | | 1.70 | - | - | x |
| | | | 0 | - | x | - |
| | | 5.0 | - | x | - | - |
| | | | - | x | - | - |
| | .300 | 5.0 | 0.60 | - | - | x |
| | | | 0.80 | - | - | x |
| | | | 0.90 | - | - | x |
| | | | 1.00 | - | - | x |
| | | | 1.09 | - | - | x |
| | | | 0 | - | x | - |
| | | 10.0 | - | x | - | - |
| | | | - | x | - | - |
| | | | 0.50 | - | - | x |
| | | | 0.65 | - | - | x |
| | | | 0.80 | - | - | x |
| | | | 0.90 | - | - | x |
| | | | 0.94 | - | - | x |
| | | | 0 | - | x | - |
| | | -5.0 | - | x | - | - |
| | | | - | x | - | - |
| | | | 2.10 | - | - | x |
| | | | 2.70 | - | - | x |
| | | | 4.70 | - | - | x |
| | | | 0 | - | x | - |
| | | -10.0 | - | x | - | - |
| | | | - | x | - | - |
| | | | 4.70 | - | - | x |

| Model | h/D | $\alpha$ (deg.) | $q/P_t$ | Wind on only | Air on only | Wind and air on |
|---|---|---|---|---|---|---|
| SYMM. | .300 | -10.0 | * | - | - | x |
| CURV. | ″ | ″ | * | - | - | x |
| ″ | ″ | ″ | * | - | - | x |
| ″ | ″ | ″ | 0 | - | x | - |

* Data not reliable due to severe negative angle producing negative pressure in forward part of plenum chamber.

## APPENDIX III, TEST PROGRAM - TWO-DIMENSIONAL FLOW VISUALIZATION

A - Wind on only
B - Air on only
C - Wind and air on
D - Jet blown under GEM
E - Jet not blown under
F - Indeterminate

| Model | $h/D$ | $\alpha$ (deg.) | $q/P_t$ | A | B | C | D | E | F |
|---|---|---|---|---|---|---|---|---|---|
| TINAJERO | .022 | 0 | - | x | - | - | - | - | - |
| | | | - | x | - | - | - | - | - |
| | | | - | x | - | - | - | - | - |
| | | | 0.46 | - | - | x | - | x | - |
| | | | 0.47 | - | - | x | - | x | - |
| | | | 0.73 | - | - | x | - | x | - |
| | | | 0.87 | - | - | x | - | x | - |
| | | | 0 | - | x | - | - | - | - |
| | | 1.18 | - | x | - | - | - | - | - |
| | | | 0.29 | - | - | x | - | x | - |
| | | | 0.38 | - | - | x | - | x | - |
| | | | 0.57 | - | - | x | - | x | - |
| | | | 0.74 | - | - | x | - | x | - |
| | | | 0.91 | - | - | x | - | x | - |
| | | | 0 | - | x | - | - | - | - |
| | | 2.36 | - | x | - | - | - | - | - |
| | | | 0.20 | - | - | x | - | x | - |
| | | | 0.36 | - | - | x | - | x | - |
| | | | 0.53 | - | - | x | - | x | - |
| | | | 0.54 | - | - | x | - | x | - |
| | | | 0 | - | x | - | - | - | - |
| | | -1.18 | - | x | - | - | - | - | - |
| | | | 0.40 | - | - | x | - | x | - |
| | | | 1.14 | - | - | x | - | x | - |
| | | | 0 | - | x | - | - | - | - |
| | | -2.36 | - | x | - | - | - | - | - |
| | | | 0.11 | - | - | x | - | x | - |
| | | | 0.54 | - | - | x | - | x | - |
| | | | 0 | - | x | - | - | - | - |

| Model | h/D | $\alpha$ (deg.) | $q/P_t$ | A | B | C | D | E | F |
|---|---|---|---|---|---|---|---|---|---|
| TINAJERO | .035 | 0 | - | x | - | - | - | - | - |
| | | | - | x | - | - | - | - | - |
| | | | - | x | - | - | - | - | - |
| | | | 0.33 | - | - | x | - | x | - |
| | | | 0.40 | - | - | x | - | x | - |
| | | | 0.55 | - | - | x | - | x | - |
| | | | 0.67 | - | - | x | - | - | x |
| | | | 1.00 | - | - | x | x | - | - |
| | | | 0 | - | x | - | - | - | - |
| | | 2.03 | - | x | - | - | - | - | - |
| | | | 0.48 | - | - | x | - | x | - |
| | | | 0.96 | - | - | x | - | x | - |
| | | | 0 | - | x | - | - | - | - |
| | | 4.07 | - | x | - | - | - | - | - |
| | | | 0.34 | - | - | x | - | x | - |
| | | | 0.69 | - | - | x | - | x | - |
| | | | 0 | - | x | - | - | - | - |
| | | -2.03 | - | x | - | - | - | - | - |
| | | | 0.43 | - | - | x | - | x | - |
| | | | 0.90 | - | - | x | - | x | - |
| | | | 1.07 | - | - | x | - | x | - |
| | | | 1.57 | - | - | x | x | - | - |
| | | | 0 | - | x | - | - | - | - |
| | | -4.07 | - | x | - | - | - | - | - |
| | | | 0.38 | - | - | x | - | x | - |
| | | | 0.58 | - | - | x | - | x | - |
| | | | 0.85 | - | - | x | - | x | - |
| | | | 1.35 | - | - | x | - | - | x |
| | | | 0 | - | x | - | - | - | - |
| | .050 | 0 | - | x | - | - | - | - | - |
| | | | - | x | - | - | - | - | - |
| | | | - | x | - | - | - | - | - |
| | | | - | x | - | - | - | - | - |
| | | | - | x | - | - | - | - | - |
| | | | 0.33 | - | - | x | - | x | - |
| | | | 0.55 | - | - | x | - | x | - |
| | | | 0.77 | - | - | x | - | x | - |
| | | | 0.93 | - | - | x | x | - | - |
| | | | 1.13 | - | - | x | x | - | - |
| | | | 0 | - | x | - | - | - | - |
| | | 5.0 | - | x | - | - | - | - | - |
| | | | - | x | - | - | - | - | - |
| | | | - | x | - | - | - | - | - |
| | | | 0.54 | - | - | x | - | x | - |

| Model | h/D | $\alpha$ (deg.) | $q/P_t$ | A | B | C | D | E | F |
|---|---|---|---|---|---|---|---|---|---|
| TINAJERO | .050 | 5.0 | 0.92 | - | - | x | - | x | - |
| | | | 1.07 | - | - | x | - | x | - |
| | | | 0 | - | x | - | - | - | - |
| | | -5.0 | - | x | - | - | - | - | - |
| | | | 0.46 | - | - | x | - | x | - |
| | | | 1.00 | - | - | x | - | x | - |
| | | | 2.15 | - | - | x | x | - | - |
| | | | 0 | - | x | - | - | - | - |
| | .100 | 0 | - | x | - | - | - | - | - |
| | | | - | x | - | - | - | - | - |
| | | | - | x | - | - | - | - | - |
| | | | 0.53 | - | - | x | x | - | - |
| | | | 0.67 | - | - | x | x | - | - |
| | | | 0.94 | - | - | x | x | - | - |
| | | | 0 | - | x | - | - | - | - |
| | | 5.0 | - | x | - | - | - | - | - |
| | | | 0.51 | - | - | x | - | x | - |
| | | | 0.83 | - | - | x | - | x | - |
| | | | 1.02 | - | - | x | x | - | - |
| | | | 0 | - | x | - | - | - | - |
| | | 10.0 | - | x | - | - | - | - | - |
| | | | 0.54 | - | - | x | - | x | - |
| | | | 0.84 | - | - | x | - | x | - |
| | | | 1.03 | - | - | x | - | x | - |
| | | | 0 | - | x | - | - | - | - |
| | | -5.0 | - | x | - | - | - | - | - |
| | | | 1.36 | - | - | x | x | - | - |
| | | | 6.22 | - | - | x | x | - | - |
| | | | 0 | - | x | - | - | - | - |
| | | -10.0 | - | x | - | - | - | - | - |
| | | | 0.54 | - | - | x | x | - | - |
| | | | 0 | - | x | - | - | - | - |
| | .150 | 0 | - | x | - | - | - | - | - |
| | | | - | x | - | - | - | - | - |
| | | | - | x | - | - | - | - | - |
| | | | 0.39 | - | - | x | x | - | - |
| | | | 1.25 | - | - | x | x | - | - |
| | | | 0 | - | x | - | - | - | - |
| | | 5.0 | - | x | - | - | - | - | - |
| | | | - | x | - | - | - | - | - |
| | | | - | x | - | - | - | - | - |

| Model | $h/D$ | $\alpha$ (deg.) | $q/P_t$ | A | B | C | D | E | F |
|---|---|---|---|---|---|---|---|---|---|
| TINAJERO | .150 | 5.0 | 0.53 | - | - | x | x | - | - |
| | | | 0.80 | - | - | x | x | - | - |
| | | | 1.06 | - | - | x | x | - | - |
| | | | 0 | - | x | - | - | - | - |
| | | 10.0 | - | x | - | - | - | - | - |
| | | | 0.43 | - | - | x | - | x | - |
| | | | 0.64 | - | - | x | x | - | - |
| | | | 0 | - | x | - | - | - | - |
| | | -5.0 | - | x | - | - | - | - | - |
| | | | - | x | - | - | - | - | - |
| | | | 0.52 | - | - | x | x | - | - |
| | | | 0 | - | x | - | - | - | - |
| | | -10.0 | - | x | - | - | - | - | - |
| | | | - | x | - | - | - | - | - |
| | | | 0.54 | - | - | x | x | - | - |
| | | | 0 | - | x | - | - | - | - |
| UPPER CURV. | .022 | 0 | - | x | - | - | - | - | - |
| | | | - | x | - | - | - | - | - |
| | | | 0.15 | - | - | x | - | x | - |
| | | | 0.32 | - | - | x | - | x | - |
| | | | 0.56 | - | - | x | - | x | - |
| | | | 0.72 | - | - | x | - | x | - |
| | | | 1.00 | - | - | x | - | x | - |
| | | | 0 | - | x | - | - | - | - |
| | | 1.18 | - | x | - | - | - | - | - |
| | | | - | x | - | - | - | - | - |
| | | | 0.47 | - | - | x | - | x | - |
| | | | 0.66 | - | - | x | - | x | - |
| | | | 0.75 | - | - | x | - | x | - |
| | | | 0.80 | - | - | x | - | x | - |
| | | | 0 | - | x | - | - | - | - |
| | | 2.36 | - | x | - | - | - | - | - |
| | | | 0.39 | - | - | x | - | x | - |
| | | | 0.51 | - | - | x | - | x | - |
| | | | 0.87 | - | - | x | - | x | - |
| | | | 0 | - | x | - | - | - | - |

| Model | $h/D$ | $\alpha$ (deg.) | $q/P_t$ | A | B | C | D | E | F |
|---|---|---|---|---|---|---|---|---|---|
| UPPER CURV. | .022 | -1.18 | - | x | - | - | - | - | - |
| | | | 0.53 | - | - | x | - | x | - |
| | | | 0.82 | - | - | x | - | x | - |
| | | | 1.17 | - | - | x | - | x | - |
| | | | 0 | - | x | - | - | - | - |
| | | -2.36 | - | x | - | - | - | - | - |
| | | | 0.48 | - | - | x | - | x | - |
| | | | 1.23 | - | - | x | - | x | - |
| | | | 0 | - | x | - | - | - | - |
| | .035 | 0 | - | x | - | - | - | - | - |
| | | | - | x | - | - | - | - | - |
| | | | 0.59 | - | - | x | - | x | - |
| | | | 0.74 | - | - | x | x | - | - |
| | | | 0.81 | - | - | x | x | - | - |
| | | | 1.06 | - | - | x | x | - | - |
| | | 2.03 | - | x | - | - | - | - | - |
| | | | - | x | - | - | - | - | - |
| | | | 0.46 | - | - | x | - | x | - |
| | | | 0.59 | - | - | x | - | x | - |
| | | | 0.75 | - | - | x | - | x | - |
| | | | 0.88 | - | - | x | x | - | - |
| | | | 0 | - | x | - | - | - | - |
| | | 4.07 | - | x | - | - | - | - | - |
| | | | - | x | - | - | - | - | - |
| | | | 0.54 | - | - | x | - | x | - |
| | | | 0.70 | - | - | x | - | x | - |
| | | | 0.87 | - | - | x | - | x | - |
| | | | 0 | - | x | - | - | - | - |
| | | -2.03 | - | x | - | - | - | - | - |
| | | | - | x | - | - | - | - | - |
| | | | 0.67 | - | - | x | - | x | - |
| | | | 0.77 | - | - | x | - | x | - |
| | | | 1.00 | - | - | x | - | x | - |
| | | | 1.16 | - | - | x | x | - | - |
| | | | 0 | - | x | - | - | - | - |
| | | -4.07 | - | x | - | - | - | - | - |
| | | | - | x | - | - | - | - | - |
| | | | 0.62 | - | - | x | - | x | - |
| | | | 1.42 | - | - | x | x | - | - |
| | | | 0 | - | x | - | - | - | - |

| Model | $h/D$ | $\alpha$ (deg.) | $q/P_t$ | A | B | C | D | E | F |
|---|---|---|---|---|---|---|---|---|---|
| UPPER CURV. | .050 | 0 | - | x | - | - | - | - | - |
| | | | - | x | - | - | - | - | - |
| | | | 0.20 | - | - | x | - | x | - |
| | | | 0.35 | - | - | x | x | - | - |
| | | | 0.51 | - | - | x | x | - | - |
| | | | 0.55 | - | - | x | x | - | - |
| | | | 0.64 | - | - | x | - | x | - |
| | | | 0.74 | - | - | x | - | x | - |
| | | | 0.77 | - | - | x | - | x | - |
| | | | 0.90 | - | - | x | - | x | - |
| | | | 0 | - | x | - | - | - | - |
| | | 5.0 | - | x | - | - | - | - | - |
| | | | 0.60 | - | - | x | - | x | - |
| | | | 0.76 | - | - | x | - | x | - |
| | | | 0.86 | - | - | x | - | x | - |
| | | | 0 | - | x | - | - | - | - |
| | | -5.0 | - | x | - | - | - | - | - |
| | | | 0.82 | - | - | x | - | x | - |
| | | | 1.09 | - | - | x | - | x | - |
| | | | 2.50 | - | - | x | - | - | x |
| | | | 0 | - | x | - | - | - | - |
| | .100 | 0 | - | x | - | - | - | - | - |
| | | | - | x | - | - | - | - | - |
| | | | 0.26 | - | - | x | - | x | - |
| | | | 0.46 | - | - | x | - | x | - |
| | | | 0.54 | - | - | x | x | - | - |
| | | | 0.96 | - | - | x | x | - | - |
| | | | 0 | - | x | - | - | - | - |
| | | 5.0 | - | x | - | - | - | - | - |
| | | | - | x | - | - | - | - | - |
| | | | 0.39 | - | - | x | - | x | - |
| | | | 0.44 | - | - | x | x | - | - |
| | | | 0.78 | - | - | x | x | - | - |
| | | | 0 | - | x | - | - | - | - |
| | | 10.0 | - | x | - | - | - | - | - |
| | | | - | x | - | - | - | - | - |
| | | | - | x | - | - | - | - | - |
| | | | 0.29 | - | - | x | - | x | - |
| | | | 0.61 | - | - | x | - | x | - |
| | | | 0.82 | - | - | x | - | x | - |
| | | | 0.92 | - | - | x | - | x | - |

| Model | $h/D$ | $\alpha$ (deg.) | $q/P_t$ | A | B | C | D | E | F |
|---|---|---|---|---|---|---|---|---|---|
| UPPER CURV. | .100 | -5.0 | - | x | - | - | - | - | - |
| | | | - | x | - | - | - | - | - |
| | | | 0.32 | - | - | x | x | - | - |
| | | | 2.03 | - | - | x | x | - | - |
| | | | 0 | - | x | - | - | - | - |
| | | -10.0 | - | x | - | - | - | - | - |
| | | | - | x | - | - | - | - | - |
| | | | 0.13 | - | - | x | - | x | - |
| | | | 4.36 | - | - | x | x | - | - |
| | | | 0 | - | x | - | - | - | - |
| LOWER CURV. | .022 | 0 | - | x | - | - | - | - | - |
| | | | - | x | - | - | - | - | - |
| | | | - | x | - | - | - | - | - |
| | | | - | x | - | - | - | - | - |
| | | | 0.10 | - | - | x | - | x | - |
| | | | 0.39 | - | - | x | - | x | - |
| | | | 0.79 | - | - | x | - | x | - |
| | | | 1.00 | - | - | x | - | x | - |
| | | | 0 | - | x | - | - | - | - |
| | | 1.18 | - | x | - | - | - | - | - |
| | | | - | x | - | - | - | - | - |
| | | | - | x | - | - | - | - | - |
| | | | 0.25 | - | - | x | - | x | - |
| | | | 0.60 | - | - | x | - | x | - |
| | | | 0.75 | - | - | x | - | x | - |
| | | | 0.81 | - | - | x | - | x | - |
| | | | 0 | - | x | - | - | - | - |
| | | 2.36 | - | x | - | - | - | - | - |
| | | | - | x | - | - | - | - | - |
| | | | 0.08 | - | - | x | - | x | - |
| | | | 0.33 | - | - | x | - | x | - |
| | | | 0.55 | - | - | x | - | x | - |
| | | | 0 | - | x | - | - | - | - |
| | | -1.18 | - | x | - | - | - | - | - |
| | | | - | x | - | - | - | - | - |
| | | | 0.26 | - | - | x | - | x | - |
| | | | 0.75 | - | - | x | - | x | - |
| | | | 1.03 | - | - | x | - | x | - |
| | | | 0 | - | x | - | - | - | - |

| Model | $h/D$ | $\alpha$ (deg.) | $q/P_t$ | A | B | C | D | E | F |
|---|---|---|---|---|---|---|---|---|---|
| LOWER CURV. | .022 | -2.36 | - | x | - | - | - | - | - |
| | | | - | x | - | - | - | - | - |
| | | | 0.09 | - | - | x | - | x | - |
| | | | 0.54 | - | - | x | - | x | - |
| | | | 0.93 | - | - | x | - | x | - |
| | | | 0 | - | x | - | - | - | - |
| | .035 | 0 | - | x | - | - | - | - | - |
| | | | - | x | - | - | - | - | - |
| | | | 0.40 | - | - | x | - | x | - |
| | | | 0.87 | - | - | x | x | - | - |
| | | | 1.03 | - | - | x | x | - | - |
| | | | 0 | - | x | - | - | - | - |
| | | 2.03 | - | x | - | - | - | - | - |
| | | | - | x | - | - | - | - | - |
| | | | 0.31 | - | - | x | - | x | - |
| | | | 0.61 | - | - | x | - | x | - |
| | | | 0.85 | - | - | x | - | x | - |
| | | | 0.85 | - | - | x | - | x | - |
| | | | 0.96 | - | - | x | - | x | - |
| | | | 0 | - | x | - | - | - | - |
| | | 4.07 | - | x | - | - | - | - | - |
| | | | 0.13 | - | - | x | - | x | - |
| | | | 0.39 | - | - | x | - | x | - |
| | | | 0.56 | - | - | x | - | x | - |
| | | | 0 | - | x | - | - | - | - |
| | | -2.03 | - | x | - | - | - | - | - |
| | | | 0.66 | - | - | x | - | x | - |
| | | | 0.92 | - | - | x | - | x | - |
| | | | 1.16 | - | - | x | - | x | - |
| | | | 1.71 | - | - | x | x | - | - |
| | | | 0 | - | x | - | - | - | - |
| | | -4.07 | - | x | - | - | - | - | - |
| | | | 0.22 | - | - | x | - | x | - |
| | | | 0.30 | - | - | x | - | x | - |
| | | | 0.54 | - | - | x | - | x | - |
| | | | 0.72 | - | - | x | - | x | - |
| | | | 0 | - | x | - | - | - | - |

| Model | $h/D$ | $\alpha$ (deg.) | $q/P_t$ | A | B | C | D | E | F |
|---|---|---|---|---|---|---|---|---|---|
| LOWER | .050 | 0 | - | x | - | - | - | - | - |
| CURV. | | | - | x | - | - | - | - | - |
| | | | 0.27 | - | - | x | - | x | - |
| | | | 0.57 | - | - | x | - | x | - |
| | | | 0.60 | - | - | x | - | x | - |
| | | | 0.88 | - | - | x | x | - | - |
| | | | 0 | - | x | - | - | - | - |
| | | 5.0 | - | x | - | - | - | - | - |
| | | | 0.25 | - | - | x | - | x | - |
| | | | 0.65 | - | - | x | - | x | - |
| | | | 0.83 | - | - | x | - | x | - |
| | | | 0.93 | - | - | x | - | x | - |
| | | | 0 | - | x | - | - | - | - |
| | | -5.0 | - | x | - | - | - | - | - |
| | | | 0.32 | - | - | x | - | x | - |
| | | | 0.71 | - | - | x | - | x | - |
| | | | 1.12 | - | - | x | x | - | - |
| | | | 0 | - | x | - | - | - | - |
| | .100 | 0 | - | x | - | - | - | - | - |
| | | | 0.27 | - | - | x | - | x | - |
| | | | 0.50 | - | - | x | - | x | - |
| | | | 0.62 | - | - | x | - | x | - |
| | | | 1.24 | - | - | x | x | - | - |
| | | | 0 | - | x | - | - | - | - |
| | | 5.0 | - | x | - | - | - | - | - |
| | | | 0.53 | - | - | x | - | x | - |
| | | | 0.76 | - | - | x | x | - | - |
| | | | 0.94 | - | - | x | x | - | - |
| | | | 0 | - | x | - | - | - | - |
| | | 10.0 | - | x | - | - | - | - | - |
| | | | 0.54 | - | - | x | - | x | - |
| | | | 0.99 | - | - | x | - | x | - |
| | | | 0 | - | x | - | - | - | - |
| | | -5.0 | - | x | - | - | - | - | - |
| | | | 0.37 | - | - | x | x | - | - |
| | | | 0 | - | x | - | - | - | - |
| | | -10.0 | - | x | - | - | - | - | - |
| | | | 0.48 | - | - | x | x | - | - |
| | | | 0 | - | x | - | - | - | - |

| Model | $h/D$ | $\alpha$ (deg.) | $q/P_t$ | A | B | C | D | E | F |
|---|---|---|---|---|---|---|---|---|---|
| SYMM. | .022 | 0 | - | x | - | - | - | - | - |
| CURV. | | | 0.18 | - | - | x | - | x | - |
| | | | 0.71 | - | - | x | - | x | - |
| | | | .100 | - | - | x | - | x | - |
| | | | 0 | - | x | - | - | - | - |
| | | 1.18 | - | x | - | - | - | - | - |
| | | | 0.58 | - | - | x | - | x | - |
| | | | 0.85 | - | - | x | - | x | - |
| | | | 0 | - | x | - | - | - | - |
| | | 2.36 | - | x | - | - | - | - | - |
| | | | 0.26 | - | - | x | - | x | - |
| | | | 0.49 | - | - | x | - | x | - |
| | | | 0 | - | x | - | - | - | - |
| | | -1.18 | - | x | - | - | - | - | - |
| | | | 0.65 | - | - | x | - | x | - |
| | | | 1.02 | - | - | x | - | x | - |
| | | | 0 | - | x | - | - | - | - |
| | | -2.36 | - | x | - | - | - | - | - |
| | | | 0.22 | - | - | x | - | x | - |
| | | | 0.39 | - | - | x | - | x | - |
| | | | 0 | - | x | - | - | - | - |
| | .035 | 0 | - | x | - | - | - | - | - |
| | | | 0.65 | - | - | x | - | x | - |
| | | | 0.78 | - | - | x | - | x | - |
| | | | 0.86 | - | - | x | x | - | - |
| | | | 0.98 | - | - | x | x | - | - |
| | | | 0 | - | x | - | - | - | - |
| | | 2.03 | - | x | - | - | - | - | - |
| | | | 0.62 | - | - | x | - | x | - |
| | | | 0.82 | - | - | x | - | x | - |
| | | | 0.86 | - | - | x | - | x | - |
| | | | 0 | - | x | - | - | - | - |
| | | 4.07 | - | x | - | - | - | - | - |
| | | | 0.69 | - | - | x | - | x | - |
| | | | 0 | - | x | - | - | - | - |
| | | -2.03 | - | x | - | - | - | - | - |
| | | | 0.83 | - | - | x | - | x | - |
| | | | 0.97 | - | - | x | - | x | - |
| | | | 1.03 | - | - | x | - | x | - |
| | | | 0 | - | x | - | - | - | - |

| Model | $h/D$ | $\alpha$ (deg.) | $q/P_t$ | A | B | C | D | E | F |
|---|---|---|---|---|---|---|---|---|---|
| SYMM. | .035 | -4.07 | - | x | - | - | - | - | - |
| CURV. | | | 0.06 | - | - | x | - | x | - |
| | | | 0.30 | - | - | x | - | x | - |
| | | | 0.85 | - | - | x | - | x | - |
| | | | 0 | - | x | - | - | - | - |
| | .050 | 0 | - | x | - | - | - | - | - |
| | | | 0.55 | - | - | x | - | x | - |
| | | | 0.70 | - | - | x | x | - | - |
| | | | 0.75 | - | - | x | x | - | - |
| | | | 0.96 | - | - | x | x | - | - |
| | | | 0 | - | x | - | - | - | - |
| | | 5.0 | - | x | - | - | - | - | - |
| | | | 0.29 | - | - | x | - | x | - |
| | | | 0.92 | - | - | x | - | x | - |
| | | | 0 | - | x | - | - | - | - |
| | | -5.0 | - | x | - | - | - | - | - |
| | | | 0.28 | - | - | x | - | x | - |
| | | | 0.99 | - | - | x | - | x | - |
| | | | 1.19 | - | - | x | x | - | - |
| | | | 2.27 | - | - | x | x | - | - |
| | | | 0 | - | x | - | - | - | - |
| | .100 | 0 | - | x | - | - | - | - | - |
| | | | 0.24 | - | - | x | - | x | - |
| | | | 0.44 | - | - | x | - | x | - |
| | | | 0.57 | - | - | x | x | - | - |
| | | | 0.57 | - | - | x | x | - | - |
| | | | 1.08 | - | - | x | x | - | - |
| | | | 0 | - | x | - | - | - | - |
| | | 5.0 | - | x | - | - | - | - | - |
| | | | 0.29 | - | - | x | - | x | - |
| | | | 0.82 | - | - | x | - | x | - |
| | | | 0.75 | - | - | x | - | x | - |
| | | | 0.93 | - | - | x | x | - | - |
| | | | 0 | - | x | - | - | - | - |
| | | 10.0 | - | x | - | - | - | - | - |
| | | | 0.40 | - | - | x | - | x | - |
| | | | 0.92 | - | - | x | - | x | - |
| | | | 0 | - | x | - | - | - | - |

| Model | $h/D$ | $\alpha$ (deg.) | $q/P_t$ | A | B | C | D | E | F |
|---|---|---|---|---|---|---|---|---|---|
| SYMM. | .100 | -5.0 | - | x | - | - | - | - | - |
| CURV. | | | 0.29 | - | - | x | - | - | x |
| | | | 1.76 | - | - | x | x | - | - |
| | | | 0 | - | x | - | - | - | - |
| | | -10.0 | - | x | - | - | - | - | - |
| | | | 0.42 | - | - | x | - | x | - |
| | | | 4.07 | - | - | x | x | - | - |
| | | | 0 | - | x | - | - | - | - |

## DISTRIBUTION

| | |
|---|---|
| USATMC(FTZAT), ATO | 1 |
| USAPRDC | 1 |
| DCSLOG | 1 |
| Rsch Anal Corp | 1 |
| ARO, Durham | 2 |
| OCRD, DA | 2 |
| USAWC | 1 |
| NATC | 1 |
| ARO, OCRD | 1 |
| DCSOPS | 1 |
| USAERDL | 2 |
| USATAC, Center Line | 4 |
| OrdBd | 1 |
| Human Engineering Lab. | 1 |
| CofT | 3 |
| USATCDA | 1 |
| USATMC | 19 |
| USATSCH | 4 |
| USATRECOM | 74 |
| TCLO, USAABELCTBD | 1 |
| USATRECOM LO, USARDG (EUR) | 3 |
| CNO | 1 |
| CNR | 3 |
| BUWEPS, DN | 2 |
| ACRD(OW), DN | 1 |
| USNSRDF | 1 |
| USNPGSCH | 1 |
| BUSHP, DN | 1 |
| USNOTS | 1 |
| Dav Tay Mod Bas | 1 |
| MCLFDC | 1 |
| MCEC | 1 |
| USASGCA | 1 |
| Canadian LO, USATSCH | 3 |
| BRAS, DAQMG (Mov & TN) | 4 |
| USASG, UK | 1 |
| Langley Rsch Cen, NASA | 2 |
| NASA, Wash., D. C. | 6 |

| | |
|---|---|
| Ames Rsch Cen, NASA | 2 |
| Lewis Rsch Cen, NASA | 1 |
| USGPO | 1 |
| ASTIA | 10 |
| USAMRDC | 1 |
| HUMRRO | 2 |
| DDRE | 1 |
| U. S. Maritime Administration | 1 |
| MOCOM | 3 |
| USSTRICOM | 1 |
| University of Maryland | 10 |

University of Maryland
Wind Tunnel Operations Dept.
College Park, Md., EXPERIMENTAL STUDIES OF THE AERODYNAMICS OF GROUND EFFECT MACHINES
Unclassified Report, TCREC 62-88

The aerodynamics of the Tinajero ground effect machine and its two-dimensional counterpart were investigated under various flight conditions.

UNCLASSIFIED

1. Ground Effect Machines
2. Contract DA 44-177-TC-776

University of Maryland
Wind Tunnel Operations Dept.
College Park, Md., EXPERIMENTAL STUDIES OF THE AERODYNAMICS OF GROUND EFFECT MACHINES
Unclassified Report, TCREC 62-88

The aerodynamics of the Tinajero ground effect machine and its two-dimensional counterpart were investigated under various flight conditions.

UNCLASSIFIED

1. Ground Effect Machines
2. Contract DA 44-177-TC-776

University of Maryland
Wind Tunnel Operations Dept.
College Park, Md., EXPERIMENTAL STUDIES OF THE AERODYNAMICS OF GROUND EFFECT MACHINES
Unclassified Report, TCREC 62-88

The aerodynamics of the Tinajero ground effect machine and its two-dimensional counterpart were investigated under various flight conditions.

UNCLASSIFIED

1. Ground Effect Machines
2. Contract DA 44-177-TC-776

University of Maryland
Wind Tunnel Operations Dept.
College Park, Md., EXPERIMENTAL STUDIES OF THE AERODYNAMICS OF GROUND EFFECT MACHINES
Unclassified Report, TCREC 62-88

The aerodynamics of the Tinajero ground effect machine and its two-dimensional counterpart were investigated under various flight conditions.

UNCLASSIFIED

1. Ground Effect Machines
2. Contract DA 44-177-TC-776

Tests of the full scale machine included external aerodynamics, control effectiveness, stability, and the effect of changing the vertical center of gravity. Tests were conducted in the University of Maryland Subsonic Wind Tunnel diffuser section and on a ground board set up in the open air. The machine was found to be basically unstable in yaw and the controls were ineffective.
The two-dimensional model, with several nose shapes was tested in a twenty four inch subsonic wind tunnel to obtain the flow patterns and pressure distributions. It was found that nose shape had no real effect on the cushion under the vehicle, but did effect the basic external aerodynamic coefficients. Significant changes in flow patterns were observed as forward speed increased.

Tests of the full scale machine included external aerodynamics, control effectiveness, stability, and the effect of changing the vertical center of gravity. Tests were conducted in the University of Maryland Subsonic Wind Tunnel diffuser section and on a ground board set up in the open air. The machine was found to be basically unstable in yaw and the controls were ineffective.
The two-dimensional model, with several nose shapes was tested in a twenty four inch subsonic wind tunnel to obtain the flow patterns and pressure distributions. It was found that nose shape had no real effect on the cushion under the vehicle, but did affect the basic external aerodynamic coefficients. Significant changes in flow patterns were observed as forward speed increased.

Tests of the full scale machine included external aerodynamics, control effectiveness, stability, and the effect of changing the vertical center of gravity. Tests were conducted in the University of Maryland Subsonic Wind Tunnel diffuser section and on a ground board set up in the open air. The machine was found to be basically unstable in yaw and the controls were ineffective.
The two-dimensional model, with several nose shapes was tested in a twenty four inch subsonic wind tunnel to obtain the flow patterns and pressure distributions. It was found that nose shape had no real effect on the cushion under the vehicle, but did effect the basic external aerodynamic coefficients. Significant changes in flow patterns were observed as forward speed increased.

Tests of the full scale machine included external aerodynamics, control effectiveness, stability, and the effect of changing the vertical center of gravity. Tests were conducted in the University of Maryland Subsonic Wind Tunnel diffuser section and on a ground board set up in the open air. The machine was found to be basically unstable in yaw and the controls were ineffective.
The two-dimensional model, with several nose shapes was tested in a twenty four inch subsonic wind tunnel to obtain the flow patterns and pressure distributions. It was found that nose shape had no real effect on the cushion under the vehicle, but did effect the basic external aerodynamic coefficients. Significant changes in flow patterns were observed as forward speed increased.